

ICLIAD 63 (3), 203-322, 2022

p-ISSN 0535-5133
e-ISSN 2477-9393

Volumen 63
No. 3
Septiembre 2022

Investigación Clínica

Universidad del Zulia
Facultad de Medicina
Instituto de Investigaciones Clínicas
"Dr. Américo Negrette"
Maracaibo, Venezuela



Investigación Clínica

<https://sites.google.com/site/revistainvestigacionesclinicas>

Revista arbitrada dedicada a estudios humanos, animales y de laboratorio relacionados con la investigación clínica y asuntos conexos.

La Revista es de Acceso Abierto, publicada trimestralmente por el Instituto de Investigaciones Clínicas “Dr. Américo Negrette”, de la Facultad de Medicina, de la Universidad del Zulia, Maracaibo, Venezuela.

Investigación Clínica está indizada en Science Citation Index Expanded (USA), Excerpta Medica/EMBASE y Scopus (Holanda), Tropical Diseases Bulletin y Global Health (UK), Biblioteca Regional de Medicina/BIREME (Brasil), Ulrich’s Periodicals, Journal Citation Reports (USA), Index Copernicus (Polonia), SIIEC Data Bases, Sección Iberoamérica (Argentina) e Infobase Index (India), Redalyc y las bases de datos: SciELO (www.scielo.org.ve), Reveneyt, LILACS, LIVECS, PERIODICA y web de LUZ: <http://www.produccioncientificaluz.org/revistas>

Américo Negrette †
Editor Fundador (1960-1971)

Editora
Elena Ryder

Slavia Ryder
Editora 1972-1990

Asistente al Editor
Lisbeny Valencia

Comité Editorial (2022-2024)

Deyseé Almarza	Jesús Mosquera
María Díez-Ewald	Jesús Quintero
Juan Pablo Hernández	Enrique Torres
Yraima Larreal	Nereida Valero
Humberto Martínez	Gilberto Vizcaíno

Asesores Científicos Nacionales (2022-2024)

Alberto Aché (Maracay)	Oscar Noya (Caracas)
Trino Baptista (Mérida)	José Núñez Troconis (Maracaibo)
Rafael Bonfante-Cabarcas (Barquisimeto)	Mariela Paoli (Mérida)
Javier Cebrian (Caracas)	Flor Pujol (Caracas)
Rodolfo Devera (Ciudad Bolívar)	Alexis Rodríguez-Acosta (Caracas)
Saul Dorfman (Maracaibo)	Martín Rodríguez (Caracas)
Jorge García Tamayo (Maracaibo)	Vanessa Romero (Maracaibo)
José Golaszewski (Valencia)	Liseti Solano (Valencia)
Liliana Gomez Gamboa (Maracaibo)	Lisbeth Soto (Valencia)
Maritza Landaeta de Jiménez (Caracas)	Marisol Soto Quintana (Maracaibo)
Jorymar Leal (Maracaibo)	Herbert Stegemann (Caracas)
Diego Martinucci (Maracaibo)	Ezequiel Trejo-Scorza (Caracas)
Edgardo Mengual (Maracaibo)	

Asesores Científicos Internacionales (2022-2024)

Carlos Aguilar Salinas (México)	Carlos Lorenzo (USA)
Francisco Alvarez-Nava (Ecuador)	Juan Ernesto Ludert (México)
Germán Añez (USA)	Valdair Muglia (Brasil)
César Cuadra Sánchez (Nicaragua)	Alejandro Oliva (Argentina)
Peter Chedraui (Ecuador)	José Antonio Páramo (España)
Marcos de Donato (México)	Isela Parra Rojas (México)
José Esparza (USA)	Joaquín Peña (USA)
Francisco Femenia (Argentina)	Mercede Pineda (España)
Hermes Flórez (USA)	Heberto Suárez (USA)
Elvira Garza-González (México)	Rodolfo Valdez (USA)
José María Gutiérrez (Costa Rica)	Gustavo Vallejo (Colombia)
Tzasna Hernández (México)	

*Para cualquier otra información dirigir
su correspondencia a:*

*Dra. Elena Ryder, Editora
Instituto de Investigaciones Clínicas
"Dr. Américo Negrette"
Facultad de Medicina, Universidad del Zulia
Maracaibo, Venezuela.*

Teléfono:

+58-0414-6305451

Correos electrónicos:

elenaryder@gmail.com

riclinicas@gmail.com

Páginas web:

*[https://sites.google.com/site/
revistainvestigacionesclinicas](https://sites.google.com/site/revistainvestigacionesclinicas)*

*[http://www.produccioncientificaluz.
org/revistas](http://www.produccioncientificaluz.org/revistas)*

*For any information please address
correspondence to:*

*Dr. Elena Ryder, Editor
Instituto de Investigaciones Clínicas
"Dr. Américo Negrette"
Facultad de Medicina, Universidad del Zulia
Maracaibo, Venezuela.*

Phone:

+58-0414-6305451

E-mails:

elenaryder@gmail.com

riclinicas@gmail.com

Web pages:

*[https://sites.google.com/site/
revistainvestigacionesclinicas](https://sites.google.com/site/revistainvestigacionesclinicas)*

*[http://www.produccioncientificaluz.
org/revistas](http://www.produccioncientificaluz.org/revistas)*



**Universidad del Zulia
Publicación auspiciada por el
Vicerrectorado Académico
Serbiluz-CONDES**

© 2022. INVESTIGACIÓN CLÍNICA

© 2022. Instituto de Investigaciones Clínicas

CODEN: ICLIAD

Versión impresa ISSN: 0535-5133

Depósito legal pp 196002ZU37

Versión electrónica ISSN: 2477-9393

Depósito legal ppi 201502ZU4667

Artes finales:

Lisbeny Valencia

lisbenyvalencia@gmail.com

EDITORIAL

Viruela del Mono, el reflejo de las infecciones olvidadas.

La viruela símica o viruela del mono es una enfermedad infecciosa de origen viral, de tipo zoonótico, ocasionada por el virus del mismo nombre, género *Orthopoxvirus*, familia *Poxviridae*. A este mismo género pertenece el virus de la variola, causante de la viruela humana, enfermedad erradicada en 1980, con la cual comparte características clínicas similares, aunque la viruela símica es mucho menos grave. Entre los reservorios naturales del virus se incluyen principalmente roedores como ratas, ardillas, lirones y conejos, la enfermedad se describió por primera vez en Europa en 1958, en monos macacos de laboratorio, de ello viene el nombre de viruela símica o viruela del mono. En el año 1970 se diagnosticó por primera vez en humanos, en un niño de la República Democrática del Congo (África central) y desde entonces se reportan miles de casos cada año en este continente, donde es considerada una enfermedad endémica.

Existen dos clados genéticos del virus, uno en África occidental y otro en África central, donde se ha presentado en forma más agresiva ¹. Al igual que en gran parte de las zoonosis, se desconoce con precisión su origen específico, estos saltos de especie ocurren bien sea porque el humano se introduce en el hábitat natural del reservorio para deforestación, o para comercialización de animales para transporte, consumo o como mascotas. Proteger la biodiversidad y los ecosistemas disminuiría de forma considerable el riesgo de propagación de las enfermedades zoonóticas.

Los datos epidemiológicos señalan, como factor determinante del aumento progresivo de los casos y brotes epidémicos, al cese de la vacunación contra la viruela a par-

tir de 1980, puesto que esta vacuna genera inmunidad cruzada contra ambos virus, además la rapidez y frecuencia de los viajes internacionales favorecen la propagación de la enfermedad. El aumento de los casos en las últimas décadas hace de esta, una más de las epidemias anunciadas.

Otro de los aspectos más destacados en el brote epidémico actual, es la vía de transmisión de persona a persona. Es bien conocida la transmisión por vía respiratoria, a través de gotas de saliva por contactos cercanos y prolongados, o por contacto directo con lesiones mucocutáneas o material contaminado. La transmisión materno infantil también ha sido descrita, a través de la placenta, pudiendo generar casos de viruela símica congénita o por contacto estrecho durante y después del nacimiento. La transmisión por contacto sexual, mayoritariamente entre hombres, ha sido también tema especial durante la epidemia en curso, el contacto físico estrecho es un factor de riesgo bien conocido para la transmisión, pero no está claro en este momento si la viruela símica puede transmitirse específicamente por vía sexual, y los fundamentos no son suficientes para que sea considerada una infección de transmisión sexual (ITS). De igual manera, la caracterización clínica ha tenido sus variaciones, sobre todo en la fase de erupción cutánea, ha sido descrito que las zonas más afectadas son el rostro (85%), por ello el riesgo de lesiones oftalmológicas y peribucales, y las extremidades, sobre todo palmas y plantas (75%); las lesiones en genitales habían sido descritas solo en un 30% de los casos; sin embargo, en los casos recientes fuera del continente africano, han ocurrido

formas atípicas de presentación, así como el mayor porcentaje de lesiones en áreas genitales, perianal y peribucal, frecuentemente sin extensión a otras zonas y de aparición anterior a la adenopatía, la fiebre, el malestar y otros síntomas asociados ². También se ha diagnosticado la infección en casos asintomáticos.

Este nuevo brote reafirma la necesidad de conocer mejor la dinámica de la transmisión, inclusive se está tratando de dilucidar cambios genómicos que pudiesen estar modificando el fenotipo, la transmisibilidad y la virulencia. Es de vital importancia hacer un buen diagnóstico clínico diferencial con enfermedades vesiculopustulosas, como la varicela, el molusco contagioso, las lesiones herpéticas, la sífilis y el impétigo. La linfadenopatía en fase prodrómica y la ubicación predominante en cara y extremidades con expansión centrífuga de las lesiones, son de considerable ayuda, tomando en cuenta las formas atípicas de presentación. El diagnóstico confirmatorio por técnicas moleculares, cultivo celular o técnicas serológicas no es accesible a todas las poblaciones.

A pesar de que las epidemias y mortalidad causadas por virus son históricas, el avance de las terapias antivirales ha sido lento; aunque los progresos son mucho más notables en las últimas décadas. Los tratamientos antirretrovirales para el control de la infección por VIH y los tratamientos curativos para Hepatitis C, son ejemplos exitosos de ello. De igual manera las terapias antivirales basadas en anticuerpos monoclonales han sido determinantes en el tratamiento y control de las infecciones virales. En el caso de la viruela del mono, se han usado antivirales como tecovirimat, cidofovir y su profarmaco derivado, brincidofovir, al igual que las inmunoglobulinas vacunales endovenosas (VIGIV), su utilización tanto para terapias pre como postexposición, está solamente disponible como reserva estratégica nacional en muy pocos países y son usadas solo bajo protocolos de ensayos controlados ³.

Aunque es una enfermedad autolimitada en la mayoría de los casos, el rango de mortalidad es amplio, entre 0 y 10% y depende no solo del estado inmunológico del paciente sino de la atención óptima de los casos. El fallecimiento ocurre, en la mayoría de los casos, por infección sobreagregada de las lesiones y sucede primordialmente en los países más pobres y con menor acceso a buenos sistemas de salud.

No hay vacunas diseñadas específicamente para proteger contra la viruela símica. Las vacunas que se están considerando para su uso en grupos vulnerables, son las vacunas basadas en el virus vaccinia, desarrolladas para prevenir la viruela. La ACAM2000, una vacuna atenuada, era la única disponible, pero con importantes efectos adversos asociados. A partir de 2019 se autorizó la Jynneos (Imvamune) con virus modificados no replicantes, la cual se considera más segura. No obstante, no está considerada aún la vacunación en forma global, solo en grupos prioritarios como personal de laboratorios de investigación de orthopoxvirus, trabajadores de salud de alto riesgo y contactos cercanos de casos confirmados.

Se hace necesario mayor aporte para la investigación y la prevención de enfermedades infecciosas, aunque estén limitadas o afecten principalmente a los países más empobrecidos, recordemos siempre, que los cambios en cualquier nación, pueden afectar al mundo entero. Actuar de manera rápida y proactiva será crucial para contenerlas. Debemos asegurarnos de aprender de las epidemias anteriores y las recientes, como la de COVID-19⁴, y compartir los recursos disponibles de manera temprana y rápida será la clave del éxito. La viruela del mono ha estado presente durante muchos años, ya es el momento de abordar las enfermedades reemergentes con un enfoque global para evitar emergencias de salud pública de importancia internacional y el desarrollo de nuevas pandemias.

Yraima Larreal

ORCID: 0000-0003-0862-9842

Monkeypox, the reflection of forgotten infections.

Monkeypox is a zoonotic infectious disease of viral origin, caused by a virus of the same family as the virus that causes smallpox, a disease officially declared eradicated in 1980 by vaccination. The cessation of this immunization, together with the speed and frequency of international travel, in addition to the commercialization of possible reservoirs, have been decisive for the increase in cases in recent decades. Changes in transmission dynamics and clinical characterization could be associated with genotypic changes of the virus. The diagnostic methods, specific viral treatments and vaccines under consideration are not very accessible to the vast majority of countries. Learning from other epidemics and acting proactively and equitably, is key to preventing the development of new pandemics.

REFERENCIAS

1. **Kaler J, Hussain A, Flores G, Keiri S, Desrosier D.** Monkeypox: A comprehensive review of transmission, pathogenesis, and manifestation. *Cureus* 2022;14(7): e26531. *doi:10.7759/cureus*.
2. **Viruela del mono 2022:** <https://www.who.int/news-room/fact-sheets/detail/monkeypox> .
3. **Bunge EM, Hoet B, Chen L, Lienert F, Weidenthaler H, Baer LR, Steffen R.** The changing epidemiology of human monkeypox—A potential threat? A systematic review. *PLoS Negl Trop Dis* 2022;16(2):e0010141.
4. **Okyay R, Bayrak E, Kaya E, Sahin A, Kocyigit B, Tasdogan A, Avci A, Zumbul H.** Another epidemic in the shadow of Covid 19 pandemic: A review of Monkeypox. *EJMO* 2022;6(2):95-99.

Role and mechanism of miR-548-3p/ DAG1 in the occurrence and malignant transformation of laryngeal carcinoma.

Jia Chen, Yu Lin Zhou, Ke Wen, Shi Huang, Nan Hou, Ling Wang and Yi Wang

Otorhinolaryngology Head and Neck Surgery, The First Affiliated Hospital of Chengdu Medical College, Chengdu, 610500, China.

Key words: laryngeal cancer; hsa-miR-548-3p; DAG1.

Abstract. The AMC-HN-8 cell line and the primary human laryngeal epithelial cell lines were utilized in this work to explore the molecular mechanism of miR-548-3p regulating the gene DAG1 to induce the occurrence and malignant transformation of laryngeal carcinoma. Non-coding RNA miR-548-3p overexpression plasmid, interference plasmid and blank plasmid were constructed, and the plasmids were transfected into AMC-HN-8 cells, respectively. Meanwhile, a non-transfected plasmid group and a human laryngeal epithelial primary cell group were set up. Five groups of cells were named as NC (Normal control), Model, Ov-miR-548-3p, Sh-miR-548-3p and Blank-plasmid group. The luciferase reporter experiment was used to analyze the regulation characteristics of hsa-miR-548-3p on dystrophin-associated glycoprotein 1 (DAG1). Immunofluorescence was used to analyze the relative expression characteristics of the protein DAG1. The cell cloning experiment was used to analyze the proliferation characteristics of AMC-HN-8. The scratch healing test was used to analyze the migration ability of AMC-HN-8. The transwell test was used to analyze the invasion ability of AMC-HN-8. The RT-PCR was used to analyze the expression level of miR-548-3p. Western blot experiments were used to analyze the expression of protein DAG1, laminin $\alpha 2$ (LAMA2) and utrophin (UTRN). The luciferase report experiment and immunofluorescence test found that the expression of DAG1 and miR-548-3p are positively correlated. Cell cloning, scratching and migration experiments identified that the activity of laryngeal cancer cells was positively correlated with the expression of DAG1. The results of Western blot analysis further strengthened the above conclusions. Through carrying out research on the cellular levels, our work has demonstrated that miR-548-3p regulated the content of protein DAG1, and then further induced malignant transformation of laryngeal carcinoma.

Papel y mecanismo de miR-548-3p/DAG1 en la aparición y transformación maligna del carcinoma de laringe.

Invest Clin 2022; 63 (3): 206 – 217

Palabras clave: cáncer de laringe; hsa-miR-548-3p; DAG1.

Resumen. En este trabajo se utilizaron la línea celular AMC-HN-8 y la línea celular epitelial laríngea humana primaria, para explorar el mecanismo molecular regulador del miR-548-3p sobre el gen DAG1 para inducir la aparición y la transformación maligna del carcinoma laríngeo. Se construyeron el plásmido de sobreexpresión de miR-548-3p de ARN no codificante, el plásmido de interferencia y el plásmido en blanco, y los plásmidos se transfectaron en células AMC-HN-8 respectivamente. Mientras tanto, se establecieron un grupo de plásmidos no transfectados y un grupo de células primarias epiteliales laríngeas humanas. Se nombraron cinco grupos de células como NC (control normal), modelo, Ov-miR-548-3p, Sh-miR-548-3p y grupo de plásmido en blanco. El experimento indicador de luciferasa se utilizó para analizar las características de regulación de hsa-miR-548-3p en la glicoproteína 1 asociada a distrofina (DAG1). Se utilizó inmunofluorescencia para analizar las características de expresión relativa de la proteína DAG1. El experimento de clonación celular se utilizó para analizar las características de proliferación de AMC-HN-8. Se utilizó la prueba de cicatrización por rascado para analizar la capacidad de migración de AMC-HN-8. La prueba de transwell se utilizó para analizar la capacidad de invasión de AMC-HN-8. Se utilizó RT-PCR para analizar el nivel de expresión de miR-548-3p. Se usó un experimento de transferencia Western (Western blot) para analizar las expresiones de la proteína DAG1, laminina $\alpha 2$ (LAMA2) y utrofina (UTRN). El experimento de reporte de luciferasa y la prueba de inmunofluorescencia encontraron que la expresión de DAG1 y miR-548-3p están positivamente correlacionadas. Los experimentos de clonación celular, rascado y migración, identificaron que la actividad de las células cancerosas de laringe se correlacionó positivamente con la expresión de DAG1. Los resultados del análisis de transferencia Western fortalecieron aún más las conclusiones anteriores. A través de la investigación a nivel celular, nuestro proyecto ha demostrado que miR-548-3p regula el contenido de la proteína DAG1 y luego induce la transformación maligna del carcinoma de laringe.

Received: 23-11-2021 Accepted: 27-03-2022

INTRODUCTION

Laryngeal cancer is a common malignant tumor among head and neck tumors. According to statistics from various places in China, it accounts for 7.9% to 35% of malig-

nant tumors in the ear, nose and throat, and ranks third in head and neck malignancies. The treatment of laryngeal cancer in China is still based on surgery¹. Surgical resection combined with radiotherapy and chemotherapy is mainly used. Laryngeal cancer is di-

vided into primary and secondary². Primary laryngeal carcinoma refers to tumors whose primary site is in the larynx, and squamous cell carcinoma is the most common. Secondary laryngeal cancer refers to the metastasis of malignant tumors from other parts to the larynx, which is relatively rare³. Symptoms of laryngeal cancer are mainly hoarseness, dyspnea, cough, dysphagia, neck lymph node metastasis, etc.⁴.

The function of DAG1 is to participate in the assembly of laminin and basement membrane, muscle membrane stability, cell survival, peripheral nerve myelination, lymph node structure, cell migration and epithelial polarization^{5,6}.

miRNA is a type of endogenous small RNA with a length of about 20-24 nucleotides, which has a variety of important regulatory effects in cells. Each miRNA can have multiple target genes, and several miRNAs can also regulate the same gene. The high degree of conservation of miRNA is closely related to the importance of its function. miRNA is closely related to the evolution of its target genes, and studying its evolutionary history helps to further understand its mechanism and function⁷. miR-548 is a larger, poorly conserved primate-specific miRNA gene family, consists of 69 human miR-548 genes located in almost all human chromosomes, and the miR-548 gene family enrichment pathway analysis showed they played important roles in various human diseases⁸. miR-548c is a member of miR-548 and the mature miR-548c-3p is obtained from it.

miR-548c-3p is low expressed in hypopharyngeal carcinoma tissues and cell lines, inhibits the proliferation, cloning, migration and invasion of FaDu cells, and promotes cell apoptosis⁹. Its expression pattern is consistent with the expression pattern of tumor suppressor genes¹⁰. miR-548c-3p targets *TP53BP2*, and the molecular axis of miR-548-3p/*TP53BP2* affects the biological functions of hypopharyngeal carcinoma cells such as proliferation, colonization, migration, invasion, cycle and apoptosis¹¹.

To explore the role and mechanism of miR-548-3p/DAG1 in the occurrence and malignant transformation of laryngeal carcinoma, the human laryngeal carcinoma cell line AMC-HN-8 and the primary human laryngeal epithelial cell line were utilized here. We found that the non-coding RNA miR-548-3p can target and regulate the gene DAG1, and then further induce malignant transformation of laryngeal carcinoma.

MATERIALS AND METHODS

Experiment design

The culture the human laryngeal carcinoma cell line AMC-HN-8 and the primary human laryngeal epithelial cell line were strictly in accordance with the requirements of aseptic cultures. The non-coding RNA miR-548-3p overexpression plasmid, interference plasmid and blank control plasmid were constructed, and the plasmids were transfected into AMC-HN-8 cells respectively. At the same time, a group of non-transfected plasmid group and a human laryngeal epithelial primary cell group were set up. Five groups of cells were named as NC group, Model group, Ov-miR-548-3p group, Sh-miR-548-3p group and Blank-plasmid group. The luciferase reporter experiment was used to analyze the regulation characteristics of miR-548-3p on gene DAG1. Immunofluorescence was used to analyze the relative expression characteristics of the protein DAG1. The cell cloning experiment was used to analyze the proliferation characteristics of laryngeal carcinoma cell lines. The scratch healing test was used to analyze the migration ability of laryngeal cancer cell lines. The transwell test was used to analyze the invasion ability of laryngeal cancer cell lines. RT-PCR was used to analyze the expression level of miR-548-3p. A Western blot was used to analyze the expression of protein DAG1, LAMA2 and UTRN.

Luciferase reporter experiment

Recombinant plasmid preparation: a recombinant plasmid containing the gene to be

tested DAG1/miR-548-3p was prepared. The reporter gene with DAG1/ miR-548-3p label and the target gene were co-transfected for 48h. Cell processing: the dual luciferase detection kit was operated according to the protocol. Fluorescence detection: a microplate reader was used for fluorescence intensity detection, and finally data analysis was performed.

Immunofluorescence analysis

In each group of cells, 1% BSA was applied for blocking at room temperature for 30 min to block non-specific epitopes. The specific primary antibody was incubated according to the recommended instructions for the antibody and let it stand overnight in a humidified box at 4°C. The slices were taken out the next day and rewarmed at room temperature for 30 min. The corresponding immunofluorescence secondary antibody was selected and then incubated at 37°C for 30 min in the dark. The nucleus was stained with DAPI under dark conditions. Anti-fluorescence quencher was added for mounting. Finally, a fluorescence microscope was used to observe and take pictures.

Cell cloning experiment

Each group of cells were taken in the logarithmic growth phase, digested with 0.25% trypsin and pipetted into single cells, and suspended in a culture medium of 10% fetal bovine serum for later use. The cell suspension was diluted in gradient multiples, and each group of cells was inoculated into a dish containing 10 mL of pre-warmed culture medium at 37°C at a gradient density of 50, 100, and 200 cells per dish, and gently rotated to make the cells uniformly dispersed. Placed it in a cell incubator at 37°C, 5% CO₂ and saturated humidity for 2-3 weeks. It was frequently observed that when there were visible clones in the petri dish, the culture were stopped. The supernatant was discarded and washed carefully with PBS twice. To fix the cells 5 mL of 4% paraformaldehyde was added for 15 minutes. The fixative solution was then removed, an appropriate amount of

GIMSA was added and the dye solution was applied to dye for 10-30 minutes, then slowly washed off with running water.

Cell scratch test

After the cells of each group were digested and counted, 8×10^5 cells were divided into 35mm² culture dishes. A marker was used to draw a line on the bottom of the dish as a mark, the culture medium was aspirated, and a 10 μ L pipette tip was used to mark the cells in the dish perpendicularly to the marker. A rinse with PBS was used to remove the marked cells, and serum-free culture medium was added to continue culturing. Pictures were taken at 24h, and the intersection of the line drawn by the marker was selected and the cell scratch as the observation point, and then observed at a fixed point.

Cell migration test

Twenty-four hours before the experiment, the cells of different groups were replaced with serum-free medium, and the culture was continued. Before inoculation, the 24-well plate and transwell chamber were soaked with 1×PBS for 5 min to moisten the chamber. The cells were digested, washed with serum-free medium, resuspended in serum-free medium, counted and diluted to adjust the cell density to 5×10^5 / mL. Then 0.2 mL cell suspension (5×10^4 cells) were inoculated into the transwell chamber, and 0.7 mL of RPMI-1640 medium containing 10% PBS was added to the lower 24-well plate, 3 replicate holes per group, and placed in a 37°C incubator for 24 hours to finish the culture. To each well of the above cells 1 mL of 4% formaldehyde solution was added, and fixed at room temperature for 10 min. The fixative solution aspirated, washed once with 1x PBS. To each well, 1mL 0.5% crystal violet solution was added, washed with 1×PBS three times after dyeing for 30 min. A cotton swab was used to carefully wipe off the cells that have not migrated in the transwell, and placed under a 200× microscope for observation.

RT-PCR analysis

The AMC-HN-8 cell and primary human laryngeal epithelial cell were treated with TRIzol reagent to extract the total RNA in the cells. Revert Aid TW first Strand cDNA Synthesis Kit was used to synthesize the first chain of DNA. QuantiNova SyBr Green PCR Kit was used to perform PCR analysis. Reaction conditions: pre-denaturation at 95°C for 1 minute, denaturation at 95°C for 30 seconds, annealing at 60°C for 30 seconds, and elongation at 72°C for 30 seconds, running 40 cycles.

Western blot analysis

Cells were collected from each group, and 200 μ L of cell lysate was added to each six-well plate. After sonication, the cells were lysed on ice for 1 hour. The lysed cell sample was centrifuged at 12,500 rpm for 15 minutes at 4°C. Then, the supernatant was transferred in the centrifuge tube to a clean centrifuge tube. β -actin protein quantification kit was used to quantify protein concentration. The measured protein samples were stored at -80°C. In Western blot electrophoresis, the protein loading concentration was 50 μ g per well. After SDS-PAGE electrophoresis, the membrane was transferred and blocked. Proteins DAG1, LAMA2 and UTRN primary antibody (1: 500, anti-human, Thermo-Fisher, USA) were diluted to use concentration. The samples were incubated overnight on a shaker at 4°C. After washing with PBS, the samples were incubated with the secondary antibody (1: 1000, anti-human, Thermo-Fisher, USA) for 30 minutes at room temperature in the dark. Finally, a developer was used for development and photography.

Statistical analysis

The experimental results are expressed as means \pm standard deviations. Quantitative variables between two groups were compared by the Student's *t* test (normal distribution) or Mann-Whitney *U* test (non-normal distribution), and one-way or two-way ANOVA was used for comparing multiple groups. Pearson χ^2 test or Fisher's exact test

were used to compare qualitative variables. Pearman's analysis was conducted for correlation analysis. Statistical analysis was performed using the SPSS 22.0 software. The figures were produced with Origin 2021 and Adobe Illustrator 2020 software.

RESULTS

miR-548-3p had a significant regulatory effect on gene DAG1

The results of this experiment are shown in Fig. 1. It can be seen from the figure that miR-548-3p was significantly increased with the expression of DAG1-wild type (WT) ($p=0.0003$) and was remarkably decreased with the expression of DAG-mutant type (MUT) ($p=0.008$), indicating that miR-548-3p has a significant regulatory effect on the gene DAG1.

The results of immunofluorescence analysis are shown in Fig. 2. The green fluorescence in the figure was emitted by the DAG1 protein A. This experiment visually indicated the difference in DAG1 protein expression between the groups, and the experimental results were consistent with the results of the luciferase report experiment B.

Protein DAG1 induced malignant transformation of laryngeal carcinoma

The cell clone formation experiment is an important technical method used to detect cell proliferation, invasiveness, and sensitivity to killing factors. The clone formation rate reflects the two important traits of cell population dependence and proliferation ability. The results of the cell cloning experiment are shown in Fig. 3. It can be seen from the figure that when miR-548-3p was overexpressed, the number of cell clones increased significantly. When miR-548-3p was interfered, cell cloning was also inhibited. This indicated that the expression of miR-548-3p was positively correlated with the malignant degree of laryngeal cancer cells.

The results of the cell scratch test are shown in Fig. 4. Cell scratch is a typical meth-

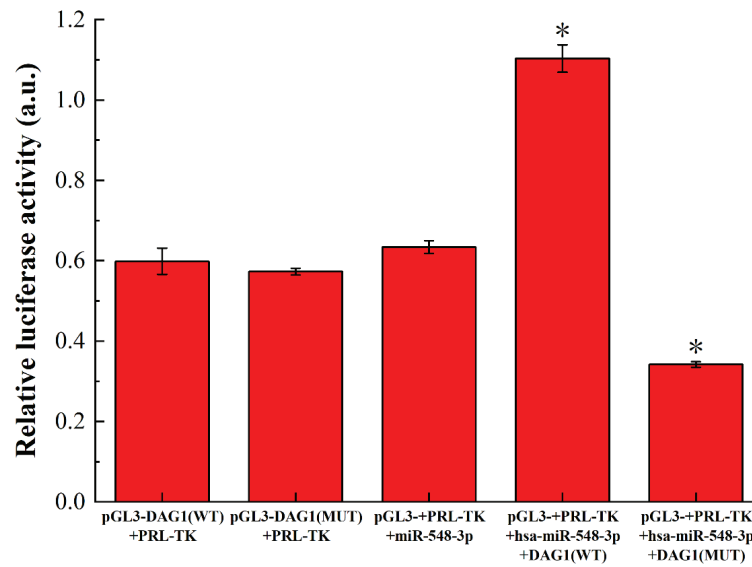


Fig. 1. The results of the dual luciferase detection experiment. miR-548-3p has a significant regulatory effect on gene DAG1 ($p < 0.05$).

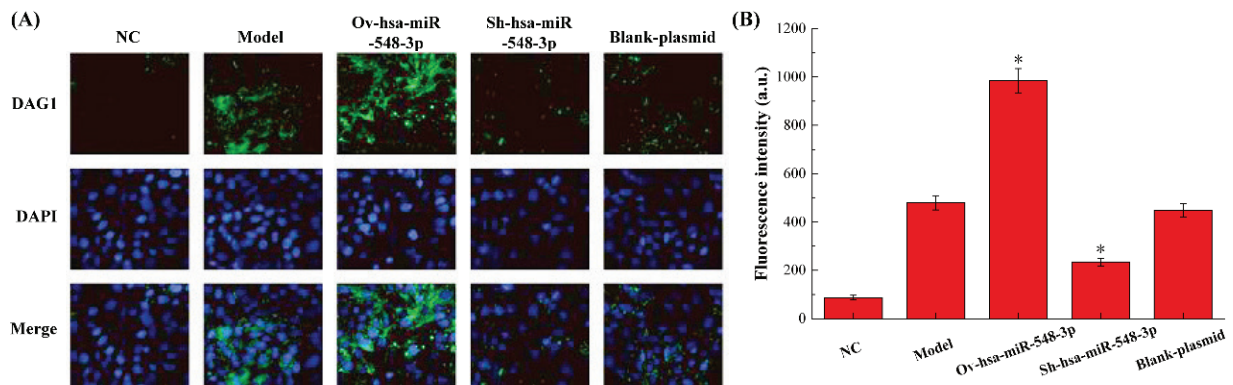


Fig. 2. The results of immunofluorescence analysis of the expression characteristics of DAG1. The expression of DAG1 protein in the Ov-miR-548-3p group and Sh-miR-548-3p group changed significantly ($p < 0.05$).

od used to detect the invasion ability of tumor cells. After 24 hours, the narrower the scratch, the stronger the cell invasion ability. From the results, we can know that overexpression of miR-548-3p significantly enhanced the migration ability of laryngeal cancer cells, while interference with the expression of miR-548-3p could inhibit the migration of laryngeal cancer cells. The blank plasmid had no effect on the expression of miR-548-3p, so the cell scratch of Model group and Blank-plasmid group was very serious.

The cell migration test is similar to the cell scratch test, which detects the strength

of cell invasion. The more cells, the stronger the tumor cell's malignant metastasis and invasion ability. The results of the cell migration test are shown in Fig. 5. Comparing the results of Fig. 4 and Fig. 5, we can find that the results of the cell migration test are consistent with the results of the cell scratch test. The three experiments of cell cloning, scratching and migration all reached a common conclusion: the overexpression of miR-548-3p enhanced the malignant transformation of laryngeal carcinoma, whereas miR-548-3p knockdown lead to inhibition of malignant transformation.

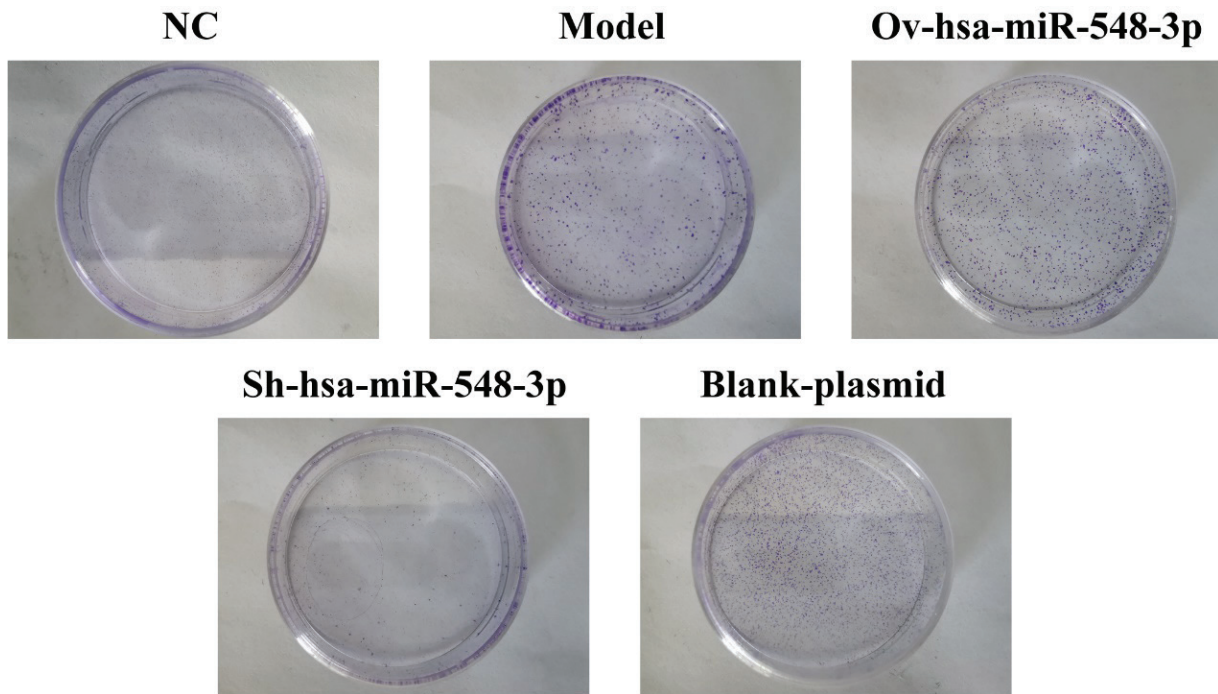


Fig. 3. The results of cell migration experiment. There was no cloning phenomenon in the NC group. The number of cell clones in the Ov-miR-548-3p group and Sh-miR-548-3p group was significantly different from that in the Model group ($p < 0.05$).

Plasmids had clear effects on the expression of miR-548-3p

The results of RT-PCR analysis are shown in Fig. 6. miR-548-3p is expressed in normal cells, so there was a certain amount of miR-548-3p in the NC group. The expression of miR-548-3p in the Model group increased significantly, and the expression of miR-548-3p increased and decreased greatly through the influence of overexpression plasmid and interference plasmid. This was positively correlated with DAG1 expression and the malignant degree of laryngeal cancer cells, confirming the correlation of the three.

Expression of the protein to be analyzed showed the same trend

The results of Western blot analysis are shown in Fig. 7. The protein DAG1 is involved in the assembly of laminin and basement

membrane, muscle membrane stability and cell survival. Its overexpression will improve the viability of cancer cells. The protein LAMA2 is the main component of the basement membrane and interacts closely with other extracellular matrix components. Its overexpression will increase the migration and invasion ability of cancer cells. UTRN is also a typical oncogene expressed protein. Its overexpression will increase the activity of cancer cells. Compared with model group, the expression of DAG1, LAMA2 and UTRN were significantly increased through overexpression of miR-548-3p plasmid, thus the expression of these proteins was obviously decreased with the treatment of interference plasmid. The expression of the above-mentioned proteins is positively correlated with malignant degree of laryngeal cancer cells, and the results of this experiment also show this.

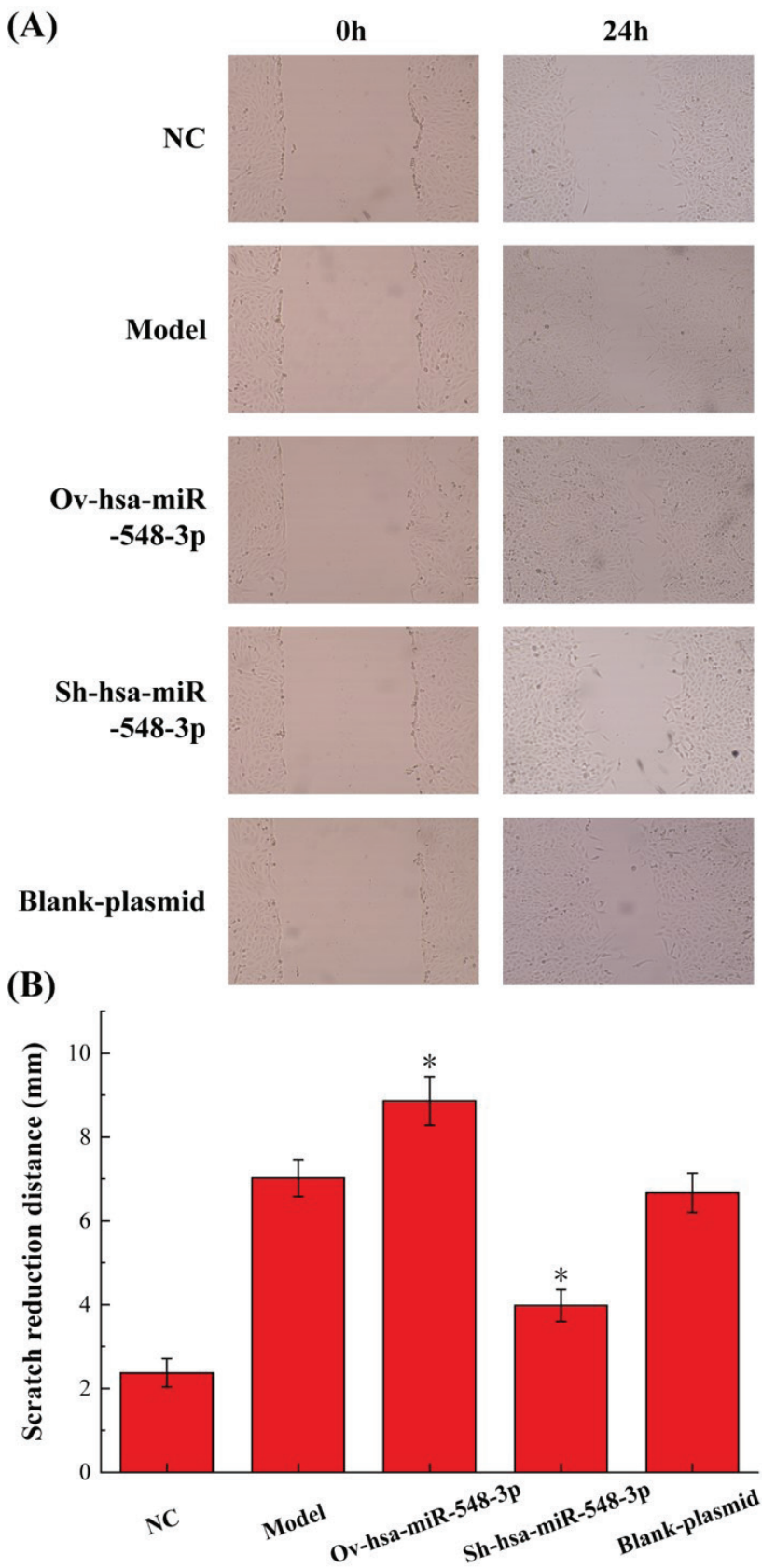


Fig. 4. The results of cell scratch test. The data of NC and Model group are consistent with the normal value.

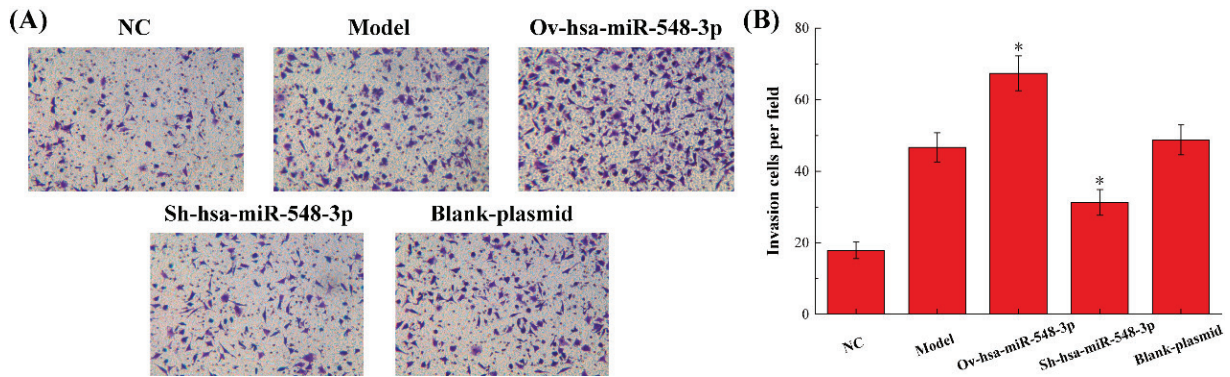


Fig. 5. The results of cell migration test. The data of NC and Model group are consistent with the normal value. The results of this experiment are consistent with the results of the cell scratch test.

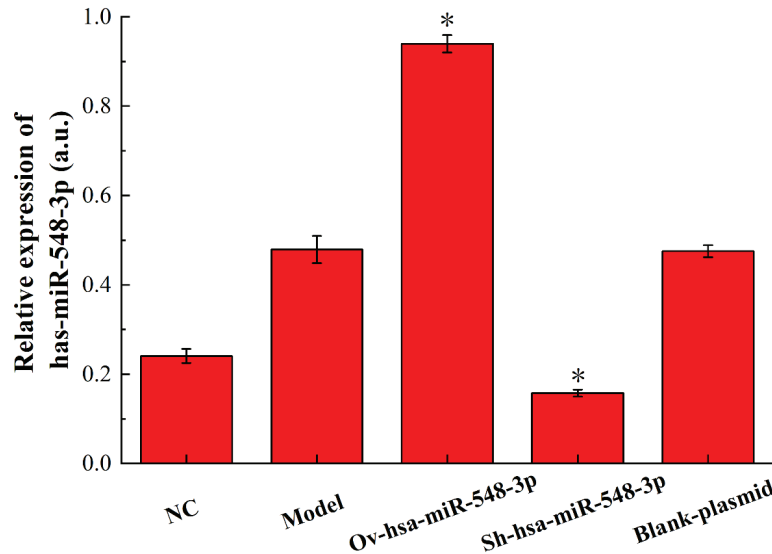


Fig. 6. The results of RT-PCR analysis. The results of this experiment are consistent with the results of the dual luciferase detection experiment and immunofluorescence analysis.

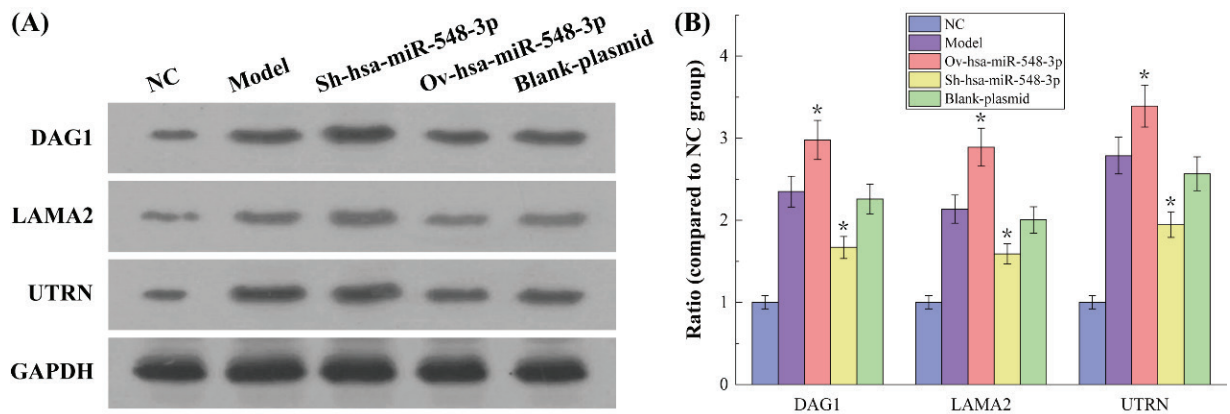


Fig. 7. The results of Western blot analysis. The data of NC and Model group are all consistent with the normal value. All the results of Ov-miR-548-3p group and Sh-miR-548-3p group were statistically different from the results of Model group ($p < 0.05$). (A) Original gel electrophoresis image. (B) The ratio of protein DAG1, LAMA2 and UTRN expression compared to NC group.

DISCUSSION

The essence of malignant tumors is abnormal cell proliferation, which locally invades surrounding normal tissues, and even metastasizes to other parts of the body through the circulatory system. From the perspective of molecular pathology, the root cause of malignant tumors is the accumulation of DNA mutations. The accumulation of mutations leads to the large expression of proteins that promote cell growth, making cell cycle control abnormal¹²⁻¹⁴. Primary laryngeal carcinoma is a kind of squamous cell carcinoma, and its malignancy ranks in the forefront of all cancers¹⁵⁻¹⁶. This project aims to promote the development of diagnosis and treatment of laryngeal cancer by identifying the underlying molecular mechanism of laryngeal cancer exacerbation.

miR-548-3p has been shown to be widely involved in the regulation of cancer genes. Luo et al pointed out that decrease of miR-548c-3p could upregulate the expression of ITGAV and contribute to tumor progression⁹. Observation of samples from oral squamous cell carcinoma patients found that miR-548-3p was increased in the OSCC group compared with the control group¹⁷. This work has indicated that miR-548-3p indirectly participates in the various processes of malignant transformation of laryngeal cancer by regulating the expression of DAG1.

In skeletal muscle, the DAG1 complex works as a transmembrane linkage between the extracellular matrix and the cytoskeleton. α -DAG1 is extracellular and binds to merosin α -2 laminin in the basement membrane, while β -DAG1 is a transmembrane protein and binds to dystrophin, which is a large rod-like cytoskeletal protein, absent in Duchenne muscular dystrophy patients. Dystrophin binds to intracellular actin cables. In this way, the DAG1 complex, which links the extracellular matrix to the intracellular actin cables, is thought to provide structural integrity in muscle tissues^{18,19}. The DAG1 complex is also known to serve as an agrin

receptor in muscle, where it may regulate agrin-induced acetylcholine receptor clustering at the neuromuscular junction. There is also evidence which suggests the function of DAG1 as a part of the signal transduction pathway because it is shown that Grb2, a mediator of the Ras-related signal pathway, can interact with the cytoplasmic domain of DAG1²⁰. DAG1 also plays an important role in the development and progression of cancer, and the regulation of DAG1 by miR-548-3p is particularly important in the progression of laryngeal cancer.

α -DAG1 is extracellular peripheral glycoprotein that acts as a receptor for extracellular matrix proteins containing laminin-G domains and receptor for laminin-2 (LAMA2) and agrin in peripheral nerve Schwann cells. It also acts as a receptor for laminin LAMA5^{21,22}. β -DAG1 is transmembrane protein that plays important roles in connecting the extracellular matrix to the cytoskeleton, which acts as a cell adhesion receptor in both muscle and non-muscle tissues. It is a receptor for both DMD and UTRN and, through these interactions, scaffolds axin to the cytoskeleton. β -DAG1 also functions in cell adhesion-mediated signaling and implicated in cell polarity^{23,24}. The direct action of DAG1 with the proteins LAMA2 and UTRN enhances the proliferation, migration and invasion ability of laryngeal cancer cells, thereby increasing the malignant degree of laryngeal cancer in all directions.

In summary, this experiment controlled the expression of miR-548-3p by adding different plasmids, and then controlled the expression of protein DAG1, and finally achieved the effect of controlling the malignant degree of laryngeal cancer. Cell cloning, scratching and migration experiments were used to determine the viability of laryngeal cancer cells. At the same time, by measuring the expression of cancer-related proteins, the regulatory effect of protein DAG1 on laryngeal cancer was further investigated. We reported the novel function of miR-548-3p in regulating laryngeal carcinoma cell mi-

gration and invasion through modulating the expression of DAG1. This provides a potential strategy for the diagnosis and treatment of laryngeal cancer. Nevertheless, more in-depth research is still needed to strengthen the conclusions of this experiment and laryngeal cancer samples are also needed to truly promote the conclusions of this work for the future diagnosis and treatment of lung cancer.

ACKNOWLEDGMENTS

We would like to acknowledge everyone for their helpful contributions in this paper.

Funding

Key project of the First Affiliated Hospital of Chengdu Medical College (No. CY-FY2018YB05).

Ethics approval and consent to participate

The research protocol has been reviewed and approved by the Ethical Committee and Institutional Review Board of The First Affiliated Hospital of Chengdu Medical College and written informed consent was obtained from all patients.

Competing interests

The authors declared that they have no competing interests.

Author's ORCID numbers

- Jia Chen: 0000-0002-9678-2523
- Yu Lin Zhou: 0000-0003-0034-093X
- Ke Wen: 0000-0002-0354-9985
- Shi Huang: 0000-0001-9811-4265
- Nan Hou: 0000-0001-9875-107X
- Ling Wang: 0000-0001-6367-2988
- Yi Wang: 0000-0001-5350-207X

Authors' contributions

Each author has made an important scientific contribution to the study and has assisted with the drafting or revising of the manuscript.

REFERENCES

1. Leemans CR, Snijders PJF, Brakenhoff RH. The molecular landscape of head and neck cancer. *Nat Rev Cancer* 2018;18(5):269-282.
2. Alshafi E, Begg K, Amelio I, Raulf N, Lucarelli P, Sauter T, Tavassoli M. Clinical update on head and neck cancer: molecular biology and ongoing challenges. *Cell Death Dis* 2019;10(8):540.
3. Hellquist H, French CA, Bishop JA, Coca-Pelaz A, Propst EJ, Paiva Correia A, Ngan BY, Grant R, Cipriani NA, Vokes D, Henrique R, Pardal F, Vizcaino JR, Rinaldo A, Ferlito A. NUT midline carcinoma of the larynx: an international series and review of the literature. *Histopathology* 2017;70(6):861-868.
4. Acero Brand FZ, Suter N, Adam JP, Faulques B, Maietta A, Soulières D, Blais N. Severe immune mucositis and esophagitis in metastatic squamous carcinoma of the larynx associated with pembrolizumab. *J Immunother Cancer* 2018;6(1):22.
5. Dai Y, Liang S, Dong X, Zhao Y, Ren H, Guan Y, Yin H, Li C, Chen L, Cui L, Banerjee S. Whole exome sequencing identified a novel DAG1 mutation in a patient with rare, mild and late age of onset muscular dystrophy-dystroglycanopathy. *J Cell Mol Med* 2019;23(2):811-818.
6. Sciandra F, Scicchitano BM, Signorino G, Bigotti MG, Tavazzi B, Lombardi F, Bozzi M, Sica G, Giardina B, Blaess S, Brancaccio A. Evaluation of the effect of a floxed Neo cassette within the dystroglycan (Dag1) gene. *BMC Res Notes* 2017;10(1):601.
7. Pathak HB, Zhou Y, Sethi G, Hirst J, Schilder RJ, Golemis EA, Godwin AK. A Synthetic lethality screen using a focused siRNA library to identify sensitizers to dasatinib therapy for the treatment of epithelial ovarian cancer. *PLoS One* 2015;10(12):e0144126.

8. **Liang T, Guo L, Liu C.** Genome-wide analysis of mir-548 gene family reveals evolutionary and functional implications. *J Biomed Biotechnol* 2012;2012:679563.
9. **Luo Z, Li D, Luo X, Li L, Gu S, Yu L, Yuanzheng Ma.** Decreased expression of miR-548c-3p in osteosarcoma contributes to cell proliferation via targeting ITGAV. *Cancer Biother Radiopharm* 2016;31(5):153-158.
10. **Rehbein G, Schmidt B, Fleischhacker M.** Extracellular microRNAs in bronchoalveolar lavage samples from patients with lung diseases as predictors for lung cancer. *Clin Chim Acta* 2015;450:78-82.
11. **Lorrai R, Gandolfi F, Boccaccini A, Ruta V, Possenti M, Tramontano A, Costantino P, Lepore R, Vittorioso P.** Genome-wide RNA-seq analysis indicates that the DAG1 transcription factor promotes hypocotyl elongation acting on ABA, ethylene and auxin signaling. *Sci Rep* 2018;8(1):15895.
12. **Ju Y, Wu X, Wang H, Li B, Long Q, Zhang D, Chen H, Xiao N, Li F, Zhang S, Yang S.** Genomic landscape of head and neck squamous cell carcinoma across different anatomic sites in Chinese population. *Front Genet* 2021;12:680699.
13. **He G, Pang R, Han J, Jia J, Ding Z, Bi W, Yu J, Chen L, Zhang J, Sun Y.** TINCR inhibits the proliferation and invasion of laryngeal squamous cell carcinoma by regulating miR-210/BTG2. *BMC Cancer* 2021;21(1):753.
14. **Chen Z, Zhang C, Chen J, Wang D, Tu J, Van Waes C, Saba NF, Chen ZG, Chen Z.** The proteomic landscape of growth factor signaling networks associated with FAT1 mutations in head and neck cancers. *Cancer Res* 2021;81(17):4402-4416.
15. **Bahig H, Lapointe A, Bedwani S, de Guise J, Lambert L, Filion E, Roberge D, Létourneau-Guillon L, Blais D, Ng SP, Nguyen-Tan PF.** Dual-energy computed tomography for prediction of loco-regional recurrence after radiotherapy in larynx and hypopharynx squamous cell carcinoma. *Eur J Radiol* 2019;110:1-6.
16. **Hughes RT, Beuerlein WJ, O'Neill SS, Porosnicu M, Lycan TW, Waltonen JD, Frizzell BA, Greven KM.** Human papillomavirus-associated squamous cell carcinoma of the larynx or hypopharynx: Clinical outcomes and implications for laryngeal preservation. *Oral Oncol* 2019;98:20-27.
17. **Garajei A, Parvin M, Mohammadi H, Allameh A, Hamidavi A, Sadeghi M, Emami A, Brand S.** Evaluation of the expression of miR-486-3p, miR-548-3p, miR-561-5p and miR-509-5p in tumor biopsies of patients with oral squamous cell carcinoma. *Pathogens* 2022;11(2):211.
18. **Perez-Ordoñez B.** Neuroendocrine carcinomas of the larynx and head and neck: challenges in classification and grading. *Head Neck Pathol* 2018;12(1):1-8.
19. **Reinhard JR, Lin S, McKee KK, Meinen S, Crosson SC, Sury M, Hobbs S, Maier G, Yurchenco PD, Rüegg MA.** Linker proteins restore basement membrane and correct LAMA2-related muscular dystrophy in mice. *Sci Transl Med* 2017;9(396).
20. **Leibovitz Z, Mandel H, Falik-Zaccai TC, Ben Harouch S, Savitzki D, Krajdjen-Haratz K, Gindes L, Tamarkin M, Lev D, Dobyns WB, Lerman-Sagie T.** Walker-Warburg syndrome and tectocerebellar dysraphia: A novel association caused by a homozygous DAG1 mutation. *Eur J Paediatr Neurol* 2018;22(3):525-531.
21. **Harris E, McEntagart M, Topf A, Lochmüller H, Bushby K, Sewry C, Straub V.** Clinical and neuroimaging findings in two brothers with limb girdle muscular dystrophy due to LAMA2 mutations. *Neuromuscul Disord* 2017;27(2):170-174.
22. **Sarkozy A, Foley AR, Zambon AA, Bönemann CG, Muntoni F.** LAMA2-related dystrophies: clinical phenotypes, disease biomarkers, and clinical trial readiness. *Front Mol Neurosci* 2020;13:123.
23. **Zhou S, Ouyang W, Zhang X, Liao L, Pi X, Yang R, Mei B, Xu H, Xiang S, Li J.** UTRN inhibits melanoma growth by suppressing p38 and JNK/c-Jun signaling pathways. *Cancer Cell Int* 2021;21(1):88.
24. **Wood CL, Suchacki KJ, van 't Hof R, Cawthorn WP, Dillon S, Straub V, Wong SC, Ahmed SF, Farquharson C.** A comparison of the bone and growth phenotype of mdx, mdx:Cmah(-/-) and mdx:Utrn (+/-) murine models with the C57BL/10 wild-type mouse. *Dis Model Mech* 2020;13(2).

Alteraciones en la producción de citocinas en respuesta a *Toxoplasma gondii* aparecen desde las etapas tempranas en pacientes co-infectados con VIH-1.

Edwin Escobar-Guevara^{1,2,3}, María de Quesada-Martínez⁴, Yhajaira Roldán-Dávila^{5,6}, Belkisyolé Alarcón de Noya⁷ y Miguel Alfonso-Díaz^{1,8}

¹Laboratorio de Inmunofisiología Celular, Escuela de Medicina “José María Vargas”, Universidad Central de Venezuela, Caracas, Venezuela.

²Cátedra de Inmunología, Escuela de Medicina “José María Vargas”, Universidad Central de Venezuela, Caracas, Venezuela.

³Laboratorio de Fisiopatología, Centro de Medicina Experimental, Instituto Venezolano de Investigaciones Científicas, Caracas, Venezuela.

⁴Cátedra de Fisiopatología, Escuela de Medicina “José María Vargas”, Universidad Central de Venezuela, Caracas, Venezuela.

⁵Servicio de Infectología, Hospital “José Ignacio Baldó”, El Algodonal, Caracas.

⁶Cátedra de Microbiología, Escuela de Medicina “José María Vargas”, Universidad Central de Venezuela, Caracas, Venezuela.

⁷Sección de Inmunología, Instituto de Medicina Tropical, Universidad Central de Venezuela, Caracas, Venezuela.

⁸Cátedra de Fisiología, Escuela de Medicina “José María Vargas”, Universidad Central de Venezuela, Caracas, Venezuela. Dirección Académica, Escuela Latinoamericana de Medicina “Salvador Allende”, Caracas, Venezuela.

Palabras clave: VIH-1; *Toxoplasma gondii*; respuesta inmunitaria; co-infección.

Resumen. Tanto el Virus de Inmunodeficiencia Humana-1 (VIH-1), como el protozoo *Toxoplasma gondii* son capaces de infectar al ser humano e invadir su sistema nervioso central (SNC). En individuos inmunocompetentes *T. gondii* causa infecciones crónicas, generalmente asintomáticas; sin embargo, la inmunodeficiencia asociada a etapas avanzadas de la infección por VIH-1, se relaciona con la pérdida del control de la infección parasitaria latente y enfermedades graves a nivel del SNC, como encefalitis toxoplásmica. Este trabajo tuvo como objetivo evaluar la evolución de la respuesta inmunitaria contra *T. gondii* en pacientes co-infectados con VIH-1, en distintas etapas de la infección viral. La respuesta contra *T. gondii* se evaluó a través de la producción *in vitro* de citocinas en respuesta a antígenos parasitarios, en individuos con serología positiva

para VIH-1 y negativa para *T. gondii* (P1), positiva para VIH-1 y *T. gondii* (P2), negativa para VIH-1 y *T. gondii* (C1) y negativa para VIH-1 y positiva para *T. gondii* (C2). Los pacientes (P1 y P2) se agruparon en *tempranos/asintomáticos* (P1A, P2A) o *tardíos/sintomáticos* (P1B/C, P2B/C) de acuerdo a su recuento de linfocitos T CD4+ en sangre periférica (>350 o <350 células/ μ L, respectivamente). La infección por VIH-1, desde etapas tempranas, se asoció con una producción de IL-2, TNF- α e IFN- γ en respuesta a *T. gondii* significativamente menor. Estos defectos pueden entorpecer la respuesta anti-*T. gondii* en pacientes co-infectados, aumentando la posibilidad de reactivación de las infecciones latentes, lo que representa un riesgo para la integridad y funcionalidad del SNC.

Alterations in the production of cytokines in response to *Toxoplasma gondii* appear from early stages in patients co-infected with HIV-1.

Invest Clin 2022; 63 (3): 218 – 234

Key words: HIV-1; *Toxoplasma gondii*; immune response; co-infection.

Abstract. Both HIV-1 and *Toxoplasma gondii* are able to invade central nervous system and affect its functionality. Advanced HIV-1 infection has been associated with defects in immune response to *T. gondii*, leading to reactivation of latent infections and the appearing of toxoplasmic encephalitis. This study evaluated changes in the immune response to *T. gondii* in different stages of HIV infection. Immune response to *T. gondii* was assessed studying cytokine production in response to parasite antigens in HIV-1-infected/*T. gondii*-non-infected (P1), HIV-1/*T. gondii* co-infected (P2), HIV-1-non-infected/*T. gondii*-non-infected (C1) and HIV-1-non-infected/*T. gondii*-infected (C2) individuals. Patients (P1 and P2) were divided in early/asymptomatic (P1A, P2A) or late/symptomatic (P1B/C, P2B/C) according to peripheral blood CD4+ T lymphocyte counts (>350 or <350/ μ L, respectively). The HIV-1 infection, from early/asymptomatic stages, was associated with significant lower production of IL-2, TNF- α and IFN- γ in response to *T. gondii*, when P2 patients were compared with C2 controls. These early defects may impair anti-parasitic response in co-infected patients, allowing to reactivation of parasitic latent infection, enhancing the risk of CNS damage and impairment of neurocognitive functions.

Recibido: 10-02-2022

Aceptado: 10-06-2022

INTRODUCCIÓN

Toxoplasma gondii es un parásito intracelular obligado, que causa una de las infecciones por protozoos más comunes en el ser humano¹, con una prevalencia global

promedio del 25,7 %². En individuos inmunocompetentes la infección por *T. gondii* es usualmente crónica y el parásito se mantiene en forma latente en el interior de quistes en los tejidos del hospedador, especialmente en el sistema nervioso central (SNC)^{3, 4}.

Durante la infección aguda los *taquizoítos* (forma del parásito en su fase de replicación rápida⁵) proliferan activamente en diversas células nucleadas que incluyen neuronas, astrocitos y otras poblaciones celulares en el cerebro⁶⁻⁸; luego, bajo la presión ejercida por la respuesta inmunitaria, los *bradizoítos* (forma del parásito en su etapa latente⁵), se ubican dentro de quistes en las células infectadas, estableciendo así la infección crónica. La producción de interferón gamma (IFN- γ), por células de la inmunidad innata⁹,¹⁰ y adaptativa^{11,12} es parte fundamental de la respuesta protectora contra *T. gondii*¹³ y conduce a la activación de macrófagos, con producción de factor de necrosis tumoral alfa (TNF- α) y a la expresión de sintasa inducible de óxido nítrico (iNOS)^{14,15}, creando un microambiente que lleva a la transformación de taquizoítos en bradizoítos¹⁶. La producción de IFN- γ también es primordial para evitar la reactivación de la infección crónica^{17,18}, y aunque diversas poblaciones celulares participan en la producción de esta citocina, el papel de los linfocitos T es esencial en la respuesta protectora efectiva^{11,12,19,20}. En esta respuesta inmunitaria contra *T. gondii*, la interleucina-2 (IL-2) media la expansión de los linfocitos T y de las células citotóxicas naturales (NK)²¹, mientras que la IL-10, con su papel modulador de la respuesta inmunitaria y su efecto anti-inflamatorio, se requiere para evitar el daño a los tejidos del hospedador^{22,23}. Es notable que los estados de inmunosupresión, como aquellos asociados con la infección avanzada por el virus de inmunodeficiencia humana-1 (VIH-1)^{24,25}, puedan conducir a la reactivación de las infecciones crónicas latentes, con ruptura de quistes y proliferación de taquizoítos, provocando una fuerte respuesta inflamatoria y la destrucción de tejidos del hospedador⁵. En el SNC la reactivación de la infección crónica usualmente se presenta como encefalitis toxoplásmica, una importante infección oportunista en pacientes con el síndrome de inmunodeficiencia adquirida (SIDA)²⁶. Debido a que la progresión de la infección por

VIH-1, así como el deterioro de la respuesta inmunitaria asociada con esta, son procesos graduales²⁷⁻²⁹, este estudio se enfocó en evaluar cómo se modifica la producción de citocinas en respuesta a *T. gondii* en las distintas etapas de la infección por VIH-1 en los pacientes co-infectados. La evaluación de la producción de citocinas hizo posible evidenciar alteraciones tempranas en la respuesta anti-*T. gondii*, que podrían disminuir la capacidad de control de las infecciones latentes, con aumento del riesgo de reactivación de la replicación parasitaria y de daños en la estructura y funcionalidad del SNC.

PACIENTES Y MÉTODOS

Se incorporaron en el estudio 34 individuos adultos seropositivos para VIH-1 y 14 seronegativos, pacientes del Servicio de Infectología del Hospital “José Ignacio Baldó” de Caracas, de la Sección de Inmunología del Instituto de Medicina Tropical y de la Escuela de Medicina “José María Vargas” de la Universidad Central de Venezuela en Caracas. Todos los participantes firmaron un consentimiento informado y el estudio fue aprobado por los comités de bioética de las instituciones participantes.

Los participantes fueron agrupados de la siguiente manera:

- **Grupo Control 1 (C1):** 5 individuos asintomáticos (2 hombres, 3 mujeres; 38 ± 4 años de edad), seronegativos para VIH-1 y *T. gondii*.
- **Grupo Control 2 (C2):** 9 individuos asintomáticos (6 hombres, 3 mujeres; 31 ± 12 años de edad), seronegativos para VIH-1 y seropositivos para *T. gondii*.
- **Grupo de Pacientes 1 (P1):** 13 individuos (8 hombres, 5 mujeres; 37 ± 9 años de edad), seropositivos para VIH-1 y seronegativos para *T. gondii*. Estos pacientes se agruparon en base a su recuento de linfocitos T CD4+ en sangre periférica de la siguiente manera:

***Grupo P1A (“temprano/asintomático”):** 5 individuos (2 hombres, 3 mujeres; 39 ± 6 años de edad), con recuentos de linfocitos T CD4+ en sangre periférica mayores a 350 células/ μ L.

***Grupo P1B/C (“tardío/sintomático”):** 8 individuos (6 hombres, 2 mujeres; 36 ± 10 años de edad), con recuentos de linfocitos T CD4+ en sangre periférica menores a 350 células/ μ L.

• Grupo de Pacientes 2 (P2): 21 individuos (16 hombres, 5 mujeres; 37 ± 10 años de edad), seropositivos para VIH-1 y *T. gondii*. Estos pacientes se agruparon en base a su recuento de linfocitos T CD4+ en sangre periférica de la siguiente manera:

***Grupo P2A (“temprano/asintomático”):** 8 individuos (5 hombres, 3 mujeres; 35 ± 10 años de edad), con recuentos de linfocitos T CD4+ en sangre periférica mayores a 350 células/ μ L.

***Grupo P2B/C (“tardío/sintomático”):** 13 individuos (11 hombres, 2 mujeres; 38 ± 9 años de edad), con recuentos de linfocitos T CD4+ en sangre periférica menores a 350 células/ μ L.

Criterios de exclusión y Toma de la muestra

La serología para VIH-1 se determinó por pruebas de ELISA y Western Blot, y la de *T. gondii* por ELISA (IgG e IgM) y avidéz. Los participantes no habían recibido terapia anti-retroviral ni anti-toxoplásmica al momento del estudio. Los criterios de exclusión incluían traumatismo cráneo-encefálico, enfermedades autoinmunes, enfermedades del SNC no asociadas a VIH-1, abuso o dependencia al alcohol o drogas ilícitas y el tratamiento con inmunosupresores. A cada participante se le tomó una muestra de sangre periférica, utilizando EDTA como anticoagulante, para la determinación de la carga viral de VIH-1,

las subpoblaciones de linfocitos T, el cultivo celular y la determinación de citocinas.

Cultivo de células mononucleares de sangre periférica

Las células mononucleares de sangre periférica (CMSP) fueron aisladas por gradiente de densidad (Histopaque 1077; Sigma-Aldrich) de las muestras de los pacientes. Las CMSP (1×10^5 células/pozo) fueron cultivadas por 72 horas, a una temperatura de 37°C y un ambiente con 5% de CO₂, por triplicado (tres pozos para cada condición), en placas de cultivo de 96 pozos (Nuncclone, Nunc), en un volumen final de 200 μ L/pozo, en medio de cultivo RPMI completo (RPMI 1640, Gibco; tampón HEPES 10 mM, Gibco; piruvato de sodio 1 mM, Sigma; aminoácidos no esenciales 1x, Gibco; L-glutamina 2 mM, Gibco; antibióticos: penicilina 100 U/mL, estreptomina 100 mg/mL, Gibco; suero bovino fetal 10%, Gibco), en tres condiciones básicas:

- **Medio:** CMSP cultivadas en condiciones basales, sin estimulación.
- **PHA:** CMSP cultivadas en presencia del estimulador policlonal fitohemaglutinina (PHA, Sigma, 5 μ g/mL)
- **SATg:** CMSP cultivadas en presencia de extracto de antígenos solubles de taquizoítos de *T. gondii* (SATg, provisto por Belkisyolé Alarcón de Noya, Instituto de Medicina Tropical, Universidad Central de Venezuela, Caracas; 1 μ g/mL). A las 72 horas de cultivo los sobrenadantes se recolectaron y almacenaron a -80°C, para ser posteriormente utilizados en la determinación de citocinas.

Determinación de citocinas

La concentración de IL-2, IL-10, TNF- α e IFN- γ en los sobrenadantes de cultivo se determinó por citometría de flujo (citómetro FACScalibur, Becton Dickinson) utilizando un estuche comercial (*Human Th1/Th2 Cytokine, Cytometric Bead Array*, Becton-Dickinson), siguiendo las instrucciones del fabricante.

te. Brevemente, los sobrenadantes de cultivo se incubaron simultáneamente con varias poblaciones de microperlas. Cada población de microperlas tenía una intensidad de fluorescencia particular, la cual podía evidenciarse con el detector FL3 del citómetro, y tenía en su superficie anticuerpos específicos para una de las citocinas (IL-2, IL-10, TNF- α o IFN- γ), de manera que podía “atrapar” dicha citocina del sobrenadante. Simultáneamente, las muestras fueron incubadas con anticuerpos detectores conjugados con ficoeritrina (PE), que eran específicos para cada una de las distintas citocinas y podían formar complejos o “sándwiches” con las citocinas unidas a las microperlas. La intensidad de fluorescencia de la PE medida en el detector FL2 del citómetro revelaba cuánta citocina se había unido a cada población de microperlas y, utilizando curvas de calibración, era posible conocer la concentración en las muestras.

Análisis estadístico

Para analizar los datos se utilizó el programa SigmaStat® (Jandel Scientific). Para estudiar las diferencias entre los grupos se utilizaron las pruebas *T de Student* o *U de Mann-Whitney*, según fuese apropiado. El coeficiente de *Pearson* se utilizó para analizar la correlación entre las variables. Las pruebas se consideraron estadísticamente significativas para valores de $p < 0,05$.

RESULTADOS

Producción de IL-2: Cuando las CMSP del grupo C2 (individuos con serología positiva para *T. gondii*, y negativa para VIH-1) fueron estimuladas durante 72 horas con antígenos de *T. gondii* (SATg), produjeron más IL-2 que cualquier otro grupo (Tablas 1 y 2), con diferencias estadísticamente significativas cuando se compararon con la producción de las mismas células cultivadas sin estimulación ($p=0,001$) (Fig. 1A, SATg vs. Medio). Por otra parte, la producción de IL-2 por las CMSP de los pacientes P2 (individuos con serología positiva para *T. gondii* y VIH-1) estimuladas con

SATg, fue significativamente menor que la del grupo C2, tanto en las etapas tempranas ($p=0,006$) como en las tardías ($p < 0,001$) (Fig. 1A, SATg). Ningún grupo incrementó su producción de IL-2 cuando las CMSP fueron cultivadas por 72 horas en presencia de PHA (Fig. 1A, PHA vs. Medio).

Producción de IL-10: La estimulación con PHA indujo una producción significativamente mayor de IL-10 en todos los grupos, al comparar con los cultivos no estimulados ($p \leq 0,029$) (Fig. 1B, PHA vs. Medio). Cuando las CMSP de los grupos C2 y P1A fueron cultivadas en presencia de SATg, produjeron cantidades significativamente mayores de IL-10 que el grupo C1 ($p=0,040$ y $p=0,016$, respectivamente) (Fig. 1B, SATg) y que sus respectivos cultivos en Medio ($p=0,001$ y $p=0,029$, respectivamente) (Fig. 1B, SATg vs. Medio). P2B/C, bajo estimulación con SATg, produjo una cantidad significativamente mayor de IL-10 que en cultivos no estimulados ($p=0,009$) (Fig. 1B, SATg vs. Medio). P1B/C evidenció producción espontánea de IL-10 en cultivos no estimulados, con valores significativamente mayores que P1A y C1 ($p=0,024$ y $p=0,042$, respectivamente) (Fig. 1B, Medio).

Producción de TNF- α : Bajo estimulación con PHA, todos los grupos produjeron una cantidad significativamente mayor de TNF- α que los cultivos en Medio ($p \leq 0,032$) (Fig. 1C, PHA vs. Medio), pero la producción de los pacientes (P1 y P2), en esta condición de estimulación policlonal, fue significativamente mayor que la de los grupos control (C1 y C2, respectivamente; $p \leq 0,029$) (Fig. 1C, PHA). C2, bajo estimulación con SATg, produjo una cantidad significativamente mayor de TNF- α que C1 ($p=0,004$) (Fig. 1C, SATg) y que su respectivo cultivo en Medio ($p=0,001$) (Fig. 1C, SATg vs. Medio). También, bajo estimulación con SATg, los dos grupos de pacientes P2 produjeron más TNF- α que los cultivos en Medio (significativo para P2B/C; $p=0,006$) (Fig. 1C, SATg vs. Medio) pero menos que C2 (significativo para P2A; $p=0,041$) (Fig. 1C, SATg).

Tabla 1
Determinación de Citocinas

C1	IL-2 (pg/mL) ^a			IL-10 (pg/mL) ^a			TNF- α (pg/mL) ^a			IFN- γ (pg/mL) ^a		
	Medio ^b	PHA ^c	STAg ^d	Medio	PHA	SATg	Medio	PHA	SATg	Medio	PHA	SATg
C1.1	26	23	35	9		36	3	5	2	43	51	25
C1.2	17	32	18		354		7		12	23	10821	43
C1.3	16	23	17	3	486	3	2	8	3	29	48	36
C1.4	17	18	19	9	750	9	3	8	2	27	41	36
C1.5	16	15	59	6	906	16	4	108	20	18	9047	
C2	IL-2 (pg/mL)			IL-10 (pg/mL)			TNF- α (pg/mL)			IFN- γ (pg/mL)		
	Medio	PHA	STAg	Medio	PHA	SATg	Medio	PHA	SATg	Medio	PHA	SATg
C2.1	14	11	196	4	1661	60	2	214	422	28	37819 ^e	41280 ^e
C2.2	13	11	143	3	750	32	3	49	82	38	8074	16263
C2.3	18	17	38	10	498	28	3	68	50	39	1483	3242
C2.4	19	19	188	3	1185	35	3	61	460	32	2391	37520 ^e
C2.5	22	16	98	10	800	49	6	473	54			
C2.6	18	16	57	25	1064	40	4	75		23	326	
C2.7	17	26	32		914	101	17			92	74225 ^e	37918 ^e
C2.8	18	22	24					527	286			
C2.9	25	20	20									
P1A	IL-2 (pg/mL)			IL-10 (pg/mL)			TNF- α (pg/mL)			IFN- γ (pg/mL)		
	Medio	PHA	STAg	Medio	PHA	SATg	Medio	PHA	SATg	Medio	PHA	SATg
P1A.1	18	28	16	18	208	35	3	757	3	31	5556	33
P1A.2	14	18	15									
P1A.3	19	15	19	3	2384	63	3	831	4	31	34044 ^e	37
P1A.4	20	17	20	13	1762	73	3	1100	7	39	34776 ^e	54
P1A.5	18	18	20	4	631	43	2	1441	21	33	25029 ^e	46
P1B/C	IL-2 (pg/mL)			IL-10 (pg/mL)			TNF- α (pg/mL)			IFN- γ (pg/mL)		
	Medio	PHA	STAg	Medio	PHA	SATg	Medio	PHA	SATg	Medio	PHA	SATg
P1B/C.1	18	18	17	19	2514	162	3	767	6	29	20010 ^e	42
P1B/C.2	19	19	17	105	1244	127	4	2310	4	33	22243 ^e	35
P1B/C.3	22	23	18	137	1984	20	36	1687	8	58	54711 ^e	45
P1B/C.4	17	23	16	6	344	7	5	411	7	33	10341	38
P1B/C.5	18	20	18	249	594	379	13	1134	33	35	7440	23
P1B/C.6	20	22	21	32	1618	167	5	316	7	56	769	48
P1B/C.7	16	19	15									
P1B/C.8	17	17		75	623		12	334		39		

Tabla 1. CONTINUACIÓN

P2A	IL-2 (pg/mL)			IL-10 (pg/mL)			TNF- α (pg/mL)			IFN- γ (pg/mL)		
	Medio	PHA	STAg	Medio	PHA	SATg	Medio	PHA	SATg	Medio	PHA	SATg
P2A.1	12	13	12	6	2787	14	7	943	4	41	8666	43
P2A.2	13	16	21									
P2A.3	21	21	24	5	780	10	8	580	62	110	50854 ^e	
P2A.4	22	21	21	5	1051	8	5	1274	7	43	3766	68
P2A.5	15	25	20	24	791	40	8	1163	18	37	71385 ^e	277
P2A.6	11	68	18	6	3428	185	2	3123	6	30	31280 ^e	42
P2A.7	21	18	23	17	187	17				58	27951 ^e	1964
P2A.8	17	22	21	34	182	142	20	884	135	18	11292	107

P2B/C	IL-2 (pg/mL)			IL-10 (pg/mL)			TNF- α (pg/mL)			IFN- γ (pg/mL)		
	Medio	PHA	STAg	Medio	PHA	SATg	Medio	PHA	SATg	Medio	PHA	SATg
P2B/C.1	12	12	12				8	1929	80	39	33603 ^e	102
P2B/C.2	20	19	20	3	1478	42	3	2364	10	31	35101 ^e	45
P2B/C.3	16	20	15	46	180	68	42	1335	94	36	20398 ^e	199
P2B/C.4	14	12	15	27	227	68				43	31413 ^e	65
P2B/C.5	19	15	27	5	507	11	4	203	206	24	32945 ^e	
P2B/C.6	18	18	21	9	824	17	2	52	4	37		39
P2B/C.7	17	19	18	11	473	129	6	874	76	40	12347	53
P2B/C.8	15	12	13	49	427	32	31	469	6	69	1436	21
P2B/C.9	17	13	17	38	668	171	10	3130	146	44	37327 ^e	1089
P2B/C.10	19	37	23	28	459	84						
P2B/C.11	18	21	18	39	1030	235	3	531	8	35	12381	61
P2B/C.12	19	20	24	16	231	22	5	1809	66	31	5201	887
P2B/C.13	18	19	21	16	1560	334	3	859	234	24	10802	774

^aLas concentraciones de IL-2, IL-10, TNF- α e IFN- γ se determinaron en el sobrenadante de los cultivos.

^bMedio: CMSP cultivadas por 72 horas en condiciones basales, sin estimulación.

^cPHA: CMSP cultivadas por 72 horas en presencia de fitohemaaglutinina (5 μ g/mL).

^dSATg: CMSP cultivadas por 72 horas en presencia de antígenos solubles de taquizoítos de *T. gondii* (1 μ g/mL).

^eLas concentraciones de IFN- γ mayores a 20.000 pg/mL se consideran más allá del rango de la curva de calibración.

Tabla 2
Producción de Citocinas – Dispersión de valores.

C1	IL-2			IL-10			TNF- α			IFN- γ		
	Medio	PHA	STAg	Medio	PHA	SATg	Medio	PHA	SATg	Medio	PHA	SATg
Mediana ^a	17	23	19	7	618	13	3	8	3	27	52	36
25% ^a	16	17	18	5	420	6	3	6	2	22	47	31
75% ^a	19	25	41	9	829	26	5	58	14	32	9491	40
n ^b	5	5	5	4	4	4	5	4	5	5	5	4
C2	IL-2			IL-10			TNF- α			IFN- γ		
	Medio	PHA	STAg	Medio	PHA	SATg	Medio	PHA	SATg	Medio	PHA	SATg
Mediana	18	17	58	7	914	41	3	75	82	35	5233	37520
25%	16	15	30	3	763	33	3	63	51	28	1484	13008
75%	19	21	155	11	1155	57	6	408	388	39	37819	38759
n	9	9	9	6	7	7	7	7	7	6	6	5
P1A	IL-2			IL-10			TNF- α			IFN- γ		
	Medio	PHA	STAg	Medio	PHA	SATg	Medio	PHA	SATg	Medio	PHA	SATg
Mediana	18	18	19	8	1196	53	3	966	5	32	29536	42
25%	17	17	16	3	419	39	2	794	3	31	15293	35
75%	19	21	20	16	2073	68	3	1271	14	36	34410	50
n	5	5	5	4	4	4	4	4	4	4	4	4
P1B/C	IL-2			IL-10			TNF- α			IFN- γ		
	Medio	PHA	STAg	Medio	PHA	SATg	Medio	PHA	SATg	Medio	PHA	SATg
Mediana	18	19	17	75	1244	144	5	767	7	35	15176	40
25%	17	18	17	22	602	20	4	353	6	33	7440	35
75%	19	22	18	129	1893	167	13	1549	8	52	22243	45
n	8	8	7	7	7	6	7	7	6	7	6	6
P2A	IL-2			IL-10			TNF- α			IFN- γ		
	Medio	PHA	STAg	Medio	PHA	SATg	Medio	PHA	SATg	Medio	PHA	SATg
Mediana	16	21	21	6	791	17	7	1053	13	41	27952	88
25%	13	17	19	5	335	11	5	884	6	32	9323	43
75%	21	24	22	22	2353	116	8	1274	62	54	45960	277
n	8	8	8	7	7	7	6	6	6	7	7	6
P2B/C	IL-2			IL-10			TNF- α			IFN- γ		
	Medio	PHA	STAg	Medio	PHA	SATg	Medio	PHA	SATg	Medio	PHA	SATg
Mediana	18	19	18	22	490	68	5	874	76	37	20398	65
25%	16	13	15	10	329	27	3	484	9	31	11189	47
75%	19	20	21	39	927	150	9	1899	133	41	33439	630
n	13	13	13	12	12	12	11	11	11	12	11	11

^aLos valores de mediana, percentil 25 y percentil 75 están expresados en pg/mL.

^bn=número de pacientes en cada grupo analizado.

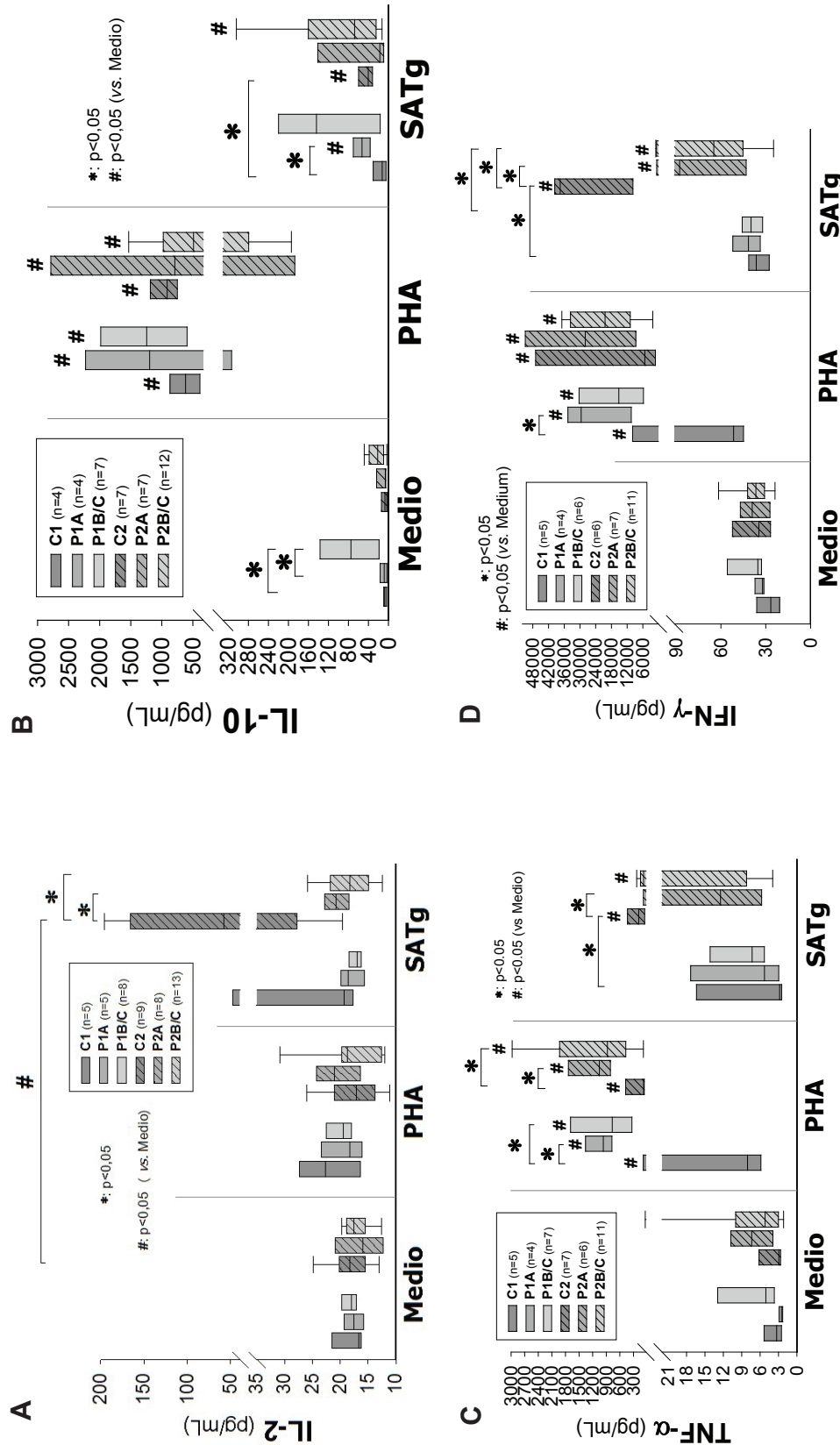


Fig. 1. Producción de Citocinas: Se representan las medianas (líneas horizontales), los percentiles 5 y 95 (cajas) y las líneas de error de las concentraciones (pg/mL) de IL-2 (A), IL-10 (B), TNF-α (C) e IFN-γ (D) en los sobrenadantes de cultivos de CMSP de individuos no infectados con VIH-1 con serología negativa (C1) o positiva (C2) para *T. gondii*; y de pacientes infectados con VIH-1, con serología negativa (P1) o positiva (P2) para *T. gondii*. Los pacientes (P1 y P2) se agruparon de acuerdo a su recuento de linfocitos T CD4+ en sangre periférica, en *tempranos/sintomáticos* (>350 células/ μ L: P1A y P2A) o *tardeos/sintomáticos* (<350 células/ μ L: P1B/C y P2B/C). Las CMSP fueron cultivadas por 72 horas en condiciones basales/sin estimulación (Medio), en presencia del estimulador policlonal fitohemaglutinina (PHA, 5 μ g/mL) o en presencia de antígenos solubles de taquizoítos de *T. gondii* (SATg, 1 μ g/mL). Los asteriscos representan diferencias estadísticamente significativas entre los grupos, el símbolo de número representa diferencias estadísticamente significativas entre un grupo en una condición determinada y su respectivo cultivo control sin estimulación (Medio).

Producción de IFN- γ : La estimulación con PHA indujo una producción significativamente mayor de IFN- γ en todos los grupos, al comparar con la condición *Medio* ($p \leq 0,029$) (Fig. 1D, *PHA* vs. *Medio*). Bajo estimulación con SATg, los grupos C2, P2A y P2B/C produjeron una cantidad significativamente mayor de IFN- γ que en *Medio* ($p=0,004$, $p=0,026$ y $p=0,006$, respectivamente) (Fig. 1D, *SATg* vs. *Medio*), y mayor que sus respectivos grupos C1, P1A y P1B/C, también bajo estimulación con SATg (significativo para C2 vs. C1: $p=0,016$; y para P2B/C vs. P1B/C: $p=0,024$) (Fig. 1D, *SATg*). Sin embargo, los pacientes P2A y P2B/C produjeron cantidades significativamente menores de IFN- γ que el grupo C2, en cultivos estimulados con SATg ($p=0,004$ y $p=0,002$, respectivamente) (Fig. 1D, *SATg*).

Correlaciones entre las producciones de citocinas: Cuando la producción de citocinas en respuesta a los antígenos de *T. gondii* (SATg) se analizó en los grupos de individuos seropositivos para el parásito (C2 y P2), se encontraron correlaciones positivas (Coeficiente de *Pearson*), estadísticamente significativas, entre la producción de IFN- γ y la producción de IL-2 ($p < 0,001$, $n=25$; Fig. 2A), entre la producción de TNF- α y la producción de IL-2 ($p < 0,001$, $n=23$; Fig. 2B), y entre la producción de TNF- α y la producción de IFN- γ ($p < 0,001$, $n=20$; Fig. 2C).

DISCUSIÓN

Los individuos inmunocompetentes son capaces de controlar la infección por *T. gondii* induciendo una respuesta inmunitaria celular temprana y fuerte^{30,32}. En esta respuesta el IFN- γ es el principal mediador de resistencia del hospedador¹³, al estimular la expresión de diferentes moléculas efectoras, tales como las trifosfatasa de guanosina inducibles por IFN (GTPasas), la sintasa inducible de óxido nítrico (iNOS) y la indolamina-2,3-dioxigenasa (IDO)^{33,34}, las cuales conducen a vigorosas respuestas inmunitarias celulares autónomas^{35,36}, con supresión

del crecimiento y/o muerte del parásito dentro de las células infectadas³³⁻³⁶. El TNF- α también juega un papel fundamental en la respuesta protectora, particularmente en el cerebro^{14,15,37-39}, al disminuir la entrada del parásito a las células, detener su proliferación e inducir su muerte. La IL-10, por su parte, ejerce un efecto regulador, al prevenir la inmunopatología potencialmente letal^{22,23,31}. Así pues, el perfil de citocinas producido en respuesta a *T. gondii*, es crítico para lograr un control efectivo de la infección, pero sin causar daños al propio hospedador^{30,32}. En los experimentos descritos en este trabajo, los individuos seropositivos para *T. gondii*, pero seronegativos para VIH-1, produjeron cantidades significativamente mayores de IFN- γ , TNF- α e IL-10 en respuesta a los antígenos parasitarios, que los individuos seronegativos para *T. gondii* y VIH-1. Por lo tanto, la producción de IFN- γ , TNF- α e IL-10, de acuerdo a los métodos aquí descritos, permite claramente distinguir entre la respuesta inmunitaria contra *T. gondii* de individuos asintomáticos seropositivos para este parásito y la de individuos seronegativos.

Por su parte, la IL-2 es importante para la función y regulación de los linfocitos T^{21,40,41} y su producción bajo estimulación con SATg, presentó correlaciones positivas con las producciones de IFN- γ y de TNF- α en los individuos seropositivos para *T. gondii*. Sin embargo, los pacientes infectados con VIH-1 y serología positiva para *T. gondii*, desde etapas tempranas/asintomáticas, produjeron cantidades significativamente menores de IL-2, TNF- α e IFN- γ en respuesta a los antígenos parasitarios que las del grupo seropositivo para *T. gondii*, pero seronegativos para VIH-1, lo cual relaciona a la infección por VIH-1 con alteraciones tempranas (además de las ya descritas en etapas avanzadas) en la respuesta contra *T. gondii*. Estas alteraciones tempranas podrían comprometer la capacidad de control de la infección latente^{13-18,37-39}, aumentando el riesgo de reactivación de la replicación parasitaria, aunque fuese de manera limitada^{42,43}, es decir, no

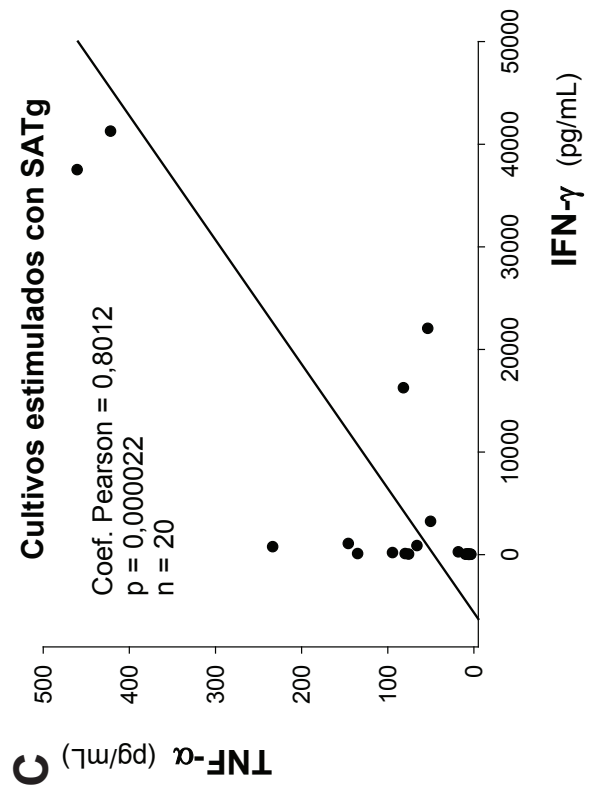
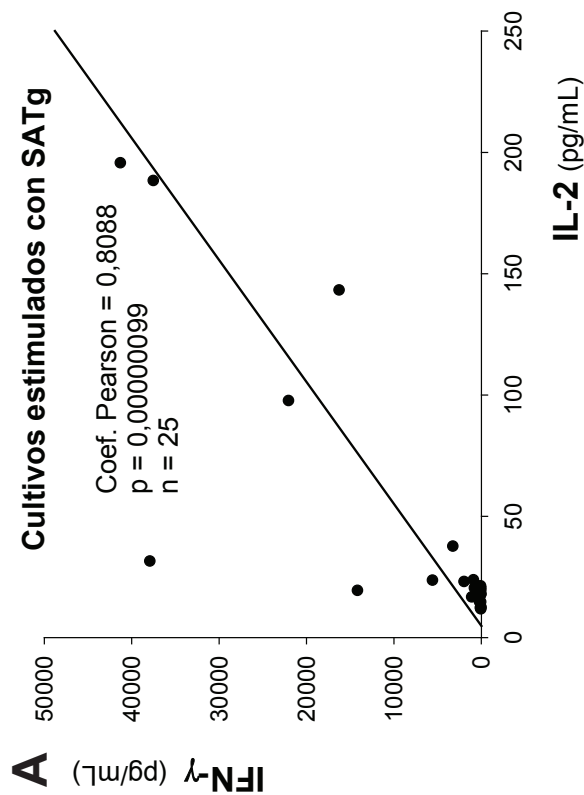
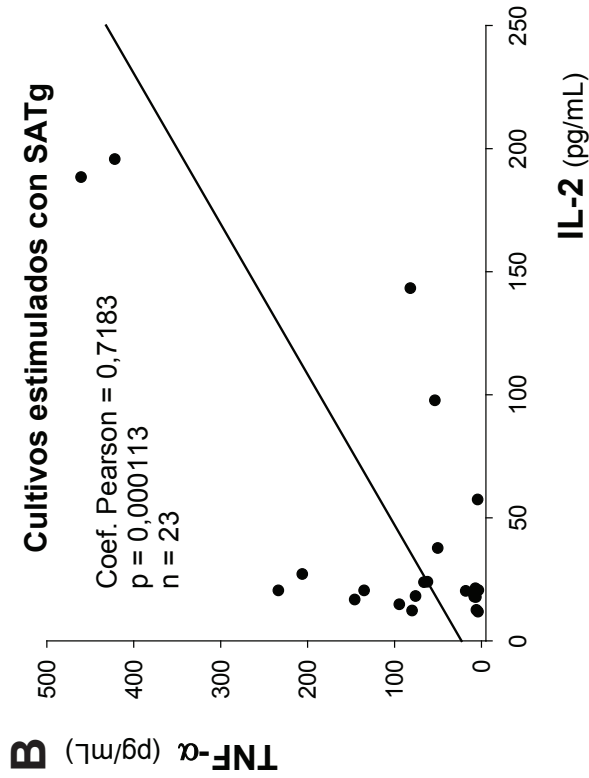


Fig. 2. Correlación entre Citocinas: Se muestran las correlaciones (Coeficiente de Pearson) entre las producciones de IFN- γ e IL-2 (A), TNF- α e IL-2 (B) y TNF- α e IFN- γ (C), bajo estimulación con SATg, en individuos seropositivos para *T. gondii*.

en una magnitud suficiente para producir encefalitis toxoplásmica (asociada sólo con etapas avanzadas de la infección por VIH-1), pero con la posibilidad de provocar daños acumulativos a nivel del SNC y de deteriorar las funciones neurocognitivas, incluso antes de llegar a etapas francamente sintomáticas. En congruencia con este razonamiento, la evaluación neurofisiológica de estos mismos grupos^{44, 45} evidenció que los pacientes infectados con VIH-1 y serología positiva para *T. gondii* presentaron deficiencias de la memoria a corto plazo^{46, 47}, del procesamiento cognitivo de estímulos visuales y auditivos^{48, 49} y de las funciones ejecutivas del lóbulo frontal^{50, 51}, significativamente mayores que las de los pacientes infectados con VIH-1 y serología negativa para *T. gondii*, desde etapas tempranas de la infección por VIH-1, sugiriendo que la neurotoxicidad está aumentada^{44, 45}, lo cual refuerza la relevancia que puede tener la pérdida gradual del control de tales infecciones latentes, al comprometer la función del sistema nervioso central, adicionalmente al deterioro que pueda generar el propio VIH-1^{52, 53}.

Con respecto a la IL-10, los resultados de este trabajo asociaron la infección por VIH-1 con producción “inespecífica”, ya que los pacientes infectados con VIH-1 y serología negativa para *T. gondii* la produjeron en respuesta a la estimulación con SATg; así como con producción “espontánea” en etapas tardías, pues este grupo produjo cantidades significativamente elevadas en cultivos sin estimulación. La IL-10 es una importante citocina reguladora^{54, 55}, cuya producción ha sido reportada como aumentada en pacientes infectados con VIH-1^{56, 57}. Este aumento se ha asociado con la inhibición de la respuesta específica contra el virus⁵⁶⁻⁵⁹, pero también con el control de la replicación viral⁶⁰⁻⁶², de manera que es difícil definir si el efecto de la IL-10 en la infección por VIH-1 es perjudicial o protector^{63, 64}. Existen diversos reportes de situaciones en las cuales la IL-10 puede presentar efectos estimuladores de la respuesta inmunitaria o pro-inflama-

torios^{65, 66}, y de otras circunstancias en las cuales se puede presentar una resistencia al efecto anti-inflamatorio de la IL-10^{65, 67}, todo lo cual hace más compleja la interpretación de la acción de la IL-10 en un contexto determinado.

Por otra parte, la infección por VIH-1 se asoció con mayor producción de TNF- α bajo estimulación con PHA, ya que todos los pacientes infectados con VIH-1 produjeron cantidades significativamente mayores que sus respectivos grupos controles sin infección por VIH-1, en esta condición de estimulación policlonal, lo cual asocia a la infección por VIH-1 con la inducción de un ambiente pro-inflamatorio⁶⁸. Es notable cómo la infección por VIH-1 puede estar asociada simultáneamente con el aumento en la producción de citocinas reguladoras (IL-10) y pro-inflamatorias (TNF- α), y cómo la co-infección con *T. gondii* puede aumentar la complejidad de esta red de citocinas⁶⁹.

También fue notable que los pacientes infectados con VIH-1 fuesen capaces de producir IFN- γ , TNF- α e IL-10 bajo estimulación con PHA, en todas las etapas de la infección viral, mostrando que mantenían esta capacidad, aun cuando presentaran defectos en la producción de estas citocinas en respuesta los antígenos parasitarios. De manera que, incluso en etapas avanzadas, los pacientes son capaces de responder con producción de citocinas dadas las condiciones apropiadas, lo cual es una oportunidad para la intervención terapéutica^{70, 71}.

Con relación a la IL-2, es importante recordar que esta citocina se produce muy rápido, es decir, pocos minutos después de la estimulación antigénica⁷². De manera que el hecho de que sólo el grupo seropositivo para *T. gondii*, pero seronegativo para VIH-1, presentara aumentos significativos en la concentración de IL-2 bajo estimulación con SATg, muestra que la producción fue lo suficientemente prolongada y/o lo suficientemente elevada como para ser detectada después de 72 horas de cultivo, mientras que la producción en los pacientes co-infectados no fue tan prolongada o tan elevada. Valdría la pena estudiar estas mismas respues-

tas inmunitarias en pacientes co-infectados tratados con medicamentos anti-*T. gondii*, a fin de evaluar si estos hallazgos se revierten, al menos parcialmente, con el tratamiento antiparasitario.

Así pues, desde etapas tempranas los pacientes co-infectados presentaron defectos en la producción de citocinas que podrían alterar el control de la replicación del parásito en el SNC, con la posibilidad de causar daños al tejido y deterioro de la función. El hecho de que en su evaluación neurocognitiva^{44, 45} estos mismos pacientes hayan presentado mayores defectos que aquellos con serología negativa para *T. gondii*, sugiere fuertemente una asociación entre los efectos tempranos sobre la respuesta inmunitaria y el aumento de las alteraciones neurocognitivas en los pacientes co-infectados, incluso en etapas “asintomáticas”. Estos resultados invitan a reconsiderar lo que es realmente la etapa “asintomática”. De hecho, varios grupos están reevaluando el concepto de que la infección crónica por *T. gondii* sea realmente “asintomática”, debido a la gran cantidad de evidencias que sugieren que esta está asociada con alteraciones neuropsiquiátricas y conductuales^{4, 73-76}. Más aún, los resultados de este trabajo enfatizan la importancia del diagnóstico temprano y el tratamiento precoz para preservar la integridad de la respuesta inmunitaria y evitar el deterioro del SNC y sus funciones⁷⁷⁻⁷⁹, y así mejorar la calidad de vida de los pacientes.

AGRADECIMIENTO

Varios miembros de nuestros laboratorios participaron en el desarrollo de este trabajo atendiendo a los pacientes, procesando y analizando muestras clínicas: Ydelys Fuentes, Riward Campelo, Alexandra Díaz, Josibel Camacho, Alexandra Rodríguez, Gustavo Rico, José Carrero, Edwin Díaz, Wolfgang Vivas y Eduardo Navarro.

Financiamiento

Este trabajo recibió financiamientos del FONACIT (G-2005000823) y del Insti-

tuto Venezolano de Investigaciones Científicas (IVIC-2009000441). EEEG recibió becas doctorales del FONACIT y el IVIC. Las instituciones que financiaron el trabajo no tuvieron parte en el diseño del estudio, en la recolección y análisis de datos, en la decisión de publicar o en la preparación del manuscrito.

Conflicto de Intereses

Los autores declaran no tener conflicto de intereses.

Contribución de los Autores

- Investigador principal y Supervisión: MAAD.
- Conceptualización y Metodología: MAAD, MEDQM, YBRD, BAN, EEEG.
- Recursos: BAN (SATg, selección de pacientes), YBRD (selección de pacientes), MAAD (selección de pacientes).
- Realización de los experimentos/Investigación: EEEG, MAAD.
- Análisis de Datos: EEEG, MAAD.
- Escritura - Preparación del manuscrito original: EEEG.
- Escritura - Revisión y edición del manuscrito: EEEG, MAAD, BAN, MEDQM, YBRD.

Número ORCID de los autores

- Edwin Eliel Escobar-Guevara: 000-0003-3093-5491
- María Esther de Quesada-Martínez: 0000-0003-2994-4788
- Yhajaira Beatriz Roldán-Dávila: 0000-0002-8742-1590
- Belkisyolé Alarcón de Noya: 0000-0002-3139-7480
- Miguel Antonio Alfonzo-Díaz: 0000-0002-3029-5191

REFERENCIAS

1. **Ferguson DJP.** *Toxoplasma gondii*: 1908-2008, homage to Nicolle, Manceaux and Splendore. Mem Inst Oswaldo Cruz 2009; 104(2): 133-148.
2. **Molan A, Nosaka K, Hunter M, Wang W.** Global status of *Toxoplasma gondii* infection: systematic review and prevalence snapshots. Trop Biomed 2019; 36(4): 898-925.
3. **Remington JS, Cavanaugh EN.** Isolation of the encysted form of *Toxoplasma gondii* from human skeletal muscle and brain. N Engl J Med 1965; 273(24):1308-10.
4. **Carruthers VB, Suzuki Y.** Effects of *Toxoplasma gondii* infection on the brain. Schizophr Bull 2007; 33(3):745-751.
5. **Dubey JP, Lindsay DS, Speer CA.** Structures of *Toxoplasma gondii* tachyzoites, bradyzoites, and sporozoites and biology and development of tissue cysts. Clin Microbiol Rev 1998; 11(2):267-299.
6. **Suzuki Y.** Immunopathogenesis of Cerebral Toxoplasmosis. J Infect Dis 2002; 186(Suppl 2):S234-240.
7. **Ghatak NR, Sawyer DR.** A morphologic study of opportunistic cerebral toxoplasmosis. Acta Neuropathol 1978; 42(3): 217-221.
8. **Halonen SK, Lyman WD, Chiu FC.** Growth and development of *Toxoplasma gondii* in human neurons and astrocytes. J Neuropathol Exp Neurol 1996; 55(11):1150-1156.
9. **Yarovinsky F.** Innate immunity to *Toxoplasma gondii* infection. Nat Rev Immunol 2014; 14:109-121.
10. **Lopez-Yglesias AH, Burger E, Camanzo E, Martin AT, Araujo AM, Kwok SF, Yarovinsky F.** T-bet dependent ILC1- and NK cell-derived IFN- γ mediates cDC1-dependent host resistance against *Toxoplasma gondii*. PLoS Pathog 2021; 17(1): e1008299.
11. **Gazzinelli RT, Hakim FT, Hieny S, Shearer GM, Sher A.** Synergistic role of CD4+ and CD8+ T lymphocytes in IFN- γ production and protective immunity induced by an attenuated *Toxoplasma gondii* vaccine. J Immunol 1991; 146(1):286-292.
12. **Gazzinelli R, Xu Y, Hieny S, Cheever A, Sher A.** Simultaneous depletion of CD4+ and CD8+ T lymphocytes is required to reactivate chronic infection with *Toxoplasma gondii*. J Immunol 1992; 149(1):175-180.
13. **Suzuki Y, Orellana MA, Schreiber RD, Remington JS.** Interferon- γ : the major mediator of resistance against *Toxoplasma gondii*. Science 1988; 240(4851):516-518.
14. **Langermans JA, Van der Hulst ME, Nibbering PH, Hiemstra PS, Fransen L, Van Furth R.** IFN- γ -induced L-arginine-dependent toxoplasmastatic activity in murine peritoneal macrophages is mediated by endogenous tumor necrosis factor- α . J Immunol 1992; 148(2):568-574.
15. **Gazzinelli RT, Eltoun I, Wynn TA, Sher A.** Acute cerebral toxoplasmosis is induced by in vivo neutralization of TNF- α and correlates with the down-regulated expression of inducible nitric oxide synthase and other markers of macrophage activation. J Immunol 1993; 151(7):3672-3681.
16. **Bohne W, Heesemann J, Gross U.** Reduced replication of *Toxoplasma gondii* is necessary for induction of bradyzoite-specific antigens: a possible role for nitric oxide in triggering stage conversion. Infect Immun 1994; 62(5):1761-1767.
17. **Suzuki Y, Conley FK, Remington JS.** Importance of endogenous IFN- γ for prevention of toxoplasmic encephalitis in mice. J Immunol 1989; 143(6):2045-2050.
18. **Wang X, Kang H, Kikuchi T, Suzuki Y.** Gamma interferon production, but not perforin-mediated cytolytic activity, of T cells is required for prevention of toxoplasmic encephalitis in BALB/c mice genetically resistant to the disease. Infect Immun 2004; 72(8):4432-4438.
19. **Sturge CR, Felix Yarovinsky F.** Complex immune cell interplay in the gamma interferon response during *Toxoplasma gondii* infection. Infect Immun 2014; 82(8):3090-3097.
20. **Kang H, Suzuki Y.** Requirement of non-T cells that produce gamma interferon for prevention of reactivation of *Toxoplasma gondii* infection in the brain. Infect Immun 2001; 69(5):2920-2927.
21. **Kupz A, Pai S, Giacomini PR, Whan JA, Walker RA, Hammoudi PM, Smith NC, Miller CM.** Treatment of mice with S4B6 IL-2 complex prevents lethal toxoplasmosis via IL-12- and IL-18-dependent interferon- γ production by non-CD4 immune cells. Sci Rep 2020; 10(1):13115.

22. **Gazzinelli RT, Wysocka M, Hieny S, Schar-ton-Kersten T, Cheever A, Kühn R, Müller W, Trinchieri G, Sher A.** In the absence of endogenous IL-10, mice acutely infected with *Toxoplasma gondii* succumb to a lethal immune response dependent on CD4+ T cells and accompanied by overproduction of IL-12, IFN- γ and TNF- α . *J Immunol* 1996; 157(2):798-805.
23. **Wilson EH, Wille-Reece U, Dzierszinski F, Hunter CA.** A critical role for IL-10 in limiting inflammation during toxoplasmic encephalitis. *J Neuroimmunol* 2005; 165(1):63-74.
24. **Wang ZD, Liu HH, Ma ZX, Ma HY, Li ZY, Yang ZB, Zhu XQ, Xu B, Wei F, Liu Q.** *Toxoplasma gondii* infection in immunocompromised patients: A systematic review and meta-analysis. *Front Microbiol* 2017; 8:389.
25. **Wong SY, Remington JS.** Biology of *Toxoplasma gondii*. *AIDS* 1993; 7(3):299-316.
26. **Luft BJ, Remington JS.** AIDS commentary. Toxoplasmic encephalitis. *J Infect Dis* 1988; 157:1-6.
27. **Boasso A, Shearer GM, Chougnat C.** Immune dysregulation in human immunodeficiency virus infection: know it, fix it, prevent it? *J Intern Med* 2009; 265(1):78-96.
28. **De Boer RJ.** Time scales of CD4+ T cell depletion in HIV infection. *PLoS Med* 2007; 4(5):e193.
29. **Roederer M, Dubs JG, Anderson MT, Raju PA, Herzenberg LA, Herzenberg LA.** CD8 naïve cell counts decrease progressively in HIV-infected adults. *J Clin Invest* 1995; 95:2061-2066.
30. **Denkers EY, Gazzinelli RT.** Regulation and function of T-cell-mediated immunity during *Toxoplasma gondii* infection. *Clin Microbiol Rev* 1998; 11(4): 569-588.
31. **Yap GS, Sher A.** Cell-mediated immunity to *Toxoplasma gondii*: initiation, regulation and effector function. *Immunobiology* 1999; 201(2):240-247.
32. **Tait ED, Christopher A, Hunter CA.** Advances in understanding immunity to *Toxoplasma gondii*. *Mem Inst Oswaldo Cruz* 2009; 104(2):201-210.
33. **Sasai M, Pradipta A, Yamamoto M.** Host immune responses to *Toxoplasma gondii*. *Int Immunol* 2018; 30(3):113-119.
34. **Fisch D, Clough B, Frickel EM.** Human immunity to *Toxoplasma gondii*. *PLoS Pathog* 2019; 15(12): e1008097.
35. **MacMicking JD.** Interferon-inducible effector mechanisms in cell-autonomous immunity. *Nat Rev Immunol* 2012; 12(5):367-82.
36. **Randow F, MacMicking JD, James LC.** Cellular self-defense: how cell-autonomous immunity protects against pathogens. *Science* 2013; 340(6133):701-706.
37. **Chao CC, Gekker G, Hu S, Peterson PK.** Human microglial cell defense against *Toxoplasma gondii*. The role of cytokines. *J Immunol* 1994; 152(3):1246-1252.
38. **Däubener W, Remscheid C, Nockemann S, Pilz K, Seghrouchni S, Mackenzie C, Hadding U.** Anti-parasitic effector mechanisms in human brain tumor cells: role of interferon- γ and tumor necrosis factor- α . *Eur J Immunol* 1996; 26(2):487-492.
39. **Janssen R, van Wengen A, Verhard E, De Boer T, Zomerdijk T, Ottenhoff THM, Van Dissel JT.** Divergent role for TNF- α in IFN- γ -induced killing of *Toxoplasma gondii* and *Salmonella typhimurium* contributes to selective susceptibility in patients with partial IFN- γ receptor 1 deficiency. *J Immunol* 2002; 169(7):3900-3907.
40. **Ross SH, Cantrell DA.** Signaling and function of IL-2 in T lymphocytes. *Annu Rev Immunol* 2018; 36:411-433.
41. **Bachmann MF, Oxenius A.** Interleukin 2: from immunostimulation to immunoregulation and back again. *EMBO Rep* 2007; 8(12):1142-1148.
42. **Escobar Guevara EE, Alfonso Díaz MA, Fernández-Mestre M, Camacho Velásquez JC, Roldán Dávila YB, Alarcón de Noya B, De Quesada ME.** HIV/*Toxoplasma gondii* co-infected patients produce lower levels of IFN- γ in response to *T. gondii* antigens, even in the asymptomatic stage of viral infection. 5th IAS Conference on HIV Pathogenesis, Treatment and Prevention, Cape Town 2009; Abstract no. WELBA104. ([http://www.iasociety.org/Default.aspx? pageId=11&abstractId=200722748](http://www.iasociety.org/Default.aspx?pageId=11&abstractId=200722748)).
43. **Escobar-Guevara EE, Alfonso-Díaz MA, Camacho-Velásquez JC, Roldán-Dávila YB, Alarcón de Noya B.** HIV/*Toxoplasma gondii*

- coinfectad patients modify their IL-2 and IL-10 production in response to *T. gondii* and HIV antigens, even in the early stage of viral infection. 9th Latin American Congress of Immunology, Chile 2009; Abstract No. 354.
44. **De Quesada ME, Marín H, Fuentes Alvarado YJ, Escobar Guevara EE, Roldán Dávila YB, Alfonzo Díaz MA.** Disorders on attention, short-term memory and executive functions in HIV/*Toxoplasma gondii* co-infected patients, in the asymptomatic stage of viral infection. 6th IAS Conference on HIV Pathogenesis, Treatment and Prevention, Rome 2011; Abstract no. CDB224. (<http://www.iasociety.org/Default.aspx?pageId=11&abstractId=200742783>).
 45. **De Quesada ME, Fuentes Alvarado YJ, Marín H, Escobar Guevara EE, Roldán Dávila YB, Alfonzo Díaz MA.** Visual and auditory event related potentials in HIV/*Toxoplasma gondii* co-infected patients, in the asymptomatic stage of viral infection. 6th IAS Conference on HIV Pathogenesis, Treatment and Prevention, Rome 2011; Abstract no. CDB225. (<http://www.iasociety.org/Default.aspx?pageId=11&abstractId=200742799>).
 46. **Sternberg S.** High-speed scanning in human memory. *Science* 1966; 153: 652-654.
 47. **Sternberg S.** In defence of high-speed memory scanning. *Q J Exp Psychol* 2016; 69(10):2020-2075.
 48. **Picton TW.** The P300 wave of the human event related potencial. *Clin Neurophysiol* 1992; 1030 9(1):456-479.
 49. **Polich J.** P300 clinical utility and control of variability. *J Clin Neurophysiol* 1998; 15(1):14-33.
 50. **Berg EA.** A simple objective technique for measuring flexibility in thinking. *J Gen Psychol* 1948; 39:15-22.
 51. **Grant DA, Berg EA.** A behavioral analysis of degree of reinforcement and ease of shifting to new responses in a Weigl-type card-sorting problem. *J Exp Psychol* 1948; 38: 404-411.
 52. **Gabuzda DH, Hirsch MS.** Neurologic manifestations of infection with human immunodeficiency virus. Clinical features and pathogenesis. *Ann Intern Med* 1987; 107(3):383-391.
 53. **González-Scarano F, Martín-García J.** The neuropathogenesis of AIDS. *Nat Rev Immunol* 2005; 5: 69-81.
 54. **Moore KW, de Waal Malefyt R, Coffman RL, O'Garra A.** Interleukin-10 and the interleukin-10 receptor. *Annu Rev Immunol* 2001; 19:683-765.
 55. **Couper KN, Blount DG, Riley EM.** IL-10: the master regulator of immunity to infection. *J Immunol* 2008; 180(9):5771-5777.
 56. **Brockman MA, Kwon DS, Tighe DP, Pavlik DF, Rosato PC, Sela J, Porichis F, Le Gall S, Waring MT, Moss K, Jessen H, Pereyra F, Kavanagh DG, Walker BD, Kaufmann DE.** IL-10 is up-regulated in multiple cell types during viremic HIV infection and reversibly inhibits virus-specific T cells. *Blood*. 2009; 114(2):346-356.
 57. **Bahraoui E, Briant L, Chazal N.** E5564 inhibits immunosuppressive cytokine IL-10 induction promoted by HIV-1 Tat protein. *Virology* 2014, 11:214.
 58. **Clerici, M, Wynn TA, Berzofsky JA, Blatt SP, Hendrix CW, Sher A, Coffman RL, Shearer GM.** Role of interleukin-10 in T helper cell dysfunction in asymptomatic individuals infected with the human immunodeficiency virus. *J Clin Invest* 1994; 93:768-775.
 59. **Taufik Y, Lantz O, Wallon C, Charles A, Dussaix E, Delfraissy JF.** Human immunodeficiency virus gp120 inhibits interleukin-12 secretion by human monocytes: an indirect interleukin-10-mediated effect. *Blood* 1997; 89(8):2842-2848.
 60. **Andrade RM, Lima PG, Filho RG, Hygino J, Milczanowski SF, Andrade AF, Lauria C, Brindeiro R, Tanuri A, Bento CA.** Interleukin-10-secreting CD4 cells from aged patients with AIDS decrease in-vitro HIV replication and tumour necrosis factor alpha production. *AIDS* 2007; 21(13):1763-1770.
 61. **Bento CA, Hygino J, Andrade RM, Sara-mago CS, Silva RG, Silva AA, Linhares UC, Brindeiro R, Tanuri A, Rosenzweig M, Klatzmann D, Andrade AF.** IL-10-secreting T cells from HIV-infected pregnant women downregulate HIV-1 replication: effect enhanced by antiretroviral treatment. *AIDS* 2009; 23(1):9-18.
 62. **Arias JF, Nishihara R, Bala M, Ikuta K.** High systemic levels of interleukin-10, interleukin-22 and C-reactive protein in Indian patients are associated with low in vitro replication of HIV-1 subtype C viruses. *Retrovirology* 2010; 7:15.

63. **Kwon DS, Kaufmann DE.** Protective and detrimental roles of IL-10 in HIV pathogenesis. *Eur Cytokine Netw* 2010; 21:208–214.
64. **Fourman LT, Saylor CF, Cheru L, Fitch K, Looby S, Keller K, Robinson JA, Hoffmann U, Lu MT, Burdo T, Lo J.** Anti-inflammatory interleukin 10 inversely relates to coronary atherosclerosis in persons with human immunodeficiency virus. *J Infect Dis* 2020; 221:510–515.
65. **Islam H, Chamberlain TC, Mui AL, Little JP.** Elevated interleukin-10 levels in COVID-19: Potentiation of pro-inflammatory responses or impaired anti-inflammatory action? *Front Immunol* 2021; 12:677008.
66. **Lu L, Zhang H, Dauphars DJ, He Y-W.** A potential role of interleukin 10 in COVID-19 pathogenesis. *Trends Immunol* 2021; 42:3–5.
67. **Barry JC, Shakibakho S, Durrer C, Simtchouk S, Jawanda KK, Cheung ST, Mui AL, Little JP.** Hyporesponsiveness to the anti-inflammatory action of interleukin-10 in Type 2 Diabetes. *Sci Rep* 2016; 6:21244.
68. **Escobar-Guevara E, Alfonzo-Díaz M.** HIV induces a pro-inflammatory/neurotoxic response in primary cultures of nervous cells, even without infection. Symposium “30 Years of HIV Science: Imagine the Future”, Institute Pasteur, 2013; Abstract No. 70/14PS. (<http://www.30yearshiv.org/Images/Public/30Y-HIV2013-Abstract-book.pdf>).
69. **Escobar EE, Alfonzo MA.** A more pro-inflammatory environment is generated in nervous cells cultures in the simultaneous presence of HIV-1 and *Toxoplasma gondii*, even with a lower parasite replication. *Front Immunol* 2013; Conference Abstract: 15th International Congress of Immunology (ICI). doi: 10.3389/conf.fimmu.2013.02.01122. (http://www.frontiersin.org/10.3389/conf.fimmu.2013.02.01122/event_abstract)
70. **Landay AL, Clerici M, Hashemi F, Kessler H, Berzofsky JA, Shearer GM.** In vitro restoration of T cell immune function in human immunodeficiency virus-positive persons: effects of interleukin (IL)-12 and anti-IL-10. *J Infect Dis* 1996; 173:1085–1091.
71. **Porichis F, Hart MG, Zupkosky J, Barblu L, Kwon DS, McMullen A, Brennan T, Ahmed R, Freeman GJ, Kavanagh DG, Kaufmann DE.** Differential impact of PD-1 and/or interleukin-10 blockade on HIV-1 specific CD4 T cell and antigen-presenting cell functions. *J Virol* 2014; 88(5):2508–2518.
72. **Sojka DK, Bruniquel D, Shwartz RH, Singh NJ.** IL-2 secretion by CD4+ T cells in vivo is rapid, transient, and influenced by TCR-specific competition. *J Immunol* 2004; 172(10):6136–6143.
73. **Dickerson F, Boronow J, Stallings C, Origoni A, Yolken R.** *Toxoplasma gondii* in individuals with schizophrenia: association with clinical and demographic factors and with mortality. *Schizophr Bull* 2007; 33(3):737–740.
74. **Flegr J.** Effects of *toxoplasma* on human behavior. *Schizophr Bull* 2007; 33(3):757–760.
75. **Flegr J.** How and why toxoplasma makes us crazy. *Trends Parasitol* 2013; 29:156–163.
76. **Milne G, Webster JP, Walker M.** *Toxoplasma gondii*: An Underestimated Threat? *Trends Parasitol* 2020; 36(12): 959–969.
77. **Chang L, Ernst T, Leonido-Yee M, Witt M, Speck O, Walot I, Miller EN.** Highly active antiretroviral therapy reverses brain metabolite abnormalities in mild HIV dementia. *Neurol* 1999; 53(4):782–789.
78. **Selnes OA.** Memory loss in persons with HIV/AIDS: assessment and strategies for coping. *AIDS Read* 2005; 15(6):289–292, 294.
79. **Wright MJ, Woo E, Foley J, Etenhofer ML, Cottingham ME, Gooding AL, Jang J, Kim MS, Castellon SA, Miller EN, Hinkin CH.** Antiretroviral adherence and the nature of HIV-associated verbal memory impairment. *J Neuropsychiatry Clin Neurosci* 2011; 23(3): 324–331.

Analysis of high risk factors for complications in the trial of vaginal delivery due to uterine scarring in a subsequent pregnancy to a cesarean section.

Ren Ye¹, Weixia Wang² and Jie Li^{1*}

¹Department of Obstetrics and Gynecology, Ningbo Women & Children's Hospital, Ningbo, China.

²Department of Obstetrics and Gynecology, Leling People's Hospital, Dezhou, China.

Key words: scarred uterus; pregnancy; vaginal trial delivery; complications; high-risk factors.

Abstract. The purpose of this work was to analyze the high-risk factors of complications in the trial of vaginal delivery of a subsequent pregnancy for scar uterus after a previous cesarean. 136 pregnant women with scar uterus with a history of cesarean who were admitted to our obstetrics department from February 2016 to March 2019 were selected and were divided into a successful group and a failed group according to the results of pregnancy and trial of labor vaginal delivery. General data of before, during, and after delivery were collected and the high-risk factors for failed vaginal delivery of scar uterine were analyzed by the logistic regression analysis. Among the 136 patients, 108 cases (79.41%) of vaginal trials were successful, and 28 cases (20.59%) of vaginal trials failed. The univariate analysis showed that the differences in gravidity, parity and the previous cesarean interval, vaginal birth history, prenatal BMI, uterine contraction, gestational age, infant weight, dilatation of the cervix, cervical Bishop score, the height of the fetal head, the thickness of the lower uterus, and whether the membranes were prematurely ruptured were statistically significant ($P < 0.05$). Logistic regression analysis showed vaginal birth history, prenatal BMI ≥ 30 kg/m², parity ≥ 2 times, cesarean interval < 2 times, dilatation of cervix ≥ 1 cm, the height of the fetal head ≥ -3 , premature rupture of the membrane and the thickness of the lower uterus of 3.0 to 3.9 cm were the high-risk factors of complications in the vaginal trial delivery of pregnancy again for scar uterus ($P < 0.05$). It is feasible for pregnant women with scar uterus to undergo vaginal delivery, but many related factors can affect the failure of trial of labor. It is necessary to pay attention to all aspects of clinical examination and choose applications strictly according to the indications.

Análisis de factores de alto riesgo para complicaciones en el trabajo de parto vaginal debidas a cicatrización uterina en un embarazo posterior a una operación cesárea.

Invest Clin 2022; 63 (3): 235 – 242

Palabras clave: cicatriz uterina; embarazo; prueba de parto vaginal; complicaciones; factores de alto riesgo.

Resumen. El propósito del presente trabajo fue analizar los factores de alto riesgo de complicaciones por cicatriz uterina en la prueba de parto vaginal del siguiente embarazo después de una cesárea previa. 136 gestantes con cicatriz uterina fueron seleccionadas con antecedente de cesárea anterior que ingresaron a nuestro servicio de obstetricia de febrero 2016 a marzo 2019, y se dividieron en un grupo exitoso y un grupo fallido según los resultados de las pruebas de embarazo y parto vaginal. Los datos generales anteriores fueron recolectados, durante y después del parto y se analizaron los factores de alto riesgo para el parto vaginal fallido de la cicatriz uterina mediante el análisis de regresión logística. Entre las 136 pacientes, 108 casos (79,41%) de las pruebas vaginales fueron exitosas y 28 casos (20,59%) de las pruebas vaginales fracasaron. El análisis univariado mostró que las diferencias en la gravidez, la paridad y el intervalo de cesárea previa, la historia de parto vaginal, el IMC prenatal, la contracción uterina, la edad gestacional, el peso del lactante, la dilatación del cuello uterino, la puntuación cervical de Bishop, la altura de la cabeza fetal, el grosor del segmento uterino inferior, y si las membranas se habían roto prematuramente fueron estadísticamente significativas ($P < 0,05$). El análisis de regresión logística mostró antecedente del parto vaginal, el IMC prenatal ≥ 30 kg/m², la paridad ≥ 2 veces, el intervalo entre cesáreas < 2 veces, la dilatación del cuello uterino ≥ 1 cm, la altura de la cabeza fetal ≥ -3 , la ruptura prematura de la membrana y el grosor del segmento uterino inferior de 3,0 a 3,9 cm fueron los factores de alto riesgo de complicaciones por cicatriz uterina en la prueba de parto vaginal de un siguiente embarazo ($P < 0,05$). Sería posible que las gestantes con cicatriz uterina vuelvan a someterse a parto vaginal, pero existen muchos factores relacionados que inciden en el fracaso del trabajo de parto. Es necesario prestar atención a todos los aspectos de la exploración física y elegir las aplicaciones estrictamente de acuerdo con las indicaciones.

Received: 15-05-2022

Accepted: 16-07-2022

INTRODUCTION

A Cesarean section is an operation to open the abdominal wall and uterus to remove the fetus that is an important operation in the field of obstetrics. It plays an important role in solving dystocia and severe

pregnancy complications; and reduces the morbidity and mortality of mothers and infants¹. At present, as the indications for cesarean section surgery and the technology of cesarean section become more and more sophisticated, China's cesarean section rate has been above the global cesarean section

warning line. Although cesarean section can significantly reduce the incidence of dystocia and postnatal adverse reactions, it can significantly increase the number of pregnant women with scar uterus after cesarean section, increase the risk of patients with scar pregnancy, placental implantation, placenta previa, and other events, which pose a certain threat to the health of mothers and infants²⁻³. In recent years, with the full popularization of the national "second child" policy, the number of women who have had a vaginal delivery again after the cesarean section has significantly increased. Related data shows that⁴, the risk of uterine rupture during the vaginal delivery of pregnant women with scar uterus is obviously increased, which easily leads to maternal and perinatal death. Reviewing relevant research findings at home and abroad⁵, most of the references mainly discuss the factors related to the success of vaginal delivery in scar uterus re-pregnancy. There are fewer factors related to the complications of vaginal delivery in scar uterus re-pregnancy, this study aims to analyze risk factors of complications in vaginal trial delivery of a subsequent pregnancy for scar uterus after cesarean section.

MATERIAL AND METHODS

Research subjects

136 pregnant women with scarred uteri with a history of cesarean section who were admitted to the obstetrics department of our hospital from February 2016 to March 2019 were selected as the research subjects. This study was approved by the ethics committee of our hospital. Inclusion criteria: 1) those aged 22 to 40 years with 37 to 41 weeks gestation; 2) the time between the last cesarean operation and this pregnancy of all pregnant women was more than 2 years; 3) the uterine scar of the pregnant woman was located at the lower section of the uterus; 4) the fetal position was normal and without absolute pelvic pelvis; 5) the pelvic bones of pregnant

women were normal; 6) the indication for the last cesarean section operation did not exist; 7) The patient and family members were informed and signed a consent form. Exclusion criteria: 1) those who had a history of two or more cesarean sections; 2) patients with intrauterine multiple births and non-term pregnancies; 3) patients with previous history of uterine rupture; 4) pregnant women with uterine tumor disease; 5) those who occur new cesarean section indications in this pregnancy; 6) those that had placenta attachment or poor continuity of muscle layer in the scar of the lower uterus. 7) products with estimated weights greater than 4000 grams were not considered. 136 pregnant women aged 22 to 40 years old, with an average age of (27.82 ± 3.84) years, 37 to 41 weeks of gestational age, an average of (39.15 ± 1.07) weeks, with two to five pregnancies, an average of (2.10 ± 1.03) times, and one to four times of parity, with an average of (1.18 ± 0.47) times, and the interval between cesarean sections was 24-168 months, with an average of (62.38 ± 25.47) months. According to the results of vaginal trial delivery, they were divided into the successful group and failed groups.

Delivery methods

After admission, pregnant women underwent detailed obstetric examinations and fetal ultrasound examinations to evaluate comprehensively their physical and pregnancy status. Pregnant women and their families chose the delivery method based on the actual situation. Continuous electronic ECG monitoring was given, and the midwife accompany the trial of pregnant women by the way of one-on-one monitoring the progress of the labor process closely. After the successful trial, it was checked whether the uterus was complete and whether the uterine scar had cracked. If the pregnant woman does not give birth within 12 hours after contraction, or if there are suspicious signs of uterine rupture and fetal distress, a cesarean section should be given immediately.

Data collection

The general information on prenatal, perinatal, and postpartum for all pregnant women was collected, including age, education, pregnancy, parity, previous cesarean sections interval, vaginal birth history, prenatal BMI, use of uterine contractions, gestational age, infant weight, admission uterine dilation of the cervix, cervical Bishop score, the height of the fetal head, lower uterine segment thickness, premature rupture of membranes, regular birth checkup, etc., and the record content was checked.

Statistical methods

All the count data in this study are expressed in [n (%)]. The comparison between the two groups was performed using the χ^2 test. Logistic regression analysis was used to analyze the high-risk factors for failed vaginal delivery of scar uterine pregnancy. $P < 0.05$ was considered statistically significant. The research data were analyzed using the SPSS21.0 software package.

RESULTS

Analysis of maternal delivery results

Among the 136 patients, 108 cases (79.41%) of successful vaginal trials were in the successful group, 28 cases (20.59%) of failed vaginal trials were in the failed group, and the reasons for 28 cases of pregnant women who failed vaginal trials and were changed to cesarean section, are shown in Table 1.

Table 1

Reasons for pregnant women who have failed vaginal trials were changed to cesarean section.

Reasons	Cases
Fetal distress	12 (42.86)
Secondary tocolytic weakness	1 (3.57)
Abnormal labor	7 (25.00)
Intrauterine infection	1 (3.57)
Other factors	7 (25.00)

Univariate analysis of factors related to failed vaginal trial delivery of scar uterine pregnancy

The univariate analysis showed that there were statistically significant differences in gravidity, parity, previous cesarean sections interval, vaginal birth history, prenatal BMI, use of uterine contraction, gestational age, infant weight, admission dilation of the cervix, cervical Bishop score, the height of the fetal head, the thickness of the lower uterus, and whether the membranes were prematurely ruptured ($P < 0.05$). See Table 2.

Influencing factors and assignments

The high-risk factors and assignments of failed vaginal trial delivery in scar uterine pregnancy, are expressed in Table 3.

Logistic regression analysis of high-risk factors for failed vaginal trial delivery in scar uterus pregnancy

Taking the failed vaginal trial delivery as the dependent variable, the statistically significant indicators in Table 2 were used as the dependent variables for evaluation (see Table 3) and were included in the logistic regression analysis model. The results showed that there was no history of vaginal delivery, $BMI \geq 30 \text{ kg/m}^2$, parity ≥ 2 times, cesarean section interval < 2 times, admission dilation of cervix $\geq 1 \text{ cm}$, the height of fetal head ≥ -3 , premature rupture of membranes, and 3.0-3.9cm of the thickness of the lower uterus are high-risk factors for complications in vaginal trial delivery in scar uterus pregnancy ($P < 0.05$) (see Table 4).

DISCUSSION

With the continuous increase in cesarean section rate in the world and the widespread application of laparoscopic myomectomy in women of childbearing age, the problem of subsequent pregnancies for scarred uterus is inevitable ⁶. With the gradual increase in cesarean section rate, the scarred uterus appears in large numbers. There are two methods of deliv-

Table 2
Univariate analysis of factors related to failed vaginal delivery of scar uterine pregnancy.

Relative factors		Successful group (n=108) (%) [*]	Failed group (n=28) (%) [*]	F	p-value ^{**}
Age	<35 years	99(91.67)	27(96.43)	0.740	0.390
	≥35 years	9(8.33)	1(3.57)		
Education	Under the high school	85(78.70)	21(75.00)	0.177	0.674
	High school or above	23(21.30)	7(25.00)		
Gravidity	<3 times	33(30.56)	12(42.56)	1.520	0.218
	≥3 times	75(69.44)	16(57.14)		
Parity	<2 times	83(76.85)	27(96.43)	5.511	0.019
	≥2 times	25(23.15)	1(3.57)		
Previous cesarean sections interval	24~36 months	55(50.93)	21(75.00)	5.227	0.022
	>36 months	53(49.07)	7(25.00)		
Vaginal birth history	Yes	67(62.04)	3(10.71)	11.825	0.001
	No	41(37.96)	25(89.29)		
Prenatal BMI	<30 kg/m ²	78(72.22)	14(50.00)	5.017	0.025
	≥30 kg/m ²	30(27.78)	14(50.00)		
Use of uterine contraction	Yes	55(50.93)	8(28.57)	7.281	0.007
	No	53(49.07)	20(71.43)		
Gestational age	<40 weeks	82(75.93)	16(57.14)	3.896	0.048
	≥40 weeks	26(24.07)	12(42.56)		
Infant weight	<3.5kg	72(66.67)	12(42.56)	5.338	0.021
	≥3.5kg	36(33.33)	16(57.14)		
Dilation of cervix	<1cm	44(40.74)	22(78.57)	12.740	<0.001
	≥1cm	64(59.26)	6(21.43)		
Cervical Bishop score	<3 scores	4(3.70)	4(14.29)	4.497	0.034
	≥3 scores	104(96.30)	24(85.71)		
Height of the fetal head	<-3	4(3.70)	4(14.29)	4.497	0.034
	≥-3	104(96.30)	24(85.71)		
The thickness of the lower uterus	3.0~3.9cm	32(29.63)	16(57.14)	7.370	0.007
	≥4.0cm	76(70.37)	12(42.56)		
Whether the membranes were prematurely ruptured	Yes	16(14.81)	10(35.71)	6.281	0.012
	No	92(85.19)	18(64.29)		
Regular birth checkup	Yes	75(69.44)	16(57.14)	1.520	0.218
	No	33(30.56)	12(42.86)		

* n= number, % (percent).

**P-value based on univariate analysis (linear regression).

Table 3
High-risk factors and assignments of failed vaginal trial delivery in scar uterine pregnancy.

Code	Variate	Assignments
X1	Gender	1=male, 2=female
X2	Education	1= under the high school, 2= high school or above
X3	Gravidity	1=<3 times, 2= \geq 3 times
X4	Parity	1=<2 times, 2= \geq 2 times
X5	Previous cesarean sections interval	1=24~36 months, 2>36 months
X6	Vaginal birth history	1=yes, 2=no
X7	Prenatal BMI	1=<30 kg/m ² , 2= \geq 30 kg/m ²
X8*	Use of uterine contraction	1=yes, 2=no
X9	Gestational age	1=<40 weeks, 2= \geq 40 weeks
X10**	Infant weight	1=<3.5kg, 2= \geq 3.5kg
X11	Dilation of cervix	1=<1cm, 2= \geq 1cm
X12	Cervical Bishop score	1=<3 scores, 2= \geq 3 scores
X13	Height of the fetal head	1=<-3, 2= \geq -3
X14	The thickness of the lower uterus	1=3.0~3.9cm, 2= \geq 4.0cm
X15	Whether the membranes were prematurely ruptured	1=yes, 2=no
X16	Regular birth checkup	1=yes, 2=no
Y	Vaginal trial delivery results	1=successful, 2=failed

* Oxytocic medications were used.

** The cut-off point of 3500 grams was taken intentionally.

Table 4
Logistic regression analysis of high-risk factors for failed vaginal delivery of scar uterine pregnancy.

Influencing factors	β	SE	Wald	p	OR	95%CI
No history of vaginal delivery	0.839	0.175	20.135	0.001	2.319	1.614~3.253
Prenatal BMI \geq 30 kg/m ²	0.078	0.021	19.561	0.001	1.120	1.041~1.132
Parity \geq 2 times	0.737	0.245	8.426	0.002	2.142	1.031~4.173
Cesarean section interval <2 times	0.086	0.021	4.167	0.012	1.169	1.022~2.637
dilation of cervix \geq 1cm	0.026	0.017	4.865	0.014	1.038	1.004~1.071
height of fetal head \geq -3	0.802	0.232	11.028	0.001	2.146	1.210~4.281
premature rupture of membranes	0.364	0.175	4.010	0.039	1.337	1.002~2.112
3.0-3.9cm of the thickness of the lower uterus	0.428	0.125	5.814	0.014	1.546	1.027~2.587

eries for scarred uterus in subsequent pregnancies, including cesarean section and vaginal delivery. A second cesarean section can reduce certain maternal and infant complications and newborn death rates, but it can increase the incidence of pain, pelvic adhesions, and surgical injuries in patients. The guided delivery in a subsequent pregnancy for scarred uterus is more economical than a second cesarean delivery, with less postpartum pain, and can reduce placental implantation and risk of placenta placement⁷⁻⁸. In recent years, the concept of vaginal trial delivery of a subsequent pregnancy for scarred uterus after the cesarean section has been accepted by obstetricians. Some scholars have found that the success rate of vaginal delivery after scar uterus for a previous cesarean section can reach 82.61%. However, there is currently no clear assessment of risk factors for vaginal trials in China, and most pregnant women have a certain degree of rejection of vaginal trials⁹⁻¹⁰. The results of this study showed that in 136 patients, 108 cases of vaginal trials were successful (79.41%), and 28 cases of vaginal trials failed (20.59%), which suggested that the scarred uterus has certain feasibility. The associated risk factors for pregnant women who have failed delivery were analyzed in this study.

Logistic regression analysis showed no history of vaginal birth, prenatal BMI ≥ 30 kg/m², parity ≥ 2 times, cesarean delivery interval <2 times, admission dilation of cervix ≥ 1 cm, the height of fetal head ≥ 3 , premature rupture of membranes and a thickness of 3.0 - 3.9cm at the lower uterus are the high-risk factors for complications in the vaginal trial of scar uterine pregnancy ($P < 0.05$). Increased prenatal BMI can increase the risk of adverse pregnancy outcomes such as hypertension and diabetes during pregnancy. Some scholars have found that pregnant women with high prenatal BMI values have a relatively slow expansion of the cervix during vaginal delivery, increasing the risk of vaginal trial failure¹¹. Relevant data show that the shorter the interval from the last cesarean section, the higher the risk of

uterine rupture in pregnant women¹². First fetal head exposure refers to the part of the fetus that first enters the pelvic entrance. Pregnant women with high first fetal head exposure have a higher incidence of dystocia¹³. Premature rupture of membranes is a common perinatal complication, which refers to the natural rupture of membranes before labor, which can lead to an increase in perinatal mortality. Relevant data¹⁴ show that the incidence of neonatal asphyxia after cesarean delivery in pregnant women with fetal head height and premature rupture of membranes has significantly increased. The thickness of the lower part of the uterus is a predictive indicator of uterine threatened rupture. When the thickness of the lower part of the uterus is low, it can increase the scar tension during labor and prone to complications such as uterine rupture¹⁵.

In summary, no history of vaginal birth, prenatal BMI ≥ 30 kg/m², parity ≥ 2 times, cesarean section interval <2 times, admission dilation of cervix ≥ 1 cm, the height of fetal head ≥ 3 , premature rupture of membranes and a thickness of 3.0 - 3.9 cm at the lower uterus are the high-risk factors for complications in the vaginal trial of scar uterine pregnancy. Therefore, a vaginal trial for pregnant women with a scarred uterus is feasible. However, there are many relevant factors affecting the failure of trial of labor, and more attention should be paid to all aspects of inspection, and choose the application strictly according to the indication.

Authors' Contribution

- Ren Ye and Weixia Wang collected the samples.
- Ren Ye and Weixia Wang analyzed the data.
- Ren Ye and Jie Li conducted the experiments and analyzed the results.

All authors discussed the results and wrote the manuscript.

Funding

The research was supported by: Ningbo key discipline women's health care (No. 2022-f27).

Conflict of interests

The authors declare no conflict of interests.

Author's ORCID numbers

- Ren Ye: 0000-0002-8366-8596
- Weixia Wang: 0000-0002-5658-8961
- Jie Li: 0000-0001-6629-7319

REFERENCES

1. **Lydonrochelle M, Holt V L, Easterling T R, Martin D P.** Risk of uterine rupture during labor among women with a prior cesarean delivery. *N Engl J Med* 2001; 345(1):3-8.
2. **Tamadon A, Park K H, Kim Y Y, Cheol Kang B, Yup Ku S.** Efficient biomaterials for tissue engineering of female reproductive organs. *Tissue Eng Regen Med* 2016 ;13(5):447-454.
3. **Patel M D, Maitra N, Patel P K, Sheth T, Vaishnov P.** Predicting successful trial of labor after cesarean delivery: Evaluation of two scoring systems. *J Obstet Gynaecol India* 2018; 68(4):276-282.
4. **Mirteymouri M, Ayati S, Pourali L, Mahmoodinia M, Mahmoodinia M.** Evaluation of maternal-neonatal outcomes in vaginal birth after cesarean delivery referred to maternity of Academic Hospitals. *J Family Reprod Health* 2016; 10(4):206-210.
5. **Rowe R, Li Y, Knight M, Brocklehurst P, Hollowell J.** Maternal and perinatal outcomes in women planning Vaginal Birth After Cesarean (VBAC) at home in England: Secondary Analysis of the Birthplace National Prospective Cohort Study. *BJOG* 2016; 123(7):1123-1132.
6. **Haq C.** Remembrances and Reflections: global health, local needs, and one very special patient. *Fam Med* 2016; 48(1):64-65.
7. **Baranov A, Gratacós E, Vikhareva O, Figueras F.** Validation of the prediction model for the success of vaginal birth after cesarean delivery at the university hospital in Barcelona. *J Matern Fetal Neonatal Med* 2017;30(24):2998-3003. doi: 10.1080/14767058.2016.1271407. Epub 2017 Jan 4.
8. **Baranov A, Salvesen KA, Vikhareva O.** Validation of prediction model for successful vaginal birth after cesarean delivery based on a sonographic assessment of hysterotomy scar. *Ultrasound Obstet Gynecol* 2018; 51(2):189-193.
9. **Clapp MA, Barth WH.** The future of cesarean delivery rates in the United States. *Clin Obstet Gynecol* 2017; 60(4):829-839.
10. **Faucher M A.** Updates from the Literature, September/October 2017. *J Mid Women's Health*, 2017, 62(5):620-624.
11. **Zafman K B, Stone J L, Factor S H.** Trends in characteristics of women choosing contraindicated home births. *J Perinat Med* 2018; 46(6):573-577.
12. **Grisaru-Granovsky S, Bas-Lando M, Drukker L, Haouzi F, Farkash R, Samueloff A, Ioscovich A.** Epidural analgesia at the trial of labor after cesarean (TOLAC): a significant adjunct to successful vaginal birth after cesarean (VBAC). *J Perinat Med* 2017; 46(3):261-269.
13. **Németh G, Molnár A.** Vaginal birth after cesarean section in light of international opinions. *Orv Hetil* 2017; 158(30):1168-1174.
14. **Committee on Practice Bulletins-Obstetrics.** Practice Bulletin No. 184: Vaginal Birth After Cesarean Delivery. *Obstet Gynecol* 2017; 130(5):e217-e233.
15. **Morton M, Fredericks Ch, Yon R, Nagy K, Bokhari Faran.** Damage control laparotomy for uterine rupture following attempted vaginal birth after cesarean. *Am Surg* 2016; 82(7): 140-141.

Effect of tetrahydroquinoline derivatives on the intracellular Ca^{2+} homeostasis in breast cancer cells (MCF-7) and its relationship with apoptosis.

Semer Maksoud¹, Adriana Mayora², Laura Colman³, Felipe Sojo^{4,5}, Adriana A. Pimentel⁶, Vladimir V. Kouznetsov⁷, Diego R. Merchán-Arenas⁷, Ángel H. Romero⁸, Francisco Arvelo^{4,5}, Juan Bautista De Sanctis⁹ and Gustavo Benaim^{10,11}

¹Department of Neurology and Experimental Therapeutics and Molecular Imaging Laboratory, Massachusetts General Hospital, MA 02129, USA.

²Instituto de Medicina Experimental. Facultad de Medicina. Universidad Central de Venezuela.

³Instituto Pasteur, Montevideo, Uruguay.

⁴Centro de Biociencias, Fundación Instituto de Estudios Avanzados (IDEA). Caracas, Venezuela.

⁵Laboratorio de Cultivo de Tejidos y Biología de Tumores, Instituto de Biología Experimental, Universidad Central de Venezuela (UCV), Caracas, Venezuela.

⁶Facultad de Farmacia, Universidad Central de Venezuela. Caracas, Venezuela.

⁷Laboratorio de Química Orgánica y Biomolecular (CMN), Universidad Industrial de Santander. Parque Tecnológico Guatiguara, Piedecuesta. Colombia.

⁸Cátedra de Química General, Facultad de Farmacia, Universidad Central de Venezuela. Caracas, Venezuela.

⁹Institute of Molecular and Translational Medicine. Palacky University. Olomouc. Czech Republic.

¹⁰Laboratorio de Señalización Celular y Bioquímica de Parásitos. Instituto de Estudios Avanzados (IDEA). Caracas, Venezuela.

¹¹Instituto de Biología Experimental, Universidad Central de Venezuela (UCV). Caracas, Venezuela.

Key words: Ca^{2+} ; apoptosis; tetrahydroquinolines; mitochondria; SERCA; NF- κ B.

Abstract. Tetrahydroquinoline derivatives are interesting structures exhibiting a wide range of biological activities, including antitumor effects. In this investigation, the effect of the synthesized tetrahydroquinolines JS-56 and JS-92 on apoptosis, intracellular Ca^{2+} concentration ($[\text{Ca}^{2+}]_i$), and the sarco(endo)plasmic reticulum Ca^{2+} -ATPase (SERCA) activity was determined on MCF-7 breast cancer cells. Colorimetric assays were used to assess MCF-7 cells viability and SERCA activity. Fura-2 and rhodamine 123 were used to measure the intracellular Ca^{2+} concentration and the mitochondrial electrochemical potential, respec-

tively. TUNEL assay was used to analyze DNA fragmentation, while caspase activity and NF- κ B-dependent gene expression were assessed by luminescence. *In silico* models were used for molecular docking analysis. These compounds increase intracellular Ca^{2+} concentration; the main contribution is the Ca^{2+} entry from the extracellular *milieu*. Both JS-56 and JS-92 inhibit the activity of SERCA and dissipate the mitochondrial electrochemical potential through processes dependent and independent of the Ca^{2+} uptake by this organelle. Furthermore, JS-56 and JS-92 generate cytotoxicity in MCF-7 cells. The effect of JS-92 is higher than JS-56. Both compounds activate caspases 7 and 9, cause DNA fragmentation, and potentiate the effect of phorbol 12-myristate-13-acetate on NF- κ B-dependent gene expression. Molecular docking analysis suggests that both compounds have a high interaction for SERCA, similar to thapsigargin. Both tetrahydroquinoline derivatives induced cell death through a combination of apoptotic events, increase $[\text{Ca}^{2+}]_i$, and inhibit SERCA activity by direct interaction.

Efecto de derivados de tetrahydroquinolinas sobre la homeostasis del Ca^{2+} intracelular en células de cáncer de mama (MCF-7) y su relación con la apoptosis.

Invest Clin 2022; 63 (3): 243 – 261

Palabras clave: Ca^{2+} , apoptosis, tetrahydroquinolinas, Mitocondria, SERCA, NF- κ B.

Resumen. Los derivados de tetrahydroquinolina son estructuras interesantes que exhiben una amplia gama de actividades biológicas, incluyendo efectos antitumorales. Se determinó el efecto de las tetrahydroquinolinas sintetizadas JS-56 y JS-92 sobre la apoptosis, concentración intracelular de Ca^{2+} ($[\text{Ca}^{2+}]_i$) y la actividad Ca^{2+} -ATPasa del retículo sarco(endo)plásmico (SERCA) en células de cáncer de mama MCF-7. Se usaron ensayos colorimétricos para evaluar la viabilidad de las células MCF-7 y la actividad SERCA. Se emplearon Fura-2 y rodamina 123 para medir la concentración de Ca^{2+} intracelular y el potencial electroquímico mitocondrial, respectivamente. El ensayo TUNEL se utilizó para analizar la fragmentación del ADN, mientras que la actividad de caspasas y la expresión génica dependiente de NF- κ B se evaluaron mediante luminiscencia. Modelos *in silico* permitieron el análisis del acoplamiento molecular. Estos compuestos aumentan la concentración de Ca^{2+} intracelular; la principal contribución es la entrada de Ca^{2+} desde el medio extracelular. Tanto JS-56 como JS-92 inhiben la actividad de SERCA y disipan el potencial electroquímico mitocondrial a través de procesos dependientes e independientes de la captación de Ca^{2+} por este orgánulo. Además, JS-56 y JS-92 generan citotoxicidad en células MCF-7. El efecto de JS-92 es mayor que JS-56. Ambos compuestos activan las caspasas 7 y 9, provocan la fragmentación del ADN y potencian el efecto del 12-miristato-13-acetato de forbol en la expresión génica dependiente de NF- κ B. El análisis de acoplamiento molecular sugiere que ambos compuestos tienen una alta interacción con SERCA, similar a la tapsigargina. Ambos derivados de tetrahydroquinolina indujeron la muerte celular a través de una combinación de eventos apoptóticos, aumento de $[\text{Ca}^{2+}]_i$ e inhibición de la actividad SERCA por interacción directa.

Received: 06-04-2022

Accepted: 10-06-2022

INTRODUCTION

Breast cancer is the most frequently diagnosed cancer and the leading cause of cancer-related death in women worldwide, with an estimated 2.3 million new cases per year and approximately more than 685,000 deaths by 2020¹. Among treatments against this disease is the use of tamoxifen (Nolvadex®) for cancer cells expressing estrogen receptors or trastuzumab (Herceptin®) for HER-2⁺ mammary tumors². Of particular interest, numerous investigations evaluate the potential of natural or synthetic compounds that stimulate apoptosis in breast cancer cells by disturbing intracellular Ca²⁺ homeostasis³⁻⁹.

Ca²⁺ possesses an essential regulatory role in differentiation, secretion, contraction, transcription, phosphorylation, and apoptosis processes. A piece of large cell machinery composed of different proteins and organelles contributes to the regulation of intracellular Ca²⁺ concentration ([Ca²⁺]_i)¹⁰. Among them is the sarco(endo)plasmic reticulum Ca²⁺-ATPase (SERCA), which allows active transport and a considerable accumulation of this cation at the endoplasmic reticulum (ER). Active transport maintains [Ca²⁺] in the ER. This concentration is approximately three orders of magnitude higher (millimolar range) than cytoplasm [Ca²⁺]

(~100 nanomolar), and similar to the extracellular *milieu*¹¹. Apoptosis is directly related to Ca²⁺ transfer from ER to mitochondria. Ca²⁺ depletion in ER can generate a phenomenon called “ER stress” in which the reduction of protein folding capacity, and consequent accumulation of these misfolded proteins, initiates different processes promoting cell death^{12,13}. The electrophoretic uniporter (MCU) induces Calcium accumulation in the mitochondria. This [Ca²⁺] increase generates an important change in electrochemical potential ($\Delta\Psi_m$)¹⁴ which may enable membrane permeabilization with consequent release of cytochrome c, caspase-9 activation and cell death¹⁵.

In this investigation, the effect of tetrahydroquinolines JS-56 and JS-92 (Fig. 1) was evaluated on Ca²⁺ homeostasis and apoptosis induction in breast cancer cells MCF-7. The tested compounds were prepared from inexpensive and commercially available isatin, 2-aminobenzonitrile (or 4-bromoaniline) and *trans*-isoeugenol, a major constituent of clove oil using a previously published two-step procedure^{16,17}. These tetrahydroquinolines have been shown to exert antitumor activity against various cancer cell lines, including MCF-7, SKBR3, PC3 and Hela cells^{16,17}; the aim of the study is to ascertain the mechanism of apoptosis induction by the compounds. Both compounds induced an in-

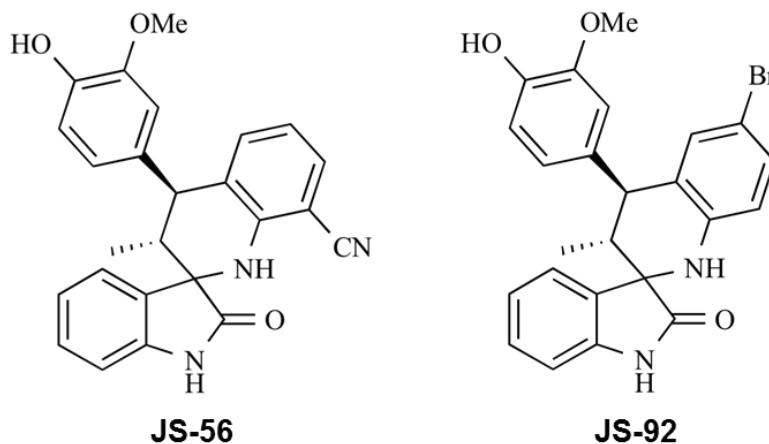


Fig. 1. Chemical structure of the tetrahydroquinolines JS-56 and JS-92.

crease in $[Ca^{2+}]_i$ caused in part through SERCA inhibition, combined with the dissipation of mitochondrial $\Delta\psi_m$. Molecular docking analysis showed that these compounds have similar ligand-protein interactions with SERCA when compared to thapsigargin (Tg). Furthermore, these tetrahydroquinolines generated apoptosis via caspase activation and DNA fragmentation. Both compounds enhanced the effect of phorbol 12-myristate-13-acetate (PMA) on the NF- κ B-dependent gene expression.

MATERIALS AND METHODS

Chemicals

The preparation of 8'-ciano-4'-(4-hydroxy-3-methoxyphenyl)-3'-methyl-3',4'-dihydro-1'*H*-spiro[indoline-3,2'-quinolin]-2-one (JS-56) and 6'-bromo-4'-(4-hydroxy-3-methoxyphenyl)-3'-methyl-3',4'-dihydro-1'*H*-spiro[indoline-3,2'-quinolin]-2-one (JS-92) was performed by following our previous reports which include the reaction of isatin and 2-aminobenzonitrile or 4-bromoaniline to give the respective ketimine-isatin derivatives and the subsequent acid-catalyzed cycloaddition reaction with *trans*-isoeugenol^{16,17}. Both compounds were purified by silica gel column chromatography and obtained as stable solids. Their structures were confirmed by various spectroscopic techniques such as EI-MS, ¹H NMR, ¹³C NMR, and IR, testing each sample as a pure chemical substance in the following biological experiments.

Cell culture

The human breast cancer cell line MCF-7 was grown in Dulbecco's Modified Eagle Medium (DMEM), supplemented with penicillin (100 U/mL), streptomycin (10,000 μ g/mL), 1% GlutaMAX™ and 10% fetal bovine serum (FBS). These cells were kept in a humidified incubator at 37°C and in an atmosphere of 5% CO₂.

Cytotoxicity assays

To evaluate the cytotoxicity in MCF-7 cells, the colorimetric reduction assay of

3-(4,5-dimethylthiazol-2-yl)-2,5-diphenyltetrazolium bromide (MTT) was performed¹⁸. Ten thousand cells were seeded in 96-well plates for 48 h allowing confluence. Cells were exposed to JS-56 and JS-92 for 24 h, at concentrations ranging from 1 to 50 μ M. In all cases, both tetrahydroquinolines were dissolved in dimethyl sulfoxide (DMSO). The final concentration of this solvent was equal to or less than 0.5%.

All appropriate controls were developed with 0.5% DMSO. After treatment, cells were incubated with 0.4 mg/mL of MTT for 2 h at 37°C. Then, the supernatant was removed, and the formazan crystals were dissolved by adding 50 μ L of DMSO. Absorbance was measured in a multi-detection microplate reader (Sinergy HT, Bio-Tek) at 570 nm. The IC₅₀ value was defined as the tetrahydroquinoline concentration causing a 50% reduction in absorbance compared to the control of untreated cells, using the Graphpad Prism 5.0 software.

Measurement of intracellular Ca²⁺ concentration

Measurements of $[Ca^{2+}]_i$ in MCF-7 cells were made using the fluorescent indicator Fura-2, essentially as previously described¹⁹. Briefly, a suspension of 1x10⁶ cells/mL was prepared in a medium containing 138 mM NaCl, 5 mM KCl, 1 mM MgCl₂, 1.5 mM CaCl₂, 5 mM glucose, 10 mM HEPES and 0.1% albumin (extracellular medium), loading cells with 200 μ M sulfinpyrazone, 0.025% pluronic acid, 0.1% albumin, and 2 μ M Fura 2 acetoxymethyl ester (Fura 2-AM) for 30 min at 25°C, in darkness and constant agitation. After loading, cells were incubated for 15 minutes in the extracellular medium and washed again using the same solution. When indicated, these experiments were also performed using the same wash buffer but without CaCl₂ (by addition of 2 mM EGTA). Fura-2 fluorescence on loaded cells suspension was monitored through a Perkin Elmer LS 55 spectrofluorimeter with a chopper device. The excitation wavelengths were set at 340 and 380 nm, while the emission was

measured at 510 nm. All experiments were carried out at 30°C, with constant agitation in a stirred cuvette.

Intracellular Ca^{2+} was calculated according to Grynkiewicz *et al.*²⁰, using the following equation: $[\text{Ca}^{2+}]_i = K_d \times (R - R_{\min}) / (R_{\max} - R) \times F_{\min(380)} / F_{\max(380)}$ where K_d is the dissociation constant of Fura-2 (224 nM). R is the ratio of emission fluorescence intensities to excitation lengths of 340/380 nm. R_{\min} and R_{\max} are ratios at 0 Ca^{2+} (6 μM digitonin plus 4 mM EGTA) and saturating Ca^{2+} (2 mM CaCl_2), respectively. $F_{\min(380)} / F_{\max(380)}$ are fluorescent values of cells exposed to digitonin plus 4 mM EGTA and 2 mM CaCl_2 , representing minimal and maximal fluorescent values.

Purification of Ca^{2+} -ATPase from the sarcoplasmic reticulum

The sarcoplasmic reticulum was obtained from the white skeletal muscle of the hind legs of rabbits, according to the method described by Eletr and Inesi²¹. The vesicles derived from the sarcoplasmic reticulum are highly enriched in Ca^{2+} -ATPase (approximately 90%). To avoid Ca^{2+} retention in the lumen of the vesicles, the ionophore A-23187 (1 μM) was added.

Evaluation of SERCA activity

The purified enzyme (2 $\mu\text{g}/\text{mL}$) was incubated for 45 min at 37°C and continuous agitation in a final volume of 250 μL of a buffer containing 100 mM KCl, 20 mM MOPS-Tris (pH 7.0), 1 mM EGTA, 10 mM MgCl_2 , 4 mM ATP, 1 μM A23817 and 1 mM CaCl_2 , obtaining 10 μM of Ca^{2+} in the medium and reaching an optimal activity of the enzyme. Inorganic phosphate production was quantified using the Fiske and Subbarow²² colorimetric assay, modified by applying ferrous sulfate as a reducing agent²³.

Determination of the mitochondrial electrochemical potential ($\Delta\psi_m$)

Mitochondrial membrane potential changes were measured using the fluorescent marker rhodamine 123, as previously

described²⁴, with the modifications introduced by Pimentel *et al.*⁶. Rhodamine 123 is a cationic fluorescent dye that allows the evaluation of the electrochemical potential of this organelle when distributed according to the $\Delta\psi_m$. Rhodamine has a maximum excitation peak of 488 nm and a maximum emission peak of 530 nm. For these experiments 3×10^5 cells/mL were resuspended in a medium containing 138 mM NaCl, 5 mM KCl, 1 mM MgCl_2 , 1.5 mM CaCl_2 , 5 mM glucose, 10 mM HEPES-KOH, pH 7.4 and then loaded with rhodamine 123 (20 $\mu\text{g}/\text{mL}$) for 45 min at 30°C. All measurements were made on a HITACHI-L-7000 spectrofluorimeter at 30°C with continuous stirring.

Determination of caspases 7 and 9 activity

We used Caspase-Glo 3/7 and Caspase-Glo 9 kits (Promega, Madison, WI) and developed the respective tests following the manufacturer's instructions. Since MCF-7 cells do not possess caspase 3²⁵, the results shown correspond to the effect of the different compounds on caspase 7 activity. In a 96-well plate, 10,000 cells/well were seeded and incubated for 48 h at 37°C in a 5% CO_2 atmosphere. Then, cells were exposed to different treatments for 24 h. Then, the cells were lysed, and the luminescence was measured with a multidetector microplate reader (Synergy HT, Bio-Tek). Staurosporine (Stau, 1 μM) was applied as an apoptosis activator (positive control), and 0.5% DMSO was used as a negative control.

Determination of DNA fragmentation

DNA fragmentation was analyzed through the "dead-end fluorimetric TUNEL (TdT-mediated dUTP Nick-End labeling) system" (Promega) kit. Cells were double-labeled with Fluorescein-12-dUTP (a specific marker of fragmented DNA) and propidium iodide (DNA marker). According to manufacturing instructions, changes in fluorescence intensity were detected by flow cytometry (Epics XL Beckman Coulter, FL). Cells incubated with staurosporine (1 μM) were used as a positive control.

Analysis of NF- κ B-dependent gene expression

In this assay, HeLa tumor cells transfected with a luciferase reporter gene whose expression is under control of a modified IL-6 promoter, which only contains a critical binding site for NF- κ B, were used. The luciferase activity was determined in a luminometer. Five thousand cells/well were seeded in 96-well plates and incubated for 48 h. Subsequently, the cells were exposed to all treatments and corresponding controls for 24 h. Then, the cells were lysed, the luciferase substrate was added, and the product was quantified by luminescence. Incubation with culture medium represents the negative control while phorbol 12-myristate 13-acetate (100 nM) was used as a positive control.

Molecular docking procedure

A 3D crystal structure from SERCA in complex with BHQ (2,5-ditert-butylbenzene-1,4-diol) and Tg was downloaded from Protein Data Bank under PDB code 2AGV. The protein corresponds to sarco(endo)plasmic reticulum Ca²⁺-ATPase from *Oryctolagus cuniculus* species, and it was crystallized with a resolution of 2.4 Å²⁶. The protein presented six co-crystallized chemical ligands: two molecules of BHQ, two molecules of Tg, and two sodium atoms. Four active sites (two for BHQ and the other two for Tg) were generated on the protein: two on α -chain and the other two on β -chain. The 3D structure was imported into the Swiss-PdbViewer v4.0.1 software²⁷. Hydrogen atoms were added to the protein structure, and minimization calculations were carried out on protein structure via AMBER force field, using the conjugate gradient method with an RMA gradient of 0.01 kcal/Åmol on Swiss-PdbViewer v4.0.1 software. The prepared protein was exported to an ArgusLab v4.0.1 program package and saved as an Agl document. Four active sites were constructed on the SERCA protein derived from BHQ and Tg inhibitors. It is well documented that both compounds, BHQ and Tg, act as SERCA inhibitors. Specifically, BHQ is an L-type Ca²⁺ channel inhibitor, blocks Ca²⁺

transport by inducing superoxide anion production²⁸. On the contrary, Tg inhibits all SERCA isozymes at similar concentrations²⁹. Both inhibitors are bound to the transmembrane domain of the enzyme close to the membrane/cytosolic interface.

Once the protein was prepared, the two tested tetrahydroquinolines JS56 and JS92 were built using ArgusLab v4.0³⁰, optimizing their respective geometries employing B3LYP/6-31G(d,p)³¹. Then, molecular docking of the two compounds and crystallized inhibitors (BHQ and TG) over the four active SERCA sites was performed employing the ArgusLab (v4.0.1) package program under Windows 7.0 environment, applying AMBER force field. The docking was achieved through their respective grid map dimensions and a grid point spacing of 0.375 Å. A flexible ligand model was used in the docking and subsequent optimization scheme. Different orientations of the ligands were scanned and ranked from their energy scores. Reproducibility of the calculated affinity and the minimum energy pose was evaluated through 10 replicates for each quinoline and crystallized inhibitor (BHQ or TS)³². The ChemScore scoring function was selected for the evaluation of ligand binding modes. Settings for genetic algorithm runs were kept at their default values; that is, the population size was 100, the selection pressure 1.1, and the number of operations was 100,000. Affinity energy is reported as the mean of the 10 replicates. The lowest energy poses (strongest-docking) for each ligand in each target protein are summarized in Table 1.

RESULTS

Effect of tetrahydroquinolines JS-56 and JS-92 on cytotoxicity in MCF-7 cells

First, the possible cytotoxicity generated by JS-56 and JS-92 on MCF-7 breast cancer cells was evaluated through an MTT assay after being treated for 24 h with different concentrations of these tetrahydroquinolines. It can be observed (Fig. 2) that both compounds

Table 1
Binding energies (kcal/mol), H-interactions, and hydrophobic interactions from molecular docking on the four studied active sites.

Binding site	Molecule	Binding energy (kcal/mol)	H-interactions (Å)	Intermolecular interactions
TG1	JS-56	-13.1366	Two hydrogen bonding (2.8596 and 2.1804 Å) between the phenolic hydrogen of the ligand and Ile-829 residue.	a) H- π interaction with Phe-834 and Phe-256. b) Hydrophobic interactions with Met-838, Tyr-837, Phe-834, Ile-829, Leu-828, Pro-827, Leu-828, Ile-765, Gln-259, Leu-260 and Val-263.
	JS-92	-12.5189	Hydrogen bonding (2.8988 Å) between the phenolic hydrogen of the ligand and Phe-834 residue	a) H- π interaction with Phe-236 and Phe-834. b) Hydrophobic interactions with Met838, Ile829, Pro827, Leu828, and 765Ile.
	Tg	-14.1626	No hydrogen bonding	a) No π - π interactions. b) Hydrophobic interactions with Met-838, Phe-834, Ile-829, Leu-828, Pro-827, Phe-776, Val-773, Val-772, Val-769, Asn-768, Ile-765, Ile-761, Pro-308, Ile-267, Val-263, Leu-260, Gln-259, Phe-256, Leu-253, Leu-249 residues.

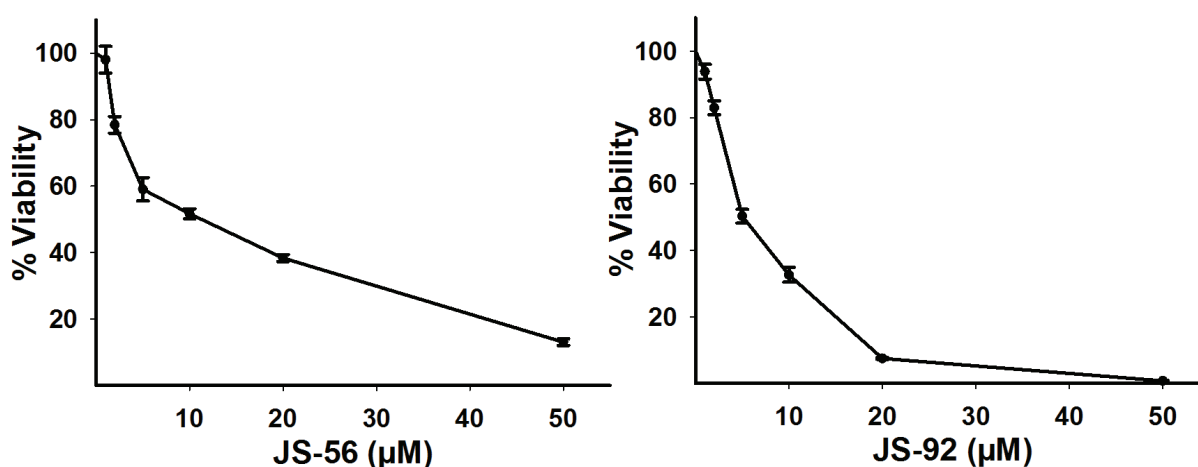


Fig. 2. Effect of tetrahydroquinolines JS-56 and JS-92 on MCF-7 cell viability. MCF-7 cells were treated with different concentrations of these compounds. Each point represents the mean \pm SD of three independent experiments. IC₅₀ values obtained for JS-56 and JS-92 were 9.74 μ M and 5.03 μ M, respectively.

induced cytotoxicity in MCF-7 cells in a dose-dependent manner, with an IC_{50} of $9.74 \mu\text{M}$ and $5.03 \mu\text{M}$ for JS-56 and JS-92, respectively. At a concentration of $50 \mu\text{M}$, JS-56 decreased cell viability by approximately 88%. At the same time, JS-92 exerted a more substantial effect than JS-56 on this cell line, being able to reduce almost 100% of MCF-7 cell viability at the same concentration.

Effect of tetrahydroquinolines JS-56 and JS-92 on intracellular Ca^{2+} mobilization

To study the effect of these tetrahydroquinolines on the $[\text{Ca}^{2+}]_i$, cells were loaded with the Ca^{2+} fluorescent indicator Fura-2. The addition of JS-56 induced a rapid increase in $[\text{Ca}^{2+}]_i$, reaching a peak followed by a continuous decrease (Fig. 3A), as a consequence of $[\text{Ca}^{2+}]_i$ regulation carried out by the cellular homeostatic machinery until it reached a new steady-state Ca^{2+} level, which is greater than

the original basal level. This response is characteristic of compounds capable of inducing the release of Ca^{2+} from the ER, with the consequent opening of plasma membrane Ca^{2+} channels (SOCE) activated by emptying this intracellular reservoir^{19,33}. The effect observed upon the addition of thapsigargin (Tg) (Fig. 3B), a potent SERCA inhibitor, was similar to that observed with JS-56. However, the maximum Ca^{2+} peak achieved with Tg was higher than JS-56. Additionally, when comparing Figures 3A and 3B, the addition of Tg after JS-56 (Fig. 3A) still induced a slight increase in $[\text{Ca}^{2+}]_i$. However, the tetrahydroquinoline did not exert any discernible effect after Tg addition (Fig. 3B).

The same experiments were performed in the absence of extracellular Ca^{2+} to determine the origin of the cation increase. Under these experimental conditions, the maximum Ca^{2+} peaks obtained with JS-56 (Fig. 3C) or Tg (Fig. 3D) were considerably lower than

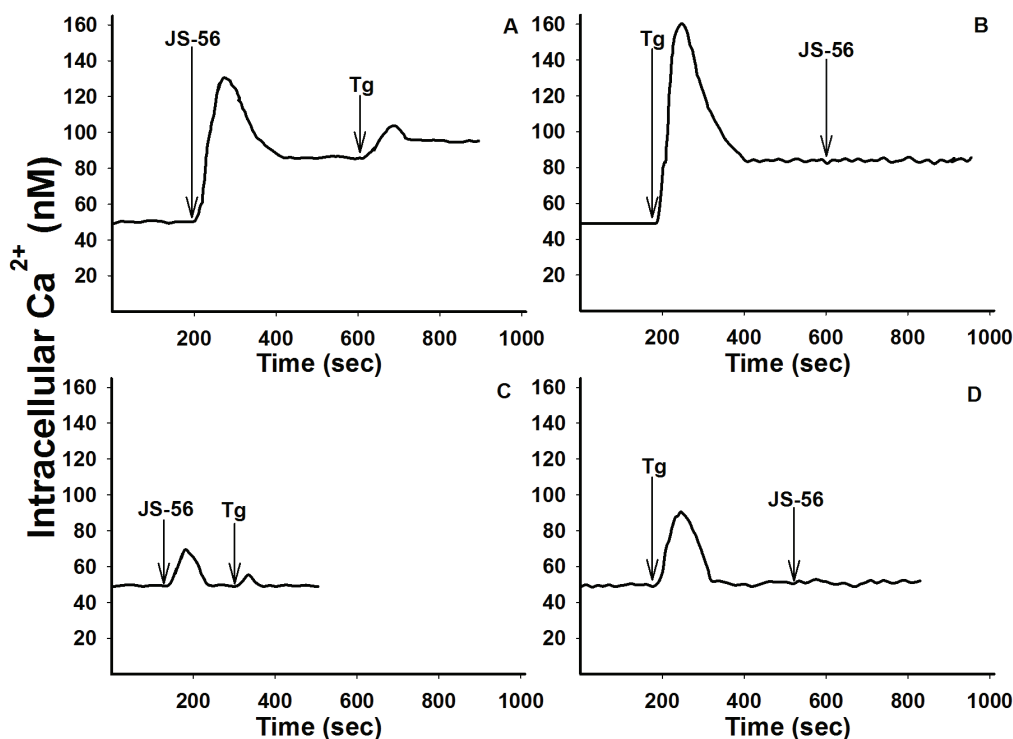


Fig. 3. Effect of tetrahydroquinoline JS-56 and thapsigargin (Tg) on $[\text{Ca}^{2+}]_i$ in MCF-7 cells. The arrows indicate the moment in which JS-56 ($20 \mu\text{M}$) and Tg ($2 \mu\text{M}$) were added, in the presence (Fig. A and B) or absence (EGTA, Fig. C and D) of 2 mM CaCl_2 . The curves are representative of at least three independent experiments.

those reached in the presence of extracellular Ca^{2+} (Figs. 3A and 3B). Furthermore, the Ca^{2+} levels obtained, after the maximum peak and the subsequent decrease, were equal to the basal levels (Figs. 3C and 3D). Moreover, when Tg was added after JS-56, a minimal rise in $[\text{Ca}^{2+}]_i$ was detected, indicating again that, different from Tg, the tetrahydroquinoline was not able to release all the Ca^{2+} from the ER (Fig. 3D). Likewise, the effect of the tetrahydroquinoline JS-92 was evaluated under the same experimental conditions, obtaining essentially the same overall results, as can be observed in Fig. 4.

Effect of tetrahydroquinolines JS-56 and JS-92 on SERCA activity

To identify a possible mechanism of action of these compounds, which could explain their effect on the increase in $[\text{Ca}^{2+}]_i$, the ability to inhibit SERCA activity was examined, considering that the results obtained were very similar to those found by the use

of Tg. Fig. 5 shows the effect of increasing concentrations of JS-56 and JS-92 on ATPase activity. Both tetrahydroquinolines inhibited SERCA activity in a dose-dependent manner. The maximum inhibitory effect of JS-56 and JS-92 on SERCA activity was 56 and 51%, respectively. Albeit none of the tetrahydroquinolines could completely inhibit the SERCA activity, these results demonstrate that part of the effect of these compounds on $[\text{Ca}^{2+}]_i$ elevation was undoubtedly due to SERCA activity inhibition.

Effect of tetrahydroquinolines JS-56 and JS-92 on the mitochondrial electrochemical potential

Mitochondria use their electrochemical membrane potential ($\Delta\psi_m$) to accumulate Ca^{2+} through the electrophoretic Ca^{2+} uniporter (MCU). The effects of the tetrahydroquinolines and Tg on the mitochondrial $\Delta\psi$ were studied by using the fluorescent marker rhodamine 123. This fluorescent indica-

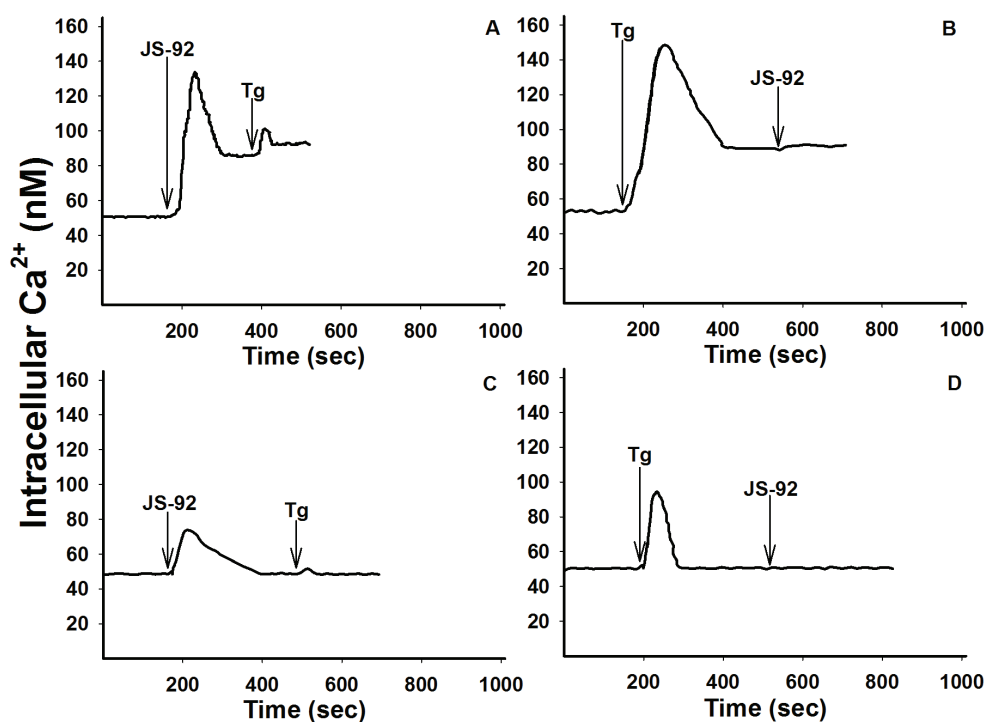


Fig. 4. Effect of tetrahydroquinoline JS-92 and thapsigargin (Tg) on $[\text{Ca}^{2+}]_i$ in MCF-7 cells. The arrows indicate the addition of JS-92 (20 μM) and Tg (2 μM), in the presence (Fig. A and B) or absence (EGTA, Fig. C and D) of 2 mM CaCl_2 . The curves are representative of at least three independent experiments.

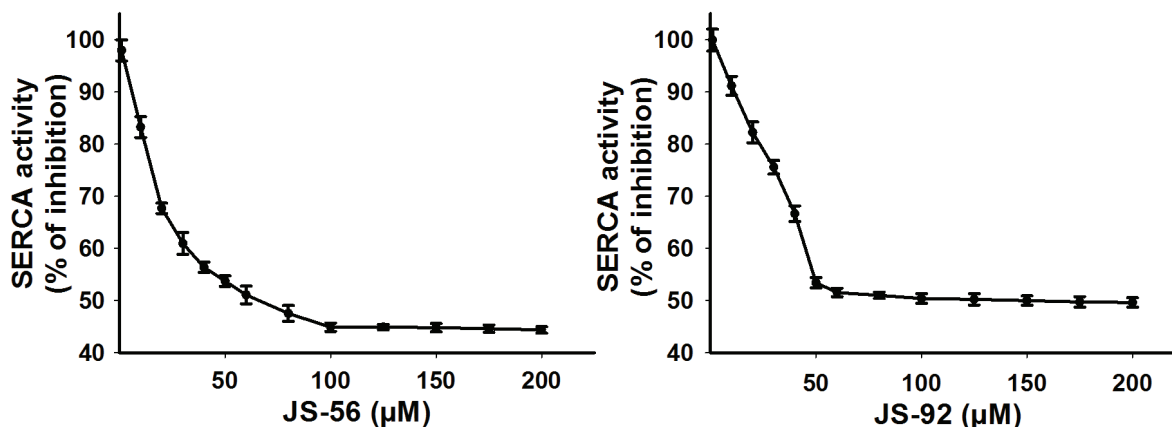


Fig. 5. Effect of tetrahydroquinolines JS-56 and JS-92 on SERCA activity. Each point represents the mean \pm SD of three independent experiments.

tor accumulates in the mitochondrial matrix according to the electrochemical gradient. Thus, an increase in fluorescence can be observed due to the mitochondrial H^+ gradient dissipation, concomitantly with the release of rhodamine 123 from the mitochondria to the cytoplasm and then to the extracellular milieu. Results from Fig. 6 demonstrate that both JS-56 and JS-92 (20 μ M) and Tg (2 μ M) produced a rapid and pronounced elevation in fluorescence due to rhodamine 123 release from mitochondria. However, the increment in rhodamine 123 fluorescence caused by Tg was more significant than those produced by the tetrahydroquinolines (Figs. 6B and 6D). It can also be noticed that JS-92 (Fig. 6C) generated an elevation of rhodamine 123 fluorescence higher than JS-56 (Fig. 6A).

The effect of Tg after the addition of the tetrahydroquinolines was less pronounced (Figs. 6A and 6C). It is worthwhile to mention that this fluorescence elevation with both Tg and tetrahydroquinolines was expected since it was due to the partial dissipation of mitochondrial $\Delta\psi$, generated by the entry of Ca^{2+} released from the ER⁶. On the other hand, after Tg application, the addition of JS-56 and JS-92 led to an additional boost in fluorescence (Figs. 6B and 6D), indicating a superior $\Delta\psi$ dissipation, which cannot be merely explained by the en-

trance of Ca^{2+} released from the ER. Thus, these results suggest that both tetrahydroquinolines can directly affect the mitochondria by Ca^{2+} -independent mechanisms. As expected, the positive control, carbonyl cyanide-4-(trifluoromethoxy)phenylhydrazone (FCCP), generated a complete collapse of the electrochemical gradient.

Effect of tetrahydroquinolines JS-56 and JS-92 on the activity of caspases 7 and 9

We then evaluated the possible effect of these tetrahydroquinolines on the induction of apoptosis in MCF-7 cells. Accordingly, the activation of caspase 9, a known caspase that initiates apoptosis, was assessed. The $1/2 IC_{50}$, IC_{50} , and $2 IC_{50}$ obtained in the MTT assay were used for both compounds. As shown in Fig. 7 (upper panel), both JS-56 and JS-92 significantly enhanced the activity of caspase-9 compared to the control in a dose-dependent manner. Sphingosine (Sph), which promotes an increase in $[Ca^{2+}]_i$ in MCF-7 cells³³, and 2,5-di-*t*-butyl-1,4-benzohydroquinone (BHQ), a known SERCA reversible-inhibitor³⁴, also elevated the activity of this initiating caspase. The positive control Stau, which activates apoptosis in MCF-7 cells³⁵, effectively activated caspase 9 at a level similar to the IC_{50} of the tetrahydroquinolines.

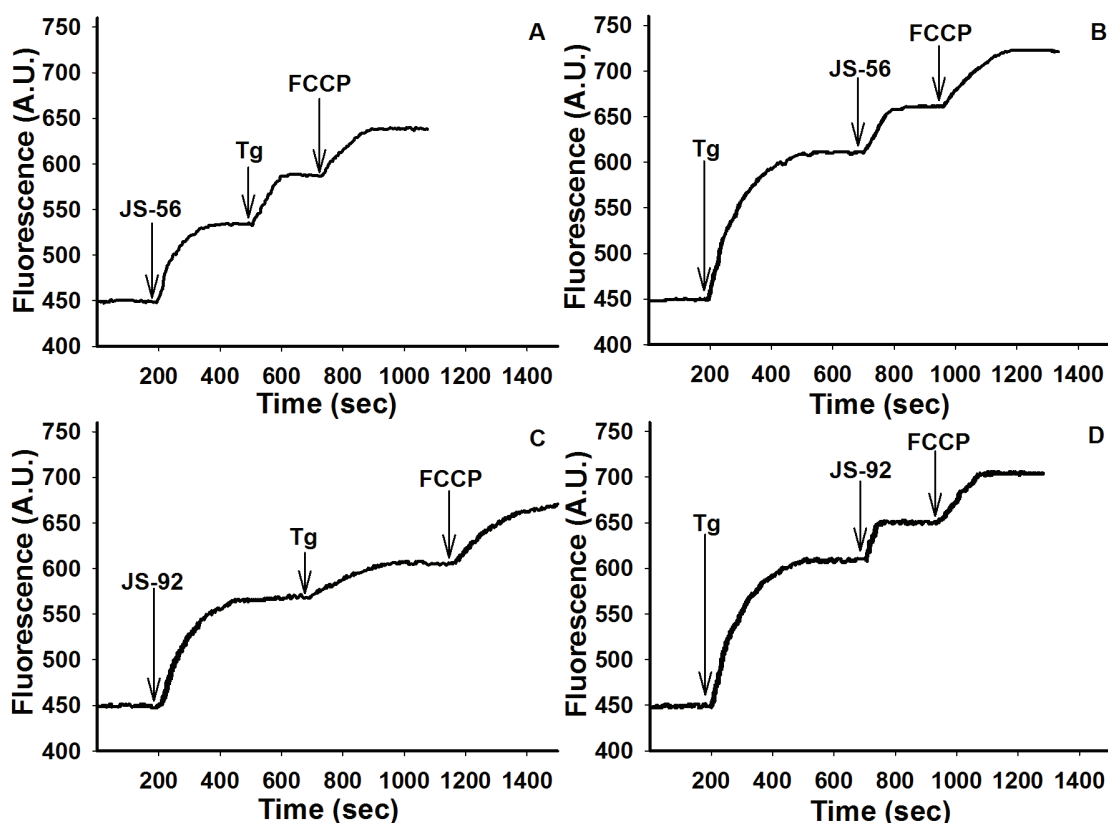


Fig. 6. Effect of tetrahydroquinolines JS-56 and JS-92 on the mitochondrial electrochemical potential in MCF-7 cells. The fluorescent marker rhodamine 123 was used for these experiments, expressing results in arbitrary units (AU) of fluorescence. The arrows indicate the moment of the addition of the different effectors: JS-56 or JS-92 (20 μ M), thapsigargin (Tg, 2 μ M), and FCCP (10 μ M). The curves are representative of at least three independent experiments.

Likewise, treatment of MCF-7 cells with both tetrahydroquinolines raised the activity of caspase 7 (Fig. 7, lower panel). Similar results were detected with the positive control Stau and the SERCA inhibitor BHQ. The activation-induced by JS-92 was slightly higher compared to the rest of the compounds. This effector caspase will be responsible for cleaving specific cell targets to promote apoptosis in these cells.

Effect of tetrahydroquinolines JS-56 and JS-92 on DNA fragmentation

An apoptotic cell is typically characterized by: changes in cell morphology, phosphatidylserine externalization, cytoplasm

contraction, shrinkage of the nucleus, and DNA fragmentation¹⁵. As a complement to the results obtained in caspases 7 and 9 activity assays, DNA fragmentation was analyzed through a TUNEL assay using Stau as a positive control. In Fig. 8, cells were divided into four populations displaying the percentage of cells in necrosis (propidium iodide, IP⁺), apoptosis (fluorescein isothiocyanate, FITC⁺), and alive (negative for both markers); apoptotic cells can either be IP⁻ or IP⁺. Apoptotic cells exhibit DNA fragmentation, which allows FITC incorporation. However, a subset of these apoptotic cells is also IP⁺, denoting that these also have a loss of plasma membrane integrity, corresponding to a

later stage of apoptosis in which cells can no longer control the passage of elements across the membrane, with eventual cell lysis in the final stage. The quantitative data is represented in Table 2.

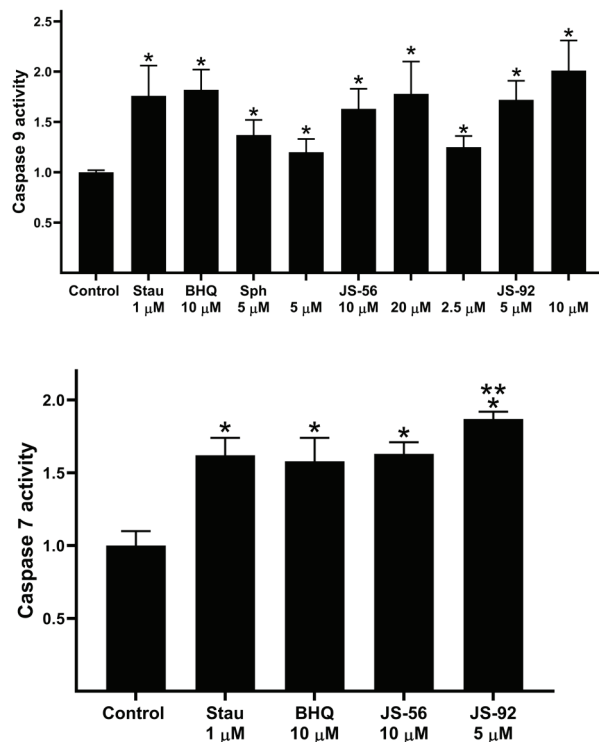


Fig. 7. Effect of tetrahydroquinolines JS-56 and JS-92 on the activity of caspases 9 (initiator) and 7 (effector). Stau (staurosporine), BHQ (2,5-di-t-butyl-1,4-benzohydroquinone) and Sph (sphingosine). The bars represent the mean \pm SD derived from three independent experiments. * and ** $p < 0.05$ compared to the control of untreated cells or treated with JS-56, respectively.

JS-56 treatment (10 μ M) for 24 h induced apoptosis, with 65.9% of FITC⁺ IP⁺ cells in this stage and only 4.3% of FITC⁺ IP⁺ cells. Treatment with Stau (1 μ M) and JS-92 (5 μ M) produced a significant percentage of FITC⁺ IP⁺ (31.5 and 46.5% for Stau and JS-92, respectively) and FITC⁺ IP⁺ cells (60.6 and 35.5% for Stau and JS-92, respectively). Hence, JS-92 has a more potent effect than JS-56, which measurements of caspase activity have also evidenced. These results are statistically significant compared to the negative control (DMSO-treated MCF-7 cells).

Effect of tetrahydroquinolines JS-56 and JS-92 on NF- κ B-dependent gene expression

The nuclear transcription factor NF- κ B regulates numerous genes involved in multiple cellular processes such as apoptosis, cell proliferation, and differentiation. To evaluate NF- κ B-dependent gene expression, HeLa tumor cells transfected with a luciferase reporter gene under the control of IL-6 promoter, which contains critical binding sites for NF- κ B, were used.

Tetrahydroquinolines JS-56 and JS-92, when added alone, were not able to increase the NF- κ B-dependent gene expression, with values similar to those observed in the negative control (Fig. 9). The luminescence measured in the negative control corresponds to the basal NF- κ B-dependent gene expression on MCF-7 cells. The NF- κ B-dependent gene expression is elevated when cells were treated with 100 nM of PMA; it has been

Table 2

Percentage of living, apoptotic, and necrotic cells after treatment with JS-56 and JS-92.

Treatment group	Percentage			
	Living cells	Apoptosis (IP-)	Apoptosis (IP+)	Necrosis
Control DMSO	93.5 \pm 4.6	0.9 \pm 0.6	0.1 \pm 0.1	4.1 \pm 1.2
Staurosporine	3.9 \pm 1.3	31.5 \pm 7.5	60.6 \pm 6.8	1.2 \pm 0.5
JS-56	25.5 \pm 9.3	65.9 \pm 4.7	4.3 \pm 2.8	1.9 \pm 1.6
JS-92	14.6 \pm 6.3	46.5 \pm 5.5	35.5 \pm 4.8	3.4 \pm 1.8

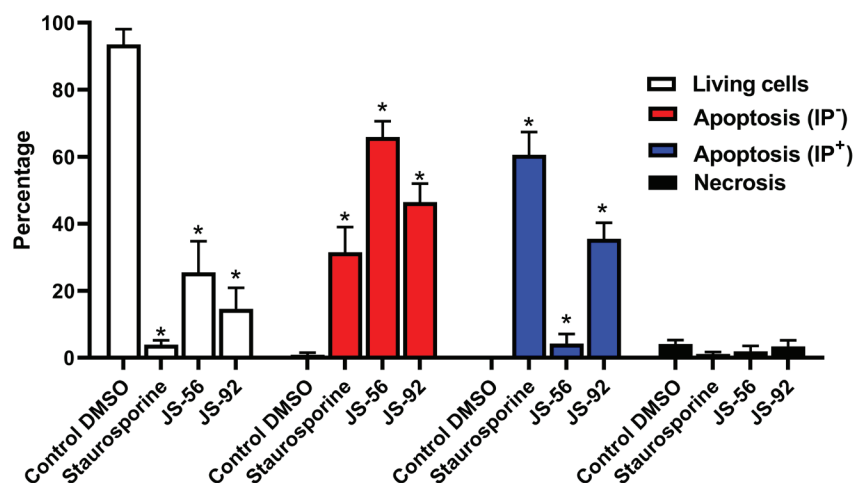


Fig. 8. Effect of tetrahydroquinolines JS-56 and JS-92 on DNA fragmentation in MCF-7 cells. The MCF-7 cells were incubated with Fluorescein-12-dUTP (fragmented DNA marker) and Propidium Iodide (IP, core marker). Cells were treated with staurosporine (1 μ M), JS-56 (10 μ M), and JS-92 (5 μ M). The bars represent the mean \pm SD derived from three independent experiments. * $p < 0.0001$ compared to the control of cells treated with DMSO.

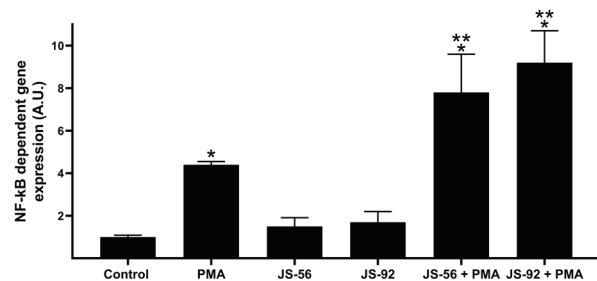


Fig. 9. Effect of tetrahydroquinolines JS-56 and JS-92 on NF- κ B-dependent gene expression. HeLa tumor cells were transfected with a luciferase reporter gene under the control of the IL-6 promoter, which contains critical binding sites for NF- κ B. Control, untreated MCF-7 cells; PMA, phorbol 12-myristate 13-acetate. * and ** $p < 0.05$ compared to the control of untreated cells or treated with PMA, respectively.

reported that PKC can activate I κ Bs kinase complexes (IKKs), which eventually leads to NF- κ B activation³⁶. Interestingly, the results demonstrate that the NF- κ B-dependent gene expression increased significantly when cells were treated with PMA plus JS-56 or JS-92, indicating an apparent effect of both compounds on the PKC-stimulated NF- κ B-dependent gene expression.

Molecular docking

The experimental results on SERCA activity obtained for the tetrahydroquinolines JS-56 and JS-92 were confirmed using molecular docking for SERCA protein (PDB code 2AGV). Interestingly, both Tg and BHQ SERCA inhibitors showed practically the same disposition as crystallized inhibitors at the respective protein binding sites, reflecting the computational package's potential for this molecular docking. In general, the tetrahydroquinolines showed a higher preference for Tg binding sites than for the BHQ active site. This effect generates a ligand-protein complex with binding energies between -12 and -13 kcal/mol at the active sites of Tg; this is in contrast to weak docking energies found at the BHQ active site for both tetrahydroquinolines. Particularly, experimental results have demonstrated that Tg exerted a more potent inhibitory activity (IC₅₀ of 0.2 nM) than BHQ (IC₅₀ of 20 nM)²⁶. The preference of these large tetrahydroquinolines for Tg binding sites may be associated with the larger box size than BHQ active sites, which may facilitate the stabilization of the inhibitor-protein complex for these bulky and inflexible molecules. It is

essential to mention that our analysis was focused on data obtained for the Tg active site from chain- α , which exhibited the lower binding energy complex.

DISCUSSION

Tetrahydroquinolines derivatives are an essential group of natural or synthetic compounds showing a wide range of biological activities. Numerous compounds capable of inducing a Ca^{2+} signal followed by a cellular response have been reported. Ca^{2+} is one of the essential ionic constituents in the body. It has a central regulatory role in differentiation, secretion, contraction, transcription, phosphorylation, and apoptosis processes¹⁰. Ca^{2+} is the component required by milk to calcify newborn bones and teeth and modulates the proliferation, differentiation, and apoptosis of mammary gland epithelial cells³⁷. The modulation of Ca^{2+} homeostasis and its signaling could represent a viable therapeutic approach in the treatment and/or prevention of breast cancer. Therefore, regulators of Ca^{2+} homeostasis or its signaling in mammary gland tumors are possible targets for drugs. In this investigation, we used the tetrahydroquinolines JS-56 and JS-92, modified derivatives from clove and cinnamon plants, to study the effect of these drugs on Ca^{2+} homeostasis and its possible relationship with apoptosis in breast cancer cells MCF-7.

In the interest of evaluating the cytotoxicity of tetrahydroquinolines JS-56 and JS-92 on MCF-7 breast cancer cells, the MTT assay was developed, allowing the determination of mitochondrial viability on treated cells. Both compounds are cytotoxic to MCF-7 cells in a dose-dependent manner, with an IC_{50} of $9.74 \mu\text{M}$ and $5.031 \mu\text{M}$ for JS-56 and JS-92, respectively. This difference may be related to the bromine atom that JS-92, instead of the cyanide atom present in JS-56. IC_{50} values for these compounds in MCF-7 cells are significantly lower than those reported previously in human dermis fibro-

blast, $92.87 \mu\text{M}$ and $42.48 \mu\text{M}$ for JS-56 and JS-92, respectively¹⁷.

Through fluorimetric techniques, we were able to perform measurements of intracellular Ca^{2+} in MCF-7 cells, aiming to find possible mechanisms of action for these compounds. The results revealed that JS-56 and JS-92 promote an increase in $[\text{Ca}^{2+}]_i$. Likewise, the Tg effect on $[\text{Ca}^{2+}]_i$ is diminished when added after the impact generated by the tetrahydroquinolines, compared to when it is initially added, allowing us to conclude that these compounds promote the release of Ca^{2+} from a compartment sensitive to Tg, namely the ER. Similar experiments were done but using a solution without CaCl_2 . Under these experimental conditions, the maximum Ca^{2+} peaks detected with JS-56, JS-92 or Tg are considerably reduced compared to those achieved in the presence of extracellular Ca^{2+} , and instead, returning to the basal level. These results show an influx of Ca^{2+} from the outside. This effect may be caused by a store-operated Ca^{2+} Entry (SOCE) or a capacitive Ca^{2+} entry induced by emptying Ca^{2+} from the ER^{19,33}.

The lack of an additive effect of Tg with tetrahydroquinolines on the $[\text{Ca}^{2+}]_i$ suggests a possible similar mechanism of action. The possible inhibitory potential of these compounds on SERCA activity was examined accordingly. Both tetrahydroquinolines inhibit the enzyme activity with similar maximum inhibitory effects of 56 and 51% for JS-56 and JS-92, respectively. This effect also indicates that different from Tg, these compounds could not completely inhibit the ATPase activity. However, part of the overall effect on the onset of apoptosis is the partial inhibition of SERCA activity. As it has been shown that Tg can induce ER stress via SERCA inhibition, JS-56 and JS-92 are likely potential candidates for generating ER stress through this identical mechanism. In this context, it is worth mentioning that SERCA targeting could represent an effective therapeutic strategy in treating pathogens and cancer cells³⁸.

The effect of both compounds on the mitochondrial membrane $\Delta\psi_m$ was determined since the accumulation of mitochondrial Ca^{2+} is a necessary event in the initiation of apoptosis via the intrinsic pathway. The primary source of the cation derives from its transfer from the ER³⁹. The results revealed that both tetrahydroquinolines generate an increase in rhodamine 123 fluorescence. Although the increment in rhodamine fluorescence caused by Tg was higher than the compounds, its effect after the addition of the tetrahydroquinolines was less pronounced, suggesting that they share part of the mechanism of action on mitochondria. The fluorescence increase after treating the cells with both Tg and tetrahydroquinolines was expected due to the partial dissipation of mitochondrial $\Delta\psi_m$. This change is generated by the entry of Ca^{2+} released from the ER⁶. When both tetrahydroquinolines were added after Tg, an additional increase in fluorescence was triggered, indicating a superior dissipation of the $\Delta\psi$. These unexpected results suggested that JS-56 and JS-92 induced a cell response independent of $[\text{Ca}^{2+}]_i$. The effects are also independent of the Ca^{2+} electrophoretic uniporter. These effects have been reported previously with concentrations higher than $1 \mu\text{M}$ ⁴⁰. Accordingly, both tetrahydroquinolines, similar to the SERCA inhibitor, could interact with the mitochondria, generating a widespread effect.

Given that the $\Delta\psi_m$ loss of the mitochondrial membrane is a hallmark event of apoptosis, the presumed activation of characteristic processes associated with programmed cell death after applying the tetrahydroquinolines was investigated. In this study, it was demonstrated that tetrahydroquinolines JS-56 and JS-92 are capable of activating caspases 7 and 9 and promoting DNA fragmentation. Activation of caspases and the percentage of cells with DNA fragmentation was higher for JS-92, which coincides with its superior cytotoxic effect. DNA fragmentation in conjunction with caspase

activation and the results demonstrating that these tetrahydroquinolines cause the dissipation of mitochondria $\Delta\psi_m$ to support the conclusion that these compounds activate apoptosis in MCF-7 cells. Additionally, after the inhibition of SERCA and the consequent reduction of the $[\text{Ca}^{2+}]$ at the ER, misfolded proteins could accumulate. The unfolded protein response could be triggered, leading the cells to death^{12,13}. By suppressing this enzyme's activity and promoting the cation's entry into the mitochondria, the release of pro-apoptotic factors from this organelle would be facilitated¹⁵. Thus, part of the potential anticancer effect of these compounds would be mediated through SERCA inhibition. Based on the accumulated evidence, we suggest that disturbances of the Ca^{2+} signal induced by these tetrahydroquinolines would trigger apoptosis by promoting ER stress and the release of proapoptotic factors from the mitochondria after the entry of Ca^{2+} into this organelle.

According to our results, JS-56 and JS-92 failed to elevate the NF- κ B-dependent gene expression. However, NF- κ B-dependent gene expression was augmented when cells were treated with PMA, an activator of PKC which upregulates NF- κ B³⁵. Interestingly, the NF- κ B-dependent gene expression is further elevated when cells were exposed to the combination of PMA and tetrahydroquinolines, possibly because these compounds enhance the affinity of PKC for PMA or modulate the PMA activity making it more potent and/or stable. Since NF- κ B is a regulator of the expression of multiple genes, additional experiments are needed to determine its putative participation in pro-apoptotic events. We do not rule out non-specific binding of other transcription factors to this NF- κ B binding site on the IL-6 promoter. Future research will confirm the participation of this transcription factor by determination of cytoplasmic/nuclear levels of p65 as well as confirmation of these results in breast cancer cells.

Based on the results that both tetrahydroquinolines may interact with the Tg bind-

ing site of SERCA, we used a docking model to test the possibility of interaction. It should be noted that both tetrahydroquinolines exhibited docking energies higher than Tg, indicating that the Tg-Ca²⁺-ATPase complex is more stable than the quinoline-Ca²⁺-ATPase complex (Table 1). These theoretical findings are in good agreement with experimental data, where Tg exhibited the higher experimental inhibitory activity (IC₅₀ of 0.2 nM) compared to the tested tetrahydroquinolines (IC₅₀ of 60 and 100 μM for JS-56 and JS-92, respectively). The high stabilization of the Tg-Ca²⁺-ATPase complex can be asso-

ciated with diverse intermolecular interactions with residues located in the Tg1 active site, including (i) a large number of hydrophobic interactions with at least 20 residues in chain A and 13 residues in chain B; (ii) from one to two strong *H*-interactions with Ile-829 and Phe-834 for JS-56 and JS-92, respectively; and (iii) *H*-π interactions between phenolic, quinolinic, or indolic rings with specific phenyl rings in Phe-834, Phe-256 or Tyr-837 (Table 1 and Fig. 10). However, it is essential to mention that these diverse interactions found for these tetrahydroquinolines are located in turn to a specific re-

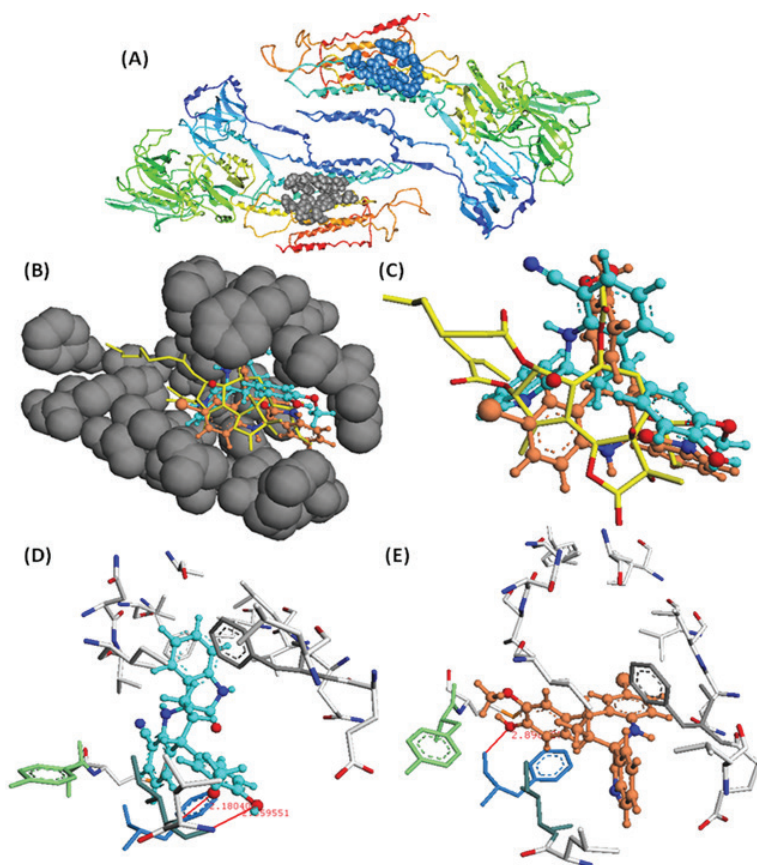


Fig. 10. Molecular docking of the tetrahydroquinolines JS-56 and JS-92 on the TG1 active site. (A) TG1 (gray ribbons) and TG2 (blue ribbons) active sites into SERCA protein; (B) Location of JS-56 (cyan color) and JS-92 (orange color) into the TG1 active site pocket of SERCA protein; (C) Superimposition between JS-56 (cyan) and JS-92 (orange) with TG1 substrate (yellow color); (D) Disposition and interactions of JS-56 (cyan) (D) and JS-92 (orange) (E) into TG1 active site. Tentative *H*-π interactions between phenolic, indolic, or quinolinic rings of JS-56 and JS-92 with Phe-236 (gray color), Phe-834 (blue color), and Phe-256 (green color) residues.

gion of the active site. At the same time, Tg, bearing a highly flexible octanoic acid residue at C2, makes hydrophobic contacts with non-polar patches on the outer surface of SERCA's trans-membrane domain and possibly with surrounding lipids, facilitating the stabilization of the ligand-protein complex. The molecular docking analysis shows that hydrophobic ligands containing long and flexible side chains are needed to design effective inhibitors of the Ca^{2+} -ATPase enzyme due to the high hydrophobic and extended nature of the Ca^{2+} -ATPase active site. Future studies will continue to evaluate these types of compounds and their effect on Ca^{2+} and apoptosis, developing new analogs with different types of chemical modifications on a more diverse panel of breast cancer cells and other types of malignancies.

Both tetrahydroquinolines derivatives, JS-56 and JS-92, induced cell death in MCF-7 cells through a combination of events. These events include the elevation of the $[\text{Ca}^{2+}]_i$, inhibiting SERCA via direct interaction, partially damaging the mitochondria, which induced activation of apoptotic pathways and consequently MCF-7 cell death. Therefore, these results show the potential that these types of compounds would have in anti-neoplastic treatment in humans. It is hoped that more powerful analogs can be developed in the future.

Funding

This work was supported by [Fondo Nacional de Ciencia, Tecnología e Investigación, Venezuela (FONACIT)] (Grants 2017000274 and 2018000010), and the [Consejo de Desarrollo Científico y Humanístico-Universidad Central de Venezuela (CDCH-UCV)] (Grant PG-03-8728-2013/2) to G.B.

Conflict of interest

The authors declare no conflicts of interest.

Authors contributions

SM: Investigation, Methodology, Data curation, Writing – original draft, Writing – review & editing. AM: Methodology, Writing – review & editing. LC: Methodology, Writing – review & editing. FS: *In silico* analysis, Writing – review & editing. AP: NF- κ B gene expression analysis. VK: *In silico* analysis, isolation and purification of natural compounds. DMA: Isolation and purification of natural compounds. AR: Methodology, Writing – review & editing. EA: *In silico* analysis, Writing – review & editing. JS: Flow cytometry analysis, Writing – review & editing. GB: Conceptualization, Formal analysis, Supervision, Funding acquisition, Writing – review & editing.

Author's ORCID numbers

- Semer Maksoud:
0000-0001-9773-9415
- Adriana Mayora:
0000-0002-6817-2066
- Laura Colman:
0000-0002-5188-880X
- Felipe Sojo:
0000-0002-6559-4845
- Adriana A. Pimentel:
0000-0002-8862-9318
- Vladimir V. Kouznetsov:
0000-0003-1417-8355
- Diego R. Merchán-Arenas:
0000-0001-9243-5914
- Ángel H. Romero:
0000-0001-8747-5153V
- Francisco Arvelo:
0000-0003-1590-358x
- Juan Bautista De Sanctis:
0000-0002-5480-4608
- Gustavo Benaim:
0000-0002-9359-5546

REFERENCES

1. **World Health Organization (WHO)**. Breast Cancer (December 2021). <https://www.who.int/news-room/fact-sheets/detail/breast-cancer>.
2. **Peart O**. Breast intervention and breast cancer treatment options. *Radiol Technol* 2015;86:535M-558M; quiz 559-62.
3. **Sergeev IN, Li S, Colby J, Ho C-T, Dushenkov S**. Polymethoxylated flavones induce Ca²⁺-mediated apoptosis in breast cancer cells. *Life Sci* 2006;80:245-253.
4. **Sareen D, Darjatmoko SR, Albert DM, Polans AS**. Mitochondria, calcium, and calpain are key mediators of Resveratrol-induced apoptosis in breast cancer. *Mol Pharmacol* 2007;72:1466-1475.
5. **Lee J-H, Li Y-C, Ip S-W, Hsu S-C, Chang N-W, Tang N-Y, Yu C-S, Chou S-T, Lin S-S, Lino C-C, Yang J-S, Chung J-G**. The role of Ca²⁺ in baicalein-induced apoptosis in human breast MDA-MB-231 cancer cells through mitochondria- and caspase-3-dependent pathway. *Anticancer Res* 2008;28:1701-1711.
6. **Pimentel AA, Felibertt P, Sojo F, Colman L, Mayora A, Silva ML, Rojas H, Dipolo R, Suarez AI, Compagnone RS, Arvelo F, Galindo-Castro I, De Sanctis JB, Chirino P, Benaim G**. The marine sponge toxin agelasine B increases the intracellular Ca²⁺ concentration and induces apoptosis in human breast cancer cells (MCF-7). *Cancer Chemother Pharmacol* 2012;69:71-83.
7. **Zhang Z, Teruya K, Eto H, Shirahata S**. Induction of apoptosis by low-molecular-weight fucoidan through calcium- and caspase-dependent mitochondrial pathways in MDA-MB-231 breast cancer cells. *BioSci Biotechnol Biochem* 2013;77:235-242.
8. **Al-Taweel N, Varghese E, Florea A-M, Büselberg D**. Cisplatin (CDDP) triggers cell death of MCF-7 cells following disruption of intracellular calcium ([Ca²⁺]_i) homeostasis. *J Toxicol Sci* 2014;39:765-774.
9. **Sehgal P, Szalai P, Olesen C, Praetorius HA, Nissen P, Christensen SB, Engedal N, Møller J V**. Inhibition of the sarco/endoplasmic reticulum (ER) Ca²⁺-ATPase by thapsigargin analogs induces cell death via ER Ca²⁺ depletion and the unfolded protein response. *J Biol Chem* 2017;292:19656-19673.
10. **Carafoli E**. Calcium signaling: A tale for all seasons. *Proc Natl Acad Sci* 2002;99:1115-1122.
11. **Carafoli E**. Intracellular calcium homeostasis. *Annu Rev Biochem* 1987;56:395-433.
12. **Breckenridge DG, Germain M, Mathai JP, Nguyen M, Shore GC**. Regulation of apoptosis by endoplasmic reticulum pathways. *Oncogene* 2003;22:8608-8618.
13. **Szegezdi E, Logue SE, Gorman AM, Samali A**. Mediators of endoplasmic reticulum stress-induced apoptosis. *EMBO Rep* 2006;7:880-885.
14. **Rizzuto R, Bernardi P, Pozzan T**. Mitochondria as all-round players of the calcium game. *J Physiol* 2000;529:37-47.
15. **Hengartner MO**. The biochemistry of apoptosis. *Nature* 2000;407:770-776.
16. **Kouznetsov V V, Bello Forero JS, Amado Torres DF**. A simple entry to novel spiro dihydroquinoline-oxindoles using Povarov reaction between 3-N-aryliminoisatins and isoeugenol. *Tetrahedron Lett* 2008; doi: 10.1016/j.tetlet.2008.07.096.
17. **Kouznetsov V, R. Merchan Arenas D, Arvelo F, S. Bello Forero J, Sojo F, Munoz A**. 4-Hydroxy-3-methoxyphenyl substituted 3-methyl-tetrahydroquinoline derivatives obtained through Imino Diels-Alder reactions as potential antitumoral agents. *Lett Drug Des Discov* 2010;7:632-639.
18. **Mosmann T**. Rapid colorimetric assay for cellular growth and survival: Application to proliferation and cytotoxicity assays. *J Immunol Methods* 1983;65:55-63.
19. **Colina C, Flores A, Castillo C, Rosario Garrido M del, Israel A, DiPolo R, Benaim G**. Ceramide-1-P induces Ca²⁺ mobilization in Jurkat T-cells by elevation of Ins(1,4,5)-P₃ and activation of a store-operated calcium channel. *Biochem Biophys Res Commun* 2005;336:54-60.
20. **Grynkiewicz G, Poenie M, Tsien RY**. A new generation of Ca²⁺ indicators with greatly improved fluorescence properties. *J Biol Chem* 1985;260:3440-3450.
21. **Eletr S, Inesi G**. Phospholipid orientation in sarcoplasmic membranes: Spin-label ESR and proton NMR studies. *Biochim Biophys Acta - Biomembr* 1972;282:174-179.

22. Fiske CH, Subbarow Y. The colorimetric determination of phosphorus. *J Biol Chem* 1925;66:375–400.
23. Benaim G, Cervino V, Lopez-Estraño C, Weitzman C. Ethanol stimulates the plasma membrane calcium pump from human erythrocytes. *Biochim Biophys Acta - Bioembr* 1994;1195:141–148.
24. Benaim G, Sanders JM, Garcia-Marchán Y, Colina C, Lira R, Caldera AR, Payares G, Sanoja C, Burgós JM, Leon-Rossell A, Concepcion JL, Schijman AG, Levin M, Oldfield E, Urbina JA. Amiodarone has intrinsic anti-*Trypanosoma cruzi* activity and acts synergistically with posaconazole. *J Med Chem* 2006;49:892–899.
25. Kagawa S, Gu J, Honda T, McDonnell TJ, Swisher SG, Roth JA, Fang B. Deficiency of caspase-3 in MCF7 cells blocks Bax-mediated nuclear fragmentation but not cell death. *Clin Cancer Res* 2001;7:1474–1480.
26. Obara K, Miyashita N, Xu C, Toyoshima I, Sugita Y, Inesi G, Toyoshima C. Structural role of countertransport revealed in Ca^{2+} pump crystal structure in the absence of Ca^{2+} . *Proc Natl Acad Sci* 2005;102:14489–14496.
27. Guex N, Peitsch MC. SWISS-MODEL and the Swiss-Pdb Viewer: An environment for comparative protein modeling. *Electrophoresis* 1997;18:2714–2723.
28. Fusi F, Saponara S, Gagov H, Sgaragli G. 2,5-Di-*t*-butyl-1,4-benzohydroquinone (BHQ) inhibits vascular L-type Ca^{2+} channel via superoxide anion generation. *Br J Pharmacol* 2001;133:988–996.
29. Lytton J, Westlin M, Hanley MR. Thapsigargin inhibits the sarcoplasmic or endoplasmic reticulum Ca-ATPase family of calcium pumps. *J Biol Chem* 1991;266:17067–17071.
30. Thompson M. ArgusLab 4.0 Planaria Software. LLC: Seattle, WA. 2004.
31. Becke AD. A new mixing of Hartree–Fock and local density-functional theories. *J Chem Phys* 1993;98:1372–1377.
32. Young DC. Computational Drug Design. Hoboken, NJ, USA: John Wiley & Sons, Inc., 2009.
33. Colina C, Flores A, Rojas H, Acosta A, Castillo C, Rosario Garrido M del, Israel A, DiPolo R, Benaim G. Ceramide increase cytoplasmic Ca^{2+} concentration in Jurkat T cells by liberation of calcium from intracellular stores and activation of a store-operated calcium channel. *Arch Biochem Biophys* 2005;436:333–345.
34. Moore GA, McConkey DJ, Kass GEN, O'Brien PJ, Orrenius S. 2,5-Di(*tert*-butyl)-1,4-benzohydroquinone - a novel inhibitor of liver microsomal Ca^{2+} sequestration. *FEBS Lett* 1987;224:331–336.
35. Tang D, Lahti JM, Kidd VJ. Caspase-8 activation and bid cleavage contribute to MCF7 cellular execution in a caspase-3-dependent manner during staurosporine-mediated apoptosis. *J Biol Chem* 2000;275:9303–9307.
36. Schmitz ML, Bacher S, Dienz O. NF- κ B activation pathways induced by T cell costimulation. *FASEB J* 2003;17:2187–2193.
37. Lee WJ, Monteith GR, Roberts-Thomson SJ. Calcium transport and signaling in the mammary gland: Targets for breast cancer. *Biochim Biophys Acta - Rev Cancer* 2006;1765:235–255.
38. Tadini-Buoninsegni F, Smeazzetto S, Gualdani R, Moncelli MR. Drug interactions with the Ca^{2+} -ATPase from sarco(endo)plasmic reticulum (SERCA). *Front Mol Biosci* 2018;5:36.
39. Demarex N. Cell biology: Apoptosis--the calcium connection. *Science* 2003;300:65–67.
40. Verecsi AE, Moreno SN, Bernardes CF, Meinicke AR, Fernandes EC, Docampo R. Thapsigargin causes Ca^{2+} release and collapse of the membrane potential of *Trypanosoma brucei* mitochondria in situ and of isolated rat liver mitochondria. *J Biol Chem* 1993;268:8564–8568.

Sub-lineages of the Omicron variant of SARS-CoV-2: characteristic mutations and their relation to epidemiological behavior.

José Luis Zambrano¹, Rossana C Jaspe², Mariana Hidalgo³, Carmen L Loureiro², Yoneira Sulbarán², Zoila C Moros¹, Domingo J Garzaro², Esmeralda Vizzi⁴, Héctor R Rangel², Ferdinando Liprandi⁴, and Flor H Pujol²

¹Laboratorio de Virología Celular, Centro de Microbiología y Biología Celular, Instituto Venezolano de Investigaciones Científicas, Caracas, Miranda, Venezuela.

²Laboratorio de Virología Molecular, Centro de Microbiología y Biología Celular, Instituto Venezolano de Investigaciones Científicas, Caracas, Miranda, Venezuela.

³Laboratorio de Inmunoparasitología, Centro de Microbiología y Biología Celular, Instituto Venezolano de Investigaciones Científicas, Caracas, Miranda, Venezuela.

⁴Laboratorio de Biología de Virus, Centro de Microbiología y Biología Celular, Instituto Venezolano de Investigaciones Científicas, Caracas, Miranda, Venezuela.

Key words: COVID-19; SARS-CoV-2; Omicron Variant of Concern; mutations; tropism.

Abstract. By the end of 2021, the Omicron variant of SARS-CoV-2, the coronavirus responsible for COVID-19, emerges, causing immediate concern, due to the explosive increase in cases in South Africa and a large number of mutations. This study describes the characteristic mutations of the Omicron variant in the Spike protein, and the behavior of the successive epidemic waves associated to the sub-lineages throughout the world. The mutations in the Spike protein described are related to the virus ability to evade the protection elicited by current vaccines, as well as with possible reduced susceptibility to host proteases for priming of the fusion process, and how this might be related to changes in tropism, a replication enhanced in nasal epithelial cells, and reduced in pulmonary tissue; traits probably associated with the apparent reduced severity of Omicron compared to other variants.

Sub-linajes de la variante Ómicron del SARS-CoV-2: mutaciones características y su relación con el comportamiento epidemiológico.

Invest Clin 2022; 63 (3): 262 – 274

Palabras clave: COVID-19; SARS-CoV-2; variante de preocupación Ómicron; mutaciones; tropismo.

Resumen. A finales de 2021 surge la variante Omicron del SARS-CoV-2, el coronavirus responsable de la COVID-19, causando preocupación inmediata, debido al aumento explosivo de casos en Suráfrica, y a su gran cantidad de mutaciones. Este estudio describe las mutaciones características de la variante Ómicron en la proteína de la Espiga (S) y el comportamiento de las sucesivas olas epidémicas asociadas a la circulación de sus sub-linajes en todo el mundo. Las mutaciones en la proteína S descritas están relacionadas con su capacidad para evadir la protección provocada por las vacunas actuales, así como su posible susceptibilidad reducida a las proteasas del hospedero para la preparación del proceso de fusión. Se infiere cómo esto podría estar relacionado con su cambio en el tropismo, con una replicación mayor en las células epiteliales nasales y menor en el tejido pulmonar, rasgos probablemente asociados a su aparente menor gravedad en comparación con otras variantes.

Received: 10-07-2022

Accepted: 22-07-2022

INTRODUCTION

SARS-CoV-2 infection, responsible for the COVID-19 pandemic, has caused more than 550 million cases and more than 6 million deaths worldwide until June 2022. This virus belongs to the family *Coronaviridae*. This family comprises enveloped viruses, with a positive sense genome of around 30,000 nt. In the case of SARS-CoV-2, the genome codes for four structural proteins (nucleocapsid or N, spike or S, membrane or M and envelope or E), 15 non-structural proteins and eight accessory proteins. The S protein contains two regions: S1, which includes the receptor-binding domain (RBD), and S2, with the furin-cleavage site and the fusion peptide. RBD, specifically the receptor binding motif (RBM), is the region responsible for the attachment to the angiotensin-converting enzyme 2 (ACE2) cellular recep-

tor (Fig. 1)^{1,2}. Two other putative receptors (Asialoglycoprotein Receptor 1 - ASGR1- and KREMEN1) have been described recently for SARS-CoV-2, which are not used by the previous SARS-CoV. The virus appears to interact with these two additional receptors through the RBD and also with N-terminal domain of the S1 region^{3,4}. These new candidates add to the list of other potential ligands that may interact with SARS-CoV-2^{5,6}.

During these two years of a high rate of replication, this virus has accumulated several mutations, allowing for its classification in more than 2000 lineages by June 2022⁷⁻⁹. Some of these lineages were denominated as variants by WHO¹⁰. These variants (lineages of viruses sharing particular types of mutations) emerged since the end of 2020, and were defined as Variants Under Monitoring (VUM), Variants of Interest (VOI), and Variants of Concern (VOC),

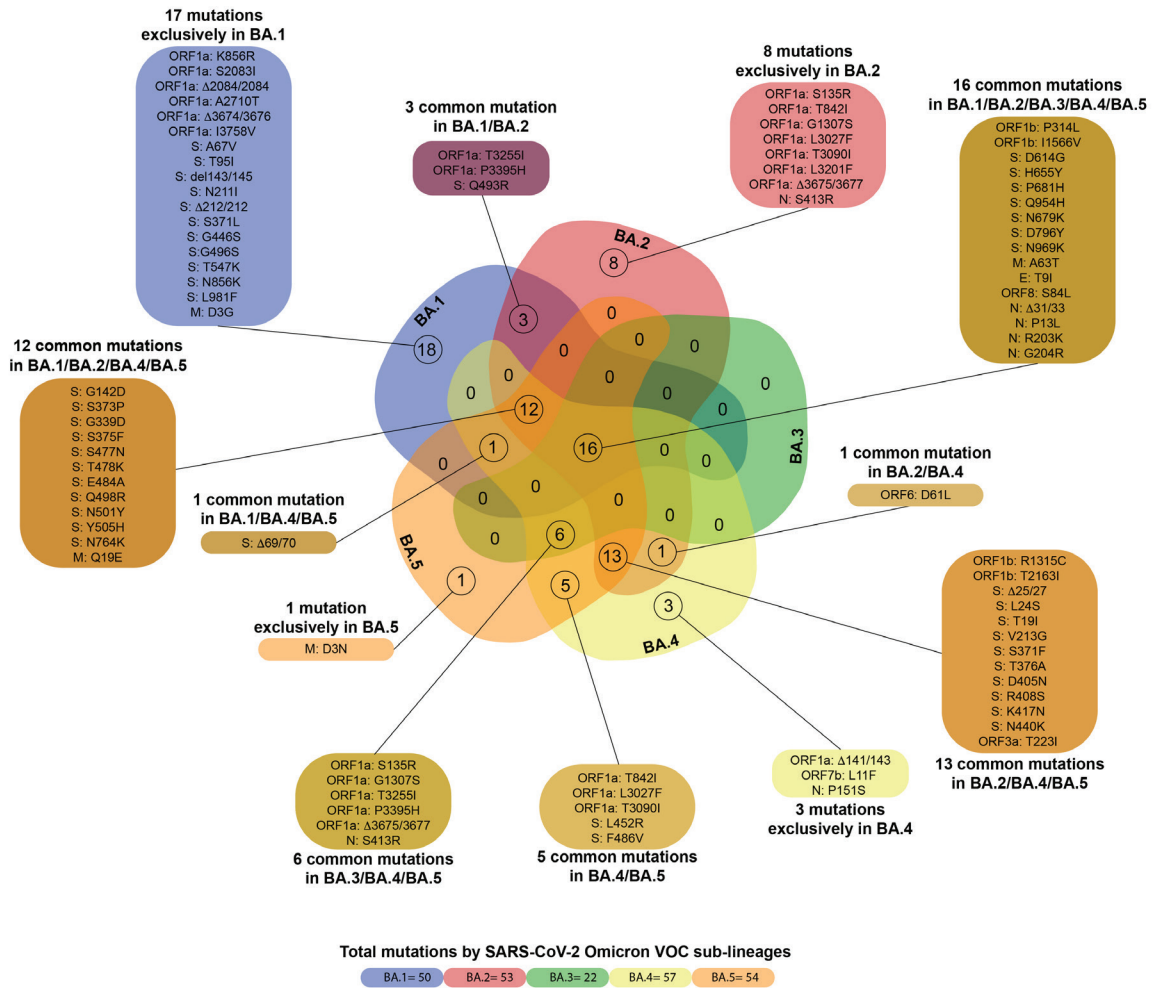


Fig. 1. Mutations of the SARS-CoV-2 Omicron VOC sub-lineages. Venn diagram showing common mutations between the SARS-CoV-2 Omicron VOC sub-lineages.

when any different phenotypic trait, such as increased transmissibility or immune evasion, among others, was suspected for the two firsts and confirmed for the last¹⁰. Until June 2022, five VOCs were described: Alpha variant, which emerged in the UK (lineage B.1.1.7), Beta variant in South Africa (B.1.351), Gamma variant in Brazil (P1), Delta variant in India (B.1.617.2), and Omicron variant, first identified in South Africa (B.1.1529). The last one was included in the list of VOCs very soon after its identification. By the end of June, only the Omicron VOC and its sub-lineages were present as a VOC¹⁰.

This variant caused immediate concern, due to the explosive increase in cases in South Africa¹¹, and the large number of mutations exhibited by this new lineage. In this study, we describe the characteristic mutations of the Omicron variant of SARS-CoV-2, and the behavior of the epidemic waves associated with the dissemination of the different sub-lineages throughout the world.

MATERIALS AND METHODS

Description of the mutations characteristic of each sub-lineage of Omicron. The identification of characteristic muta-

tions of the five sub-lineages of Omicron was performed using the following databases: SARS-CoV-2 lineages (Cov-lineages.org), Outbreak.info and; GISAID EpiFlu™ (https://www.gisaid.org/). The Venn diagram was made in Bioinformatics & Systems Biology UGent/VIB (bioinformatics.psb.ugent.be), and edited in Illustrator CC (ver. 23.0.1).

Analysis of the frequency of Omicron VOC in the world from November 2021 to May 2022. The number of sequences of Omicron VOC available at the GISAID database (https://www.gisaid.org/) on June 26, 2022 was compared to the total number of sequences for each month, between November 2021 and May 2022.

Frequency of Omicron VOC sub-lineages in the world. The number of sequences reported for each Omicron VOC sub-lineage, together with the date of the first and peak detection, were analyzed from “SARS Cov2-Lineages.” https://cov-lineages.org/lineage_list.html⁹, and accessed on June 26, 2022.

Analysis of the epidemic waves caused by the Omicron VOC in different countries. The peak number of cases caused by the circulating Omicron VOC was analyzed in selected countries, and compared with the previous highest peak of cases occurring in the same country, using the Worldometer database (https://www.worldometers.info/coronavirus/, accessed on July 1, 2022).

RESULTS

Key mutations of the Omicron variant

The Omicron variant exhibits a large number of mutations in its genome, particularly in the S protein (Fig. 1). Five sub-lineages of the Omicron variant have already been identified, which exhibit some differences with the original B.1.1.529 lineage and between them (Figs. 1 and 2). Additionally, a recombinant BA.1/BA.2 sub-lineage has also been described (Table 1).

The number of mutations exhibited by the different sub-lineages of Omicron VOC ranges from 22 for BA.3 to 57 in BA.4. Key mutations of the S protein and present in almost all the sub-lineages are shown in Fig. 2. The S371L, K417N, and N440K mutations, although not present in all the BA.1 isolates, are however also frequently found, according to a search in GISAID database (data not shown) In the case of BA.3, many key mutations present in the other lineages of Omicron, such as D405N, K417N, N440K, T478K, E484A and N501Y, were found in most sequences of lineage BA.3 available in the GISAID database (data not shown).

Of particular relevance is the absence of the deletion of the amino acids 69 and 70 in the S protein in the BA.2 sub-lineage, which instead possesses a deletion of the amino acids 25 to 27⁹ (Fig. 1). Another important mutation acquired by the BA.4 and

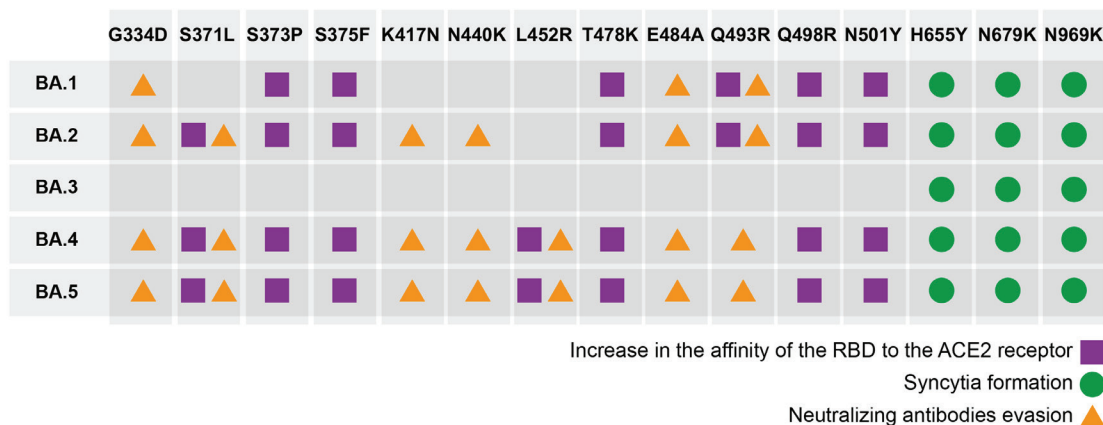


Fig. 2. Key mutations in the different Omicron VOC sub-lineages.

Table 1
Description of Omicron VOC sub-lineages.

Omicron main lineage	Sub-lineages ¹	Date of first detection	Date of peak detection ²	Number of sequences ³
BA.1	50 (54)	2/9/21	4/1/22	2166293
BA.2	53 (108)	11/10/21 ⁴	28/3/22	1625851
BA.3	2	23/11/21	3/2/22	745
BA.4	1 (4)	10/1/22	25/5/22	13334
BA.5	2 (15)	5/1/22	30/5/22	27560
XE ⁵	1	19/1/22	28/3/22	2438

Information from (9), accessed on June 26, 2022.

¹ The effective number of sub lineages is shown, with the number of proposed ones indicated under parentheses.

² Date when the highest number of sequences were available was June 26, 2022. This date may change, particularly for lineages BA.4 and BA.5, which are more actively disseminating in June 2022.

³ The number of total sequences tentatively assigned to this lineage is shown.

⁴ An earlier date of detection is reported for sub-lineage BA.2.3 (29/9/21).

⁵ Recombinant BA.1/BA.2.

BA.5 sub-lineages is the L452R mutation (Fig. 2), a key mutation in the Delta VOC, which was previously identified, particularly in some Californian variants. The sub-lineage BA.2.12.1 carries the mutation L452Q, previously described in the C.37 VOI⁹.

Omicron dissemination and sub-lineages

Soon after its emergence, the Omicron VOC displaced very rapidly the other lineages circulating in the world, mainly the Delta VOC (Fig. 3). At the end of June 2022, the Omicron VOC was the only VOC recognized by the WHO, although some Delta VOC isolates were still described in the GISAID database.

At the end of June 2022, the most frequent lineages found in several parts of the world were the sub-lineages BA.2.12.1, BA.4 and BA.5. These 3 lineages are expected to circulate abundantly in the next months of 2022. Very few sequences of sub-lineage BA.3 were available at GISAID database (Table 1).

Table 2 shows some representative patterns of the epidemic waves caused by the Omicron VOC and its successive sub-lineages. Generally, the Omicron VOC dissemination caused an epidemic wave of unprecedented magnitude, when compared to the

previous waves. Exceptions to this are India and Iran, for which the ratio of Peak number of cases with Omicron VOC/Peak number of cases before Omicron VOC (PNO/PNBO) was below 1 (Table 2). Additionally, this ratio is highly variable between countries, being generally lower in American countries, compared to European ones, for example. The second epidemic wave of Omicron VOC, due to the dissemination of sub-lineages such as BA.2, BA.4 and BA.5, was observed earlier in many countries of Europe, while in America, for example, some countries were suffering an ongoing peak at the end of June 2022 (Table 2).

Several factors may have affected the analysis. The testing capacity of each country, which ranged in July 1, 2022, from five tests/million inhabitants in Algeria, to 21,890,462 tests/million inhabitants in Denmark (<https://www.worldometers.info/coronavirus/>), may have limited more accurate estimation of cases during the epidemic waves, particularly during the Omicron VOC one. With the highest testing capacity, Denmark exhibited a high PNO/PNBO of 11.54 (Table 2). The intensity of the Delta VOC epidemic wave, which was particularly high in some Asian countries, like India and Iran,

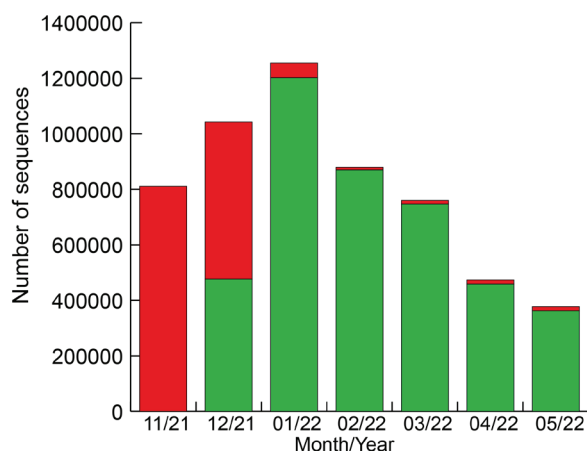


Fig. 3. Frequency of Omicron VOC around the world from November 2021 to May 2022. Green: Omicron VOC. Red: other lineages, mainly Delta VOC. From GISAID (<https://www.gisaid.org/> accessed on June 26, 2022). In November 2021, only 3217 sequences of Omicron were available out of 810820 total sequences.

led to a reduction of this ratio in these countries, probably combined with saturated testing capacities. PNO/PNBO is of particular interest in countries like South Korea (83.58), Australia (59.61) and New Zealand (unassigned since no peak in the number of cases was observed before the Omicron wave (Table 2). In Colombia and Venezuela, for example, the PNO/PNBO was close to 1 (Table 2). In addition to possible testing saturation during the Omicron VOC wave in these countries, the lower severity associated with this variant, particularly in young persons, may have reduced the demand for testing in some groups.

DISCUSSION

Soon after its identification, the Omicron variant was declared as a VOC, especially due to the huge number of mutations it harbors¹¹. Of the more than 30 mutations present in the Omicron variant in the S protein, around half of them are located in the RBD¹². Some of these mutations can be used detecting of this VOC by rapid methods¹³. Seven produce a modest increase in the affinity

of the RBD for the ACE2 receptor: Q493R, N501Y, S371L, S373P, S375F, Q498R, and T478K^{12,14}. It has been shown that Omicron VOC can infect murine cell lines¹⁵. At least two of the substitutions responsible for the increase in affinity for the human ACE2 receptor are also responsible for the increase in binding to mouse ACE2: Q493R and Q498R^{15,16}. Furthermore, the molecular spectrum of Omicron-acquired mutations was significantly different from the spectrum for viruses that evolved in human patients. However, it resembles the spectra associated with virus evolution in a mouse cellular environment. These observations lead to the suggestion that the progenitor of Omicron might have jumped from humans to mice, accumulating mutations conducive to infecting that host, then jumping back into humans, indicating an interspecies evolutionary trajectory for the Omicron outbreak¹⁵. Thus, this increased propensity for reverse zoonosis makes this variant more likely than previous variants to establish an animal reservoir of SARS-CoV-2.

Recent studies show that Omicron VOC exhibit a replication enhanced in human primary nasal epithelial cells, and reduced in pulmonary cells¹⁷⁻²⁰. This trait appears to be related to the fact that, unlike other SARSCoV-2 variants, Omicron is capable of efficiently entering cells in a TMPRSS2-independent manner, via the endosomal route. This enables Omicron to infect a greater number of cells in the respiratory epithelium, allowing it to be more infectious at lower exposure doses and resulting in enhanced transmissibility¹⁷. Syncytia formation depends on the fusogenic activity of the S2 region of the S protein after cleavage by the TMPRSS2. The Omicron also forms fewer syncytia than other lineages^{20,21}. The authors suggest that this phenotypic trait may be due to the presence of the mutation N969K. The role of syncytia formation in the pathogenic effect of SARS-CoV-2 remains a matter of debate²². Other substitutions, such as N679K and H655Y, may be contributing to

Table 2
Omicron VOC epidemic waves in selected countries.

Country	Pop (M hab)	Cases ¹ (M)	PNBO ²	PNO ³	PNO /PNBO	SOP ⁴
America						
USA	334.9	89.4 (1)	310,438 (8/1/21)	908,909 (14/1/22)	2.93	140,047 (23/6/22)
Brazil	215.6	32.4 (3)	115,041 (23/6/21)	282,050 (3/2/22)	2.45	75,106 (30/6/22)
Argentina	45	9.4 (13)	41,080 (27/5/21)	139,853 (14/1/22)	3.40	8,314 (26/5/22)
Colombia	52	6.2 (18)	33,594 (26/6/21)	35,575 (15/1/22)	1.06	3,403 (28/6/22)
Mexico	131.6	6 (20)	28,953 (19/8/21)	60,552 (20/1/22)	2.09	32,216 (30/6/22)
Chile	19.4	4 (31)	9151 (9/4/22)	39,840 (10/2/22)	4.35	13,104 (17/5/22)
Venezuela	28.3	0.5 (86)	1,786 (4/4/21)	2,646 (30/1/22)	1.48	199 (24/6/22)
Africa						
South Africa	60.8	4 (30)	26,645 (3/7/21)	37,875 (12/12/22)	1.42	10,017 (11/5/22)
Asia						
India	1,407	43.5 (2)	414,433 (6/5/21)	347,254 (20/1/22)	0.88	19118 (30/6/22)
South Korea	51.3	18.4 (9)	7434 (17/12/21)	621,328 (17/3/22)	83.58	10,437 (29/6/22)
Iran	86.1	7.2 (17)	50,228 (17/8/21)	39,819 (7/2/22)	0.79	4,615 (5/4/22)
Hong Kong	7.6	1.2 (55)	absent	79,876 (3/3/21)	+++	2,352 (30/6/22)
Europe						
France	65.6	31.1 (4)	83,321 (7/11/20)	501,635 (25/1/22)	6.02	217,480 (29/3/22)
UK	68.6	22.7 (6)	83,088 (30/12/20)	275,618 (5/1/22)	3.32	109,320 (22/5/22)
Italy	60.3	18.6 (7)	41,386 (13/11/20)	228,740 (18/1/22)	5.53	100,823 (20/4/22)
Denmark	5.8	3 (39)	4,508 (18/2/20)	52,009 (10/2/22)	11.54	2,407 (28/6/22)
Oceania						
Australia	26.1	8.2 (16)	2,528 (9/10/21)	150,702 (13/1/22)	59.61	67,379 (30/3/22)
New Zealand	5	1.3 (53)	absent	24,106 (2/3/22)	+++	8,331 (28/6/22)

¹Cases: Total number of cases in millions (M) until July 1, 2022 (position in the ranking of cases).

²PNBO: Peak number of cases before Omicron VOC (date). ³PNO: Peak number with Omicron VOC (date).

⁴SOP: Secondary Omicron VOC peak (date).

this particular phenotype in Omicron VOC. The N679K substitution is located in the QTQTN motif upstream of the furin cleavage site (QTQTK in the Omicron VOC). The cleavage site is known to play an important role in viral pathogenesis. Its deletion attenuates viral replication in respiratory cells *in vitro* and attenuates disease *in vivo*²². The substitution N679K in the QTQTN motif of the Omicron VOC has been shown to reduce the affinity of the protein for furin, resulting in

a reduced susceptibility to serine proteases on the cell surface for entry^{23,24}. The substitution H655Y, in contrast, has been shown to enhance viral replication and spike protein cleavage²⁵.

One of the most striking characteristics of the Omicron VOC is its ability to evade protective immunity induced by previous infection or vaccination^{26,27}. In fact, it is believed that the increase in transmissibility of this variant is primarily due to its ability to

evade previous protective immunity rather than to of a higher affinity of its S protein for the ACE2 receptor²⁸. Several mutations of Omicron VOC could impair neutralizing antibodies (Nabs) with different specificities. Specifically, mutations K417N, G446S, E484A, and Q493R induce escape of NAbs in Group A-D, whose epitope overlaps with the ACE2-binding motif. Group E (S309 site) and F (CR3022 site) NAbs, which often exhibit broad *Sarbecovirus* neutralizing activity, are still somehow effective against the Omicron VOC, but mutations G339D, N440K, and S371L may induce resistance to a subset of Nabs²⁷.

The Omicron VOC also exhibits an insertion of 3 amino acids (EPE) in the N-terminal region of the S protein, at residue 214. This insertion of EPE has not been observed in other major variants of SARS-CoV-2 and may induce a structural change, which might be associated with a decrease in neutralizing antibody binding ability to this region. This genomic insertion has also been suggested to be incorporated into SARS-CoV-2 by recombination with another coronavirus or even other respiratory pathogens^{29,30}. The mutation L452R present in sub-lineages BA.4 and BA.5, may confer to these Omicron VOC sub-lineages an increased immune evasion^{31,32}, and may also contribute to the dissemination of these lineages. The sub-lineages more frequent in June 2022, BA.2.12.1, BA.4 and BA.5, exhibit an increased potential of breakthrough infection after vaccination and infection, even with a previous infection with another Omicron VOC³³⁻³⁵.

In contrast, the sub-lineage BA.3 of the Omicron VOC did not exhibit wide dissemination, compared to the other ones. This may be related to the absence of many key mutations exhibited by the other sub-lineages, related to increased transmissibility and immune evasion (Figs. 1 and 2). However, the number of mutations found in this sub-lineage is also variable among different isolates, and some of those key mutations are also frequently found.

Several lines of evidence suggest that the Omicron VOC is highly more transmissible than all previous variants, in addition to the reduced sensitivity to the immune protection conferred by vaccines and previous infections. The effective and basic reproduction numbers of the Omicron variant have been estimated to be 3.8 and 2.5 times higher than that of the Delta variant, respectively, which was the previous VOC displaying the highest reproduction numbers³⁶.

From this significant increase in transmissibility and resistance to previous immunity, it could be inferred at a first glance, that the clinical course of the Omicron VOC might be more severe. However, the changed tropism of this variant, to a virus infecting more the upper respiratory airway, compared to the lungs, suggests that is the contrary. Indeed, several studies point to a less severe clinical course of infection with the Omicron VOC, compared to the infection caused by the Delta VOC.

The first evidence comes from *in vitro* and animal model infections, where the Omicron VOC exhibited an attenuated phenotype³⁷. The early studies of the Omicron VOC in South Africa also suggested a reduced odd of severity for the patients infected with this VOC³⁸. This trend was confirmed in a retrospective observational study³⁹. The same observation was found among US Veterans⁴⁰. Children in Israel were less prone to develop multisystem inflammatory syndrome (MISC), a common sequel of COVID-19 in children, during the Omicron VOC wave, than during the Delta and Alpha VOC waves⁴¹.

The emergence of Omicron VOC and its sub-lineages led to an abrupt epidemic peak worldwide⁴². However, differences in the intensity of the epidemic peak caused by the Omicron VOC were however observed between countries. For example, countries such as South Korea, Australia, and New Zealand were characterized by a successful control of COVID-19 during the pandemic⁴³⁻⁴⁵, until the Omicron VOC wave. The increased transmission ability of the Omicron VOC al-

lowed it to spread widely even in countries with previous highly successful control measures. Finally, the great disparities in vaccination coverage between countries⁴⁶, also had a profound influence on the intensity of the Delta and Omicron VOC waves.

In conclusion, the Omicron VOC displays a great number of mutations, some of them already present in previous lineages. Although associated with a high attack rate and immune evasion, this variant seems to be associated with lower severity, compared to previous ones. A probable explanation for this somehow attenuated phenotype could be related to its resistance to the cleavage of TMPRSS2 and probably furin, and its reduced ability to form syncytia, leading to increased tropism for epithelia over the lungs. The reduced effectivity observed for various vaccines to protect against infection with this variant has not hampered its effectiveness in reducing the morbidity and mortality of COVID-19, particularly with a booster dose, which still induces neutralizing antibodies⁴⁷. The well-known non-pharmacological preventive interventions (mask, social distancing, ventilation and frequent hand hygiene), together with vaccination, are still the most effective measures to reduce the burden of this highly contagious variant.

Funding

This study was supported by IVIC, Ministerio del Poder Popular de Ciencia, Tecnología e Innovación de Venezuela.

Conflict of interest

The authors declared that they have no competing interests.

Authors contribution

Design of the study and writing of the manuscript: JLZ, RCJ, FL, FHP. Data analysis: JLZ, RCJ, MH, YS, CLL, ZCM, DJG, EV, HRR, FHP. All the authors read and approved the final version of the manuscript.

Author's ORCID numbers

- José Luis Zambrano:
0000-0001-9884-2940
- Rossana C Jaspe:
0000-0002-4816-1378
- Mariana Hidalgo:
0000-0002-8307-8254
- Yoneira Sulbarán:
0000-0002-3170-353X
- Carmen L Loureiro:
0000-0003-3665-1107
- Zoila C Moros:
0000-0001-6322-9230
- Domingo J Garzaro:
0000-0002-9956-5786
- Esmeralda Vizzi:
0000-0001-6865-1617
- Héctor R Rangel:
0000-0001-5937-9690
- Ferdinando Liprandi:
0000-0001-8084-8252
- Flor H Pujol:
0000-0001-6086-6883

REFERENCES

1. V'kovski P, Kratzel A, Steiner S, Stalder H, Thiel V. Coronavirus biology and replication: implications for SARS-CoV-2. *Nat Rev Microbiol* 2020; 19(3): 155–170. *Doi: 10.1038/s41579-020-00468-6*.
2. Pujol FH, Zambrano JL, Jaspe RC, Loureiro CL, Vizzi E, Liprandi F, Rangel HR. Biología y evolución del coronavirus causante de la COVID-19. *Rev Soc Venezol Microbiol* 2020; 40:63-73.
3. Gu Y, Cao J, Zhang X, Gao H, Wang Y, Wang J, He J, Jiang X, Zhang J, Shen G, Yang J, Zheng X, Hu G, Zhu Y, Du S, Zhu Y, Zhang R, Xu J, Lan F, Qu D, Xu G, Zhao Y, Gao D, Xie Y, Luo M, Lu Z. Receptome profiling identifies KREMEN1 and ASGR1 as alternative functional receptors of SARS-CoV-2. *Cell Res* 2022;32(1):24-37. *Doi: 10.1038/s41422-021-00595-6*.

4. Hoffmann M, Pöhlmann S. Novel SARS-CoV-2 receptors: ASGR1 and KREMEN1. *Cell Res* 2022;32(1):1-2. *Doi: 10.1038/s41422-021-00603-9*.
5. Rangu R, Wander PL, Barrow BM, Zraika S. Going viral in the islet: mediators of SARS-CoV-2 entry beyond ACE2. *J Mol Endocrinol* 2022;69(2):R63-R79. *Doi: 10.1530/JME-21-0282*.
6. Eslami N, Aghbash PS, Shamekh A, Entezari-Maleki T, Nahand JS, Sales AJ, Baghi HB. SARS-CoV-2: Receptor and Coreceptor Tropism Probability. *Curr Microbiol* 2022;79(5):133. *Doi: 10.1007/s00284-022-02807-7*.
7. Rambaut A, Holmes EC, O'Toole Á, Hill V, McCrone JT, Ruis C, du Plessis L, Pybus OG. A dynamic nomenclature proposal for SARS-CoV-2 lineages to assist genomic epidemiology. *Nat Microbiol*. 2020;5(11):1403-1407. *Doi: 10.1038/s41564-020-0770-5*.
8. O'Toole Á, Scher E, Underwood A, Jackson B, Hill V, McCrone JT, Colquhoun R, Ruis C, Abu-Dahab K, Taylor B, Yeats C, du Plessis L, Maloney D, Medd N, Attwood SW, Aanensen DM, Holmes EC, Pybus OG, Rambaut A. Assignment of epidemiological lineages in an emerging pandemic using the pangolin tool. *Virus Evol* 2021;7(2):veab064. *Doi: 10.1093/ve/veab064*.
9. "SARS Cov2-Lineages." https://cov-lineages.org/lineage_list.html. [Accessed on June 26, 2022].
10. World Health Organization. "Tracking SARS-CoV-2 variants." <https://www.who.int/en/activities/tracking-SARS-CoV-2-variants/>. [Accessed on June 26, 2022].
11. Viana R, Moyo S, Amoako DG, Tegally H, Scheepers C, Althaus ChL, Anyaneji UJ, Bester PhA, Boni MF, Chand M, Choga WT, Colquhoun R, Davids M, Deforche K, Doolabh D, du Plessis L, Engelbrecht S, Everatt J, Giandhari J, Giovanetti M, Hardie D, Hill V, Hsiao NY, Iranzadeh A, Ismail A, Joseph Ch, Joseph R, Koopile L, Kosakovsky Pond SL, Kraemer MUG, Kuate-Lere L, Laguda-Akingba O, Leseledi-Mafoko O, Lessells RJ, Lockman Sh, Lucaci AG, Maharaj A, Mahlangu B, Maponga T, Mahlakwane K, Makatini Z, Marais G, Maruapula D, Masupu K, Mats-
haba M, Mayaphi S, Mbhele N, Mbulawa MB, Mendes A, Mlisana K, Mnguni A, Mohale Th, Moir M, Moruisi K, Mosepele M, Motsatsi G, Motswaledi MS, Mphoyakgosi Th, Msomi N, Mwangi PN, Naidoo Y, Ntuli N, Nyaga M, Olubayo L, Pillay S, Radibe B, Ramphal Y, Ramphal U, San JE, Scott L, Shapiro R, Singh L, Smith-Lawrence P, Stevens W, Strydom A, Subramoney K, Tebeila N, Tshiabuila D, Tsui J, van Wyk S, Weaver S, Wibmer CK, Wilkinson E, Wolter N, Zarebski AE, Zuze B, Goedhals D, Preiser W, Treurnicht F, Venter M, Williamson C, Pybus OG, Bhiman J, Glass A, Martin DP, Rambaut A, Gaseitsiwe S, von Gottberg A, de Oliveira T. Rapid epidemic expansion of the SARS-CoV-2 Omicron variant in Southern Africa. *Nature* 2022;603(7902):679-686. *Doi: 10.1038/s41586-022-04411-y*.
12. Kumar S, Thambiraja TS, Karuppanan K, Subramaniam G. Omicron and Delta variant of SARS-CoV-2: A comparative computational study of spike protein. *J Med Virol* 2022;94(4):1641-1649. *Doi: 10.1002/jmv.27526*.
13. Jaspe RC, Zambrano JL, Hidalgo M, Sulbaran Y, Loureiro CL, Moros ZC, Garzaro DJ, Liprandi F, Rangel HR, Pujol FH. Detection of the Omicron variant of SARS-CoV-2 by restriction analysis targeting the mutations K417N and N440K of the Spike protein. *Invest. Clin* 2022;63(1):92-99. *Doi: 10.54817/IC.v63n1a08*.
14. Ortega JT, Jastrzebska B, Rangel HR. Omicron SARS-CoV-2 Variant Spike Protein Shows an Increased Affinity to the Human ACE2 Receptor: An *In Silico* Analysis. *Pathogens* 2021;11(1):45. *Doi: 10.3390/pathogens11010045*.
15. Wei C, Shan KJ, Wang W, Zhang S, Huan Q, Qian W. Evidence for a mouse origin of the SARS-CoV-2 Omicron variant. *J Genet Genomics* 2021;48(12):1111-1121. *Doi: 10.1016/j.jgg.2021.12.003*.
16. Yan K, Dumenil T, Le TT, Tang B, Bishop C, Suhrbier A, Rawle DJ. Passage of SARS-CoV-2 in cells expressing human and mouse ACE2 selects for mouse-adapted and ACE2-independent viruses. *bioRxiv* 2021; 12.16.473063. *doi: 10.1101/2021.12.16.473063*.

17. Peacock TP, Brown JC, Zhou J, Thakur N, Sukhova K, Newman J, Kugathasan R, Yan AWC, Furnon W, De Lorenzo G, Cowton VM, Reuss D, Moshe M, Quantrell JL, Platt OK, Kaforou M, Patel AH, Palmarini M, Bailey D, Barclay WS. The altered entry pathway and antigenic distance of the SARS-CoV-2 Omicron variant map to separate domains of spike protein. *bioRxiv* 2021;12.31.474653; *Doi*: 10.1101/2021.12.31.474653.
18. Hui KPY, Ho JCW, Cheung MC, Ng KC, Ching RHH, Lai KL, Kam TT, Gu H, Sit KY, Hsin MKY, Au TWK, Poon LLM, Peiris M, Nicholls JM, Chan MCW. SARS-CoV-2 Omicron variant replication in human bronchus and lung ex vivo. *Nature* 2022; 603(7902):715-720. *Doi*: 10.1038/s41586-022-04479-6.
19. Abdelnabi R, Foo CS, Zhang X, Lemmens V, Maes P, Slechten B, Raymenants J, André E, Weynand B, Dallmeier K, Neyts J. The omicron (B.1.1.529) SARS-CoV-2 variant of concern does not readily infect Syrian hamsters. *Antiviral Res.* 2022; 198:105253. *Doi*: 10.1016/j.antiviral.2022.105253.
20. Zhao H, Lu L, Peng Z, Chen LL, Meng X, Zhang C, Ip JD, Chan WM, Chu AW, Chan KH, Jin DY, Chen H, Yuen KY, To KK. SARS-CoV-2 Omicron variant shows less efficient replication and fusion activity when compared with Delta variant in TMPRSS2-expressed cells. *Emerg Microbes Infect.* 2022;11(1):277-283. *Doi*: 10.1080/22221751.2021.2023329.
21. Rajah MM, Hubert M, Bishop E, Saunders N, Robinot R, Grzelak L, Planas D, Dufloo J, Gellenoncourt S, Bongers A, Zivaljic M, Planchais C, Guivel-Benhassine F, Porrot F, Mouquet H, Chakrabarti LA, Buchrieser J, Schwartz O. SARS-CoV-2 Alpha, Beta, and Delta variants display enhanced Spike-mediated syncytia formation. *EMBO J* 2021; 40(24):e108944. *Doi*: 10.15252/embj.2021108944.
22. Koch J, Uckeley ZM, Lozach PY. SARS-CoV-2 variants as super cell fusers: cause or consequence of COVID-19 severity? *EMBO J* 2021;40(24):e110041. *Doi*: 10.15252/embj.2021110041.
23. Vu MN, Lokuğamage KG, Plante JA, Scharton D, Johnson BA, Sotcheff S, Swetnam DM, Schindewolf Cr, Alvarado RE, Crocquet-Valdes PA, Debbink K, Weaver SC, Walker DH, Routh AL, Plante KS, Menachery VD. QTQTN motif upstream of the furin-cleavage site plays key role in 9SARS-CoV-2 infection and pathogenesis. *bioRxiv* 2021;12.15.472450; *Doi*: 10.1101/2021.12.15.472450.
24. Jawaid MZ, Baidya A, Jakovcevic S, Lusk J, Mahboubi-Ardakani R, Solomon N, Gonzalez G, Arsuaga J, Vazquez M, Davis RL, Cox DL. Computational study of the furin cleavage domain of SARS-CoV-2: delta binds strongest of extant variants. *bioRxiv* 2022; 01.04.475011. *doi*: 10.1101/2022.01.04.475011.
25. Escalera A, Gonzalez-Reiche AS, Aslam S, Mena I, Laporte M, Pearl RL, Fossati A, Rathnasinghe R, Alshammary H, van de Guchte A, Farrugia K, Qin Y, Bouhaddou M, Kehrer T, Zuliani-Alvarez L, Meekins DA, Balaraman V, McDowell C, Richt JA, Bajic G, Sordillo EM, Dejosez M, Zwaka TP, Krogan NJ, Simon V, Albrecht RA, van Bakel H, Garcia-Sastre A, Aydilto T. Mutations in SARS-CoV-2 variants of concern link to increased spike cleavage and virus transmission. *Cell Host Microbe* 2022; 30(3):373-387.e7. *Doi*: 10.1016/j.chom.2022.01.006.
26. Dejnirattisai W, Huo J, Zhou D, Zahradník J, Supasa P, Liu C, Duyvesteyn HME, Ginn HM, Mentzer AJ, Tuekprakhon A, Nutalai R, Wang B, Dijokaite A, Khan S, Avinoam O, Bahar M, Skelly D, Adele S, Johnson SA, Amini A, Ritter TG, Mason C, Dold C, Pan D, Assadi S, Bellass A, Omo-Dare N, Koeckerling D, Flaxman A, Jenkin D, Aley PK, Voysey M, Costa Clemens SA, Naveca FG, Nascimento V, Nascimento F, Fernandes da Costa C, Resende PC, Pauvolid-Correa A, Siqueira MM, Baillie V, Serafin N, Kwatra G, Da Silva K, Madhi SA, Nunes MC, Malik T, Openshaw PJM, Baillie JK, Semple MG, Townsend AR, Huang KA, Tan TK, Carroll MW, Klenerman P, Barnes E, Dunachie SJ, Constantinides B, Webster H, Crook D, Pollard AJ, Lambe T; OPTIC Consortium; ISARIC4C Consortium, Paterson NG, Williams MA, Hall DR, Fry EE, Mongkolsapaya J, Ren J, Schreiber G, Stuart DI, Sreaton GR. SARS-CoV-2 Omi-

- cron-B.1.1.529 leads to widespread escape from neutralizing antibody responses. *Cell* 2022;185(3):467-484.e15. *Doi: 10.1016/j.cell.2021.12.046.*
27. Cao Y, Wang J, Jian F, Xiao T, Song W, Yisimayi A, Huang W, Li Q, Wang P, An R, Wang J, Wang Y, Niu X, Yang S, Liang H, Sun H, Li T, Yu Y, Cui Q, Liu S, Yang X, Du S, Zhang Z, Hao X, Shao F, Jin R, Wang X, Xiao J, Wang Y, Xie XS. Omicron escapes the majority of existing SARS-CoV-2 neutralizing antibodies. *Nature*. 2022; 602(7898):657-663. *Doi: 10.1038/s41586-021-04385-3.*
 28. Yao L, Zhu KL, Jiang XL, Wang XJ, Zhan BD, Gao HX, Geng XY, Duan LJ, Dai EH, Ma MJ. Omicron subvariants escape antibodies elicited by vaccination and BA.2.2 infection. *Lancet Infect Dis*. 2022; S1473-3099(22)00410-8. *Doi: 10.1016/S1473-3099(22)00410-8.*
 29. Nersisyan S, Zhiyanov A, Zakharova M, Ishina I, Kurbatskaia I, Mamedov A, Galatenko A, Shkurnikov M, Gabibov A, Tonevitsky A. Alterations in SARS-CoV-2 Omicron and Delta peptides presentation by HLA molecules. *PeerJ* 2022;10:e13354. *Doi: 10.7717/peerj.13354.*
 30. Qin S, Cui M, Sun S, Zhou J, Du Z, Cui Y, Fan H. Genome Characterization and Potential Risk Assessment of the Novel SARS-CoV-2 Variant Omicron (B.1.1.529). *Zoonoses* 2021; Vol. 1(1). *Doi: 10.15212/ZOONOSES-2021-0024.*
 31. Motozono C, Toyoda M, Zahradnik J, Saito A, Nasser H, Tan TS, Ngare I, Kimura I, Uriu K, Kosugi Y, Yue Y, Shimizu R, Ito J, Torii S, Yonekawa A, Shimono N, Nagasaki Y, Minami R, Toya T, Sekiya N, Fukuhara T, Matsuura Y, Schreiber G. Genotype to Phenotype Japan (G2P-Japan) Consortium, Ikeda T, Nakağawa S, Ueno T, Sato K. SARS-CoV-2 spike L452R variant evades cellular immunity and increases infectivity. *Cell Host Microbe* 2021; 29(7):1124-1136.e11. *Doi: 10.1016/j.chom.2021.06.006.*
 32. Deng X, Garcia-Knight MA, Khalid MM, Servellita V, Wang C, Morris MK, Sotomayor-González A, Glasner DR, Reyes KR, Gliwa AS, Reddy NP, Sanchez San Martin C, Federman S, Cheng J, Balcerek J, Taylor J, Streithorst JA, Miller S, Sreekumar B, Chen PY, Schulze-Gahmen U, Taha TY, Hayashi JM, Simoneau CR, Kumar GR, McMahon S, Lidsky PV, Xiao Y, Hemarajata P, Green NM, Espinosa A, Kath C, Haw M, Bell J, Hacker JK, Hanson C, Wadford DA, Anaya C, Ferguson D, Frankino PA, Shivram H, Lareau LF, Wyman SK, Ott M, Andino R, Chiu CY. Transmission, infectivity, and neutralization of a spike L452R SARS-CoV-2 variant. *Cell* 2021;184(13):3426-3437.e8. *Doi: 10.1016/j.cell.2021.04.025.*
 33. Qu P, Faraone J, Evans JP, Zou X, Zheng YM, Carlin C, Bednash JS, Lozanski G, Mallampalli RK, Saif LJ, Oltz EM, Mohler PJ, Gumina RJ, Liu SL. Neutralization of the SARS-CoV-2 Omicron BA.4/5 and BA.2.12.1 Subvariants. *N Engl J Med* 2022; 386(26):2526-2528. *Doi: 10.1056/NEJMc2206725.*
 34. Cao Y, Yisimayi A, Jian F, Song W, Xiao T, Wang L, Du S, Wang J, Li Q, Chen X, Yu Y, Wang P, Zhang Z, Liu P, An R, Hao X, Wang Y, Wang J, Feng R, Sun H, Zhao L, Zhang W, Zhao D, Zheng J, Yu L, Li C, Zhang N, Wang R, Niu X, Yang S, Song X, Chai Y, Hu Y, Shi Y, Zheng L, Li Z, Gu Q, Shao F, Huang W, Jin R, Shen Z, Wang Y, Wang X, Xiao J, Xie XS. BA.2.12.1, BA.4 and BA.5 escape antibodies elicited by Omicron infection. *Nature* 2022. *Doi: 10.1038/s41586-022-04980-y.*
 35. Hachmann NP, Miller J, Collier AY, Ventura JD, Yu J, Rowe M, Bondzie EA, Powers O, Surve N, Hall K, Barouch DH. Neutralization Escape by SARS-CoV-2 Omicron Subvariants BA.2.12.1, BA.4, and BA.5. *N Engl J Med* 2022. *Doi: 10.1056/NEJMc2206576.*
 36. Liu Y, Rocklöv J. The effective reproductive number of the Omicron variant of SARS-CoV-2 is several times relative to Delta. *J Travel Med*; 29(3): taac037. *Doi: 10.1093/jtm/taac037.*
 37. Shuai H, Chan JF, Hu B, Chai Y, Yuen TT, Yin F, Huang X, Yoon C, Hu JC, Liu H, Shi J, Liu Y, Zhu T, Zhang J, Hou Y, Wang Y, Lu L, Cai JP, Zhang AJ, Zhou J, Yuan S, Brindley MA, Zhang BZ, Huang JD, To KK, Yuen KY, Chu H. Attenuated replication and pathogenicity of SARS-CoV-2 B.1.1.529 Omicron. *Nature* 2022; 603(7902):693-699. *Doi: 10.1038/s41586-022-04442-5.*
 38. Wolter N, Jassat W, Walaza S, Welch R, Moultrie H, Groome M, Amoako DG, Eve-

- ratt J, Bhiman JN, Scheepers C, Tebeila N, Chiwandire N, du Plessis M, Govender N, Ismail A, Glass A, Mlisana K, Stevens W, Treurnicht FK, Makatini Z, Hsiao NY, Parboosing R, Wadula J, Hussey H, Davies MA, Boule A, von Gottberg A, Cohen C. Early assessment of the clinical severity of the SARS-CoV-2 omicron variant in South Africa: a data linkage study. *Lancet* 2022;399(10323):437-446. *Doi: 10.1016/S0140-6736(22)00017-4*.
39. Jassat W, Abdool Karim SS, Mudara C, Welch R, Ozougwu L, Groome MJ, Govender N, von Gottberg A, Wolter N, Wolmarans M, Rousseau P; DATCOV author group, Blumberg L, Cohen C. Clinical severity of COVID-19 in patients admitted to hospital during the omicron wave in South Africa: a retrospective observational study. *Lancet Glob Health* 2022;10(7):e961-e969. *Doi: 10.1016/S2214-109X(22)00114-0*.
40. Mayr FB, Talisa VB, Castro AD, Shaikh OS, Omer SB, Butt AA. COVID-19 disease severity in US Veterans infected during Omicron and Delta variant predominant periods. *Nat Commun*. 2022;13(1):3647. *Doi: 10.1038/s41467-022-31402-4*.
41. Levy N, Koppel JH, Kaplan O, Yechiam H, Shahar-Nissan K, Cohen NK, Shavit I. Severity and incidence of multisystem inflammatory syndrome in children during 3 SARS-CoV-2 pandemic waves in Israel. *JAMA* 2022; 327(24):2452-2454. *Doi: 10.1001/jama.2022.8025*.
42. Jaspe RC, Sulbaran Y, Loureiro CL, Moros ZC, Marulanda E, Bracho F, Ramírez NA, Canonico Y, D'Angelo P, Rodríguez L, Castro J, Liprandi F, Rangel HR, Pujol FH. Detection of the Omicron variant of SARS-CoV-2 in international travelers returning to Venezuela. *Travel Med Infect Dis* 2022; 48:102326. *Doi: 10.1016/j.tmaid.2022.102326*.
43. Kang J, Jang YY, Kim J, Han SH, Lee KR, Kim M, Eom JS. South Korea's responses to stop the COVID-19 pandemic. *Am J Infect Control*. 2020; 48(9):1080-1086. *Doi: 10.1016/j.ajic.2020.06.003*.
44. Baker MG, Wilson N, Anglemeyer A. Successful Elimination of Covid-19 Transmission in New Zealand. *N Engl J Med*. 2020; 383(8):e56. *Doi: 10.1056/NEJMc2025203*.
45. Paterson DL, Rickard CM. Letter From Australia: A Never-Ending Pandemic? *Ann Intern Med*. 2021; 174(12):1743-1744. *Doi: 10.7326/M21-3295*.
46. Chen Z, Zheng W, Wu Q, Chen X, Peng C, Tian Y, Sun R, Dong J, Wang M, Zhou X, Zhao Z, Zhong G, Yan X, Liu N, Hao F, Zhao S, Zhuang T, Yang J, Azman AS, Yu H. Global diversity of policy, coverage, and demand of COVID-19 vaccines: a descriptive study. *BMC Med*. 2022; 20(1):130. *Doi: 10.1186/s12916-022-02333-0*.
47. Bowen JE, Addetia A, Dang HV, Stewart C, Brown JT, Sharkey WK, Sprouse KR, Walls AC, Mazzitelli IG, Logue JK, Franko NM, Czudnochowski N, Powell AE, Dellota Jr E, Ahmed K, Ansari AS, Cameroni E, Gori A, Bandera A, Posavad CM, Dan JM, Zhang Z, Weiskopp D, Sette A, Crotty S, Iqbal NT, Corti D, Geffner J, Snell G, Grifantini R, Chu HY, Veesler D. Omicron spike function and neutralizing activity elicited by a comprehensive panel of vaccines. *Science*. 2022; 19 Jul. *Doi: 10.1126/science.abq02*.

Calcinosis escrotal idiopática: Reporte de un caso.

Vanessa Bouquett¹ y Letmarié Sánchez²

¹Hospital Francisco Antonio Rísquez. Caracas, Venezuela.

²Unidad de Inmunología Clínica Diagnóstica. Caracas, Venezuela.

Palabras clave: calcinosis idiopática; calcinosis cutis.

Resumen. El calcio participa en muchos procesos fisiológicos. La calcinosis cutis es una enfermedad de depósito de calcio en la dermis. La calcinosis escrotal idiopática (CEI) es una forma común de calcinosis cutis idiopática. Se presenta el caso de un paciente masculino de 28 años de edad, con clínica de masas múltiples en escroto, de color blanco, tamaños variados, no dolorosas. Los niveles de calcio y fósforo se mostraron dentro de los rangos normales, característico de calcinosis de tipo idiopática, mientras que la vitamina D y la PTH se mostraron fuera de los límites normales. Se realiza una cirugía menor de las lesiones nodulares circunscritas, de diversos tamaños y de bordes regulares. El examen histológico post-biopsia confirmó el diagnóstico de calcinosis cutis. Se prescribió una dieta baja en calcio como método preventivo a largo plazo. A pesar de lo infrecuente de esta condición debe tenerse en cuenta al realizar un diagnóstico diferencial. Su etiología es aún desconocida y puede presentarse de manera asintomática. Lo importante es brindar al paciente una mejor calidad de vida, evitar incomodidades y baja autoestima debido al aspecto estético.

Idiopathic scrotal calcinosis. A case report.

Invest Clin 2022; 63 (3): 275 – 282

Key words: idiopathic calcinosis; calcinosis cutis.

Abstract. Calcium participates in many physiological processes. Calcinosis cutis is a disease caused by calcium deposition in the dermis. Idiopathic scrotal calcinosis (ICS) is a common form of idiopathic calcinosis cutis. A 28-year-old male patient was evaluated, with symptoms of multiple white masses in the scrotum, of various sizes, not painful. Calcium and phosphorus levels were within normal ranges, characteristic of idiopathic calcinosis, while vitamin D and PTH were outside the normal limits. Minor surgery was performed on circumscribed nodular lesions of various sizes with regular borders. Post-biopsy histological examination confirmed the diagnosis of calcinosis cutis. A low-calcium diet was prescribed as a long-term preventive method. Despite the infrequency of this condition, it should be taken into account when making a differential diagnosis. Its etiology is still unknown and it can present asymptotically. The important thing is to provide the patient with a better quality of life, avoid discomfort and low self-esteem due to the aesthetic aspect.

Recibido: 29-01-2022

Aceptado: 06-05-2022

INTRODUCCIÓN

El calcio constituye del 1 al 2% del peso corporal total de un individuo¹. Regula las principales funciones de los queratinocitos epidérmicos, incluida la proliferación, diferenciación y adhesión célula-célula. Al menos tres hormonas reguladoras controlan la concentración de calcio iónico en el suero: la hormona paratiroidea (PTH), la calcitonina y la 1,25-dihidroxitamina D₃ (1,25 (OH) 2D₃)².

El depósito de calcio y fosfatos a nivel extraesquelético se presenta frecuentemente por la precipitación de sales amorfas, sin embargo, no hay evidencia clara acerca de los fenómenos metabólicos que rigen estos depósitos³.

La calcinosis cutis es una enfermedad de depósito de calcio en la dermis; existen 5 formas en las cuales puede presentarse: metastática, distrófica, iatrogénica, calcifilaxis e idiopática. En la forma metastática,

el paciente tiene niveles séricos anormales de calcio, fósforo o ambos; en la forma distrófica, el paciente tiene niveles normales de calcio y fósforo, pero las condiciones locales como la inflamación favorecen la formación de depósitos de calcio; la forma iatrogénica depende del uso terapéutico o diagnóstico, de sustancias que contienen calcio o fosfato. La calcifilaxis o arteriopatía urémica calcificante, es una entidad que se define como la calcificación de la capa media de vasos de pequeño y mediano tamaño de la dermis y tejido celular subcutáneo, que conduce secundariamente a la isquemia y a la necrosis del tejido afecto. Si no se cumplen los criterios para ninguna de las anteriores, se considera calcinosis cutis idiopática⁴.

Aspectos éticos legales

El estudio del caso fue aprobado por el Comité de Bioética del Hospital Francisco Antonio Rísquez (Caracas – Venezuela). El

paciente aceptó la presentación del caso, mediante consentimiento informado. Fue informado sobre la confidencialidad de sus datos personales y de sus derechos irrenunciables como paciente.

Presentación del caso clínico

Paciente masculino de 28 años de edad, quien hizo referencia a inicio de la enfermedad actual hace 10 años aproximadamente, caracterizada por la presencia de masas múltiples en escroto, de color blanco, tamaños variados, no dolorosas (Fig. 1); además refirió infección del área en diversas ocasiones, la cual mejoraba con antibioterapia, mas no desaparecían. No se hallaron antecedentes patológicos, médicos, alérgicos o quirúrgicos; tampoco refirió la patología en ningún familiar. Padre fallecido con antecedentes de hipertensión arterial, madre viva aparentemente sana, y tres hermanos vivos sin patologías adyacentes. Respecto a los hábitos dietéticos, se realizó un recordatorio de 24 horas de un día típico para conocer hábitos y cuantificar ingesta diaria de calcio en la dieta. En cuanto a los aspectos psicosociobiológicos; refirió hábito tabáquico (3 cigarrillos cada 2 días), hábitos alcohólicos ocasionales, ingesta diaria de café, y en cuanto a su ocupación informó ser médico general.

Al examen físico se observó: piel y mucosas hidratadas, cuello cilíndrico simétrico, tiroides no palpable, sin dificultad para deglutir, tórax simétrico y normo expansible, con ruidos cardiacos rítmicos sin soplo, ni galope. A nivel abdominal presentó un abdomen blando, depresible, globoso a expensas de panículo adiposo, no doloroso. En su región genital, se evidenciaron lesiones bilaterales en escroto de diámetros variables; la mayor de 2cm de diámetro aproximadamente y la menor de 0,2 cm; de color blanco, no dolorosas, de consistencia sólida a la palpación y adheridas a plano subcutáneo.

A fin de determinar el tipo de calcinosis presentada por el paciente, se ordenaron pruebas de laboratorio de rutina, además de

la determinación de niveles de calcio y fosfato sérico, niveles de PTH, de vitamina D y un perfil 20. Para observar la extensión de la calcificación se practicó ecograma testicular y biopsia de las lesiones.

RESULTADOS

Los resultados de las pruebas de laboratorio pueden observarse en la Tabla 1, donde los niveles de calcio y fósforo se muestran dentro de los rangos normales, característico de calcinosis de tipo idiopática, mientras que la vitamina D y la PTH se mostraron alterados en comparación con los límites normales; haciendo énfasis en que estos dos parámetros pueden jugar un papel fundamental en la formación de calcinosis.

Por otro lado, el ecograma de piel y partes blandas mostró calcinosis en ambos escrotos, la mayor de 1,5cm, con bordes regulares, lisos y simétricos.



Fig. 1. Masas múltiples en escroto características de calcinosis.

Tabla 1
Pruebas de laboratorio.

Indicadores	Resultados	Rangos aceptables
Hemoglobina (g/dL)	12,9	12,0 – 15,1g/dL
Hematocrito (%)	37,4	35 – 46%
Velocidad de sedimentación medular (fL)	89	79,0 – 97,0fL
Monocitos (%)	8,9	0,2 – 10%
Eosinófilos (%)	0,9	1,0 – 3,0%
Sodio (mEq/L)	139	134,0 – 146,0mEq/L
Potasio (mEq/L)	3,7	3,50 – 5,00mEq/L
Cloro (mEq/L)	102	91,0 – 110,0mEq/L
Calcio (mg/dL)	8,5	8,0 – 10,5mg/dL
Fosforo (mg/dL)	3,5	2,5 – 5,1mg/dL
Vitamina D25-hidroxi Total	93,5	15,01 – 30,01ng/dL
Parathormona (pg/mL)	400	7,5 – 65pg/mL
pH	7,39	7,31 – 7,42
PCO ₂ (mmHg)	39	39,0 a 55,0mmHg
PO ₂ (mmHg)	35	35,0 – 60,0mmHg
Bicarbonato (mmol/L)	23,3	22,0 – 28,0mmol/L
SatO ₂ (%)	64	38,0 – 80,0%
CO ₂ T (mmol/L)	24,5	23,0 a 29,0mmoL/L
Calciuria (mg/24horas)	80	42,0 – 390,0 mg/24horas
Fosfaturia (mg/24horas)	800	657,3 – 934,5mg/24horas

Desde el punto de vista dietético el recordatorio de 24 horas arrojó que el paciente mantenía una ingesta de calcio de 800mg al día, encontrándose dentro de los requerimientos diarios (1000mg/día) establecidos para adulto⁵.

En vista de los hallazgos obtenidos a través del ecograma que mostró imágenes hiperecogénicas compatibles con calcinosis y los

resultados de laboratorio específicos solicitados, se decidió realizar una cirugía menor, en la cual se observaron lesiones nodulares circunscritas, de diversos tamaños y bordes regulares, sobre los cuales, previa asepsia y antisepsia, se infiltró un anestésico local y se realizó una incisión elíptica, haciendo excisión de cada una (Fig. 2). El resultado del procedimiento fue satisfactorio y posteriormente se procedió a hacer disección de un nódulo, cuyo contenido estaba formado por una pasta semisólida, blanquecina, carente de olor (Fig. 3).

Para la confirmación del diagnóstico, el fragmento de piel reseca fue enviado al Departamento de Anatomía Patológica, donde fue descrita macroscópicamente de la siguiente forma: se reciben 3 fragmentos de piel, el mayor mide de 3,8 x 2 a 1 x 0,9 cm y el menor mide 2 x 1,5 cm, con una superficie cutánea de color pardo claro, observándose múltiples lesiones nodulares entre 0,6 y 1,4 cm, redondeadas y de consistencia dura, la superficie de corte es sólida y blanquecina (Fig. 4).

Se incluyó una muestra representativa para estudio histológico (2B CC/rm), con un hallazgo diagnóstico histológico compatible con calcinosis cutis. En el comentario del estudio se observó: “Se aprecian nódulos de material calcificado, con inflamación mixta y reacción gigante-celular de tipo cuerpo extraño y sin criterios de malignidad”.

Dado lo anterior se decidió mantener una dieta baja en calcio (800 mg/día) de forma preventiva a largo plazo con buena aceptación por parte del paciente^{1,6}.

DISCUSIÓN

La calcinosis escrotal es un desorden idiopático benigno, que se presenta como una lesión de consistencia dura, como roca, o como pápulas blandas y lisas o nódulos en el escroto. Pueden infectarse o presentar inflamación posterior al trauma y muy rara vez afecta el pene⁷.



Fig. 2. Incisión elíptica, posterior a exceresis de cada lesión.



Fig. 3. Ejemplo de nódulo resecaado.



Fig. 4. Escala de las lesiones descritas por el Departamento de Anatomía Patológica. Macroscópicamente se reciben 3 fragmentos de piel, el mayor mide de 3.8x2 a 1x0.9cm y el menor mide 2x1.5cm, con una superficie cutánea de color pardo claro, observándose múltiples lesiones nodulares entre 0.6 y 1.4cm, redondeadas y de consistencia dura, la superficie de corte es sólida y blanquecina.

Los nódulos generalmente crecen lentamente en años o décadas, pero en múltiples reportes de casos, se han desarrollado rápidamente en meses⁷. El tamaño de los nódulos varía desde varios milímetros hasta el más grande reportado de 7 cm. La recurrencia es poco común, aunque se han reportado 4 pacientes que han presentado recurrencia luego de la extirpación⁴.

Aún se ignora su etiopatogénesis, varios autores postulan el lento adelgazamiento y eventual desaparición del recubrimiento epitelial de la pared del aparato folicular y la formación de pequeños quistes de inclusión epidérmica, al fragmentarse por estímulos irritativos externos en personas susceptibles, que permiten la salida de la queratina hacia la dermis circunvecina con su consecuente calcificación y respuesta inflamatoria resultante⁸. Por el contrario, otros autores plantean la hipótesis de que la calcinosis escrotal podría ser originada por la degeneración del músculo dartos⁹.

La edad promedio de los pacientes con diagnóstico de calcinosis escrotal varía entre 20 y 49 años con una edad media de 31,4 años¹⁰, lo cual coincide con la edad del sujeto de estudio en este caso (28 años).

En cuanto al diagnóstico ante un paciente con calcinosis cutis o que se sospecha de la misma, se recomienda realizar una serie de

estudios analíticos y pruebas de imagen que permitan orientar el tipo de calcificación y acercarnos a su etiología. Cuando se altera el metabolismo fosfo-cálcico, los niveles de calcio y fósforo son frecuentemente normales porque existe una elevación de los niveles de PTH. De manera ideal, debe usarse el calcio iónico, pero tiene problemas de procesamiento y alto coste para su uso sistemático. Empleando el calcio total es recomendable ajustar para los niveles de albúmina (o proteínas plasmáticas), dado que el calcio se une de forma importante a las proteínas¹¹. Para realizar un diagnóstico diferencial se debe tener en cuenta el esteatocistoma y otros tumores de localización escrotal como xantomas, hidrocele o hematocele calcificados¹².

Tal como se mencionó en la publicación de Jimenez-Gallo y col.¹¹, se realizaron, para el momento del diagnóstico, pruebas complementarias para la orientación etiológica del paciente con calcinosis cutis: hemograma, pruebas de funcionamiento renal, valores de electrolitos, calcio y fósforo, de PTH (para evaluar hiperparatiroidismo), y de vitamina D (para descartar hiperavitaminosis D). En este caso los resultados obtenidos estuvieron en relación con las características que han sido descritas, en cuanto a las pruebas clínicas alteradas de PTH y vitamina D, en esta patología¹¹.

Por otro lado, dentro de las características de la calcificación metastásica se encuentran la hipervitaminosis D, el hiperparatiroidismo, la sarcoidosis (producción de vitamina D por los granulomas sarcoideos), el síndrome de leche y alcalinos (excesivo consumo de antiácidos o comidas que tienen calcio) y neoplasias malignas (mecanismo destructivo metastásico o paraneoplásico), lo que coincide con los resultados del estudio de hiperavitaminosis D y PTH elevados¹¹.

Así mismo, Soto-Miranda y col. en su reporte de caso y revisión bibliográfica¹³ observaron que el sujeto de estudio presentó niveles elevados de PTH (382 UD), y recomendaron que con valores por encima de 600 pg/mL, debe realizarse paratiroidectomía de emergencia. En este caso no fue necesaria la paratiroidectomía, ya que se indicaron tratamiento y dieta.

En cuanto al tratamiento de la calcinosis cutis, se han llevado a cabo diversas terapias con escasos resultados, estos dependientes de la enfermedad o causa subyacente. Pueden usarse medicamentos para tratar las lesiones, pero su éxito ha sido irregular; para lesiones pequeñas entre los medicamentos que pueden ayudar se incluyen: warfarina, ceftriaxona e inmunoglobulina intravenosa (IVIG). El gel de hidróxido de aluminio actúa como quelante del fósforo a nivel intestinal, impidiendo su absorción. El probenecid actúa disminuyendo niveles de fósforo sérico. El EDTA disódico administrado por vía intravenosa, disminuye los niveles de calcemia. El etridonato disódico disminuye la formación de cristales de hidroxiapatita *in vitro*. La warfarina, a dosis de 1mg/día disminuye los niveles tisulares de ácido gamma-carboxi-glutámico, que está probablemente implicado en el desarrollo de la calcificación. En los episodios agudos de inflamación de un nódulo calcificado, es útil el tratamiento con colchicina. Para lesiones más grandes, los medicamentos que pueden ayudar incluyen: diltiazem, bisfosfonatos, probenecid e hidróxido de aluminio. La exéresis quirúrgica generalmente va seguida de recidivas, por ello sólo está indicada cuando los nódulos son dolorosos, existen infecciones recurrentes, trastornos funcionales, severos problemas estéticos, compresión nerviosa o en úlceras secretantes. Es importante mencionar que existe un elevado porcentaje de regresiones espontáneas¹⁰.

En cuanto a las nuevas opciones de tratamiento, se encuentra el trasplante de células madre hematopoyéticas (TCMH). Esto se ha utilizado para tratar algunas enfermedades autoinmunes¹⁰. La terapia con láser y la litotricia por ondas de choque (una terapia de ultrasonido que se usa para romper los cálculos renales), han mostrado resultados satisfactorios ya que reducen el tamaño y el dolor en los pacientes con calcinosis¹⁴.

Investigación Clínica 63(3): 2022

La cirugía sigue siendo actualmente el único tratamiento recomendado que proporciona excelentes resultados estéticos y permite la confirmación patológica del diagnóstico. Como la enfermedad se limita a la dermis escrotal, la escisión se circunscribe a la piel¹⁵.

A pesar de lo infrecuente de esta condición médica, la calcinosis cutis escrotal puede ser una de las patologías que deben tenerse en cuenta al realizar un diagnóstico diferencial; su etiología es aún desconocida, aunque tiene diversas vertientes ideológicas. Así mismo, se puede presentar de manera asintomática, reflejo de ello son los pocos casos que vemos en la práctica médica profesional diaria. Sin embargo, es importante enfocarse en su tratamiento oportuno, lo cual le brindará al paciente una mejor calidad de vida, y evitará incomodidades y baja autoestima debido al aspecto estético.

AGRADECIMIENTO

Agradecemos al paciente que tan amablemente permitió realizar el diagnóstico, tratamiento y uso de los datos para su publicación y divulgación científica. Además agradecemos al Hospital Dr. Francisco Antonio Rísquez por el uso de sus espacios, instalaciones y del personal del área de la salud que colaboró en todo el proceso.

Financiamiento

Dicha investigación fue financiada por los propios investigadores.

Conflicto de competencia

Esta investigación no tiene ningún conflicto de intereses.

Número ORCID de los autores

- Vanessa Bouquett:
0000-0001-6489-2691
- Letmarié Sánchez:
0000-0003-0818-5962

REFERENCIAS

1. **Macías-Tomei C, Palacios C, Mariño-Elizondo M, Carías D, Noguera D, Chávez-Pérez JF.** Valores de referencia de calcio, vitamina D, fósforo, magnesio y flúor para la población venezolana. *ALAN* 2013;63(4):362–378. Disponible en: http://ve.scielo.org/scielo.php?script=sci_arttext&pid=S0004-06222013000400011&lng=es.
2. **Bringhurst F, Demay MB, Krane SM, Kronenberg HM.** Metabolismo óseo y mineral en salud y enfermedad. In: Longo DL, Kasper DL, Jameson J, Fauci AS, Hauser SL, Loscalzo J. eds. *Harrison. Principios de Medicina Interna*, 18e. McGraw Hill; 2012. Accessed abril 24, 2022. <https://accessmedicina.mhmedical.com/content.aspx?bookid=1622§ionid=101851699>
3. **Iglesias-Gamarra A, Patarroyo PM, Rondón F, Rodríguez AI, Restrepo JF.** Calcinosis Universal: una manifestación atípica de las colagenosis: ¿Es una vía común o vías diferentes del proceso inflamatorio? *Rev Esp Enf Metabolic Oseas*. 2002;11(2):50–58. <http://www.elsevier.es el 02/09/2016>.
4. **Lei X, Liu B, Cheng Q, Wu J.** Idiopathic scrotal calcinosis: report of two cases and review of literature: Idiopathic scrotal calcinosis. *Int J Dermatol* 2012;51(2):199–203. <doi.org/10.1111/j.1365-4632.2011.04922.x>
5. **Palacios C.** Lo nuevo en los requerimientos de calcio, propuesta para Venezuela. *An Venez Nutr* 2007; 20(2):99-107.
6. **Fernández A, Sosa P, Setton D.** Calcio y nutrición, Buenos Aires: Sociedad Argentina de Pediatría; 2011:1-19 [actualizado Jul 2011, 2022/04/06]. Disponible en:<http://www.sap.org.ar/docs/calcio.pdf>
7. **Priego NA, López GM, Morales CJA, Díaz LNCA, Velarde CA, Cortez BR, Cortés AY.** Tumor escrotal de comportamiento incierto. Calcinosis idiopática. *Rev Mex Urológ* 2007;67(4):223–266. Disponible en: <https://www.medigraphic.com/cgi-bin/new/resumen.cgi?IDARTICULO=29132>
8. **Pérez-Elizondo AD, Del Pino Rojas GT.** Lesiones noduliformes en el escroto en un paciente de 35 años. *Medicina General* 2012;1(5):244-245. Disponible en: <https://dialnet.unirioja.es/servlet/articulo?codigo=6346671>.

9. **Andola S, Karangadan S, Patil S.** Idiopathic scrotal calcinosis: A case series. *Indian J Dermatopathol Diagn Dermatol* 2014;1(2):86-89. doi.org/10.4103/2349-6029.147312.
10. **Ortiz LJ, Sánchez JL.** Dermatology diagnosis. Idiopathic calcinosis cutis. *Bol Asoc Med P R.* 1987;79(12):491-492. Disponible en: <http://bases.bireme.br/cgi-bin/wxis-lind.exe/iah/online/?IsisScript=iah/iah.xis&src=google&base=ADOLEC&lang=p&nxtAction=lnk&exprSearch=66485&indexSearch=ID>
11. **Jiménez-Gallo D, Ossorio-García L, Linares-Barrios M.** Calcinosis cutis y calcifilaxis. *Actas Dermo-sifiliográficas* 2015; 106(10):785-794. Disponible en: <https://doi.org/10.1016/j.ad.2015.09.001>
12. **Morales MMC, Martínez ME.** Presentación de un caso de calcinosis idiopática del escroto. Congreso Virtual Hispanoamericano de Anatomía Patológica. Habana-Cuba, 2004. Disponible en: <https://conganat.uninet.edu/6CVHAP/autores/trabajos/T077/index.html>.
13. **Soto-Miranda MÁ, Goné-Fernández A, Huesca, ARY.** Calciphylaxis of the penis. A case report and literature review. *Cirugía y cirujanos* 2007; 75(2), 113-117. Disponible en: <https://www.medigrafiac.com/cgi-bin/new/resumenI.cgi?IDREVISTA=10&IDARTICULO=12102&IDPUBLICACION=1270>.
14. **Jayarajah U, de Silva L, de Silva C, Senviratne S.** Idiopathic scrotal calcinosis: A case report of a rare entity. *Case Rep Urol* 2019;2019:6501964. Disponible en: <http://dx.doi.org/10.1155/2019/6501964>.
15. **Sultan-Bichat N, Menard J, Perceau G, Staerman F, Bernard P, Reguiaï Z.** Treatment of calcinosis cutis by extracorporeal shock-wave lithotripsy. *J Am Acad Dermatol* 2012;66(3):424-429. Disponible en: <http://dx.doi.org/10.1016/j.jaad.2010.12.035>.

The benefits of peritoneal dialysis (PD) solution with low-glucose degradation product in residual renal function and dialysis adequacy in PD patients: A meta-analysis.

Sheng Chen¹, Jieshuang Jia², Huimin Guo³ and Nan Zhu²

¹Department of Nephrology, Ningbo Medical Center Lihuili Hospital, Ningbo, Zhejiang, China.

²Department of Nephrology, Shanghai General Hospital, Shanghai, China.

³Department of Nuclear Medicine, Shandong Provincial Hospital Affiliated to Shandong First Medical University, Jinan, Shandong, China.

Key words: glucose degradation products; peritoneal dialysis solution; residual renal function; dialysis adequacy; meta-analysis.

Abstract. The peritoneal effects of low-glucose degradation product (GDP)-containing peritoneal dialysis (PD) solutions have been extensively described. To systematically evaluate the efficacy and safety of low GDP solution for PD patients, specifically the effect on residual renal function (RRF) and dialysis adequacy, we conducted a meta-analysis of the published randomized controlled trials (RCTs). Different databases were searched for RCTs that compared low GDP-PD solutions with conventional PD solutions in the treatment of PD patients with continuous ambulatory peritoneal dialysis (CAPD) and automated peritoneal dialysis (APD). The outcomes of RCTs should include RRF and may include small solute clearance, peritoneal transport status, nutritional status, and all-cause mortality. Seven studies (632 patients) were included. Compared with the conventional solution, low-GDP solution preserved RRF in PD patients over time (MD 0.66 mL/min, 95% CI 0.34 to 0.99; $p < 0.0001$), particularly in one year of treatment ($p < 0.01$), and improved weekly Kt/V (MD 0.11, 95% CI 0.05 to 0.17; $p = 0.0007$) without an increased 4-hour D/Per (MD 0.00, 95% CI -0.02 to 0.02; $p = 1.00$). Notably, the MD of RRF and urine volume between the two groups tended to decrease as time on PD progressed up to 24 months. Patients using low GDP PD solutions did not have an increased risk of all-cause mortality (MD 0.97, 95% CI 0.50 to 1.88; $p = 0.93$). Our meta-analysis confirms that the low GDP PD solution preserves RRF, improves the dialysis adequacy without increasing the peritoneal solute transport rate and all-cause mortality. Further trials are needed to determine whether this beneficial effect can affect long-term clinical outcomes.

Beneficios de la solución de diálisis peritoneal (DP), con producto de degradación bajo en glucosa, en la función renal residual y la adecuación de la diálisis en pacientes en DP: un metanálisis.

Invest Clin 2022; 63 (3): 283 – 303

Palabras clave: productos de degradación de glucosa; solución de diálisis peritoneal; función renal residual; adecuación de diálisis; metanálisis.

Resumen. Los efectos peritoneales de las soluciones de diálisis peritoneal (DP) que contienen productos de degradación bajos en glucosa (PIB) se han descrito ampliamente. Para evaluar sistemáticamente la eficacia y la seguridad de la solución de PIB bajo para pacientes en DP, específicamente el efecto sobre la función renal residual (RRF) y la adecuación de la diálisis, realizamos un metanálisis de los ensayos controlados aleatorios (ECA) publicados. Se realizaron búsquedas en diferentes bases de datos de ECA que compararan la solución de DP de bajo PIB con la solución de DP convencional en el tratamiento de pacientes con EP con CAPD y APD. Los resultados de los ECA deben incluir la RRF y pueden incluir la depuración de solutos pequeños, el estado nutricional, el estado del transporte peritoneal y la mortalidad por todas las causas. Se incluyeron siete estudios (632 pacientes). En comparación con la solución convencional, la solución de bajo PIB preservó la FRR en pacientes con EP a lo largo del tiempo (DM 0,66 mL/min, IC del 95%: 0,34 a 0,99; $p < 0,0001$), particularmente en un año de tratamiento ($p < 0,01$), y mejoró el Kt/V semanal (DM 0,11, IC del 95%: 0,05 a 0,17; $p = 0,0007$), sin un aumento de D/Per a las 4 horas (DM 0,00, IC del 95%: -0,02 a 0,02; $p = 1,00$). Los pacientes que usaron una solución para DP con bajo contenido de GDP no tuvieron un mayor riesgo de mortalidad por todas las causas (DM 0,97; IC del 95%: 0,50 a 1,88; $p = 0,93$). Nuestro metanálisis confirma que la solución de DP de bajo PIB preserva la FRR, mejora la adecuación de la diálisis sin aumentar la tasa de transporte peritoneal de solutos y la mortalidad por todas las causas. Se necesitan más ensayos para determinar si este efecto beneficioso puede afectar los resultados clínicos a largo plazo.

Received: 06-01-2022 Accepted: 22-04-2022

INTRODUCTION

Peritoneal dialysis (PD) has become an established form of renal replacement therapy for patients with end-stage renal disease (ESRD) in the past thirty years¹. In 2008, there were approximately 196,000 PD patients worldwide, representing 11% of the

dialysis population² and the number is increasing by at least 6% per annum³.

Conventional peritoneal dialysis solutions (CS) are acidic and contain high levels of glucose degradation products (GDPs) as a result of the heat sterilization process⁹. GDPs as a major factor in the bioincompatibility of peritoneal solutions¹⁰, exert poten-

tially negative effects on both the structural and functional deterioration of peritoneum and systemic metabolic disturbance, leading to treatment failure and an increase in cardiovascular morbidity and mortality¹¹. Residual renal function (RRF) plays a vital role in the prognosis of patients on dialysis⁴, which evaluates the excretion of small solute and middle-molecular uremic toxins⁵, salt and water homeostasis, acid-base balance, nutritional status and associated survival⁶⁻⁸. Accumulating evidence from epidemiological and experimental researches^{10,12-14} reveals that low-GDP peritoneal dialysis solutions (LS) may play a role in retarding RRF loss in PD patients¹⁴. However, not all clinical trials show encouraging results of the perceived advantages that LSs have on RRF^{15,16}. The impact of the low GDP in RRF protection and other beneficial effects remain insufficiently described, even though there has been interest in evaluating the systemic biocompatibility of these solutions¹⁷. Therefore, we conducted a meta-analysis to examine the effect of LS on RRF and other related factors known to affect PD in PD patients compared with CS.

SUBJECTS AND METHODS

Study Inclusion and Exclusion Criteria

Studies that met all the following basic criteria were included in our meta-analysis: (1) a randomized controlled trial (RCT) for patients on continuous ambulatory peritoneal dialysis (CAPD) or automated peritoneal dialysis (APD) as the treatment of ESRD; (2) LS was compared with CS. The crossover randomized trials or RCTs that did not assess RRF were excluded.

Search Strategy

We identified eligible RCTs by searching the PubMed, Embase, Wiley, Scopus, Ovid databases and abstracts presented at the annual meetings of the American Society of Nephrology (ASN), the National Kidney

Foundation (NKF), and the European Renal Association (ERA), from inception to July 2014, using appropriate Medical Subject Headings (MeSH) and text words: peritoneal dialysis, glucose degradation products, bio-compatible solution, low-GDP, APD, CAPD in combination with “residual renal function”. Further, the reference lists of retrieved articles were then searched for additional relevant studies. No language restrictions were imposed.

Study Selection

We included RCTs examining the effect of LSs on RRF in PD patients >18 years old compared with CSs. PD modality was restricted as either CAPD or APD. The outcomes of RCTs should include the RRF value, which is measured as the arithmetic means of residual renal clearances of urea and creatinine by collecting 24-hour urine volume. Other endpoints for the evaluation may include small solute clearance, peritoneal solute transport rate (PSTR), nutritional status, and all-cause mortality of PD patients. The study had at least 12 months of duration of follow-up without restriction on sample size. Two investigators (NZ and JW), independently, screened titles and abstracts of all electronic citations to select studies that met the inclusion criteria for further analysis. All articles identified by the investigators were retained.

Study Validity Assessment

We used the Cochrane Collaboration's bias tool and Jadad score for assessing the risk of bias for the included studies. The first approach incorporates assessment of randomization (sequence generation and allocation sequence concealment), blinding (participants, personnel, and outcome assessors), completeness of outcome data, selection of outcomes reported, and other sources of bias. The items were scored with “yes,” “no,” and “unclear”¹⁸. The Jadad scale score ranged from 0 to 5 points about the randomization, double-blinding, and withdrawals and dropouts¹⁹.

Data Extraction

Two investigators extracted the useful data independently and reached a consensus on all eligible data. Relevant information was obtained by contacting the corresponding authors of the respective studies.

Study characteristics were extracted from all included trials with respect to year of publication, the study sample, baseline characteristics of the trials, follow-up, and the following reported outcomes of different follow-up months (baseline, 6, 12, and 24 months): (1) RRF (mL/min) (2) total weekly urea clearance (total Kt/V) and peritoneal urea clearance (peritoneal Kt/V), (3) total creatinine clearance (total CrCl) (L/week/1.73m²), and peritoneal creatinine clearance (peritoneal CrCl) (L/week/1.73m²), (4) daily urine volume (UV) (mL), daily peritoneal ultrafiltration (UF) (mL) and daily glucose exposure (g), (5) dialysate-to-plasma ratio of creatinine at 4 hours of peritoneal equilibration test (PET) (D/Pcr) and D/D0 glucose at 4 hours (D/D0 glucose), (6) blood pressure (mmHg) including systolic blood pressure (SBP) and diastolic blood pressure (DBP), (7) nutritional data, including serum albumin (g/dL), subjective global assessment (SGA) and normalized protein nitrogen appearance (nPNA) (g/kg/day), (8) all-cause mortality.

Data Synthesis and Analysis

Continuous outcomes results were presented as the mean difference (MD) and its 95% confidence intervals (CIs). Dichotomous outcomes were reported as the risk ratio (RR) and 95% CIs. Statistical pooling was performed with a random-effect model, *via* generic inverse variance weighting. All the statistical analyses in this meta-analysis were performed using Review Manager 5 software (RevMan 2012) for the meta-analysis.

Hypothesis testing was set at the two-tailed and results were considered statistically significant at 0.05 level. The I² statistic was calculated as a measure of statistical heterogeneity, and I² values of 25%, 50%, and

75% corresponded to low, medium, and high levels of heterogeneity. When heterogeneity was found (I²>25%), sensitivity analysis was performed in an attempt to explain the findings. When doing a pool for some outcome assessment, we excluded the study which has the significant difference at baseline to keep two groups in all studies have the consistent outcome at the baseline. For each parameter estimate, an integrated analysis was given, finally.

The meta-analysis was performed in accordance with the recommendations by Preferred Reporting Items for Systematic reviews and Meta-Analyses (PRISMA) workgroup²⁰.

RESULTS

Study Characteristics

A total of 223 potentially relevant citations were identified and screened, of which 197 were selectively excluded from the study because they were not clinical RCTs or did not expose the outcome of interest. Twenty-six articles were retrieved for detailed evaluation. Overall, seven RCTs were included with a combined total of 632 patients^{3,15,17,21-24} (Fig. 1).

The details of the characteristics and the demographic data of the RCTs included in our analysis were summarized in Table 1. These studies varied in sample size, and follow-up duration differed from 12 to 24 months, spanning nearly 10 years. The mean age of the populations ranged from 51~62 years and the mean of body mass index (BMI) ranged from 23~28.4 kg/m². The prevalence of diabetes in the patients was from 11%~56%. More than half of the patients in both groups used angiotensin converting-enzyme inhibitors (ACEI) or angiotensin II receptor blockers (ARB) and half of the patients in both groups used diuretics in two studies^{3,23}. All trials evaluated the LS (Balance: Fresenius Medical Care) compared with a CS (Stay•Safe: Fresenius Medical Care). Almost all studies included incident CAPD patients except the Choi *et*

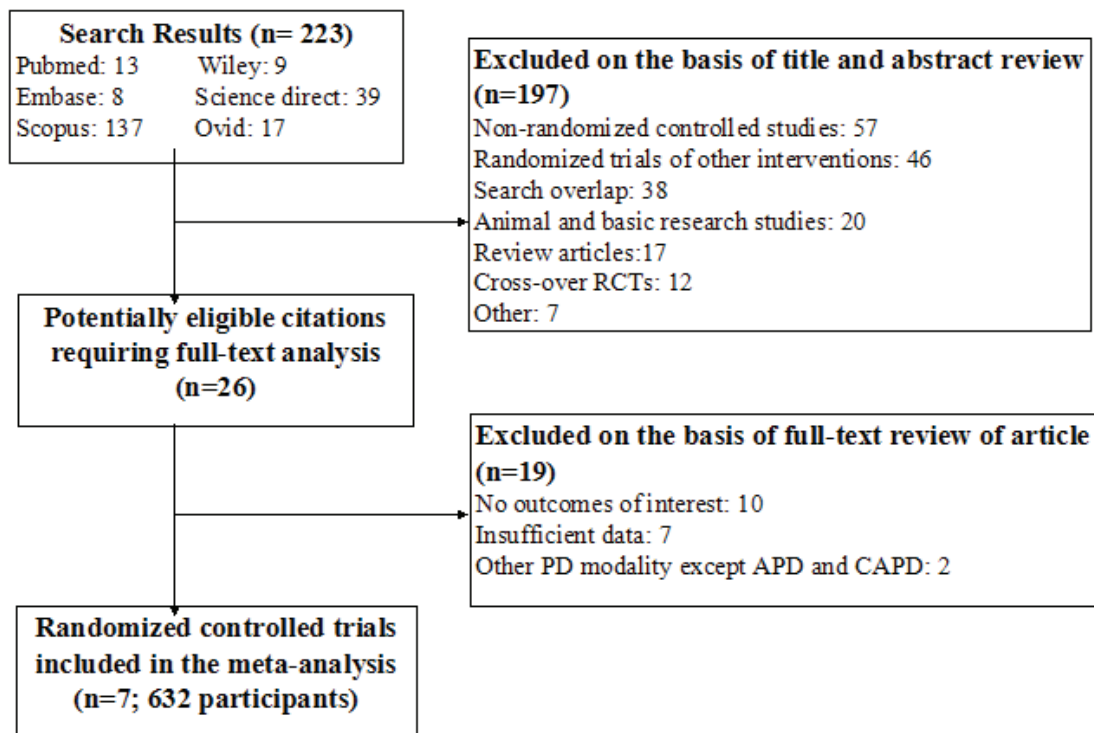


Fig 1. Flow chart showing the number of citations retrieved by individual searches and the number of trials included in the review.

*al.*²¹ study, and patients with CAPD modality except the balANZ Trial³.

Baseline of outcomes in these included studies were shown in Table 2. Kim *et al.*²² demonstrated that there were no significant differences of all outcomes between the two groups except CrCl (LS group, 95.5 ± 5.0 vs. CS group, 78.6 ± 11.8 L/week/ 1.73m^2 , $p < 0.05$) and nPNA (LS group, 0.85 ± 0.07 vs. CS group, 1.06 ± 0.11 g/kg/day, $p < 0.05$). The D/Per at the baseline was higher in the LS group than in the CS group in the two trials studied by Kim *et al.*²³ and Park *et al.*¹⁷. Moreover in the study by Park *et al.*¹⁷ peritoneal CrCl and was higher in the LS group, peritoneal UF volume was lower in the LS group at baseline in keeping with higher peritoneal transport characteristics in this group. Szeto *et al.*¹⁵ showed that at baseline, the CS group had a better nutritional status than the LS group (serum albumin, $p = 0.004$ and SGA, $p = 0.023$), but the difference disappeared in 12 months.

Quality Assessment

Two investigators assessed the quality of the included studies independently. All RCTs were considered fair to good quality (Fig. 2). Allocation methods and concealment were generally, incompletely reported and therefore difficult to assess. Allocation concealment was adequate in four studies (43%). Six studies (86%) were classified as low risk of performance bias and only one study was unclearly reported. However, no information about the blinding of outcome assessment (detection bias) of the studies was provided. Completeness of outcome reporting and intention-to-treat analysis methodology was applied in 29% of included studies. Selective reporting was observed in six studies (86%). No other significant biases were identified in these seven studies, except an unclear description of participant details in four studies. The Jadad score was 3 or higher (Table 1), even though the method of random se-

Table 1
Characteristics of the included RCTs in this analysis.

Study or Author Year	Country	Peritoneal dialysis (PD)	PD solution (L/C)	Modality (L/C)	Sample size, n (L/C)	Mean age, year (L/C)	Male, n (L/C)	Follow-up duration, month	% DM, (L/C)	BMI(kg/ m ²)(L/C)	Charlson's Index score (L/C)	ACEI/ARB, (%) (L/C)	diuretics, (%) (L/C)	Sum of Score
Bajo <i>et al.</i> 2011	Spain	Incident CAPD	Balance versus Stay-safe	CAPD	13/20	62/59	10/9	24	11/38	NA	NA	NA	NA	3
balANZ Trial	New Zealand, Australia, Singapore	Incident CAPD	Balance versus Stay-safe	CAPD / APD	91/91	59.3/57.9	52/48	24	33/34	27.7/28.4	NA	44.0/45.1	44/50.5	4
Choi <i>et al.</i> 2008	Korea	Prevalent CAPD	Balance versus Stay-safe	CAPD	51/53	52.6/55.4	20/27	12	18/19	24.5/24.3	NA	NA	NA	3
Kim <i>et al.</i> 2003	South Korea	Incident CAPD	Balance versus Stay-safe	CAPD	16//10	51.6/56.1	NA	12	38/30	NA	NA	NA	NA	3
Kim <i>et al.</i> 2008	Korea	Incident CAPD	Balance versus Stay-safe	CAPD	48/43	55.3/52.8	31/24	12	56/42	22.7/23.5	NA	64.6/58.1	52.1/55.8	3
Park <i>et al.</i> 2012	Korea	Incident CAPD	Balance versus Stay-safe	CAPD	79/67	52.2/52.6	37/30	12	52/55	22.9/22.6	4.06/3.99	65.8/78.1	NA	4
Szeto <i>et al.</i> 2007	Hongkong	Incident CAPD	Balance versus Stay-safe	CAPD	25/25	60.9/55.0	16/14	12	40/32	23.0/23.3	5.4/4.68	NA	NA	4

Note: data are presented as mean or median (range). NA, not available. L/C, neutral pH and low-GDP PDSs/conventional PDSs; DM, diabetes mellitus; BMI, body mass index; ACEi, angiotensin-converting enzyme inhibitor; ARB, angiotensin II receptor blocker.

Table 2
The baseline of outcomes in the included RCTs.

Study or Author Year	Bajo <i>et al.</i> 2011	baMANZ Trial		Choi <i>et al.</i> 2008		Kim <i>et al.</i> 2003		Kim <i>et al.</i> 2008		Park <i>et al.</i> 2012		Szeto <i>et al.</i> 2007		
Groups	LS	CS	LS	CS	LS	CS	LS	CS	LS	CS	LS	CS	LS	CS
sample size (n)	13	91	91	53	16	10	48	43	79	67	25	25	25	25
RRF (mL/min)	7.0±4.3	5.8±3.9	7.0±6.0	7.9±17.7	8.9±22.9	4.3±0.4	3.2±1.2	6.84±6.69	5.71±3.76	3.9±3.1	3.7±2.6	3.91±2.09	3.67±2.27	3.67±2.27
Kt/V	NA	NA	NA	1.9±0.4	1.9±0.4	2.83±0.17	2.52±0.29	2.41±1.01	2.08±0.59	2.4±0.6	2.3±0.6	2.28±0.35	2.23±0.62	2.23±0.62
peritoneal Kt/V	NA	NA	NA	1.8±0.3	1.7±0.3	NA	NA	1.63±0.4	1.46±0.4	1.7±0.4	1.7±0.5	NA	NA	NA
CrCl (L/week/1.73m ²)	NA	NA	NA	55.2±15.2	55.9±22.8	95.5±5.0*	78.6±11.8	90±47.7	78±27.7	84.1±30.9	77.5±27.9	NA	NA	NA
peritoneal CrCl (L/week/1.73m ²)	NA	NA	38.3±9.0	36.3±11.9	48.3±6.3	NA	NA	44.6±10.1	39.6±10.7	41.4±7.3*	37.9±6.9	NA	NA	NA
urine volume (mL/d)	NA	NA	1556.0±691.0	1501.0±682.0	385.5±330.7	447.1±278.4	NA	783.0±630.0	698.0±430.0	880.0±732.0	717.0±536.0	870.0±620.0	900.0±710.0	900.0±710.0
peritoneal UF (mL/d)	NA	NA	700 (2700 to 3500)	1110.8±555.2	921.2±498.0	NA	NA	865.0±338.0	923.0±430.0	621.0±520.0*	962.0±527.0	560.0±600.0	560.0±690.0	560.0±690.0
glucose load (g/d)	NA	NA	121.5±35.3	123.6±36.3	145.1±38.3	155. ±44.3	NA	121.0±21.1	121.0±48.7	100.8±11.1*	109.1±10.3	100.7±14.6	100.9±17.7	100.9±17.7
D/Per	NA	NA	0.67±0.1	0.62±0.1	NA	NA	0.69±0.02	0.66±0.03	0.72±0.1*	0.67±0.1	0.74±0.12*	0.69±0.12	NA	NA
D/P0 glucose	NA	NA	NA	NA	NA	NA	0.28 ±0.02	0.3 ±0.03	0.32 ±0.14	0.35 ±0.14	NA	NA	NA	NA
SBP (mmHg)	NA	NA	139.8±21.4	138.9±21.8	NA	NA	NA	NA	NA	131.6±19.3	131.4±20.8	NA	NA	NA
DBP (mmHg)	NA	NA	76.6±11.3	78.1±11.0	NA	NA	NA	NA	NA	82.2±11.9	81.3±12.1	NA	NA	NA
Serum alb (g/dL)	NA	NA	3.8±0.5	3.7±0.6	3.6±0.3	3.5±0.4	3.4±0.1	3.7±0.2	3.39±0.56	3.6±0.6	3.6±0.5	3.28±0.44*	3.65±0.41	3.65±0.41
SGA	NA	NA	NA	NA	6.0±0.7	6.1±0.9	NA	NA	NA	5.9±1.2	5.7±1.1	4.83±0.87*	5.24±0.78	5.24±0.78
nPNA (g/kg/d)	NA	NA	1.05±0.25	1.06±0.26	0.9±0.2	0.9±0.2	0.85±0.07*	1.06±0.11	0.92±0.23	0.91±0.18	0.9±0.25	1.07±0.19	1.18±0.19	1.18±0.19

Note: data are presented as mean±SD or median (range). NA, not available. Bold indicates the parameters have significant differences between the two groups and asterisk (*) indicates p<0.05 versus CS group. RRF, mean of creatinine clearance (Cr) and urea clearance (Curea); Kt/V, total weekly urea clearance; peritoneal Kt/V, weekly peritoneal urea clearance; CrCl, total creatinine clearance; peritoneal CrCr, peritoneal creatinine clearance; peritoneal UF, peritoneal ultrafiltration; D/Per, dialyrate-to-plasma creatinine ratio at 4 hours of peritoneal equilibration test (PEF); D/D0 glucose, D/D0 glucose at 4 hours of PEF; SBP, systolic blood pressure; DBP, diastolic blood pressure; SGA, subjective global assessment; nPNA, normalized protein nitrogen appearance.

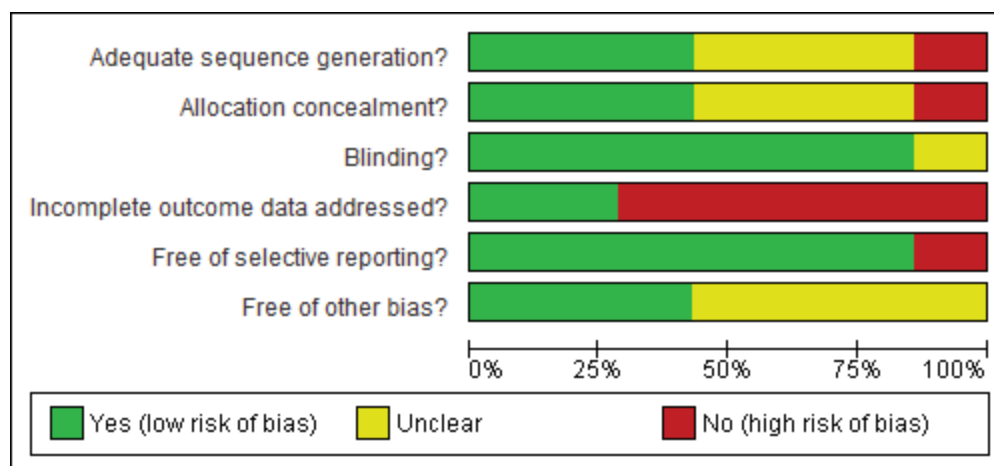


Fig 2. Risk of bias graph: each risk of bias item is presented as percentages across all included studies.

quence generation, blinding of participants and allocation concealment were not mentioned in most studies.

Outcome Measurement

PD patients in these different studies were followed up for different periods, which may have influenced the effectiveness of the outcomes of this analysis. Therefore, subgroup analysis was used to decrease clinical heterogeneity according to the follow-up periods.

Residual Renal Function

Two studies^{17,23} of seven RCTs were undertaken to calculate the RRF of 226 patients after 6 months of follow-up, and indicated that LS group was beneficial for preserving RRF compared with the control group (MD 1.28 mL/min, 95% CI 0.52 to 2.03, $p=0.0009$; $I^2=0\%$). Similar results were obtained after 12 months of follow-up in all studies including 520 patients (MD 0.60 mL/min, 95% CI 0.18 to 1.02, $p=0.005$; $I^2=11\%$). The balANZ Trial³ followed up 24 months and RRF was measured at baseline, 12 and 24 months, as well as the study by Bajo *et al.*²⁴, and the pooled data indicated no difference between the two groups ($p=0.76$). As the studies duration continued from 6 to 24 months, the difference of RRF between

the two groups was reduced gradually. This should be commented in the abstract and/or conclusions. Considering the heterogeneity, exclusion of the study²⁴ with a small sample size did not materially change the results of the meta-analysis or the subgroup analyses. Overall, the use of LS induced a reduction in RRF decline compared with the control group (MD 0.66 mL/min, 95% CI 0.34 to 0.99; $p<0.0001$; $I^2=4\%$; Fig. 3).

Daily Urine Volume

Three studies^{3,17,23} with a total of 377 patients and five studies^{3,15,17,21,23} with a total of 462 patients showed the 24h urine volume separately at 6 and 12 months. The 24h urine volume in the LS group was higher than that in the CS group (MD 155.42 mL/d, 95% CI 37.84 to 273.00; $p=0.01$) at 6 months. A total of 238 patients were followed up in the LS groups and 224 patients were followed up in the CS groups after 1 year's study. Patients with the LS had more daily urine volume than the CS group (MD 158.93 mL/d, 95% CI 83.22 to 234.64; $p<0.0001$). Only the balANZ Trial³ reported the urine volume at 24 months follow-up, and there was no significant difference between the two groups. As the study duration continued from 12 to 24 months, the MD of the residual urine volume decreased from

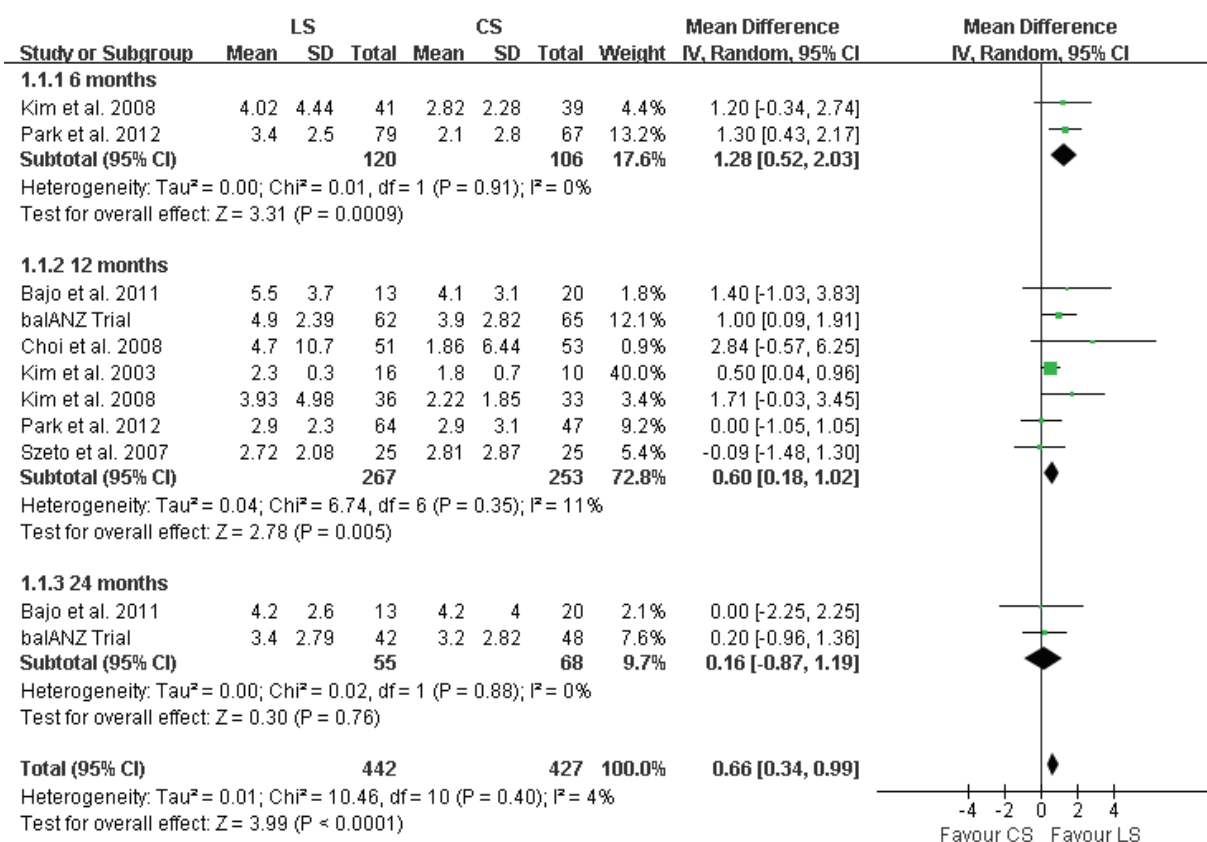


Fig 3. Effect of low-GDP PD solution on RRF (mL/min).

158.93 mL/d to 115.00 mL/d. The pooled urine volume in patients using LS was greater than using CS (MD 153.15 mL/d, 95% CI 96.62 to 209.68; $p < 0.00001$; $I^2 = 0\%$; Table 2). Overall, our meta-analysis indicated that the LS had a significant effect on RRF with an increase in daily urine output compared with the CS group.

Small solute clearance

At 6 months, Kim *et al.*²³ and Park *et al.*¹⁷ published the data of total Kt/V and peritoneal Kt/V showing that there was no statistical difference between the two groups ($p = 0.99$; $p = 0.18$). After one year follow up, five studies involving 360 patients reported the effect of LS on total Kt/V in PD patients^{15,17,21-23}. Compared to the CS group, the LS group showed significantly increased Kt/V (MD 0.13, 95% CI 0.06 to 0.20; $p = 0.0002$).

Overall, we found that patients with LS had higher total Kt/V than with CS (MD 0.11, 95% CI 0.05 to 0.17; $p = 0.0007$; $I^2 = 0\%$) (Fig. 4) and the CS group had a higher peritoneal Kt/V than the LS group (MD -0.10, 95% CI -0.20 to -0.01; $p = 0.03$; $I^2 = 0\%$) (Table 2).

Our subgroup analyses showed no statistical differences of total CrCl and peritoneal CrCl between the LS and CS groups at 6 and 12 months (Table 2). We excluded the total CrCl data of the follow-up period from the study performed by Kim *et al.*²² who reported the significant difference between the two groups at baseline but no statistical difference observed at 12 months. The study by Park *et al.*¹⁷ was excluded because this study published that peritoneal CrCl was higher in the LS group at baseline and there was no significant difference after 6 months.

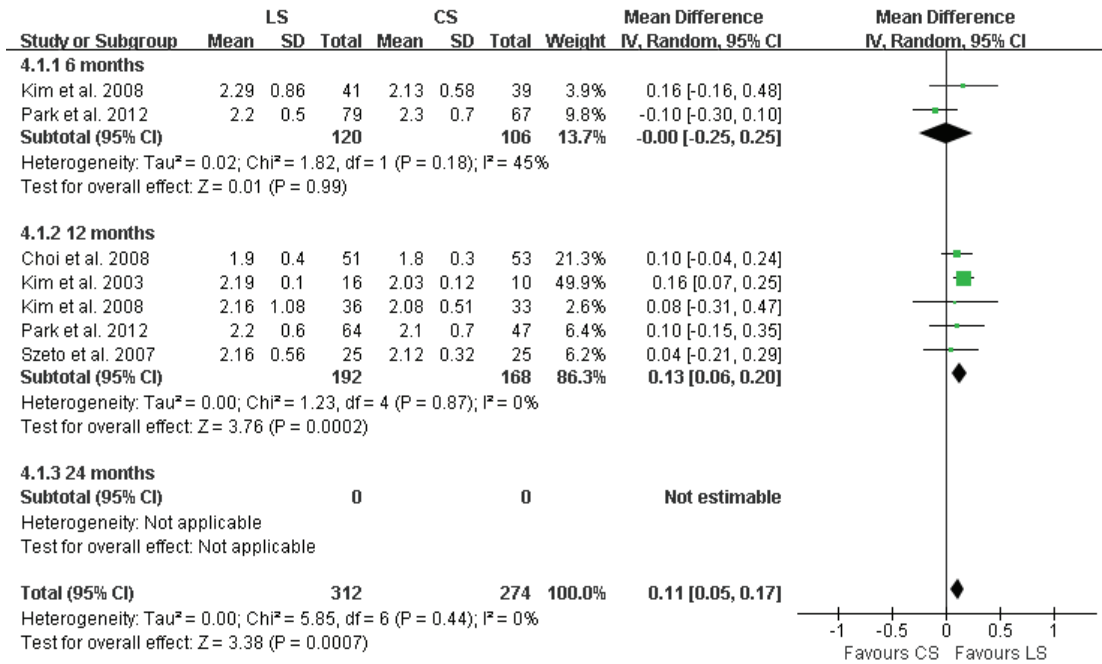


Fig. 4. Effect of low-GDP PD solution on total Kt/V.

Peritoneal Ultrafiltration and Glucose Load

Five studies ^{3,15,17,21,23} published the daily peritoneal UF volume in the follow-up period. Park *et al.*¹⁷ indicated that the CS group had higher UF than the LS group at baseline and 6 months. After exclusion of this study, we pooled the data at 6 months, showing the higher UF in the CS group (MD -261.97 mL/d, 95% CI -427.73 to -96.21; p=0.002). In the subgroup analyses of 12 months, Choi *et al.*²¹ who included all prevalent PD patients with more than half number of anuric, revealed the outcome that UF was significantly higher in the LS group than in the CS group at all follow-up visits. The exclusion of this study did materially change the results of the meta-analysis or the subgroup analyses. Table 3 showed that patients with the LS had less daily peritoneal UF volume than the CS (MD -193.45 mL/d, 95% CI -315.36 to -71.54;

p=0.002; I²=36%). The subgroup analyses of glucose load suggested that there was no statistically significant difference between patients using the LS and CS at 6 and 12 months.

Blood Pressure

The balANZ Trial ³ and the study by Park *et al.*¹⁷ followed up the blood pressure of the two groups. There was no significant difference between the two groups in controlling blood pressure during 1 year of follow-up (SBP, p=0.91; DBP, p=0.59) (Table 3).

Peritoneal Solute Transport Rate

Five studies ^{3,17,21-23} published the D/Per. In the study by Kim *et al.*²³, the D/Per was higher in the LS group than in the CS group, and this difference persisted throughout the treatment period. Similar results were obtained from Park *et al.*¹⁷, but after 6 months, the D/Per showed no difference between the two groups. The patients of two groups in these three included stud-

Table 3
Comparison of low glucose degradation products (GDP) versus standard glucose dialysate.

Outcome or subgroup title	No. of studies	No. of patients (LS/CS)	Statistical method	Effect size	p	Heterogeneity
Residual renal function						
6 months	2	120/106	Mean Difference (IV, Random, 95% CI)	1.28 [0.52, 2.03]	0.0009	I2=0%
12 months	7	267/253	Mean Difference (IV, Random, 95% CI)	0.60 [0.18, 1.02]	0.005	I2=11%
24 months	2	55/68	Mean Difference (IV, Random, 95% CI)	0.16 [-0.87, 1.19]	0.76	I2=0%
Total		442/427	Mean Difference (IV, Random, 95% CI)	0.66 [0.34, 0.99]	<0.0001	I2=4%
Daily Urine Volume						
6 months	3	196/181	Mean Difference (IV, Random, 95% CI)	155.42 [37.84, 273.00]	0.01	I2=0%
12 months	5	238/224	Mean Difference (IV, Random, 95% CI)	158.93 [83.22, 234.64]	<0.0001	I2=7%
24 months	1	42/48	Mean Difference (IV, Random, 95% CI)	115.00 [-146.33, 376.33]	0.39	
Total		476/453	Mean Difference (IV, Random, 95% CI)	153.15 [96.62, 209.68]	<0.00001	I2=0%
Peritoneal Ultrafiltration						
6 months	2	117/114	Mean Difference (IV, Random, 95% CI)	-261.97 [-427.73, -96.21]	0.002	I2=0%
12 months	3	123/124	Mean Difference (IV, Random, 95% CI)	-200.57 [-389.25, -11.88]	0.04	I2=48%
24 months	1	42/48	Mean Difference (IV, Random, 95% CI)	65.00 [-234.81, 364.81]	0.67	
Total		282/286	Mean Difference (IV, Random, 95% CI)	-193.45 [-315.36, -71.54]	0.002	I2=36%
glucose load						
6 months	3	203/185	Mean Difference (IV, Random, 95% CI)	1.35 [-1.76, 4.47]	0.40	I2=0%
12 months	5	250/234	Mean Difference (IV, Random, 95% CI)	0.25 [-3.25, 3.74]	0.89	I2=0%
24 months	1	42/48	Mean Difference (IV, Random, 95% CI)	4.30 [-17.76, 26.36]	0.70	
Total		495/467	Mean Difference (IV, Random, 95% CI)	0.90 [-1.41, 3.21]	0.45	I2=0%
Small solute clearance						
total Kt/V						
6 months	2	120/104	Mean Difference (IV, Random, 95% CI)	-0.00 [-0.25, 0.25]	0.99	I2=45%
12 months	5	192/168	Mean Difference (IV, Random, 95% CI)	0.13 [0.06, 0.20]	0.0002	I2=0%
24 months	0					

Table 3. Continuación

Outcome or subgroup title	No. of studies	No. of patients (LS/CS)	Statistical method	Effect size	p	Heterogeneity
Total		312/274	Mean Difference (IV, Random, 95% CI)	0.11 [0.05, 0.17]	0.0007	I ² =0%
Peritoneal Kt/V						
6 months	2	120/106	Mean Difference (IV, Random, 95% CI)	-0.08 [-0.19, 0.04]	0.18	I ² =0%
12 months	2	100/80	Mean Difference (IV, Random, 95% CI)	-0.16 [-0.33, 0.01]	0.06	I ² =0%
24 months	0					
Total		220/186	Mean Difference (IV, Random, 95% CI)	-0.10 [-0.20, -0.01]	0.03	I ² =0%
total CrCl						
6 months	2	120/106	Mean Difference (IV, Random, 95% CI)	4.82 [-6.96, 16.61]	0.42	I ² =45%
12 months	3	151/133	Mean Difference (IV, Random, 95% CI)	3.60 [-2.48, 9.67]	0.25	I ² =34%
24 months	0					
Total		271/239	Mean Difference (IV, Random, 95% CI)	3.39 [-0.75, 7.53]	0.11	I ² =17%
Peritoneal CrCl						
6 months	1	48/43	Mean Difference (IV, Random, 95% CI)	1.50 [-2.91, 5.91]	0.05	
12 months	2	99/96	Mean Difference (IV, Random, 95% CI)	-0.08 [-2.09, 1.93]	0.94	I ² =0%
24 months	1	91/91	Mean Difference (IV, Random, 95% CI)	2.00 [-1.07, 5.07]	0.20	
Total		238/230	Mean Difference (IV, Random, 95% CI)	0.67 [-0.90, 2.24]	0.40	I ² =0%
Peritoneal Solute Transport Rate						
D/Per						
6 months	0					
12 months	2	54/40	Mean Difference (IV, Random, 95% CI)	0.00 [-0.02, 0.02]	1	I ² =0%
24 months	1	37/47	Mean Difference (IV, Random, 95% CI)	0.00 [-0.04, 0.04]	1	
Total		91/87	Mean Difference (IV, Random, 95% CI)	0.00 [-0.02, 0.02]	1	I ² =0%
D/D0 glucose						
6 months	1	41/39	Mean Difference (IV, Random, 95% CI)	-0.05 [-0.11, 0.01]	0.09	
12 months	2	52/43	Mean Difference (IV, Random, 95% CI)	-0.03 [-0.06, 0.00]	0.08	I ² =40%

Table 3. Continuación

Outcome or subgroup title	No. of studies	No. of patients (LS/CS)	Statistical method	Effect size	p	Heterogeneity
24 months	0					
Total		93/82	Mean Difference (IV, Random, 95% CI)	-0.03 [-0.05, -0.01]	0.01	I2=17%
Blood Pressure						
systolic blood pressure						
6 months	2	155/142	Mean Difference (IV, Random, 95% CI)	0.96 [-3.67, 5.60]	0.68	I2=0%
12 months	2	126/113	Mean Difference (IV, Random, 95% CI)	2.89 [-2.41, 8.18]	0.29	I2=0%
24 months	1	42/48	Mean Difference (IV, Random, 95% CI)	-10.80 [-19.24, -2.36]	0.01	
Total		323/303	Mean Difference (IV, Random, 95% CI)	-0.29 [-5.04, 4.46]	0.91	I2=53%
diastolic blood pressure						
6 months	2	155/142	Mean Difference (IV, Random, 95% CI)	1.01 [-1.84, 3.85]	0.49	I2=0%
12 months	2	126/113	Mean Difference (IV, Random, 95% CI)	1.10 [-1.88, 4.07]	0.47	I2=0%
24 months	1	42/48	Mean Difference (IV, Random, 95% CI)	-3.10 [-8.51, 2.31]	0.26	
Total		323/303	Mean Difference (IV, Random, 95% CI)	0.53 [-1.40, 2.45]	0.59	I2=0%
Nutritional Status						
Serum albumin						
6 months	3	203/185	Mean Difference (IV, Random, 95% CI)	-0.09 [-0.28, 0.10]	0.35	I2=59%
12 months	5	225/209	Mean Difference (IV, Random, 95% CI)	-0.16 [-0.28, -0.05]	0.005	I2=45%
24 months	1	42/48	Mean Difference (IV, Random, 95% CI)	-0.20 [-0.41, 0.01]	0.06	
Total		470/442	Mean Difference (IV, Random, 95% CI)	-0.14 [-0.23, -0.05]	0.002	I2=45%
nPNA						
6 months	3	203/185	Mean Difference (IV, Random, 95% CI)	-0.02 [-0.07, 0.02]	0.29	I2=0%
12 months	5	250/234	Mean Difference (IV, Random, 95% CI)	-0.03 [-0.07, 0.01]	0.18	I2=0%
24 months	1	42/48	Mean Difference (IV, Random, 95% CI)	0.00 [-0.12, 0.12]	1	
Total		495/467	Mean Difference (IV, Random, 95% CI)	-0.02 [-0.05, 0.00]	0.10	I2=0%
SGA score						
6 months	1	79/67	Mean Difference (IV, Random, 95% CI)	0.20 [-0.19, 0.59]	0.31	

Table 3. Continuación

Outcome or subgroup title	No. of studies	No. of patients (LS/CS)	Statistical method	Effect size	p	Heterogeneity
12 months	2	115/100	Mean Difference (IV, Random, 95% CI)	0.36 [-0.02, 0.73]	0.06	I ² =45%
24 months	0	0	Mean Difference (IV, Random, 95% CI)			
Total		194/167	Mean Difference (IV, Random, 95% CI)	0.33 [0.08, 0.57]	0.009	I ² =21%
all-cause mortality		Total events (LS/CS)				
6 months	0					I ² =0%
12 months	5	9/10	Odds Ratio (M-H, Fixed, 95% CI)	0.80 [0.32, 2.03]	0.64	I ² =0%
24 months	2	10/9	Odds Ratio (M-H, Fixed, 95% CI)	1.18 [0.46, 3.03]	0.73	
Total		19/19	Odds Ratio (M-H, Fixed, 95% CI)	0.97 [0.50, 1.88]	0.93	I ² =0%

ies ^{3,21,22} had high average transport status. Overall, there was no statistically significant difference in the D/Per between the two groups (MD 0.00, 95% CI -0.02 to 0.02; p=1.00; I²=0%) (Table 3).

However, two studies ^{22,23} with a difference on D/D0 glucose were small sample trials. The pooled analysis suggested that the CS had a higher D/D0 than the LS (MD -0.03, 95% CI -0.05 to -0.01; p=0.01; I²=17%) (Table 3).

Overall, the D/Per and D/D0 glucose of all patients included in this subgroup analysis indicated that both the LS group and the CS group had high-average transport characteristics of peritoneal membrane ⁶.

Nutritional Status

Our meta-analysis indicated that patients using the LS had lower serum albumin than the CS (MD -0.14 g/dL, 95% CI -0.23 to -0.05; p=0.002; I²=45%) (Table 3).

In the meta-analysis of five studies ^{3,15,17,21,23}, we found there was no significant difference in nPNA between the two groups (MD -0.02 g/kg/d, 95% CI -0.05 to 0.00; p=0.10; I²=0%) (Table 3).

Only two studies ^{17,21}, publishing the data of SGA were small sample trials. We found that the LS group had a better SGA score than the CS group (MD 0.33, 95% CI 0.08 to 0.57; p=0.009; I²=21%) (Table 3).

All-cause Mortality

All seven studies ^{3,15,17,21-24} published the effect of LS on patients' survival. No patient died in the two groups at 6-month follow-up. At 12 months five studies ^{15,17,21-23} involving 417 patients and at 24 months two studies involving 215 patients were included in the subgroup analysis, suggesting that there was no significant difference between the two groups, respectively (Table 3).

DISCUSSION

Our study suggests that low GDP solution preserves RRF in PD patients over time,

particularly in one year of treatment, and improves the dialysis adequacy especially the urea clearance without increasing the peritoneal solute transport rate. In addition, low-GDP solution was found to have no benefits on blood pressure, nutritional status and all-cause mortality.

The low GDP solution preserves more RRF as they may cause less intraperitoneal inflammation, thereby reducing peritoneal ultrafiltration and fluid losses. It is supported by a crossover designed RCT by EURO-BALANCE¹⁴, which showed more urine volume and better clearance of both urinary urea and creatinine with the neutral pH low GDP glucose containing dialysates alongside lower serum concentrations of AGE markers. In addition, these findings were also confirmed by several clinical trials, suggesting better preservation of RRF compared with the conventional PD solutions^{3,23}. The improved preservation of RRF with low GDP solution was observed at all study time points⁴⁰. Kim *et al.*²³ firstly declared the beneficial effect of low GDP solution on RRF with more urine volume in a prospective RCT. The balANZ trial³, as the largest RCT, observed that the rate of decline of renal function did not reach statistical significance in the first and the second year, but there was a significant delay in time to anuria. However, these beneficial effects on RRF were not substantiated by other studies^{15,17,21,22,24}. Szeto *et al.*¹⁵ failed to show any difference in RRF and urine output between the two groups because the small sample size was not adequately powered to elucidate the effect on RRF. Similarly, Fan *et al.*¹⁶ reported negative results from a larger number of patients, which was due to the lack of homogeneity for the patients in each study group. Therefore, meta-analysis, differing from included single study, can exert statistical power and result in a highly reliability outcome. The benefits of low-GDP solution are biologically plausible, as GDPs have been demonstrated to exert nephrotoxic effects directly on renal

tubular cells¹¹. One potential and underpinning mechanism is that low-GDP solution better preserves RRF in PD patients *via* reduction of GDP and the AGE in the systemic circulation²⁷. The other possible reason for the beneficial effect of low GDP solution on RRF could be that decreased peritoneal UF results in more urine output and higher residual renal clearance^{28,29}.

Weekly Kt/V is an important parameter for evaluating PD treatment adequacy. Our data indicate that although the use of the low GDP dialysates was not associated with increasing creatinine clearance (either total CrCl or peritoneal CrCl) or decreasing blood pressure (either SBP or DBP), it exhibited significant benefit in weekly Kt/V in 12 months of treatment. While patients using conventional PD solutions had a small advantage in the peritoneal Kt/V ($p=0.03$) which was consistent with the analysis of peritoneal UF ($p=0.002$) despite similar glucose load ($p=0.73$) (Supplementary Figure S3 and S6). Our study analyzed the nutritional status including serum albumin, nPNA and SGA score, which is important to evaluate the adequacy of peritoneal dialysis and CAPD patients survival³⁶. However, serum albumin suffered from a moderate level of statistical heterogeneity, which could not be satisfactorily explained³⁷. Improved nutritional status with low GDP PD solution was confirmed by the increase of SGA in the LS group. Inconsistency of these parameters for evaluating nutritional status may be due to heterogeneity among studies²⁷.

Most of the clinical studies find that low GDP solution reduces peritoneal UF accompanied by high average PSTR, whereas our review revealed that low GDP solution improved the dialysis adequacy with no expense of PSTR represented by D/Per and D/D0 glucose at 4 hours. Two studies by Choi *et al.*²¹ and Tranaeus *et al.*³⁰ showed similar findings but with a high level of clinical heterogeneity. McDonald *et al.*³¹ thought that the reduction of peritoneal UF was an important

cause of technique failure. However, excessive peritoneal UF may also play a causal role in the decline of RRF by provoking intravascular volume depletion^{32,33}. Thus, it is difficult to delimit UF volume as a clinical outcome, which is affected by many other variables such as fluid status, UV, PSTR and glucose load³⁴.

PSTR has been recognized as an important factor for the assessment of clinical outcomes, including technical failure and patient survival³⁵. Although the study by Kim *et al.*²³ was excluded for analyzing the effect of low GDP PD solution on PSTR because of a difference at baseline, the significant difference still existed at 6 and 12 months. It also supported our outcome that low GDP solution contributed to the lower UF without the difference of PSTR. Taken together, our results highlighted that the assessment for PSTR should be focused on process carefully rather than just an absolute value at the end of the study³⁴.

Concerning the survival advantage with low GDP PD solution, retrospective studies from Korea^{38,39} suggested that the biocompatible solution improved the survival in patients with PD and reduced mortality risk by 39%. However, our data showed that low GDPs in PD solution have no statistical impact on the survival of PD patients at 1 year or even longer follow-up period.

Several limitations of this study should be considered. First, most of the studies included patients who were receiving RAS (renin-angiotensin system) blockers that might be effective in slowing the decrease in RRF in PD patients. In addition, the primary endpoints of the studies and the dose of peritoneal dialysis in patients were different. Furthermore, RCTs investigating the effects of neutral pH, low GDP PD solution on RRF and adequacy were limited in number and publication bias. The Balance® (Fresenius Medical Care, Bad Homburg, Germany), the only one particular solution analyzed in our meta-analysis, may not enough to represent the neutral pH, low GDP PD solutions. At

last, PD treatment adequacy should be interpreted clinically rather than be evaluated by solute and fluid removal²⁸.

CONCLUSIONS

This meta-analysis suggests that low GDP PD solution significantly preserved residual renal function and improved dialysis adequacy without increasing the peritoneal solute transport rate (Table 4). Future randomized trials with adequate statistical power are needed to determine whether low GDP PD solution affects long-term clinical outcomes.

ACKNOWLEDGEMENTS

We would like to acknowledge everyone for their helpful contributions on this paper.

Ethics approval and consent to participate

The ethic approval was obtained from the Ethic Committee of Ningbo Medical Center Lihuili Hospital.

Consent to publish

All of the authors have consented to publish this research.

Competing interests

All authors declare no conflict of interest.

Funding

National Natural Science Foundation of China (No. 81700621).

Authors' contributions

Each author has made an important scientific contribution to the study and has assisted with the drafting or revising of the manuscript.

Table 4
 Summary of findings for the main comparison
Low-glucose degradation product versus standard glucose dialysate
Patient or population: PD patients
Setting: community

Outcomes	Relative effect (95% CI)	No of Participants (studies)	Quality of the evidence (Grade)	Comments
Residual renal function	MD 0.66 (0.34, 0.99)	442 (11)	high	Benefits reached significance as the study duration continued from 6 to 12 months
Daily Urine Volume	MD 153.15 (96.62, 209.68)	476 (9)	high	Benefits reached significance as the study duration continued from 6 to 12 months
Small solute clearance total Kt/V	MD 0.11 (0.05, 0.17)	312 (7)	high	Benefit reached significance after one year followed up
Peritoneal Kt/V	MD -0.10 (-0.20, -0.01)	220 (4)	moderate	Benefit reached significance after one year followed up
total CrCl	MD 3.39 (-0.75, 7.53)	271 (5)	Very low	
Peritoneal CrCl	MD 0.67 (-0.90, 2.24)	238 (4)	Very low	Benefit reached significance at 6 months followed up
Peritoneal Ultrafiltration	MD -193.45 (-315.36, -71.54)	282 (6)	high	Benefits reached significance as the study duration continued from 6 to 12 months
glucose load	MD 0.90 (-1.41, 3.21)	495 (9)	Very low	
Blood Pressure				
systolic blood pressure	MD -0.29 (-5.04, 4.46)	323 (5)	Very low	

Table 4. CONTINUACIÓN
Low-glucose degradation product versus standard glucose dialysate
Patient or population: PD patients

Outcomes	Relative effect (95% CI)	No of Participants (studies)	Quality of the evidence (Grade)	Comments
diastolic blood pressure	MD 0.53 (-1.40, 2.45)	323 (5)	Very low	
Peritoneal Solute Transport Rate				
D/Per	MD 0.00 (-0.02, 0.02)	91 (3)	Very low	
D/D0 glucose	MD -0.03 (-0.05, -0.01)	91 (3)	high	
Nutritional Status				
Serum albumin	MD -0.14 (-0.23, -0.05)	470 (9)	high	Benefit reached significance after one year followed up
nPNA	MD -0.02 (-0.05, 0.00)	495 (9)	Very low	
SGA score	MD 0.33 (0.08, 0.57)	194 (3)	high	
All-cause mortality	OR 0.97 (0.50, 1.88)	19 (7)	Very low	

REFERENCES

1. Krediet RT. 30 years of peritoneal dialysis development: The past and the future. *Perit Dial Int* 2007;27 Suppl 2:S35-41.
2. Jain AK, Blake P, Cordy P, Garg AX. Global trends in rates of peritoneal dialysis. *J Am Soc Nephrol* 2012;23:533-544.
3. Johnson DW, Brown FG, Clarke M, Boudville N, Elias TJ, Foo MW, Jones B, Kulkarni H, Langham R, Ranganathan D, Schollum J, Suranyi M, Tan SH, Voss D. Effects of biocompatible versus standard fluid on peritoneal dialysis outcomes. *J Am Soc Nephrol* 2012;23:1097-1107.
4. Rumpsfeld M, McDonald SP, Johnson DW. Peritoneal small solute clearance is nonlinearly related to patient survival in the Australian and New Zealand peritoneal dialysis patient populations. *Perit Dial Int* 2009;29:637-646.
5. Tam P. Peritoneal dialysis and preservation of residual renal function. *Perit Dial Int* 2009;29 Suppl 2:S108-110.
6. Cho Y, Badve SV, Hawley CM, Wiggins K, Johnson DW. Biocompatible peritoneal dialysis fluids: Clinical outcomes. *Int J Nephrol* 2012;2012:812609.
7. Termorshuizen F, Korevaar JC, Dekker FW, van Manen JG, Boeschoten EW, Krediet RT. The relative importance of residual renal function compared with peritoneal clearance for patient survival and quality of life: An analysis of the Netherlands Cooperative Study on the Adequacy of Dialysis (NECOSAD)-2. *Am J Kidney Dis* 2003;41:1293-1302.
8. Wang AY. The "heart" of peritoneal dialysis. *Perit Dial Int* 2007;27 Suppl 2:S228-232.
9. Diaz-Buxo J, Clark SC, Ho CH, Jensen LE. New pH-neutral peritoneal dialysis solution, low in glucose degradation products, in a double-chamber bag. *Adv Perit Dial* 2010;26:28-32.
10. Wieslander A, Linden T. Glucose degradation and cytotoxicity in pd fluids. *Perit Dial Int* 1996;16 Suppl 1:S114-118.
11. Chan TM, Yung S. Studying the effects of new peritoneal dialysis solutions on the peritoneum. *Perit Dial Int* 2007;27 Suppl 2:S87-93.
12. Witowski J, Bender TO, Gahl GM, Frei U, Jorres A. Glucose degradation products and peritoneal membrane function. *Perit Dial Int* 2001;21:201-205.
13. Plum J, Lordnejad MR, Grabensee B. Effect of alternative peritoneal dialysis solutions on cell viability, apoptosis/necrosis and cytokine expression in human monocytes. *Kidney Int* 1998;54:224-235.
14. Williams JD, Topley N, Craig KJ, Mackenzie RK, Pischetsrieder M, Lage C, Passlick-Deetjen J. The euro-balance trial: The effect of a new biocompatible peritoneal dialysis fluid (balance) on the peritoneal membrane. *Kidney Int* 2004;66:408-418.
15. Szeto CC, Chow KM, Lam CW, Leung CB, Kwan BC, Chung KY, Law MC, Li PK. Clinical biocompatibility of a neutral peritoneal dialysis solution with minimal glucose-degradation products--a 1-year randomized control trial. *Nephrol Dial Transplant* 2007;22:552-559.
16. Fan SL, Pile T, Punzalan S, Raftery MJ, Yaqoob MM. Randomized controlled study of biocompatible peritoneal dialysis solutions: Effect on residual renal function. *Kidney Int* 2008;73:200-206.
17. Park SH, Do JY, Kim YH, Lee HY, Kim BS, Shin SK, Kim HC, Chang YK, Yang JO, Chung HC, Kim CD, Lee WK, Kim JY, Kim YL. Effects of neutral pH and low-glucose degradation product-containing peritoneal dialysis fluid on systemic markers of inflammation and endothelial dysfunction: A randomized controlled 1-year follow-up study. *Nephrol Dial Transplant* 2012;27:1191-1199.
18. Justo P, Sanz AB, Egido J, Ortiz A. 3,4-dideoxyglucosone-3-ene induces apoptosis in renal tubular epithelial cells. *Diabetes* 2005;54:2424-2429.
19. Jadad AR, Moore RA, Carroll D, Jenkinson C, Reynolds DJM, Gavaghan DJ, McQuay HJ. Assessing the quality of reports of randomized clinical trials: Is blinding necessary? *Controlled clinical trials* 1996;17:1-12.
20. Moher D, Liberati A, Tetzlaff J, Altman DG. Preferred reporting items for systematic reviews and meta-analyses: The prisma statement. *Ann Intern Med* 2009;151:264-269.

21. Choi HY, Kim DK, Lee TH, Moon SJ, Han SH, Lee JE, Kim BS, Park HC, Choi KH, Ha SK, Han DS, Lee HY. The clinical usefulness of peritoneal dialysis fluids with neutral ph and low glucose degradation product concentration: An open randomized prospective trial. *Perit Dial Int* 2008;28:174-182.
22. Kim YL, Do J, Park SH, Cho K, Park J, Yoon K, Cho DK, Lee EG, Kim IS. Low glucose degradation products dialysis solution modulates the levels of surrogate markers of peritoneal inflammation, integrity, and angiogenesis: Preliminary report. *Nephrology (Carlton)* 2003;8 Suppl:S28-32.
23. Kim SG, Kim S, Hwang Y-H, Kim K, Oh JE, Chung W, Oh K-H, Kim HJ, Ahn C. Could solutions low in glucose degradation products preserve residual renal function in incident peritoneal dialysis patients? A 1-year multicenter prospective randomized controlled trial (balnet study). *Perit Dial Int* 2008;28:S117-S122.
24. Bajo MA, Pérez-Lozano ML, Albar-Vizcaino P, del Peso G, Castro M-J, Gonzalez-Mateo G, Fernández-Perpén A, Aguilera A, Sánchez-Villanueva R, Sánchez-Tomero JA. Low-gdp peritoneal dialysis fluid ('balance') has less impact in vitro and ex vivo on epithelial-to-mesenchymal transition (emt) of mesothelial cells than a standard fluid. *Nephrol Dial Transplant* 2011;26:282-291
25. Mujais S, Nolph K, Gokal R, Blake P, Burkart J, Coles G, Kawaguchi Y, Kawanishi H, Korbet S, Krediet R, Lindholm B, Oreopoulos D, Rippe B, Selgas R. Evaluation and management of ultrafiltration problems in peritoneal dialysis. International society for peritoneal dialysis ad hoc committee on ultrafiltration management in peritoneal dialysis. *Perit Dial Int* 2000;20 Suppl 4:S5-21.
26. Piraino B, Bernardini J, Brown E, Figueiredo A, Johnson DW, Lye WC, Price V, Ramalakshmi S, Szeto CC. Ispd position statement on reducing the risks of peritoneal dialysis-related infections. *Perit Dial Int* 2011;31:614-630
27. Kim S, Oh J, Chung W, Ahn C, Kim SG, Oh KH. Benefits of biocompatible pd fluid for preservation of residual renal function in incident capd patients: A 1-year study. *Nephrol Dial Transplant* 2009;24:2899-2908.
28. Bargman JM, Thorpe KE, Churchill DN. Relative contribution of residual renal function and peritoneal clearance to adequacy of dialysis: A reanalysis of the canusa study. *J Am Soc Nephrol* 2001;12:2158-2162.
29. Haag-Weber M, Kramer R, Haake R, Islam MS, Prischl F, Haug U, Nabut JL, Deppisch R. Low-gdp fluid (gambrosol trio) attenuates decline of residual renal function in pd patients: A prospective randomized study. *Nephrol Dial Transplant* 2010;25:2288-2296.
30. Tranaeus A. A long-term study of a bicarbonate/lactate-based peritoneal dialysis solution--clinical benefits. The bicarbonate/lactate study group. *Perit Dial Int* 2000;20:516-523.
31. McDonald S, Hurst K. Thirty fourth annual report. Australian & New Zealand Dialysis & Transplant Registry Report. Adelaide, South Australia. 2011.
32. Konings CJ, Kooman JP, Schonck M, Gladziwa U, Wirtz J, Bake AWVDW, Gerlag PG, Hoorntje SJ, Wolters J, Van Der Sande FM. Effect of icodextrin on volume status, blood pressure and echocardiographic parameters: A randomized study. *Kidney Int* 2003;63:1556-1563.
33. Konings CJ, Kooman JP, Gladziwa U, van der Sande FM, Leunissen KM. A decline in residual glomerular filtration during the use of icodextrin may be due to underhydration. *Kidney Int* 2005;67:1190-1191.
34. Cho Y, Johnson DW, Craig JC, Strippoli GF, Badve SV, Wiggins KJ. Biocompatible dialysis fluids for peritoneal dialysis. *Cochrane Database Syst Rev* 2014;3:CD007554.
35. Davies SJ, Phillips L, Russell GI. Peritoneal solute transport predicts survival on capd independently of residual renal function. *Nephrol Dial Transplant* 1998;13:962-968.
36. Chung SH, Lindholm B, Lee HB. Influence of initial nutritional status on continuous ambulatory peritoneal dialysis patient survival. *Perit Dial Int* 2000;20:19-26.
37. Cho Y, Johnson DW, Badve SV, Craig JC, Strippoli GF, Wiggins KJ. The impact of neutral-ph peritoneal dialysates with reduced glucose degradation products on clinical outcomes in peritoneal dialysis patients. *Kidney Int* 2013;84:969-979.

38. Lee HY, Park HC, Seo BJ, Do JY, Yun SR, Song HY, Kim YH, Kim YL, Kim DJ, Kim YS, Ahn C, Kim MJ, Shin SK. Superior patient survival for continuous ambulatory peritoneal dialysis patients treated with a peritoneal dialysis fluid with neutral ph and low glucose degradation product concentration (balance). *Perit Dial Int* 2005;25:248-255.
39. Lee HY, Choi HY, Park HC, Seo BJ, Do JY, Yun SR, Song HY, Kim YH, Kim YL, Kim DJ, Kim YS, Kim MJ, Shin SK. Changing prescribing practice in capd patients in korea: Increased utilization of low gdp solutions improves patient outcome. *Nephrol Dial Transplant* 2006;21:2893-2899.
40. Htay H, Johnson DW, Wiggins KJ, Badve SV, Craig JC, Strippoli GF, Cho Y. Bio-compatible dialysis fluids for peritoneal dialysis. *Cochrane Database Syst Rev* 2018; 26:10(10).

Evaluación de actividad física como coadyuvante terapéutico para pacientes con enfermedad inflamatoria intestinal: una revisión.

Diego Fernández-Lázaro^{1,2}, Nuria Hernández-Burgos^{1,3}, Raúl Cobreros Mielgo⁴ y Sandra García-Lázaro⁵

¹Departamento de Biología Celular, Genética, Histología y Farmacología, Facultad de Ciencias de la Salud, Universidad de Valladolid, Campus de Soria, 42003 Soria, España.

²Grupo de Investigación en Neurobiología, Facultad de Medicina, Universidad de Valladolid, Valladolid, España.

³Servicio de Medicina Interna, Hospital Enrest Luch Martín, Calatayud, España.

⁴Departamento de Fisioterapia, Instituto de Biomedicina (IBIOMED), Universidad de León, Campus de Vegazana, León, España.

⁵Departamento de Fisioterapia, Facultad de Ciencias de la Salud, Universidad de Valladolid, Campus de Soria, Soria, España.

Palabras clave: actividad física; enfermedad inflamatoria intestinal; coadyuvante terapéutico; fatiga; biomarcadores; calidad de vida.

Resumen. La enfermedad inflamatoria intestinal (EII) incluye la enfermedad de Crohn (EC) y la colitis ulcerosa (CU). El tratamiento farmacológico en la EII presenta pérdida de eficacia y efectos secundarios, por esta razón es necesario el planteamiento de estrategias alternativas, como la práctica de actividad física (AF), como coadyuvante terapéutico. El propósito de este estudio fue evaluar la efectividad de las intervenciones de AF como herramienta para aumentar la condición física, la calidad de vida relacionada con la salud (CVRS) y mejorar la sintomatología en pacientes con EC y CU, identificando el componente de AF óptimo. Se realizó una revisión mediante una búsqueda en las bases electrónicas de datos Medline (PubMed), SciELO y Cochrane Library Plus, que incluyó ensayos controlados aleatorios de los últimos 10 años que relacionaran la EII y la AF, hasta el 31 de enero de 2022. Se incluyeron 4 estudios con un total de 133 pacientes. La realización de AF de pacientes con EII (CU y EC) aumentó ($p > 0.05$) la capacidad física, la masa muscular esquelética, la densidad mineral ósea y la CVRS, incrementando significativamente ($p < 0,05$) el estado de ánimo. Además, disminuyó significativamente ($p < 0,05$) la inflamación intestinal y las manifestaciones extraintestinales. Se observó una tendencia de reducción ($p > 0,05$) de la fatiga, la tensión arterial y la restauración de la microbiota. La AF moderada y realizada regularmente durante un mínimo de 8 semanas, favorece la mejoría del paciente con EII a nivel físico, psicológico, la CVRS y la sintomatología.

Evaluation of physical activity as a therapeutic adjuvant for patients with inflammatory bowel disease: A systematic review.

Invest Clin 2022; 63 (3): 304 – 322

Key words: physical activity; inflammatory bowel disease; therapeutic adjuvant; fatigue; biomarkers. quality of life.

Abstract. Inflammatory bowel disease (IBD) includes Crohn's disease (CD) and ulcerative colitis (UC). Pharmacological treatment in IBD presents a loss of efficacy and side effects, inviting to consider alternative strategies, such as the practice of physical activity (PA), as a therapeutic adjuvant. The purpose of this review was to evaluate the effectiveness of PA interventions as a tool to increase physical fitness, and health-related quality of life (HRQoL) and improve the symptomatology in patients with CD and UC, identifying the optimal PA component. The review was performed, by searching the electronic databases Medline (PubMed), SciELO, and Cochrane Library Plus, including randomized controlled trials from the last 10 years that related to IBD and PA, until January 31, 2022. We found four studies with a total of 133 patients. The performance of PA in patients with IBD (UC and CD) increases ($p > 0.05$) physical capacity, skeletal muscle mass, bone mineral density, and HRQoL, significantly ($p < 0.05$) increasing mood. In addition, it significantly ($p < 0.05$) decreases intestinal inflammation and extraintestinal manifestations. A trend of reduction ($p > 0.05$) of fatigue, blood pressure, and microbiota restoration was observed. Moderate PA and performed regularly for a minimum of eight weeks, favors the improvement of the IBD patient at the physical, psychological, HRQoL, and symptomatology levels.

Recibido: 13-04-2022 Aceptado: 24-06-2022

INTRODUCCIÓN

La enfermedad inflamatoria intestinal (EII) engloba un conjunto de enfermedades crónicas, idiopáticas y autoinflamatorias. La EII incluye, principalmente, dos trastornos de etiología desconocida que son: la enfermedad de Crohn (EC) y la colitis ulcerosa (CU)^{1,2}. La EC y la CU están asociadas a factores genéticos, estímulos ambientales y alteraciones del sistema inmunológico, lo que condiciona una exacerbación desequilibrada de la respuesta inmune e inflamatoria en la mucosa intestinal en sujetos genéticamente predispuestos, jugando un papel re-

levante en ellos los factores ambientales³⁻⁵. Ambas enfermedades pueden aparecer en adolescentes y adultos y afectan por igual a hombres y mujeres. La prevalencia es de 318,5/100.000 habitantes – año en EC y 286,3/100.000 habitantes – año en CU, y la incidencia es de 23,82/100.000 habitantes – año en EC y 57,7/100.000 habitantes – año en CU para los países desarrollados. A nivel mundial aproximadamente cinco millones de personas entre los 15 y los 35 años están afectadas de EC y CU⁶⁻⁸. En España se ha observado un aumento de su incidencia en los últimos años con un 42,2% de casos de EC y 87,8% de CU (7). Estas elevadas cifras

posicionan a la EII como un problema importante de salud pública y, además, supone una elevada carga a los sistemas de salud ⁹.

La EII es una enfermedad crónica y hasta la fecha no se ha descubierto ningún tratamiento que sea curativo. No obstante, se dispone de una amplia batería de fármacos que permiten tener un adecuado control de los síntomas; entre ellos, los 5-ASA o los antiinflamatorios esteroideos (AIEs), inmunosupresores como la azatioprina, antibióticos (ciprofloxacina, metronidazol, claritromicina, rifaximina y cotrimoxazol), terapias biológicas como anti-TNF- α (infliximab, adalimumab y golimumab); sin embargo, si estos tratamientos farmacológicos se utilizan durante largos periodos, además de perder eficacia no están exentos de riesgos, reacciones adversas y efectos secundarios sistémicos que complican la salud del paciente con EII¹⁰. En virtud de ello, se hace necesario el planteamiento de alternativas terapéuticas que sean eficaces para el control de la EII y eviten los riesgos asociados a los tratamientos farmacológicos¹¹. En este sentido, se ha descrito la efectividad de la actividad física (AF) como terapia coadyuvante no farmacológica en otras enfermedades crónicas, tales como el cáncer de mama, la enfermedad renal crónica, enfermedades cardiovasculares y diabetes mellitus tipo II. En estos casos, se ha observado que no solo mejora el rendimiento físico de los pacientes, sino que se reducen los signos clínicos e induce cambios psicológicos asociados tanto a la enfermedad como al tratamiento, consiguiéndose una mejor calidad de vida relacionada con la salud (CVRS) ¹²⁻¹⁸.

De forma general, los niveles habituales de AF en pacientes con EII son muy bajos, lo que repercute en un inadecuado control de la enfermedad e incrementa la recurrencia. Por esta razón, se ha recomendado el entrenamiento regular con ejercicios aeróbicos (AE) y de fuerza (Fz), como terapia complementaria para las personas con EII por sus posibles efectos beneficiosos sobre la condición física, la salud mental y porque ayu-

da a contrarrestar algunas complicaciones específicas de la EII al mejorar la densidad mineral ósea, la respuesta inmunológica, la pérdida de peso, la fatiga, y la inflamación. ¹⁹⁻²¹. Por todo lo anterior, en el presente trabajo se revisaron diferentes estudios que evaluaron el efecto de las intervenciones de AF sobre la condición física, la sintomatología, y la CVRS en pacientes con EII (EC o CU) y, además, se trató de identificar el componente de la actividad física más adecuado.

MATERIAL Y MÉTODOS

Estrategia de búsqueda

El presente estudio es una revisión narrativa, llevada a cabo entre octubre del 2021 y enero del 2022, cuyo objetivo fue analizar la literatura actualizada sobre las intervenciones de actividad física sobre adultos con EII (EC o CU). La búsqueda bibliográfica se realizó en las bases de datos electrónicas: Medline (PubMed), SciELO y Cochrane Library Plus. Los términos utilizados en la búsqueda primaria estaban relacionados con la AF y la EII en diferentes combinaciones usando los operadores booleanos "OR" / "AND" como nexo de búsqueda: "Inflammatory bowel disease", "Crohn's disease", "Physical exercise", "Physical activity", "Exercise therapy", "Physical treatment", "Adaptations", "Markers", "Effects", "Analysis", "Biomarkers", "Indicators", "Activity", "Pathways", "Health-related quality of life", "Quality of life", "Inflammation", "Fatigue" and "Microbiota".

Una vez ubicados los artículos en las bases de datos, se cotejaron los títulos de la búsqueda para identificar duplicados y posibles publicaciones que añadir. Posterior a la lectura de cada resumen, se procedió a la revisión a texto completo de los artículos seleccionados.

Criterios de inclusión

La selección de los registros se basó en los siguientes criterios a) Adultos diagnosticados de EII (CU o EC) (excluyendo estudios

en animales y/o *in vitro*), b) Estudios que evaluaron los efectos de una intervención de AF, c) Ensayos clínicos aleatorios (excluyendo registros editoriales, revisiones, notas y cualquier otro estudio no original), d) Estudios que evalúen como resultados (primarios, secundarios o de seguridad) modificaciones físicas, biológicas, psicológicas y de calidad de vida, e) Estudios con información clara sobre la intervención y la duración de la AF, f) Estudios publicados en los últimos 10 años. Los registros que no cumplieran los criterios fueron excluidos de esta revisión narrativa.

RESULTADOS

En la Tabla 1 se analiza la información respecto a los datos obtenidos en las fuentes de estudio, situación del paciente con EII, diseño de estudio, características de los participantes y protocolo de intervención de AF como medida no farmacológica en pacientes con EII. El diseño de los 4 estudios²²⁻²⁵ incluidos en la revisión son ensayos controlados aleatorios (ECAs). Fueron incluidos un total de 133 adultos diagnosticados de EII (CU o EC); 55 hombres y 78 mujeres ≥ 18 años. Todos los estudios excluían a personas que presentasen alto nivel previo de AF y comorbilidades que impidiesen la práctica de AF propuesta en la intervención de los estudios²²⁻²⁵. Con respecto a la EII, distinguiendo entre EC y CU, se contaba con que todos los pacientes tuviesen en común un bajo nivel de actividad de la enfermedad; es decir, se encontrasen en fase de remisión de la enfermedad. Para ello se tomaron como referencia los biomarcadores clínicos calprotectina fecal (CF) $< 150 \mu\text{g}/\text{g}$ y un índice de actividad de la enfermedad de Crohn *Crohn's Disease Activity Index* (CDAI) < 150 puntos. Esto permitió una adecuada comparación entre los cuatro estudios²²⁻²⁵ al encontrarse los pacientes en el mismo estadio de la enfermedad. Además, Klare y col.²⁴, emplearon como indicador del estado de la enfermedad

el índice de Rachmilewitz (IR) < 11 puntos y Jones y col.²⁵ incluyeron una adherencia farmacológica estable de duración > 4 semanas. La intervención de ejercicio para Cronin y col.²², fue de un total de 24 sesiones en 8 semanas, en el que se sometía a los pacientes a AF AE y de Fz, incluyendo todos los grupos musculares (superior, central e inferior). Tew y col.²³, realizaron un estudio de 36 sesiones en 12 semanas en el que se centraban únicamente en la AF aeróbica, dividiendo el grupo intervención en dos subgrupos, uno de intensidad moderada y otro de alta intensidad. La intervención de Klare y col.²⁴, tuvo una duración de 30 sesiones en 10 semanas en las cuales se realizaba trote o carrera supervisada y controlada como elemento de AF aeróbica. Por otro lado, Jones y col.²⁵, realizaron un estudio de mayor duración con 78 sesiones durante 12 semanas, en el que se realizaba ejercicio de impacto junto con ejercicios de resistencia en cada sesión.

La adherencia a su intervención de AF fue elevada de 68%²², 87.5%²³ y 62%²⁵, el estudio restante no especificó la adherencia de participación²⁴. Tres de los estudios realizaron sus intervenciones con supervisión completa²²⁻²⁴; el estudio de Jones y col.²⁵, en cambio, realizó supervisión gradual que fue disminuyendo conforme avanzaba la intervención.

Los principales resultados y conclusiones de cada uno de los estudios incluidos en esta revisión²²⁻²⁵ se reportan en la Tabla 2. También se observó mejoría en la tensión arterial (TA) y la frecuencia cardíaca (FC) en reposo en tres de los estudios^{22, 23, 25}, Klare y col.²⁴, fueron los únicos en no indicar sus variaciones. Tew y col.²³ y Jones y col.²⁵, evaluaron la escala de fatiga con Escala de Fatiga para EII (IBD-F), ya que es un problema que afecta a estos pacientes, observando una reducción de esta. El microbioma intestinal únicamente se valoró en el estudio de Cronin y col.²², en el que se observó un aumento de la Archaea α -diversidad, aunque manteniendo los mismos niveles de Archaea β -diversidad.

Tabla 1
Resumen de las características generales de los estudios incluidos en la revisión que investigan el impacto del ejercicio físico en pacientes con enfermedad inflamatoria intestinal.

Autor/es – Año – País	Población	Diseño de estudio	Estado de la enfermedad inflamatoria intestinal	Intervención
Cronin y col. ²² 2019 Irlanda	n=20(15♂;5♀) Edad: 25 ± 6,5 años GC: n = 7 (86%♂;14%♀) GAF: n=13 (69%♂;31%♀) Adherencia AF: 87,5% Supervisión completa	Ensayo controlado aleatorizado. Exclusión: comorbilidades que impedirían la práctica de AF, alto nivel previo de AF, brotes de la enfermedad, tratamiento con corticosteroides en las dos semanas previas	Remisión de enfermedad (CF < 150 μg/g; CDAI < 150 puntos)	8 semanas, 3 veces/semana. 24 sesiones. 60 min/sesión 5 min calentamiento AE: 18- 32 min intensidad moderada, 5-7 Escala de Borg 10 puntos. Trote/ carrera en cinta o ciclismo estacionario. Fz: intensidad del 70% del valor de IRM. Progresivo de 15% a 20%. 7 máquinas de resistencia, 3 series * 8 repeticiones – Parte superior del cuerpo: press hombros y pecho, flexiones laterales y remo en Fowler. – Parte inferior del cuerpo: extensión + flexión de pierna, retroceso de glúteo y presión en pierna – Músculos centrales: rizos abdominales y rotación del torso
Tew y col. ²³ 2019 Reino Unido	n = 36 (17 ♂; 19 ♀) Edad: 36 ± 11,2 años Tres grupos de estudio: GC: n = 11 (64%♂;36%♀) AEMI: n = 12 (25%♂;75%♀) ANAI: n = 13 (54%♂;46% ♀) Adherencia AF: 68% Supervisión completa	Ensayo controlado aleatorizado. Exclusión: comorbilidades que impedirían la práctica de AF, alto nivel previo de AF, embarazadas y personas con poca tolerancia a la punción de extracción sanguínea	Remisión de enfermedad (CF < 150 μg/g; CDAI < 150 puntos)	12 semanas, 3 veces/semana. 36 sesiones AF: ciclismo de pierna cicloergómetro. 38 min/sesión AEMI – 28 min/sesión ANAI – 5 min calentamiento (al 15% de IRM) – AEMI: 30 episodios de 1 min al 35% IRM. 30 min FC: 68% del máximo – ANAI: 10 episodios de 1 min al 90% de IRM + 10 episodios de 1 min al 15% de IRM. 20 min FC: 92% del máximo – 3 min enfriamiento al 15% de IRM

Tabla 1. Continuación

Autor/es – Año – País	Población	Diseño de estudio	Estudio de enfermedad inflamatoria intestinal	Intervención
Klare y col. ²⁴ 2015 Alemania	n=30 (8♂ (27%); 22♀ (73%)) Edad: 41,1 ± 14,1 años GC: n= 15 (33%♂; 67%♀) GAF: n =15 (20%♂;80%♀) Adherencia AF: no especificada Supervisión completa	Ensayo controlado aleatorizado. Exclusión: comorbilidades que impedirían la práctica de AF, alto nivel previo de AF y alta actividad de la EII (CDAI ≥220 o RI II)	Pacientes en remisión de enfermedad o en fase activa leve (CDAI ≤150 puntos o IR ≤11 puntos).	10 semanas, 3 veces/semana 30 sesiones AE: trote o carrera progresiva supervisada de intensidad moderada. 2 horas a la semana (40 min/sesión).
Jones y col. ²⁵ 2020 Reino Unido	n = 47 (32♂; 15♀) Edad: 49 ± 3,1 años GC:n=23(33%♂;67%♀) GAF:n=24(30%♂;70%♀) Adherencia AF: 62% Supervisión gradual	Ensayo controlado aleatorizado. Exclusión: comorbilidades que impedirían la práctica de AF, alto nivel previo de AF, intervenciones quirúrgicas importantes recientes, embarazo, participación en ensayos clínicos simultáneos	Pacientes con CF <250µg/g enfermedad levemente activa (CDAI <150 puntos) y medicación estable (>4 semanas de tratamiento)	26 semanas, 3 veces/semana 78 sesiones 5 min calentamiento (aumento de FC y estiramientos dinámicos) Sesión: 50 min de EFim + Fz EFim: 10-15 repeticiones de saltos diferentes + 5 min salto de cuerda Fz: 2-3 series con 10-15 repeticiones para 8 ejercicios diferentes de intensidad moderada-alta. Principales grupos musculares: parte superior, sección media y parte inferior del cuerpo. 5 min enfriamiento estiramientos estáticos

Abreviaturas: (N) Número de participantes; (♂) Hombres; (♀) Mujeres; (±) Más/Menos; (GC) Grupo de control; (%) Porcentaje; (GAF) Grupo de actividad física; (AF) Actividad física; (CF) Calprotectina fecal; (<) Menor de; (µg/g); Microgramos por gramo; (CDAI) Índice de actividad de la enfermedad de Crohn; (Min) Minutos; (AE) Aeróbico; (Fz) Fuerza; (LRM) Una repetición máxima; (*) Signo de multiplicación; (+) Más; (AEMI) Grupo aeróbico moderada intensidad; (ANAII) Grupo anaeróbico alta intensidad; (FC) Frecuencia cardíaca; (EII) Enfermedad inflamatoria intestinal; (≥) Mayor o igual de; (IR) Índice de Rachmi-lewitz; (≤) Menor o igual de; (>) Mayor de; (EFim) Ejercicio de impacto.

Tabla 2. Resumen de la evaluación, los resultados y las conclusiones obtenidas de los estudios incluidos en la revisión que investigan el impacto del ejercicio físico en pacientes con enfermedad inflamatoria intestinal.

Autor/es – Año – País	Población	Evaluación	Resultados GAF Vs. GC	Conclusiones
Cronin y col. ²² 2019 Irlanda	n=20 ♂ y ♀ Edad: 25±6,5 años	Resistencia: 70% del valor de IRM. Función física: 5-7 Escala de Borg 10 puntos. Función digestiva: colonoscopia DMO: Rx Función biológica: análisis sangre/heces. CVRS: cuestionario SF-36 Función psicológica: HADS, STAI, BDI-II	<ul style="list-style-type: none"> ↔ VO2max ↓ TA ↓* FC ↔ Estado físico ↔ Fatiga ↑* Grasa corporal ↑ Masa muscular ↓ Inflamación intestinal: - ↓ Citocinas proinflamatorias (IL-8, IL-6 y TNF-α) - ↑ Citocinas antiinflamatorias (IL-10) - ↓ PCR <p>Microbiota intestinal:</p> <ul style="list-style-type: none"> - ↑ Archaea α-diversidad - = Archaea β-diversidad = Actividad de la enfermedad ↔ Manifestaciones extraintestinales ↑ DMO ↔ CVRS ↔ Estado de ánimo 	La AF combinada a corto plazo provoca modificaciones beneficiosas en la composición corporal de los pacientes, convirtiéndose en una estrategia económica en la prevención y tratamiento no farmacológico de la EII y los trastornos metabólicos relacionados con ella. Esta terapia mejora la sintomatología de la enfermedad y aporta a los pacientes un incremento en su CVRS.
Tew y col. ²³ 2019 Reino Unido	n=36 (17♂;19♀) Edad: 36 ± 11,2 años	Resistencia: - 15% del valor de 1MR en calentamiento, 35% GEFM, 90% ↓ FC GEFI - FC 68% máx. GEFM, 92% GEFI. Función física: - IPAQ - IBD-F Scale Función digestiva: colonoscopia Función biológica: análisis de sangre/heces Función psicológica: - Cuestionario EQ-5D-5 - Escala HADS	<ul style="list-style-type: none"> ↑* VO2max ↓ TA ↓ FC ↑ Estado físico ↓ Fatiga ↓ Grasa corporal ↑ Masa muscular ↓ Inflamación intestinal - ↔ Citocinas proinflamatorias (IL-8, IL-6 y TNF-α) - ↔ Citocinas antiinflamatorias (IL-10) - ↔ PCR ↔ Microbiota intestinal ↓ Actividad de la enfermedad ↓ Manifestaciones extraintestinales ↔ DMO ↑ CVRS ↑ Estado de ánimo 	Tanto el AEMI como el ANAI se consideran adecuados en adultos con EC en fase de remisión. Se considera una terapia adyuvante beneficiosa que disminuye la sintomatología intestinal y mejora la CVRS.

Tabla 2. Continuación

Autor/es – Año – País	Población	Evaluación	Resultados	Conclusiones
Klare <i>et al.</i> ²⁴ 2015 Alemania	n=30, 8♂;22♀ Edad: 41,1±14,1 años	Función física: IBDQ-32 Función digestiva: IBDQ-32 CDAI DMO: Rx Función biológica: análisis sangre/heces. Función psicológica: Cuestionario EQ-5D-5	<p>↑VO2max ↓TA ↓FC ↑ Estado físico ↓ Fatiga ↓ Grasa corporal ↑ Masa muscular ↓* Inflamación intestinal – ↓ Citocinas proinflamatorias (IL-8, IL-6 y TNF-α) – ↓ Citocinas antiinflamatorias (IL-10) – ↑ PCR ↓ Microbiota intestinal: ↓* Actividad de la enfermedad ↓ Manifestaciones extraintestinales ↑ DMO ↑ CVRS ↑* Estado de ánimo</p>	<p>La AF realizada de manera continua, es un tratamiento adyuvante indicado para mejorar la CVRS y la sintomatología en los pacientes con EII en fase activa leve. El aumento de PCR puede ser indicativo de la inflamación producida por la práctica inicial de AF, reduciendo el resto de los marcadores inflamatorios.</p>

Tabla 2. Continuación

Autor/es – Año – País	Población	Evaluación	Resultados	Conclusiones
Jones <i>et al.</i> 25 2020 Reino Unido	n = 47 (32♂; 15♀) Edad: 49 ± 3, 1 años	Función física: – IBDQ-32 – Toma de TA y FC – IBD Fatigue Scale Función digestiva: – IBDQ-32 – CDAI DMO; Rx Función biológica: análisis sangre/heces. Función psicológica: – IBDQ-32 – EQ-5D-5	↑VO2max ↔ TA ↓FC ↑ Estado físico ↓ Fatiga ↓ Grasa corporal ↑ Masa muscular ↓* Inflamación intestinal – ϕ Citocinas proinflamatorias (IL-8, IL-6 y TNF- α) – ϕ Citocinas antiinflamatorias (IL-10) – ↓ PCR ϕ Microbiota intestinal: ↓ Actividad de la enfermedad ↓* Manifestaciones extraintestinales ↑ DMO ↑ CVRS ↑ Estado de ánimo	La AF que combina ejercicio aeróbico que aumente la FC, y ejercicios de impacto, en personas con EI, mejoró su función muscular, su DMO y su CVRS, evidenciando su utilidad en reducir el riesgo de complicaciones futuras y fracturas osteoporóticas.

Abreviaturas: (GAF) Grupo de actividad física; (GC) Grupo de control; (N) Número de participantes; (♂) Hombres; (♀) Mujeres; (\pm) Más/Menos; (TA) Tensión arterial; (FC) Frecuencia cardiaca; (%) Porcentaje; (IRM) Una repetición máxima; (CVRS); Calidad de vida relacionada con la salud; (Rx) Radiografía; (SF-36) Short Form 36 Questionnaire; (HADS) Hospital Anxiety and Depression Scale; (STAI) State Trait Anxiety Inventory; (BDI-II) Beck Depression Inventory II; (VO2max) Consumo máximo de oxígeno; (ϕ) No se especifica; (↓*) Disminución significativa; (↓) Disminución; (↑*) Aumento significativo; (↑) Aumento; (=) No hay cambios; (↔) Sin cambios estadísticamente significativos; (IL) Interleucinas; (TNF- α) Factor de necrosis tumoral Alfa; (PCR) Proteína C reactiva; (AF) Actividad física; (EI) Enfermedad inflamatoria intestinal; (AEM) Grupo aeróbico moderada intensidad; (ANAD) Grupo anaeróbico alta intensidad; (IPAQ) Cuestionario internacional de actividad física-largo; (IBD-F Scale) Escala de fatiga en enfermedad inflamatoria intestinal; (EQ-5D-5) Cuestionario EuroQol-5D; (EC) Enfermedad de Crohn; (IBDQ-32) Cuestionario de 32 ítems sobre calidad de vida para la enfermedad inflamatoria intestinal; (ECG) Electrocardiograma; (CAI) Índice de actividad de la enfermedad de Crohn; (IR) Índice de Rachmilewitz; (DMO) Densidad mineral ósea.

DISCUSIÓN

El objetivo de este estudio fue evaluar el impacto de las intervenciones de AF en pacientes con EII. Los resultados más relevantes de esta revisión son que la realización de AF por pacientes con CU y EC mejora de la capacidad física, el cambio de los parámetros antropométricos (aumento de la masa muscular esquelética y disminución de grasa corporal), incrementa la CVRS; además, tiene efectos positivos sobre la función muscular, la fatiga y la densidad mineral ósea (DMO)²²⁻²⁵. Por otro lado, no indujo inflamación intestinal y las manifestaciones extra-intestinales; asimismo, no se infirieron cambios sustanciales en la microbiota intestinal. Para proporcionar un análisis más claro, en esta revisión se agruparon los resultados más relevantes.

Metodología en la realización de actividad física

La prescripción de AF se realizó en fase de remisión²²⁻²⁴, estado quiescente²⁵, y media²⁵ o baja²⁴ actividad con unos niveles CDAI < 150²²⁻²⁵ y de CF < 250 $\mu\text{g}/\text{g}$ ²⁵, que indica remisión clínica con algún grado de inflamación residual en la mucosa intestinal y con bajo riesgo de enfermedad recidiva²⁶. Actualmente, las directrices de AF en EII se sustentan en datos de ejercicio en individuos con baja actividad de la enfermedad, pero no sobre pacientes con exacerbación de la EII²⁷. De esta manera, es posible que la elección del estadio (remisión o baja actividad de la EII) de enfermedad del paciente para la práctica de AF esté determinado por la falta de estudios en este grupo de pacientes de alto riesgo²⁵. La AF no está exenta de riesgos en este tipo de pacientes; un alto número de ellos la abandonan por las posibles complicaciones que surgen durante su realización tales como es el dolor articular por la disminución de la masa ósea, la fatiga y debilidad²⁸.

La planificación de la AF en EII se basa en el uso de diferentes tipos de ejercicio que

incluyen trabajo aeróbico (AE)²²⁻²⁵, anaeróbico (ANE)²³ y de Fz²²⁻²⁵. Tew *et al.*²³, propone un entrenamiento de las capacidades aeróbicas (frecuencia cardíaca máxima al 68%) y anaeróbicas (frecuencia cardíaca máxima al 92%) en cicloergómetro a intensidades exigentes. El ejercicio combinado (AE + Fz) es empleado utilizando intensidades medias/altas de AE (5-7 Escala de Borg 10 puntos) y altas de Fz (70% repetición máxima)²². Estas intensidades medias/altas también son utilizadas por Jones y col.²⁵ con trabajo exclusivo de Fz, mediante los ejercicios con bandas elásticas de resistencia y ejercicios de alto impacto, que obligan a despejar los pies del suelo, lo que requiere un nivel de fuerza muscular considerable para realizarse.

En tres estudios^{22,23,25} incluidos en esta revisión, el trabajo físico se ha implementado a intensidades elevadas en pacientes con EII. Esto supone una novedad para pacientes con EII, donde tradicionalmente la AF a una intensidad de baja a moderada se ha considerado la adecuada²⁴, para evitar una posible exacerbación de la enfermedad²¹. El trabajo de Fz en intensidades exigentes²²⁻²⁵ desarrollaría hipertrofia muscular tras un proceso de inflamación local, derivada del daño sobre el músculo esquelético²⁹, que podría incrementar el riesgo de recurrencia y recrudescer la inflamación. Por otra parte, la AE/ANE de alta intensidad²²⁻²³ puede inducir una inflamación sistémica leve y un aumento de citocinas inflamatorias en pacientes con EII activa o en remisión³⁰. Además, se ha observado que el ejercicio extenuante en deportistas sanos provoca una colitis isquémica con diarrea sanguinolenta, fiebre y altos niveles de fatiga³¹. Asumiendo estas consideraciones e interpretando el adagio hipocrático "*primun non nocere*", Klare y col.²⁴ realizaron la intervención más conservadora de AE a intensidades que permitían a los participantes seguir hablando mientras corrían y bajo supervisión médica.

La contribución de la AF para modular el estado de salud y controlar algunos de los factores de riesgo en personas que padecen

enfermedades crónicas, debe realizarse de manera regular y continuada¹⁹. Se ejecutaron entre 24 y 78 sesiones de AF con una frecuencia de 3 sesiones/semana con una duración de entre 2-3 horas/semana²²⁻²⁵. Este conjunto ordenado y sistemático de prescripción de AF es similar en cuanto a los componentes (tipo de ejercicio, intensidad, duración, frecuencia) aplicados en otras enfermedades crónicas y que han conseguido óptimos resultados en el estado de salud de los pacientes^{12, 13}. De esta forma, podrían quedar desterradas aquellas directrices de prescripción intensidad baja y duración corta en la AF de pacientes con EII.

La supervisión médica completa²²⁻²⁴ o gradual²⁵ es necesaria en pacientes con EII que practican AF. En tres estudios²²⁻²⁵ un total de diez pacientes han padecido efectos adversos relacionados con la AF como son: dolor leve abdominal (n=1)²⁴, náuseas y mareos (n=3)²⁵, anemia leve (n=1), estrés (n=1), deshidratación y nutrición inadecuada (n=4)²³. Es probable que estos cuadros leves sean derivados de no cumplir los requerimientos extra de nutrición e hidratación que requiere la práctica de AF³². Debería ajustarse el incremento calórico y de líquidos en función del tipo y tiempo dedicado a la AF y a las características del paciente. De este modo se permite conservar el volumen sanguíneo, el sistema cardiovascular y termorregulador, la reposición de glucógeno hepático y muscular³³ que son esenciales en los pacientes con EII.

Impacto de la actividad física sobre los factores físicos/fisiológicos modificables de los pacientes que padecen enfermedad inflamatoria intestinal.

La EII, como enfermedad crónica autoinmune, impacta negativamente el estado físico del paciente quien se ve limitado para realizar sus actividades diarias más comunes⁹. La frecuencia cardíaca (FC) es uno de los marcadores para valorar la severidad de la EII³⁴ y ofrece datos cuantificables sobre la condición física^{24, 25, 27}. La realización de

AF programada (AE, ANE, Fz) produjo una disminución de la FC mejorando la condición física^{22, 23, 25}. La disminución de la FC contribuye a la tolerancia de la AF, permitiendo la elevación gradual de las cargas en el entrenamiento (volumen e intensidad) y a la progresión en los resultados físicos^{35, 36}. La mejora de niveles basales de FC, por la AF, permite disminuir el riesgo de episodios isquémicos, muerte súbita, y mortalidad por fallo cardiovascular³⁷. Por lo tanto, en la EII el control de la FC constituye un objetivo terapéutico razonable mediado por la AF.

En tres de los estudios²³⁻²⁵, se indicó que a través de la realización de AF (AE, ANE, Fz) se mejoró el volumen máximo de oxígeno (VO₂máx) y se incrementó en el estado físico general de los pacientes con EII. Estos pacientes con EII tienen disminuida de forma considerable la tolerancia al ejercicio y la capacidad física²⁴; con la práctica de AF se revierte esta situación en EII, de la misma forma que ocurre con otras enfermedades crónicas¹³. Estas mejoras en la condición física influirían en los descensos de la fatiga que fue evaluada con Escala de Fatiga en Enfermedad Inflamatoria Intestinal (IBD-F Scale)^{23, 25}. La fatiga es un síntoma común e incapacitante, de carácter transitorio y/o crónica (mayor de 6 meses), en pacientes con EII activa o en remisión clínica³⁸. La reducción de la fatiga implicaría una menor sensación de cansancio, aumento de los niveles de energía y una mayor Fz muscular³⁹. Por lo tanto, les permitiría realizar sus actividades cotidianas, estimularía la concentración y la memoria, incrementaría las actividades de ocio, mejoraría el rendimiento en el ámbito laboral y en el estudio⁴⁰.

La hipertensión arterial (HTA) es un posible efecto adverso de algunos tratamientos médicos como la ciclosporina, el tacrolimus o los corticoesteroides sistémicos⁴¹. El control de la HTA por la AF se observó en dos estudios de esta revisión^{22, 23}, que incluían el ejercicio concurrente (AE + Fz)²² e intensidades medias-altas de AF en cicloergómetro²³. Es conocido que los efectos hemodiná-

micos de la práctica regular de AF mejoran la función cardiovascular, estabilizando/modulando la tensión arterial (TA) ⁴². Otro mecanismo de control de la TA sea probablemente por la restauración de la disbiosis de los pacientes con EII ²² por la acción de la AF ⁴³.

La AF se ha asociado con beneficios para la salud sobre el índice de masa corporal (IMC), la DMO, y la masa muscular ¹⁹. De este modo, los programas de AF son de especial interés para los pacientes con EII, quienes sufren problemas de baja DMO, reducida masa muscular y con unos porcentajes de comorbilidad entre obesidad y EII del 15-40% ⁴⁴. Todas las intervenciones de AF ²²⁻²⁵ consiguieron disminuir la grasa corporal, siendo significativa la realizada con trabajo físico concurrente ⁴⁵. El control de la masa grasa reduce el grado de obesidad que, en pacientes de EII, es considerado como un factor riesgo de enfermedad recidiva, de pérdida de respuesta a la terapia farmacológica y de complicaciones postquirúrgicas ⁴⁶.

Mediante la absorciometría de energía dual de rayos X, se observó que en la AF ^{22, 24, 25}, tanto el entrenamiento AE como el entrenamiento de Fz, muestra efectos positivos sobre el metabolismo óseo, los cuales parecen generarse más por un efecto de disminución de la tasa de pérdida de hueso, que por un aumento de la DMO. La desmineralización ósea y la osteoporosis son complicaciones comunes asociadas a la EII; la prevalencia de baja masa ósea en el 30% de los pacientes y la DMO media sería un 10% menor que en la población general ⁴⁷. El mantenimiento de DMO, haría reducir el riesgo de sufrir fracturas y la posibilidad de mantener el tratamiento con glucocorticoides para el control de la EII ⁴⁹. El entrenamiento de Fz estimula más intensamente la DMO que AF aeróbica por efecto directo sobre la formación osteoblástica, e indirecto por la masa muscular que actuará sobre el tejido óseo por medio

de una serie de fuerzas localizadas producidas por la contracción muscular ⁵⁰.

La hipertrofia muscular generada por la realización de AF produce aumento de la tensión mecánica, provoca estrés metabólico y daños musculares que activan la respuesta de inflamación, lo que posibilita la exacerbación de la enfermedad ²¹. Sin embargo, con todos los programas de AF ²²⁻²⁵ se obtuvieron incrementos en la masa muscular sin exacerbaciones de la EII y/o lesiones musculares y sin generar inflamación sistémica con niveles circulantes de la proteína C reactiva (PCR) estables ²³ o incluso menores ²²⁻²⁵. La ganancia de masa muscular reportada después de programas de entrenamiento quizá sea una de las adaptaciones más importantes en el paciente con EII, y que podría ratificar la idoneidad de protocolo de ejercicio derivada de AF ²²⁻²⁵. Los programas de entrenamiento que superan la tolerancia de los pacientes de EII hacen también disminuir la concentración de glucógeno a niveles incapacitantes ³⁰, ya que la inflamación del intestino induce una mala absorción de los alimentos. Las mejoras en la masa muscular en pacientes con EII que practican AF programada, podría deberse a la reducción de la expresión de proteínas anti-apoptóticas, Bcl-2 y Bcl-XL, (mantenimiento de la musculatura) ¹⁵, la secreción en el músculo esquelético humano de IL-15 (factor anabólico muscular) ⁵⁰, y la sobreexpresión factor coactivador 1- α del receptor de proliferación de peroxisomas (PGC-1 α) ⁵¹, preservando la masa muscular por bloqueo de *mammalian target of rapamycin complex 1* (mTORC1) ⁵².

Todos estos resultados convierten a la AF como una intervención activa y multidisciplinaria, para optimizar el estado de salud en el paciente por la mitigación de factores físicos/fisiológicos, responsables las complicaciones en EII. Además, superar las limitaciones físicas y clínicas podría acrecentar el interés y la adherencia a programas de AF dirigida a EII.

Acción biológica de los beneficios del ejercicio en los pacientes de EII

El efecto protector de la AF en la EII puede atribuirse a su efecto antiinflamatorio²²⁻²⁵. El mecanismo antiinflamatorio directo responsable se produce a través de la liberación de interleucinas (IL) IL-6 e IL-15, disminución de las citocinas pro-inflamatorias (IL-8, factor de necrosis tumoral alfa (TNF- α)) y estimulación de la acción antiinflamatoria de IL-10^{22, 24}, por su papel regulador de la respuesta inmune sobre algunas citoquinas, macrófagos y linfocitos T⁵³. Adicionalmente, la acción de IL-6 como mioquina antiinflamatoria- está mediada por sus efectos inhibidores sobre TNF- α e IL-1 y su activación de IL-1ra e IL-10, aunque se debe considerar su efecto dual como antiinflamatorio y proinflamatorio^{21, 27,30}. También la adrenalina es otro posible factor que inhibe la producción de TNF- α ⁵⁴ y de este modo, el control del proceso de inflamatorio que haría disminuir la actividad de la EII²³⁻²⁵ y las manifestaciones extraintestinales²³⁻²⁵. Con ello se logra disminuir a 1 ó 2 deposiciones diarias (lo que aminora la deshidratación, ayudando a la recuperación de la concentración osmótica fisiológica entre 50 y 125 mOsm/kg) y reducir los espasmos intestinales^{3, 22, 55}.

Los péptidos similares al glucagón, la irisina y la proteína secretada, ácida y rica en cisteína (SPARC), también aumentan con la AF. Todos ellos, contribuyen a la remodelación y la reparación de la mucosa intestinal dañada en los procesos de EII^{21, 27, 30}. La importancia de mantener el epitelio intestinal es porque la reducción de la integridad de la barrera intestinal ocasionaría un aumento de la permeabilidad intestinal; ello posibilita el paso a la circulación sanguínea de lipopolisacáridos y otros componentes del peptidoglicano de la pared celular bacteriana, que desencadenan la inflamación de bajo grado asociada a la HTA y la obesidad en pacientes con EII⁵⁶.

Los niveles más altos de AF y una óptima capacidad cardiorrespiratoria se asocian con una mayor diversidad bacteriana fecal,

lo que genera y mantiene la heterogeneidad en la microbiota⁴³. El óptimo equilibrio microbiano contribuye al adecuado ecosistema intestinal que es esencial en la promoción de salud y la prevención de enfermedades crónicas no transmisibles como las enfermedades inflamatorias⁵⁷. La AF concurrente y prolongada (8 semanas) de media / alta intensidad (AE: 5-7 escala Borg; Fz 70% repetición máxima (RM)) induce una mayor diversidad microbiota *Archaea- α* ²⁴ (cuya función principal es evitar la colonización de especies como el *Clostridium difficile*). Estos resultados son similares a estudios en voluntarios sanos, con un programa de ejercicio moderado⁵⁸ y en atletas profesionales^{59, 60}. La AF realizada durante un periodo de tiempo prolongado y con intensidad progresiva, disminuye el recuento leucocitario causante de la destrucción del microbioma intestinal y regula la actividad del intestino^{23, 24}.

Efectos de la realización de actividad física en la calidad de vida de los pacientes

Es común la afectación de las enfermedades crónicas en el ámbito psicológico. Los pacientes con EII relacionan su afectación psicológica con el deterioro físico, los propios síntomas de la enfermedad y las comorbilidades que se asocian a ella, causándoles un aminoramiento del estado de ánimo y de su CVRS^{3, 61}. Aunque Cronin y col.²² no reportan cambios en el estado de ánimo de los pacientes en su estudio, Tew y col.²³, Klare y col.²⁴ y Jones y col.²⁵ concluyeron que la AF puede establecer mejorías de forma significativa en el bienestar general y el estado de ánimo de los pacientes, lo que mejora su CVRS y aumenta su satisfacción y percepción psicológica con su estado de salud.

Las mejoras reportadas en la CVRS vendrían derivadas de la optimización física, fisiológica y biológica, logradas por la AF como terapia adyuvante²²⁻²⁵. En su conjunto, estos efectos positivos derivados de la AF proporcionarían una estrategia de afrontamiento ante el anhelo constante de ser personas sanas ante los demás y poder superar el hecho

de vivir constantemente con la amenaza e incertidumbre de sentirse constantemente personas enfermas. Además, ayudaría a superar el posible aislamiento laboral, familiar y social debido a la imposibilidad de predecir cuándo y por qué se va a desencadenar una fase de actividad de la enfermedad.

Por lo reportado anteriormente, se podría establecer que el AF combinada de AE y Fz -aplicada con intensidad moderada- es lo más adecuado para obtener mejoras sobre el estado físico y los resultados de salud en pacientes con EII. En este sentido, proponemos un protocolo sencillo y de fácil implementación de AF para pacientes con EII (CU o EC) (Fig. 1). La AF podría consistir, inicialmente, en un calentamiento breve de 5 minutos de duración, que permita activar los grupos musculares que se van a ejercitar. La parte principal de la sesión de AF comenzaría con 20 minutos de ejercicios de Fz sobre los grupos musculares del tren superior e inferior y del tronco del cuerpo; es decir sobre los músculos principales que componen el core (abdominales, lumbares, músculos de la pelvis, glúteos y musculatura de la columna). Se continuaría con 30 minutos de AE, que podría realizarse sobre una bicicleta estática, o con carrera continua moderada en cinta o al aire libre en un terreno sin dificultades orográficas. Finalmente, proponemos una fase de “*cool down*” o vuelta a la calma de 5 minutos de duración mediante estiramientos suaves. El objetivo de la vuelta a la calma serviría de ayuda a los pacientes con EII a regenerarse tras la AF, lo que podría proporcionar beneficios a nivel físico (prevenir lesiones, mareos y dolores) y mental.

Esta revisión tuvo, como principal limitación, la escasa cantidad de estudios y el bajo número de pacientes (n=133) incluidos. Sin embargo, los estudios seleccionados son ECAs, que se consideran los “*gold standards*” para examinar si existe una relación de causa-efecto entre la realización de AF y los posibles beneficios en pacientes¹³. Además, todos los estudios incluidos analizan grupos población con las mismas características (edad, capacidad física previa y estado de la enfermedad).

En conclusión, la realización de AF concurrente a intensidad moderada durante un periodo de tiempo mínimo de 8 semanas, con tres sesiones a la semana, alcanza resultados notables en los pacientes con EC y CU, tanto a nivel físico como a nivel psicológico, o sobre el control de síntomas de la enfermedad y sus exacerbaciones, siendo bien tolerada por los adultos con EII. Se ha observado un aumento en la masa muscular, la DMO y



Fig. 1. Protocolo de actividad física de ejercicio combinado de actividad aeróbica y fuerza para pacientes con enfermedad inflamatoria intestinal.

el VO₂máx, a su vez que disminuyen la grasa corporal, y la actividad y la inflamación intestinales al controlarse la producción de citoquinas inflamatorias. También se observa una mejora en la CVRS y el estado de ánimo de los pacientes. Estos resultados podrían posicionar a la AF como una intervención coadyuvante, activa y multidisciplinaria para optimizar el estado de salud en la EII.

AGRADECIMIENTO

Los autores quieren agradecer su colaboración al Grupo de Investigación en Neurobiología del Departamento de Biología Celular, Genética, Histología y Farmacología de la Facultad de Medicina de la Universidad de Valladolid.

Financiamiento

Esta investigación no ha recibido financiación externa.

Conflictos de interés

Los autores declaran no tener ningún conflicto de intereses.

Contribuciones de los autores

D.F.-L. y N.H.-B.: concibieron y diseñaron la investigación, analizaron e interpretaron los datos, redactaron el artículo y aprobaron la versión final presentada para su publicación; R.C.M. y S.G.-L.: analizaron e interpretaron los datos, revisaron críticamente el artículo. Todos los autores han leído y aceptado la versión publicada del manuscrito.

Número ORCID de los autores

- Diego Fernández-Lázaro:
0000-0002-6522-8896
- Nuria Hernández-Burgos:
0000-0001-7996-4571

- Raúl Cobreros Mielgo:
0000-0002-4281-9044
- Sandra García-Lázaro:
0000-0001-9439-7413

REFERENCIAS

1. **Oviedo C, Yañez M, Pennacchiotti V.** Frequency of oral manifestation in patients with inflammatory bowel disease in Chile. *Int J Odontostomatol* 2017; 11: 267–271. Disponible en: [https://www.scielo.cl/scielo.php?script=sci_abstract&pid=S0718-381X2017000300267&lng=en&nrm=iso#:~:text=Of%20these%20patients%2C%2037%20%25%20presented,recurrent%20oral%20ulcer%20\(ROU\).](https://www.scielo.cl/scielo.php?script=sci_abstract&pid=S0718-381X2017000300267&lng=en&nrm=iso#:~:text=Of%20these%20patients%2C%2037%20%25%20presented,recurrent%20oral%20ulcer%20(ROU).)
2. **Meligrana N, Quera R, Figueroa C, Ibáñez P, Lubascher J, Kronberg U.** Factores ambientales en el desarrollo y evolución de la enfermedad inflamatoria intestinal. *Rev Med Chile* 2019; 147: 212–220. Disponible en: https://www.scielo.cl/scielo.php?pid=S0034-98872019000200212&script=sci_arttext&tlng=en
3. **World Gastroenterology Organization (WGO).** Practice Guideline Inflammatory bowel disease (IBD). *World Gastroenterology Organisation [Internet]* 2022 [citado, 2022 febrero 10] Disponible en: <https://www.worldgastroenterology.org/guidelines/global-guidelines/inflammatory-bowel-disease-ibd>.
4. **Yamamoto-Furusho JK, Bosques-Padilla FJ, Charúa-Guindic L, Cortés-Espinosa T, Miranda-Cordero RM, Saez A, Ledesma I.** Inflammatory bowel disease in Mexico: epidemiology, burden of disease, and treatment trends. *Rev Gastroenterol México* 2020; 85: 246–256. Disponible en: <https://pubmed.ncbi.nlm.nih.gov/32143974/>.
5. **The European Federation of Crohn's & ulcerative colitis associations (EFCCA).** What is inflammatory bowel disease? *European Federation of Crohn's & ulcerative colitis associations* 2022 [Internet] [citado, 2022 febrero 10] Disponible en: <https://www.efcca.org/en/what-ibd>.

6. **Ng S, Shi H, Hamidi N, Underwood F, Tang W, Benchimol E.** Worldwide incidence and prevalence of inflammatory bowel disease in the 21st century: a systematic review of population-based studies. *Lancet* 2017; 390: 2769–2778. Disponible en: <https://pubmed.ncbi.nlm.nih.gov/29050646/>.
7. **Puig L, Ruiz De Morales J, Dauden E, Andreu J, Cervera R.** La prevalencia de diez enfermedades inflamatorias inmunomediadas (IMID) en España. *Rev Esp Salud Pública* 2019; 93: 1–14. Disponible en: https://scielo.isciii.es/scielo.php?script=sci_abstract&pid=S1135-57272019000100069.
8. **Velásquez JR.** Enfermedad de Crohn. Enfoque diagnóstico y terapéutico de las primeras visitas. *Rev Colomb Gastroenterol* 2014; 29: 404–416. Disponible en: <https://revistagastrocol.com/index.php/rcg/article/view/438>.
9. **Büsch K, Sonnenberg A, Bansback N.** Impact of inflammatory bowel disease on disability. *Curr Gastroenterol Rep* 2014; 16: 414. Disponible en: <https://pubmed.ncbi.nlm.nih.gov/25231757/>.
10. **Seyedian SS, Nokhostin F, Malamir MD.** A review of the diagnosis, prevention, and treatment methods of inflammatory bowel disease. *J Med Life* 2019; 12: 113–122. Disponible en: <https://pubmed.ncbi.nlm.nih.gov/31406511/>.
11. **Ponferrada A.** Efectos adversos de fármacos en EII Efectos adversos de fármacos. 2015. Grupo Español de Trabajo en Enfermería de Crohn y Colitis Ulcerosa [Internet] 2015 Disponible en: <https://geteccu.org/pacientes/efectos-adversos-de-farmacos-en-eii>.
12. **Fernández-Lázaro D, Mielgo-Ayuso J, Caballero-García A, Córdova-Martínez A, Lázaro MP, Fernández-Lázaro CI.** Physical activity in oncological breast cancer patients: non-pharmacological sports medical therapy? Systematic review. *Arch med Deport* 2020; 198: 266–274. Disponible en: <https://dialnet.unirioja.es/servlet/articulo?codigo=7660871>.
13. **Fernández-Lázaro D, Mielgo-Ayuso J, Lázaro-Asensio MP, Martínez AC, Caballero-García A, Fernández-Lázaro CI.** Intradialytic physical exercise in chronic kidney disease: A systematic review of health outcomes. *Arch Med Deport* 2020; 37: 419–429. Disponible en: <https://dialnet.unirioja.es/servlet/articulo?codigo=7772527>
14. **Ramírez-Vélez R.** Physical activity and health-related quality of life: a systematic review of current evidence. *Rev Andal Med Deport* 2010. 3: 110-120 Disponible en: <https://www.elsevier.es/es-revista-revista-andaluza-medicina-del-deporte-284-articulo-actividad-fisica-calidad-vida-relacionada-X1888754610543999>.
15. **Llopis PQ, García-Galbis M.** Control glucémico a través del ejercicio físico en pacientes con diabetes mellitus tipo 2; revisión sistemática. *Nutr Hosp* 2015; 31: 1465–1472. Disponible en: https://www.mendeley.com/catalogue/0b1fc2f8-388f-3490-9119-9be525e2b952/?utm_source=desktop&utm_medium=1.19.8&utm_campaign=open_catalog&userDocumentId=%7Be86582ab-f1cc-325e-9458-cc6941414b32%7D.
16. **Defilippis E, Tabani S, Warren R, Christos P, Bosworth B, Scherl E.** Exercise and self-reported limitations in patients with inflammatory bowel disease. *Dig Dis Sci* 2016; 61: 215–220. Disponible en: <https://pubmed.ncbi.nlm.nih.gov/26254773/>
17. **Cordero A, Masiá MD, Galve E.** Ejercicio físico y salud. *Rev Esp Cardiol* 2014; 67: 748–753. Disponible en: <http://www.revespcardiol.org/es-ejercicio-fisico-salud-articulo-S0300893214002656>.
18. **Candón-Liñán Á, Sánchez-Olliver AJ, Galancho-Reina I, Suárez-Carmona W, González JA.** Ejercicio físico, obesidad e inflamación. *EmásF, revista digital de educación física* 2016; 41: 65-82. Disponible en: <https://dialnet.unirioja.es/servlet/articulo?codigo=5558014>.
19. **Narula N, Fedorak R.** Exercise and inflammatory bowel disease. *Can J Gastroenterol* 2008; 22: 497-504. Disponible en: <https://pubmed.ncbi.nlm.nih.gov/18478136/>.
20. **Reboredo M, Pinheiro B, Chebli J.** Physical exercise programmes in patients with inflammatory bowel disease. *J Crohns colitis* 2017; 11: 1286. Disponible en: <https://pubmed.ncbi.nlm.nih.gov/28369347/>.
21. **Bilski J, Brzozowski B, Mazur A, Sliwowski Z, Brzozowski T.** The role of physical exercise in inflammatory bowel disease. *Biomed Res Int* 2014; 2014: 429031. Dis-

- ponible en: <https://pubmed.ncbi.nlm.nih.gov/24877092/>.
22. **Cronin O, Barton W, Moran C, Sheehan D, Whiston R, Nugent H, Mccarthy Y, Molloy C, O'sullivan O, Cotter PD, Molloy MG, Shanahan F.** Moderate-intensity aerobic and resistance exercise is safe and favorably influences body composition in patients with quiescent inflammatory bowel disease: a randomized controlled cross-over trial. *BMC Gastroenterol* 2019; 19: 29. Disponible en: <https://pubmed.ncbi.nlm.nih.gov/30755154/>.
 23. **Tew GA, Leighton D, Carpenter R, Anderson S, Langmead L, Ramage J, Faulkner J, Coleman E, Fairhurst C, Seed M, Bottoms L.** High-intensity interval training and moderate-intensity continuous training in adults with Crohn's disease: a pilot randomised controlled trial. *BMC Gastroenterol* 2019; 19: 1–11. Disponible en: <https://pubmed.ncbi.nlm.nih.gov/30696423/>.
 24. **Klare P, Nigg J, Nold J, Haller B, Krug A, Mair S, Thoeninger CK, Christle JW, Schmid RM, Halle M, Hubber W.** The impact of a ten-week physical exercise program on health-related quality of life in patients with inflammatory bowel disease: a prospective randomized controlled trial. *Digestion* 2015; 91: 239–247. Disponible en: <https://pubmed.ncbi.nlm.nih.gov/25823689/>.
 25. **Jones K, Baker K, Speight R, Thompson N, Tew G.** Randomised clinical trial: combined impact and resistance training in adults with stable Crohn's disease. *Aliment Pharmacol Ther* 2020; 52: 964–975. Disponible en: <https://pubmed.ncbi.nlm.nih.gov/33119156/>.
 26. **D'haens G, Ferrante M, Vermeire S, Baert F, Noman M, Moortgat L, Geens P, Iwens D, Aerdenl, Van Assche G, Olmen GV, Rutgeerts P.** Fecal calprotectin is a surrogate marker for endoscopic lesions in inflammatory bowel disease. *Inflamm Bowel Dis.* 2012; 18: 2218–2224. Disponible en: <https://pubmed.ncbi.nlm.nih.gov/22344983/>.
 27. **Engels M, Cross R, Long M.** Exercise in patients with inflammatory bowel diseases: current perspectives. *Clin Exp Gastroenterol* 2017; 11: 1–11. Disponible en: <https://pubmed.ncbi.nlm.nih.gov/29317842/>.
 28. **Eckert KG, Abbasi-Neureither I, Köppel M, Huber G.** Structured physical activity interventions as a complementary therapy for patients with inflammatory bowel disease – a scoping review and practical implications. *BMC Gastroenterol* 2019; 19: 115. Disponible en: <https://pubmed.ncbi.nlm.nih.gov/31266461/>.
 29. **Fernández-Lázaro D, Díaz J, Caballero A, Córdova A.** The training of strength-resistance in hypoxia: effect on muscle hypertrophy. *Rev Biomed* 2019; 39: 212–220. Disponible en: <https://pubmed.ncbi.nlm.nih.gov/31021559/>.
 30. **Papadimitriou K.** Effect of resistance exercise training on Crohn's disease patients. *Intest Res* 2020; 19: 275–281. Disponible en: <http://www.irjournal.org/journal/view.php?number=892>.
 31. **Holik D, Včev A, Milostić-Srb A, Salinger Ž, Ivanišević Z, Včev I, Miškulin M.** The effect of daily physical activity on the activity of inflammatory bowel diseases in therapy-free patients. *Acta Clin Croat* 2019; 58: 202-212. Disponible en: <https://pubmed.ncbi.nlm.nih.gov/31819315/>.
 32. **Manonelles P, De Teresa C, Alacid F, Álvarez J, Del Valle M, Gaztañaga T, Gondra J, Luengo E, Martínez P, Gil N.** Deporte recreacional saludable. Documento de consenso de la sociedad española de medicina del deporte (SEMED-FEMEDE). *Arch Med del Deport* 2016; 33: 8–41. Disponible en: <https://dialnet.unirioja.es/servlet/articulo?codigo=6273644>.
 33. **González-Gross M, Gutiérrez A, Mesa JL, Ruiz-Ruiz J, Castillo MJ.** La nutrición en la práctica deportiva: Adaptación de la pirámide nutricional a las características de la dieta del deportista. *Arch Latinoam Nutr* 2001; 51: 321–331. Disponible en: http://ve.scielo.org/scielo.php?script=sci_arttext&pid=S0004-06222001000400001.
 34. **De la Morena F, Gisbert JP.** Anemia y enfermedad inflamatoria intestinal. *Rev Esp Enferm Dig.* 2008; 100: 285-293. Disponible en: https://scielo.isciii.es/scielo.php?script=sci_arttext&pid=S1130-01082008000500007.
 35. **Marins JCB, Marins NM, Fernández M.** Aplicaciones de la frecuencia cardiaca máxima en la evaluación y prescripción de ejercicio.

- Apunt Med l'Esport. 2010; 45: 251–258. Disponible en: <https://dialnet.unirioja.es/servlet/articulo?codigo=3664676>.
36. **Bernal-Reyes F, Peralta-Mendivil A, Gavattono-Nogales HH, Placencia-Camacho L.** Principios de entrenamiento deportivo para la mejora de las capacidades físicas. *Biotecnia* 2014; 16: 42-49. Disponible en: <https://dialnet.unirioja.es/servlet/articulo?codigo=7930481>.
 37. **López-Sendón J, López E.** Reducción de la frecuencia cardiaca. Otras oportunidades terapéuticas. *Rev Española Cardiol* 2007; 7: 53-57. Disponible en: <http://www.revespcardiol.org/es-reduccion-frecuencia-cardiaca-otras-opportunidades-articulo-S113135870775776X>.
 38. **Vogelaar L, Spijker A, Van der Woude C.** The impact of biologics on health-related quality of life in patients with inflammatory bowel disease. *Clin Exp Gastroenterol* 2009; 2: 101-109. Disponible en: <https://pubmed.ncbi.nlm.nih.gov/21694833/>.
 39. **Chavarria-Herbozo CM.** Prevalencia y factores asociados a la fatiga en pacientes con enfermedad inflamatoria intestinal. [Tesis doctoral] Madrid: Univ. Autónoma de Madrid; 2018. Disponible en: <https://dialnet.unirioja.es/servlet/tesis?codigo=150883>.
 40. **D'Silva A, Fox DE, Nasser Y, Vallance JK, Quinn RR, Ronksley PE.** Prevalence and risk factors for fatigue in adults with inflammatory bowel disease: a systematic review with meta-analysis. *Clin Gastroenterol Hepatol.* 2021; 20: 995-1009.e7. Disponible en: <https://pubmed.ncbi.nlm.nih.gov/34216824/>.
 41. **Benítez EM.** Protocolos diagnóstico-terapéuticos de gastroenterología, hepatología y nutrición pediátrica SEGHNPAEP. *Ergón.* 2010; 1: 157-269. Disponible en: <https://www.seghnp.org/documentos/protocolos-diagnostico-terapeuticos-de-gastroenterologia-hepatologia-y-nutricion>.
 42. **Quiroz-Mora CA, Serrato-Ramírez DM, Bergonzoli-Peláez G.** Factores asociados con la adherencia a la actividad física en pacientes con enfermedades crónicas no transmisibles. *Rev Salud Pública* 2018; 20: 460–464. Disponible en: <https://doi.org/10.15446/rsap.V20n4.629597>.
 43. **Ortiz-Alvarez L, Xu H, Martinez-Tellez B.** Influence of exercise on the human gut microbiota of healthy adults: a systematic review. *Clin Transl Gastroenterol* 2020; 11: e00126. Disponible en: <https://pubmed.ncbi.nlm.nih.gov/32463624/>.
 44. **Rozich J, Dulai P, Fumery M, Sandborn W, Singh S.** Progression of elderly onset inflammatory bowel diseases: a systematic review and meta-analysis of population-based cohort studies. *Clin Gastroenterol Hepatol* 2020; 18: 2437-2447. Disponible en: <https://pubmed.ncbi.nlm.nih.gov/32142940/>.
 45. **Taylor K, Scruggs P, Balemba O, Wiest M, Vella C.** Associations between physical activity, resilience, and quality of life in people with inflammatory bowel disease. *Eur J Appl Physiol* 2018; 118: 829–836. Disponible en: <https://pubmed.ncbi.nlm.nih.gov/29411129/>.
 46. **Estay C, Simian D, Escaffi MJ, Figueroa C, Ibáñez P, Lubascher J, Kronberg U, Flores L, Quera R.** Obesidad y enfermedad inflamatoria intestinal. *Gastroenterol. latinoam* 2017; 28: 177-184. Disponible en: <http://gastrolat.org/DOI/PDF/10.0716/gastrolat2017n3000.04.pdf>
 47. **Vavricka S, Schoepfer A, Scharl M, Lakatos P, Navarini A, Rogler G.** Extraintestinal manifestations of inflammatory bowel disease. *Inflamm Bowel Dis* 2015; 21: 1982–1992. Disponible en: <https://pubmed.ncbi.nlm.nih.gov/26154136/>.
 48. **Cano S, Rubio C, Fernández R, Centeno O, Daniel C.** Metabolismo mineral óseo en la enfermedad inflamatoria intestinal. *Rev Osteoporos Metab Min.* 2009; 1: 21–28. Disponible en: <https://www.redalyc.org/pdf/3609/360933648004.pdf>.
 49. **Bird SP, Tarpennig KM, Marino FE.** Designing resistance training programmes to enhance muscular fitness: a review of the acute programme variables. *Sports Med* 2005; 35: 841-851. Disponible en: <https://pubmed.ncbi.nlm.nih.gov/16180944/>.
 50. **Pedersen B, Febbraio M.** Muscles, exercise and obesity: skeletal muscle as a secretory organ. *Nat Rev Endocrinol* 2012; 8: 457–465. Disponible en: <https://pubmed.ncbi.nlm.nih.gov/22473333/>.
 51. **Sandri M.** Signaling in muscle atrophy and hypertrophy. *Physiology.* Bethesda 2008;

- 23: 160–170. Disponible en: <https://pubmed.ncbi.nlm.nih.gov/18556469/>.
52. **Mounier R, Lantier L, Leclerc J, Sotiropoulos A, Foretz M, Viollet B.** Antagonistic control of muscle cell size by AMPK and mTORC1. *Cell Cycle* 2011; 10: 2640–2646. Disponible en: <https://pubmed.ncbi.nlm.nih.gov/21799304/>.
53. **Pérez R, Carlos J.** Interleukin-10 and Coronary Disease. *Rev Española Cardiol* 2012; 55: 738–750. Disponible en: <https://www.sciencedirect.com/science/article/abs/pii/S0300893202766931>.
54. **Beery RM, Li E, Fishman LN.** Impact of pediatric inflammatory bowel disease diagnosis on exercise and sports participation: Patient and parent perspectives. *World J Gastroenterol* 2019; 25: 4493–4501. Disponible en: <https://pubmed.ncbi.nlm.nih.gov/31496627/>.
55. **Escribano LI, Rodríguez AS, Centeno G.** Etiopathogenic diagnosis protocol of chronic diarrhea. *Medicine* 2020; 13: 38–44. Disponible en: <https://www.medicineonline.es/es-protocolo-diagnostico-etiotopogenico-diarrea-cronica-articulo-S0304541220300056?referer=seccion>.
56. **Salvo-Romero E, Alonso-Cotoner C, Pardo-Camacho C, Casado-Bedmar M, Vicario M.** Función barrera intestinal y su implicación en enfermedades digestivas. *Rev Esp Enferm Dig* 2015; 107: 686–696. Disponible en: https://scielo.isciii.es/pdf/diges/v107n11/es_revision.pdf.
57. **Álvarez J, Fernández-Real JM, Guarner F, Gueimonde M, Rodríguez JM, Saenz M.** Gut microbes and health 2021; 44: 519–535. Disponible en: <https://www.sciencedirect.com/science/article/pii/S0210570521000583>.
58. **Cronin O, Barton W, Skuse P, Penney N, Garcia-Pérez I, Murphy E.** A Prospective metagenomic and metabolomic analysis of the impact of exercise and/or whey protein supplementation on the gut microbiome of sedentary adults. *MSystems* 2018; 3: 18–44. Disponible en: <https://pubmed.ncbi.nlm.nih.gov/29719871/>.
59. **Barton W, Penney N, Cronin O, Garcia-Pérez I, Molloy M, Holmes E.** The microbiome of professional athletes differs from that of more sedentary subjects in composition and particularly at the functional metabolic level. *Gut* 2018; 67: 625–633. Disponible en: <https://pubmed.ncbi.nlm.nih.gov/28360096/>.
60. **Petersen LM, Bautista EJ, Nguyen H, Hanson BM, Chen L, Lek SH.** Community characteristics of the gut microbiomes of competitive cyclists. *Microbiome* 2017; 51: 1–13. Disponible en: <https://microbiomejournal.biomedcentral.com/articles/10.1186/s40168-017-0320-47>.
61. **Colmenarez G, Armania E.** Calidad de vida en pacientes con enfermedad inflamatoria intestinal. *Bol Med Postgrado* 2018; 34: 17–23. Disponible en: <https://revistas.uclave.org/index.php/bmp/article/view/2526>.

Contents

EDITORIAL

Monkeypox, the reflection of forgotten infections.

Larreal Y (*E-mail: yracimalarreal@gmail.com*) 203
<https://doi.org/10.54817/IC.v63n3a00>

ORIGINAL PAPERS

Role and mechanism of miR-548-3p/DAG1 in the occurrence and malignant transformation of laryngeal carcinoma (English).

Chen J, Zhou YL, Wen K, Huang S, Hou N, Wang L, Wang Y
(*E-mail: y_xwang5566@126.com*) 206
<https://doi.org/10.54817/IC.v63n3a01>

Alterations in the production of cytokines in response to *Toxoplasma gondii* appear from early stages in patients co-infected with HIV-1 (Spanish).

Escobar-Guevara EE (*E-mail: edscobar@gmail.com*), de Quesada-Martínez ME,
Roldán-Dávila YB, Alarcón de Noya B, Alfonso-Díaz MA 218
<https://doi.org/10.54817/IC.v63n3a02>

Analysis of high risk factors for complications in the trial of vaginal delivery due to uterine scarring in a subsequent pregnancy to a cesarean section (English).

Ye R, Wang W, Li J (*E-mail: taomu36311039913@163.com*) 235
<https://doi.org/10.54817/IC.v63n3a03>

Effect of tetrahydroquinoline derivatives on the intracellular Ca²⁺ homeostasis in breast cancer cells (MCF-7) and its relationship with apoptosis (English).

Maksoud S, Mayora A, Colman L, Sojo F, Pimentel AA, Kouznetsov VV, Merchán-Arenas DR, Romero AH, Arvelo F, De Sanctis JB, Benaim G (*E-mail: gbenaim@gmail.com*) 243
<https://doi.org/10.54817/IC.v63n3a04>

Sub-lineages of the Omicron variant of SARS-CoV-2: characteristic mutations and their relation to epidemiological behavior (English).

Zambrano JL, Jaspe RC, Hidalgo M, Loureiro CL, Sulbarán Y, Moros ZC, Garzaro DJ, Vizzi E, Rangel HR, Liprandi F, Pujol FH (*E-mail: fhpujol@gmail.com*) 262
<https://doi.org/10.54817/IC.v63n3a05>

CASE REPORT

Idiopathic scrotal calcinosis. A case report (Spanish).

Bouquett V, Sánchez L (*E-mail: lemasq212@gmail.com*) 275
<https://doi.org/10.54817/IC.v63n3a06>

REVIEWS

The benefits of peritoneal dialysis (PD) solution with low-glucose degradation product in residual renal function and dialysis adequacy in PD patients: A meta-analysis (English).

Chen S, Jia J, Guo H (*E-mail: guohuiminmail@126.com*), Zhu N. 283
<https://doi.org/10.54817/IC.v63n3a07>

Evaluation of physical activity as a therapeutic adjuvant for patients with inflammatory bowel disease (Spanish).

Fernández-Lázaro D (*E-mail: diego.fernandez.lazaro@uva.es*), Hernández-Burgos N, Cobreros Mielgo R, García-Lázaro S. 304
<https://doi.org/10.54817/IC.v63n3a08>

Contenido

EDITORIAL

Viruela del Mono, el reflejo de las infecciones olvidadas.

Larreal Y (*Correo electrónico: yrcaimalarreal@gmail.com*) 203
<https://doi.org/10.54817/IC.v63n3a00>

TRABAJOS ORIGINALES

Papel y mecanismo de miR-548-3p/DAG1 en la aparición y transformación maligna del carcinoma de laringe (Inglés).

Chen J, Zhou YL, Wen K, Huang S, Hou N, Wang L, Wang Y
(*Correo electrónico: y_wang5566@126.com*) 206
<https://doi.org/10.54817/IC.v63n3a01>

Alteraciones en la producción de citosinas en respuesta a *Toxoplasma gondii* aparecen desde las etapas tempranas en pacientes coinfectados con VIH-1 (Español).

Escobar-Guevara EE (*Correo electrónico: edscobar@gmail.com*), de Quesada-Martínez ME, Roldán-Dávila YB, Alarcón de Noya B, Alfonso-Díaz MA 218
<https://doi.org/10.54817/IC.v63n3a02>

Análisis de factores de alto riesgo para complicaciones en el trabajo de parto vaginal debidas a cicatrización uterina en un embarazo posterior a una operación cesárea (Inglés).

Ye R, Wang W, Li J (*Correo electrónico: taomu36311039913@163.com*) 235
<https://doi.org/10.54817/IC.v63n3a03>

Efecto de derivados de tetrahydroquinolinas sobre la homeostasis del Ca²⁺ intracelular en células de cáncer de mama (MCF-7) y su relación con la apoptosis (Inglés).

Maksoud S, Mayora A, Colman L, Sojo F, Pimentel AA, Kouznetsov VV, Merchán-Arenas DR, Romero AH, Arvelo F, De Sanctis JB, Benaim G
(*Correo electrónico: gbenaim@gmail.com*) 243
<https://doi.org/10.54817/IC.v63n3a04>

Sub-linajes de la variante Ómicron del SARS-CoV-2: mutaciones características y su relación con el comportamiento epidemiológico (Inglés).

Zambrano JL, Jaspe RC, Hidalgo M, Loureiro CL, Sulbarán Y, Moros ZC, Garzaro DJ, Vizzi E, Rangel HR, Liprandi F, Pujol FH (*Correo electrónico: fhpujol@gmail.com*) 262
<https://doi.org/10.54817/IC.v63n3a05>

REPORTE DE CASO

Calcinosis escrotal idiopática: Reporte de un caso (Español).

Bouquett V, Sánchez L (*Correo electrónico: lemasq212@gmail.com*) 275
<https://doi.org/10.54817/IC.v63n3a06>

REVISIONES

Beneficios de la solución de diálisis peritoneal (DP), con producto de degradación bajo en glucosa, en la función renal residual y la adecuación de la diálisis en pacientes en DP: un metanálisis (Inglés).

Chen S, Jia J, Guo H (*Correo electrónico: guohuiminmail@126.com*), Zhu N 283
<https://doi.org/10.54817/IC.v63n3a07>

Evaluación de actividad física como coadyuvante terapéutico para pacientes con enfermedad inflamatoria intestinal (Español).

Fernández-Lázaro D (*Correo electrónico: diego.fernandez.lazaro@uva.es*), Hernández-Burgos N, Cobreros Mielgo R, García-Lázaro S 304
<https://doi.org/10.54817/IC.v63n3a08>